NTNU – Trondheim
Norwegian University of
Science and Technology

Transferability of Petrophysical, Lithological and Mineralogical Datasets for the Kai Formation and the Brygge Formation

Between the Fields; Heidrun, Åsgard and
Aasta Hansteen in the Norwegian Sea

Helene Kristiansen Andersen

Geology
Submission date: May 2015
Supervisor: Mai Britt E. Mørk, IGB
Co-supervisor: Georg Röser, Statoil
Rune Langlo Pedersen, Statoil

Norwegian University of Science and Technology
Department of Geology and Mineral Resources Engineering

Proposed topic

Transferability of data between geological areas

In the effort of saving costs, it is desirable to transfer data gathered on one geological field to another adjacent field or to areas even further away. Various datasets are of interest, such as stress data (XLOT), mechanical properties and geotechnical behaviour (formation collapse as a barrier) or the presence of permeable zones with flow potential within tight formations. While it is already common practice to use datasets from adjacent offset wells, no methodological approach has been established so far, leading to a substantial risk of working with false assumptions. In order to minimize the risk of inappropriate use of offset data, questions of similarity of formations and conditions need to be addressed. A broad approach, including an assessment of log data, mineralogy, regional geology, sediment provenance, depositional environment, burial/unloading history, diagenesis, etc. is necessary to make a statement about the transferability of data.

Within the scope of this master thesis it is suggested to compare one or two specific formations on at least two operating oilfields on the Norwegian Continental Shelf (NCS) and their respective counterparts in the North Sea or Barents Sea. The suggested datasets of interest for possible transferability are mechanical properties with respect to formation collapse as a barrier in the permanent plug and abandonment of oil wells. Standard log data from existing wells in addition to logs with special meaningfulness to rock mechanics should be looked into and investigated for similar trends and value ranges. Existing mineralogical data should be investigated and additional XRD data should be acquired using Statoil cuttings samples from representative wells. Extensive literature research regarding sediment provenance, depositional environment, burial/unloading and tectonical history, as well as diagenesis of the respective formations in the different areas should be used to complete the investigation. An assessment of the most practical way to approach questions of data transferability including a statement regarding the connected uncertainties should be the targeted end result of the thesis.

Suggested parameters:

Formation	Kai Fm., Brygge Fm.
Fields on NCS	Heidrun, Åsgard, Tyrihans
Offset area	Aasta Hansteen
Datasets	GR, RES, DEN/NEU, Sonic, XRD, (geomechanical data from lab tests?)

Abstract

Transferability of datasets between fields is of great interest in the current economic situation. Transferability is the ability to use the same set of data in two or more separate places without doing further testing. In order to optimize the cost efficiency during drilling operations it is important to know what is most efficient, conventional testing or transfer of datasets. To investigate transferability, the topic of using shale formations as hydraulic barriers was chosen. Three fields were selected for the investigation: the Heidrun Field, the Åsgard Field and the Aasta Hansteen Field. From each field several wells were picked based on the availability of datasets from the two chosen formations, linked to petrophysical logs, lithological descriptions and mineralogical analyses. The mineralogical analyses were based on x-ray diffraction data. The Kai Formation was chosen as it has already been confirmed as a hydraulic barrier on the Heidrun Field; in the reference well which was used for the comparison of the datasets. The Brygge Formation has not been confirmed as a barrier and was mostly used as an extension to the Kai Formation, to have a larger set of available data. The transferability of both formations was assessed.

The transferability of the petrophysical logs, the lithological descriptions and the mineralogical analyses within and between the Heidrun and Åsgard Fields proved possible for the Kai Formation, and the likelihood of using it as barrier in the extended area is relatively high. The Brygge Formation also proved possible to correlate between the two fields. However since it has not been proven as a barrier, no conclusion was drawn concerning its ability to act as a barrier. Between the Heidrun and Åsgard Field and the Aasta Hansteen it was hard to correlate the formations and finding a possible barrier interval is most likely impossible. The method used for the comparison was a broad approach and can be used for similar types of projects. However, to optimize the method, especially for the topic of shale formation as a barrier, more information is needed concerning rockmechanical and geochemical aspects. At this point there is no conclusive statement to how and why some shale formations act as a barrier and it is necessary to answer this before the method can be optimized. The method in itself works quite well when considering the question of transferability. Nevertheless, the amount of work and difficulty in finding suitable data is probably less cost efficient than doing the conventional tests during drilling operations.

Sammendrag

Overføring av datasett mellom felt og brønner er svært viktig med dagens økonomiske situasjon. Overførbarhet er muligheten til å bruke de samme typene datasett på to eller flere separate steder, uten å gjøre flere undersøkelser. For å øke effektiviteten under boreoperasjoner må man vite hva som er mest effektivt av konvensjonell testing og overføring av datasett. For å undersøke overførbarhet av datasett, ble det valgt et tema for å representere datasettene; bruken av leireformasjoner som hydrauliske barrierer på Heidrun Feltet, Åsgard Feltet og Aasta Hansteen Feltet. Fra hvert felt ble noen få brønner plukket ut basert på tilgjengeligheten av datasett (petrofysiske logger, litologiske beskrivelser og mineralogiske XRD analyser) i leireformasjonene. Kai Formasjonen ble valgt fordi den allerede har blitt bekreftet som en barriere på Heidrun Feltet i referansebrønnen som ble brukt som grunnlag for sammenligningen av datasettene. Brygge Formasjonen har ikke blitt bekreftet som en barriere og ble mest brukt for å supplere Kai Formasjonen med tilgjengelige datasett. Overførbarheten av begge formasjonene ble undersøkt.

Overføringen av de petrofysiske loggene, de litologiske beskrivelsene og de mineralogiske analysene var gjennomførbare på og mellom Heidrun Feltet og Åsgard Feltet for Kai Formasjonen, og sannsynligheten for å kunne bruke leireformasjonen som en barriere over et større område er relativt høy. Det var også mulig å korrelere datasettene i Brygge Formasjonen mellom de to feltene, men siden den ikke har blitt bekreftet som en hydraulisk barriere er det ikke mulig å dra noen konklusjoner angående formasjonens barriereegenskaper. Det var vanskeligere å korrelere datasettene mellom Heidrun og Åsgard Feltet og Aasta Hansteen Feltet, og å finne et mulig barriereintervall ville vært nesten umulig. Metoden som ble brukt til sammenligningen var relativt generell og kan bli brukt i lignende prosjekter. For å optimalisere metoden, spesielt for dette temaet om bruken av leireformasjoner som barriere, er det nødvendig med mer informasjon om bergmekaniske og geokjemiske aspekter. Per dags dato finnes det ingen bekreftet teori for hvorfor og hvordan noen leireformasjoner har de riktige barriereegenskapene, mens andre ikke. For å optimalisere metoden for overførbarhet av datasett må dette spørsmålet besvares. Metoden å sammenligne og korrelere datasettene fungerte bra, men basert på mengden arbeid og kostandene som ligger i et slikt prosjekt vil det mest sannsynlig være mer effektivt og kostnad- besparende å gjennomføre de konvensjonelle testene.

Acknowledgment

On the completion of my master thesis at the Norwegian University of Science and Technology I would like to acknowledge and express my gratitude to all my supervisors and fellow students.

- My supervisor at NTNU, Professor Mai Britt E. Mørk, for all the guidance and help throughout the year writing the thesis.
- My co-supervisors in Operation Geology, Statoil; Georg Röser and Rune Langlo Pedersen for all the help, discussions and guidance throughout the process. In addition, Anikken Bjerge and Zain Bilgrami for all the patience and answers to all my field related questions.
- Statoil and all the partners for granting access to and providing all the necessary data and covering the expenses for transporting the cutting samples from Weahterford Laboratories.

Helene Kristiansen Andersen Trondheim, 15.5.2015

Table of Contents

List of Figures

List of tables

List of abbreviations

Logs:

Bbl – barrel

Cali – caliper

CBL – cement bond log

Cmt – cement

Dt – sonic

FIT – formation integrity test

GR – gamma ray

Imp. – impedance

LOT – leak off test

LWD – logging while drilling

MD – measured depth

MSL – mean sea level

MWD – measuring while drilling

NCS – Norwegian continental shelf

NPHI – neutron log

P&A – plug and abandonment

Pef – photoelectric effect

RHOB – density

RKB (KB) – rotary kelly bushing

Rt – resistivity

SS - subsea

TVD – true vertical depth

VDL – variable density log

Lithology:

Clst – claystone

Lst – limestone

Slst – siltstone

Sst – sandstone

Mineralogy:

Amph – amphibole

Bar – barite

Calc – calcite

Chl – chlorite

Fsp – feldspar

I/S – illite/smectite

Ill – illite

Kaol – kaolinite

Kfsp (K-fsp) – kalifeldspar

Mi/ill – mica/illite

ML – mixed layer clay

Plag – plagioclase

Pyr - pyrite

Qtz – quartz

SEM – scanning electron microscope

Smec – smectite

Syl – sylvite

Ver - vermiculite

XRD – x-ray diffraction

Zeo - zeolite

1 Introduction

In the changing economic environment of the oil industry, it is becoming increasingly important to save costs. To meet the new demands from the industry and the society, pre-existing methods and data are combined in order to increase the efficiency of operations and production. This thesis is an effort to gather existing data on fields and formations on the Halten Terrace, and looking into the possibility of transferring the data to other fields and areas. It will be a broad approach to investigate a variety of geological datasets, which in the end will result in a statement concerning the transferability of data. The secondary goal of this thesis is to establish a methodological approach to the question of transferability between fields, based on the comparison of two established fields on the Halten Terrace and one offset area further north.

The assessment will be based on the geotechnical behavior of the geological formations, by that meaning the formations ability to act as a hydraulic seal after collapsing on to the casing string. This is important during the plug and abandonment (P&A) of wells, and will become progressively more common during the next phase of drilling operations on the Norwegian Continental Shelf (NCS). During P&A operations, cement is commonly used to plug the well and seal the annulus, to make sure there will be no leakage after the abandonment. In an attempt to reduce the costs of P&A operations, the possibility of using the downhole formations as hydraulic barriers is a good alternative. The purpose of the hydraulic barrier is to provide a laterally continuous and impermeable seal which will permanently plug the annulus along the casing, so no fluids can flow to the surface.

The best way to compare the formations will be by using various petrophysical, lithological and mineralogical datasets. An assessment of standard log data, mineralogy, regional geology, provenance, burial history and digenesis is required. Finding the right method is important to reduce the risk of incorrect use of the datasets and to address the questions of similarities and differences between the formations. The chosen formations are the Kai Formation and the Brygge Formation. The chosen fields on the Halten Terrace are the Heidrun Field and the Åsgard Field and from the offset area, the Aasta Hansteen Field. Additional data acquisition might be necessary to collect more data if there is any missing information for any of the fields.

Another important aspect to consider is the economical factor. To what extent is it actually cost efficient to execute the transferability of data? At what point will the cost of obtaining and analyzing the necessary information exceed the cost of performing conventional tests offshore? This aspect will not be investigated as a topic, but will be considered during the assessment of the transferability of data.

1.1 Transferability of datasets

In this context, transferability is the ability to use the same data in two or more separate places without doing further tests or investigation. The main question is then, to what extent is it possible to use gathered data from one field directly on another field? The data is based on existing well data from the fields and formations to be investigated. The datasets will be compared to the interval in the formation, in which the desired properties have already been confirmed. The interval with the required properties will be used as a reference for comparing the other intervals investigated in the thesis. The question of transferability can be considered both vertically and laterally. The difference is that, if the formations are compared laterally, all the properties can be correlated without taking into account the vertical difference in the formations. This will be a study of the relationship between mineralogy, lithology and log response as a function of burial depth and lateral extension.

1.2 Plug and abandonment operations

Plug and abandonment (P&A) are an important part of the well-life cycle anywhere in the world. Plugging of the old well occurs prior to drilling a sidetrack to another part of the field, or when the well is to be permanently abandoned. The aim, according to today's requirements in the Norwegian sector, is to permanently seal off and plug the well for eternity. Offshore Norway the importance of completely sealing the well is critical due to the proximity of the coast and the wildlife in the area (Liversidge et al., 2006). Therefore, there are strict requirements for P&A operations on the Norwegian Continental Shelf. The NORSOK standard is developed by the Norwegian oil industry to take into account the requirements for safety and to avoid the consequences of any catastrophe on a climatic scale in the North Sea. The standards are modified and based on the international standards ISO and EN (Williams et al., 2009). The part of the standard describing drilling and well operations, is the NORSOK Standard D-010 (The Standards Organisation in Norway (NORSOK), 2004). In the D-010 standard, all the requirements for the design and the execution of the well and the operations are described in detail. The design requirements concern the placement of barriers, depth,

materials, distance to the source of possible leakage and the need for double barriers. According to the D-010 Standard, the properties required for the barrier are the following:

- Impermeable
- Long term integrity
- Non-shrinking
- Ductile – (non-brittle) – able to withstand mechanical loads/impact
- Resistant to different chemicals/substances
- Wetting, to ensure bonding to steel

In addition, it states that; "*Permanent well barriers shall extend across the full cross section of the well, include all annuli and seal both vertically and horizontally*" (The Standards Organisation in Norway (NORSOK), 2004). Figure 1.1 is an illustration of how the barrier is meant to fulfill this requirement.

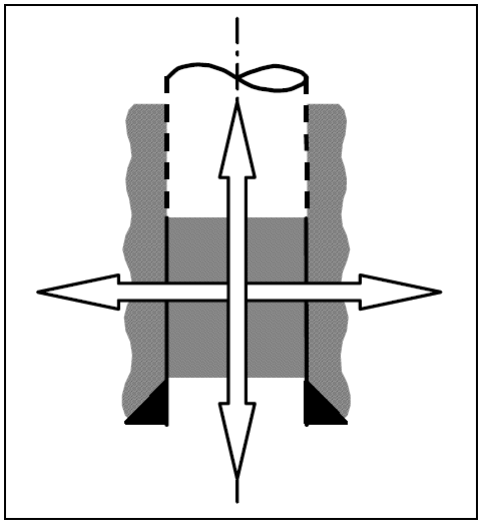

Figure 1.1 Well barrier element. The figure shows that the permanent well barrier shall include the annuli and seal both horizontally and vertically (The Standards Organisation in Norway (NORSOK), 2004).

To ensure the barriers have the required properties they have to be tested. All intervals considered to have the right properties as barriers have to be logged, using a sonic logging tool to acquire the Cement Bond Log (CBL) and Variable Density Log (VDL). These logs will show if the barrier has sufficient bonding to the casing and if it covers the sufficient interval. A pressure test is necessary to ensure that the well barrier elements can withstand the maximum pressure applied to the barrier. There are multiple risks and uncertainties concerning barriers made of cement, often related to the design and placement of the barriers,

cement volume, pump parameters, contamination and cement shrinkage (The Standards Organisation in Norway (NORSOK), 2004). If any of these properties are not fulfilled according to the standard, or there is any suspicion of potential risks, it might be necessary with remedial actions such as perforating the casing and cement squeezing. All the possible solutions are costly and time consuming; in addition it might damage the casing, which is undesirable since it is a part of the barrier (Williams et al., 2009). A second option is using a shale formation as an annular barrier.

1.3 Shale formation as a barrier

If the requirement of double barriers or the properties of the cement barrier is not fulfilled, it is possible to use collapsed shale formations as a hydraulic barrier. The requirements for using shale as a barrier are the following according to Williams et al. (2009).

- Verification of the shale properties using wireline logs
- Adequate strength to withstand maximum pressure exerted on formation
- Displacement mechanism satisfying the requirements for a barrier
- Suitable interval, length and completely surrounding the casing

To verify these properties, the first step is to acquire the CBL and the VDL. These will ascertain if there is good bonding between the formation and the casing, sufficient interval and circumference around annulus. If the formation is previously untested, a strength test is necessary. Figure 1.2 from the Williams et al. (2009) report illustrates how a log can show good and poor bonding. The test is meant to verify the strength of the formation, in addition to making sure there is no possibility of a fluid communication system in the formation (Williams et al., 2009). The possible strength tests are; Formation Integrity Test (FIT), Leak Off Test (LOT) or Extended Leak Off Test (XLOT). When a formation has been tested and qualified as a barrier, it can be used to confirm the same formation in other wells on the same field. The only requirement is a statement from a senior geologist, confirming the similarities of the tested formation to the formation in question.

The senior geologist must decide if the formation shows sufficient evidence based on logs and seismic data to qualify it as a barrier without doing a pressure test. Previously, the decision has been done based on comparison of the CBL and VDL logs. For a geologist to make a decision, it is necessary to have all the relevant information about the formation. To be able to qualify the formation it is important to understand why some formations show the necessary properties of formation collapse, while other formations do not.

To understand how the formation can be used as a barrier it is essential to understand the displacement mechanism. The mechanism for formation collapse is most likely one of the following or a combination of the following (Williams et al., 2009):

- Shear or tensile failure
- Compaction and/or consolidation
- Liquefaction
- Thermal expansion
- Chemical effects
- Creep

All of these factors play a role in the behavior of the formation, it is however most likely that the formation collapse is a combination of shear failure and creep, according to Williams et al. (2009). A reduction in mud weight behind the casing may initiate the collapse, and the natural creep that occurs in the formation ensures good bonding to the casing (Williams et al., 2009). This makes sense for a shale formation, however, the problem with the shale formations on the NCS is that the same formation might show good bonding in one well and poor bonding in the next well. There is no accepted answer to why only parts of the same formation show formation collapse. However, it is not in the scope of this thesis to answer the question of formation collapse.

Most likely there are several factors contributing to the differences in the formations. This thesis will have a petrophysical, lithological and mineralogical approach to the question of transferability; therefore an extensive literature research is necessary to describe geological history, structural setting, mineralogy and diagenesis.

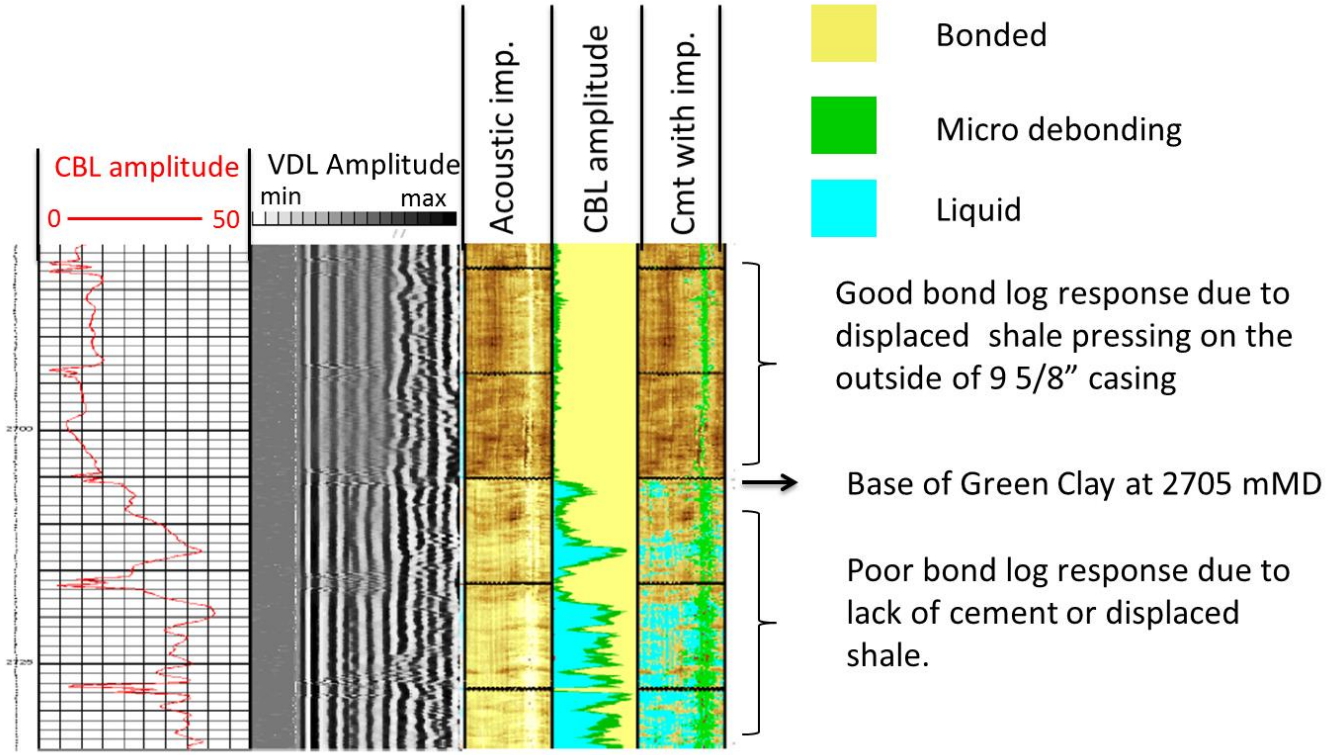

Figure 1.2 Bonding between casing and the formation. Example showing a cement bond log (CBL) and a variable density log (VDL), and how it can be used to determine if the there is good bonding between the casing and the formation or the cement (cmt), modified from Williams et al. (2009).

1.4 Approach to study

The goal of this thesis is to establish a method for transferring datasets and in the end form a statement of the viability of this method. The question of transferability between the fields will be approached by an in-depth comparison of the various datasets available from the wells on the three fields. Access has been granted from Statoil and their partners to the wells from each field. The access includes information for petrophysical logs, lithological descriptions and mineralogical reports.

Even though the Norwegian Continental Shelf is one of the best studies petroleum areas in the world, there are limitations to the availability of data when it comes to the formations in the overburden. In most wells the data collection is most extensive in the reservoir section, meaning the overburden section is usually not as well covered. Some difficulties will therefore be encountered when looking at the shale sections in the overburden.

The first step in the assessment of transferability is to define the reference well for the comparison of fields. The reference is the well, in which the formation of interest has already been confirmed as a hydraulic barrier. For this interval it is necessary to gather all available information and combine it with information from the additional data acquisition. The cuttings from the interval will be analyzed using x-ray diffraction to determine the mineralogy. This practical approach will help in determining the time and cost aspect of this kind of project, since the secondary goal is to make a statement to the feasibility of transferability. This will in the end be a part of the methodology for transferability of various datasets. The reference well is located in the Heidrun Field and will be a combination of well 0 and well 0.2 and the interval used as a hydraulic barrier is in the Kai Formation. The confirmation of the Kai Formation in well 0 makes it possible to use it as barrier in other wells on the Heidrun Field. The Brygge Formation has not yet been confirmed as a barrier in any of the fields on the Halten Terrace; and can therefore not be used as a barrier. Compared to the Kai Formation, the Brygge Formation has a lot more available datasets concerning petrophysical logs, lithology and mineralogy, making it easier to correlate and compare across the fields.

With access to a great amount of data, the first objective is to get a good overview and organize the material in a logical manner. In this case, it will be easiest organizing the data for each field, and then compare and correlate them in the results and the discussion. With this method it will be easier to see missing data, and determine if more information is needed for each field. The goal is to have enough information to be able to compare and correlate the formations across the fields. An important detail to note is that the datasets from the different fields are not always the same and there might be datasets not available for parts of the two formations. This is another reason why it was decided to look at both formations. In addition, some of the wells have been chosen mostly to support and strengthen the datasets in the other wells and will be used as supplementary wells. In addition, the previous studies done on the mineralogy in the Kai and Brygge Formations by Marcussen et al. (2009) and Peltonen et al. (2008) will be used in the discussion to compare results and trends.

2 Area of study and geological formations

The area of investigation for this thesis is the Mid-Norwegian margin, from the Trøndelag Platform to the Nyk High (63°N – 67°N) and is shown on the map (Figure 2.1) and in Figure 2.2 (Blystad et al., 1995).

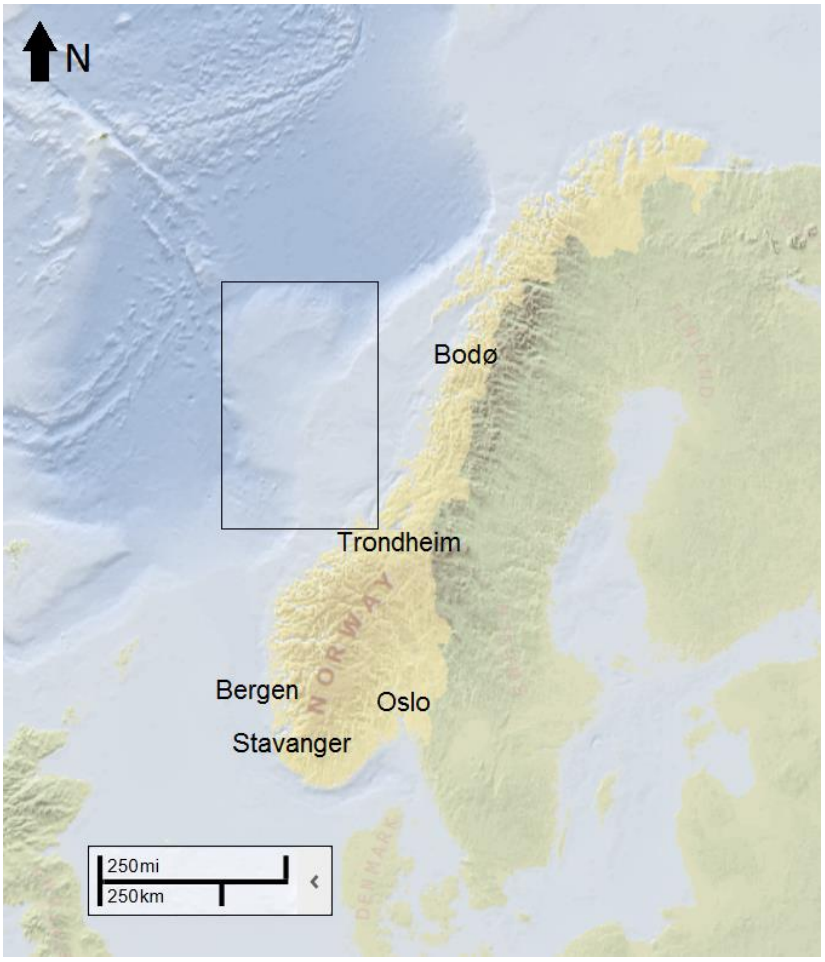

Figure 2.1 Map of study area. The figure shows the area of investigation on the Mid-Norwegian margin, modified from The Norwegian Petroleum Directorate (2014a).

The area consists of several segments in form of basins, terraces and structural highs, separated by distinct features such as fracture zones, horsts, grabens and fault complexes, and some of them will be described below and are shown in Figure 2.2.

The Halten Terrace is the location for the Åsgard and the Heidrun Fields. The Halten Terrace is defined between 64°N and 65°N, and is approximately 80km wide and 130km long and covers an area of 10,000km^2. It is bounded by the Trøndelag Platform to the east and by the

Dønna Terrace in the north. The Nordland Ridge is one of the structural highs in the area is the northeastern boundary to the Halten Terrace. The ridge is considered to be a sub-element of the Trøndelag Platform, and is the separation between the Dønna Terrace and the Helgeland Basin (Blystad et al., 1995). Westward is the Vøring Basin and the Vøring Marginal High. Southwest, the Møre Basin and the Møre Marginal High can be found (Blystad et al., 1995). These will not be of great importance in the thesis, but are mentioned in the literature research. The most northern part of the area to be investigated is the Nyk High, where the Aasta Hansteen Field is located. This is an elongated structural high and is located at 67°N. It stretches approximately 75km in the NE-SW trending strike direction, and it is only 15-20km wide (Blystad et al., 1995).

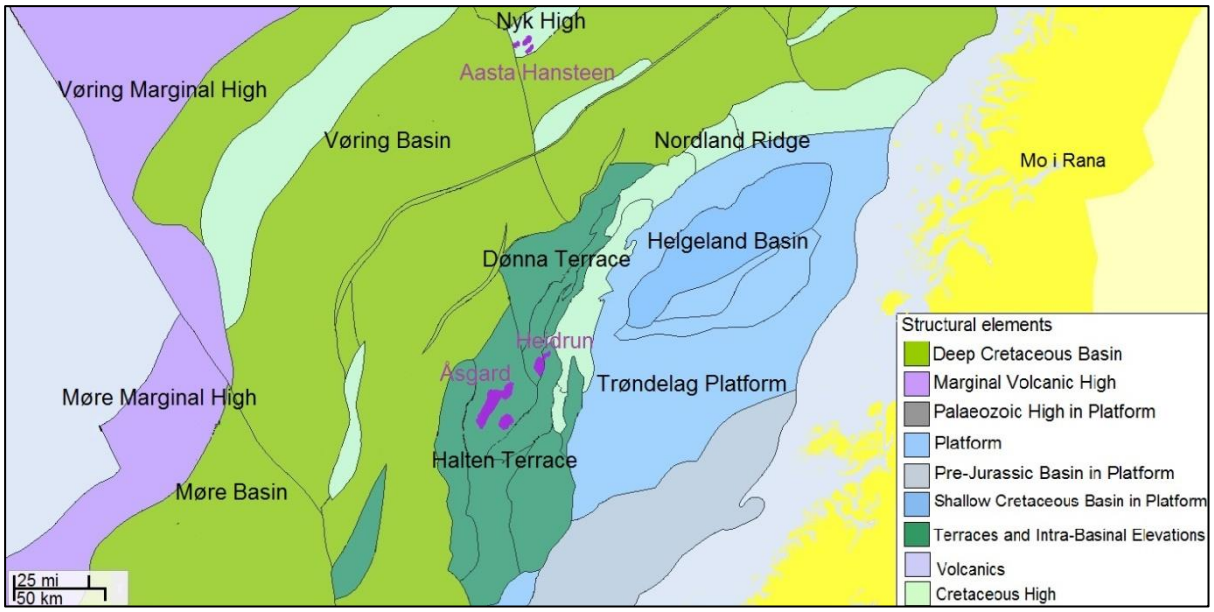

Figure 2.2 Structural map of the study area. Map showing the area of interest with the various basins, platforms and structural highs on the Mid-Norwegian Margin. The location of the Åsgard, Heidrun and Aasta Hansteen Fields are marked by the purple colour on the map, modified from The Norwegian Petroleum Directorate (2014a).

2.1 Fields

The Heidrun and Åsgard Fields are located in the northern part of the Halten Terrace (Figure 2.2). The Heidrun Field is located approximately 40 km northeast of the Åsgard Field. The Aasta Hansteen Field is located on the Nyk High further north, close to the Vøring Basin. The distance between the Halten Terrace and the Aasta Hansteen Field is approximately 190 km.

2.1.1 The Heidrun Field

The Heidrun Field was discovered on the Halten Terrace (Figure 2.3) in 1985, when drilling exploration well 6507/7-2 (Jackson et al., 2006 , The Norwegian Petroleum Directorate, 2014b). The well is located approximately 190 km off the Norwegian coast and is situated in the northern part of the Halten Terrace with water depths of approximately 345m. The reservoir rocks were located in Middle and Late Jurassic (2203-2217mTVD). After initial calculations Heidrun was proved to be a giant oil field with around 750 million bbl. of recoverable oil (Whitley, 1992). The Kai and Brygge Formations are located between 1454 mTVD and 1944 mTVD in the overburden section of the discovery well.

2.1.2 The Åsgard Field

The Åsgard Field (Figure 2.3) was discovered in 1981, while drilling the exploration well 6507/11-1, with the purpose of testing the sequence between the seabed and the Triassic boundary. The reservoir section was found in Early and Middle Jurassic, in the interval 2358 – 2596 mTVD. The overburden Kai and Brygge Formations are in the interval between 1407 mTVD to 2010 mTVD. The discovery is located approximately 200km west for the Norwegian coastline (Torsoy, 2000) and at water depths between 240 and 300m (The Norwegian Petroleum Directorate, 2014c). The Åsgard discovery has later been divided into three subfields; Midgard, Smørbukk and Smørbukk South. However, to make development and production as effective as possible, they are treated as one entity (Torsoy, 2000).

2.1.3 The Aasta Hansteen Field

Aasta Hansteen was not discovered until 1997, when the exploration well 6707/10-1 was drilled to test a tilted fault block on the Nyk High (Figure 2.4). Hydrocarbon indication was discovered in the Late Cretaceous interval between 2977 mTVD and 4241 mTVD. The overburden formations (Kai and Brygge Formation) are located above 2142 mTVD. The field is situated 320km west of the Norwegian coastline, outside Bodø and the water depth in the area is around 1270m. Production will not start until 2017 (The Norwegian Petroleum Directorate, 2014c).

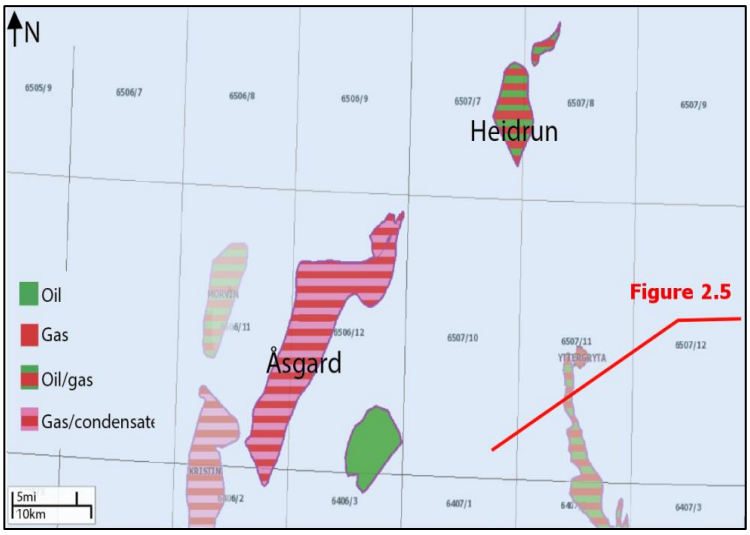

Figure 2.3 Map of the Heidrun and Åsgard Fields. Overview of the location of Heidrun and Åsgard Fields on the Halten Terrace, modified from The Norwegian Petroleum Directorate (2014a). The red line shows the approximate location of the seismic line in Figure 2.5. The line extends further east and is modified from Eidvin et al. (2007).

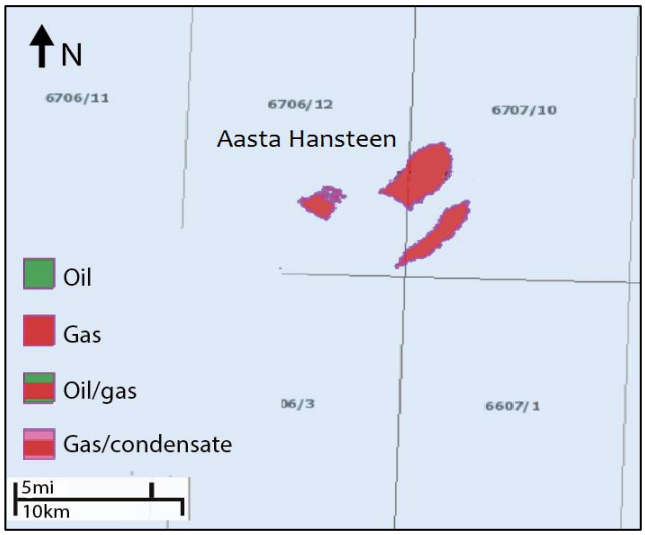

Figure 2.4 Map of the Aasta Hansteen Field. Overview of the location of the Aasta Hansteen Field on the Nyk High, modified from The Norwegian Petroleum Directorate (2014a)

2.2 Formations

2.2.1 The Brygge Formation (Early Eocene – Early Miocene)

The Brygge Formation is found across most of the Halten Terrace, except on the Nordland Ridge. It is of Early Eocene to Early Miocene age (Hordaland Group) and the depositional environment was mainly marine. It was defined in well 6407/1-3, in the interval between 2212.5 mTVD and 1762.5 mTVD, with a thickness of 450 m. The formation is clay-dominated with sandstone, siltstone, limestone or marl stringers. In addition, it is common to find pyrite, glauconite and shell fragments (Dalland et al., 1988). On the Halten Terrace, it consists mostly of clay, while out in the Møre and Vøring basin it consists mostly of ooze-deposits (Chand et al., 2011 , Eidvin et al., 2007). The deposition of the formation was a result of a regional uplift and erosion in Paleocene, with following subsidence and transgression (Eidvin et al., 2007). The upper part of the formation is broken up by a characteristic polygonal fault system (Eidvin et al., 2007 , Berndt et al., 2003 , Chand et al., 2011).

2.2.2 The Kai Formation (Early Miocene – Late Pliocene)

The age of the Kai Formation on the Halten Terrace is Early Miocene to Late Pliocene (Lower Nordland Group). It can be found on most of the Halten Terrace, except only on parts

of the Nordland Ridge. The formation was defined in the well 6407/1-2, in the interval between 1690 mTVD and 1419 mTVD, with a thickness of 271m. It consists of varying amounts of clay, silt and sand with limestone stringers. Glauconite, pyrite and shell fragments are commonly found in the formation. Varying amounts of sand have been recorded across the Halten Terrace. The depositional environment was generally marine, with great variations in water depth (Dalland et al., 1988). The Kai Formation is coeval with the Molo Formation to the east and the Utsira Formation to the south (Løseth and Henriksen, 2005 , Eidvin et al., 2007). The same polygonal fault system, found in the Brygge Formation, can also be found in the Kai Formation (Berndt et al., 2003 , Chand et al., 2011 , Eidvin et al., 2007).

The sequence of the formations can be seen in Figure 2.5. The Brygge Formation is underlying the Kai Formation and the Molo Formation. In addition it is possible to see the configuration of the two latter formations.

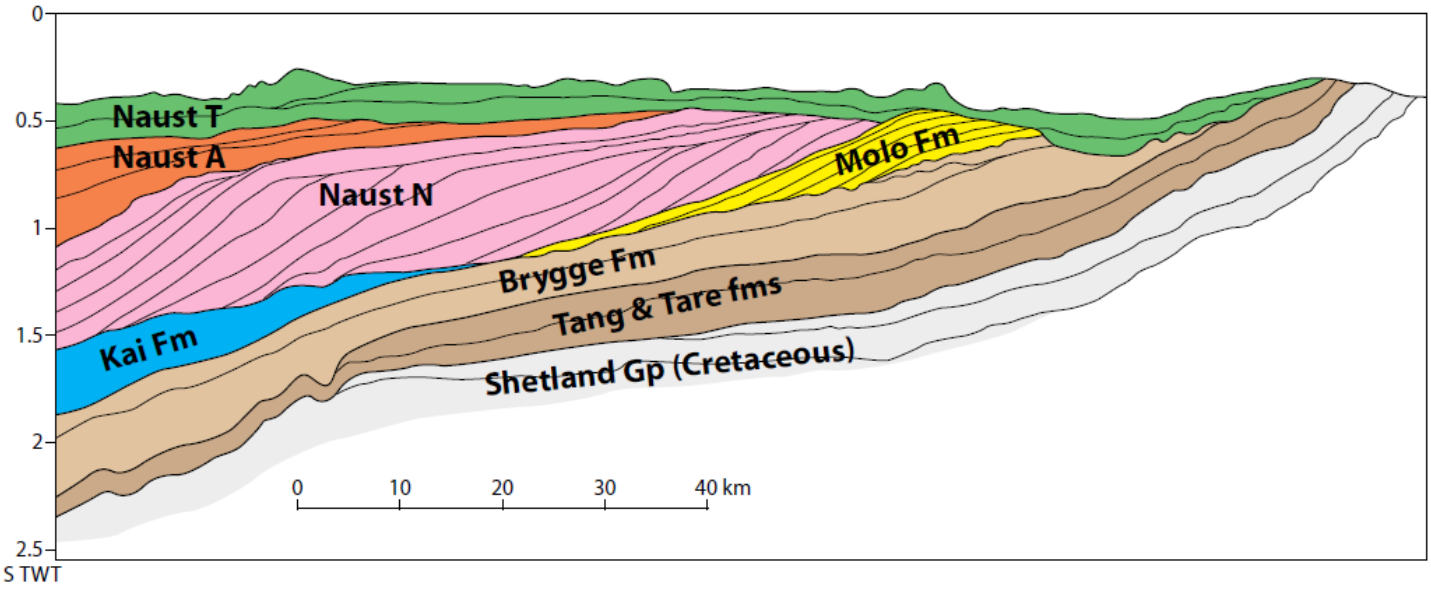

Figure 2.5 Cenozoic sequence of formations. Overview of the Cenozoic formations on the Halten Terrace, based on geoseismic (Eidvin et al., 2007). The approximate location of the line can be seen in Figure 2.3.

2.3 Previous studies

The Norwegian Sea and the North Sea are two of the world's best studied basins; however most of the studies have been done on the possible reservoir sandstones and carbonates, and not on the overburden mudstones. Recently, there has been more interest in the Cenozoic formations after the discovery of hydrocarbon indications. Forsberg and Locat (2005) did a mineralogical and microstructural study of the Cenozoic sediments to investigate the mechanisms behind the Storegga Slide. Marcussen et al. (2009) studied the physical properties of the Cenozoic mudstones in the northern North Sea and Peltonen et al. (2008) studied the mineralogical control on mudstone compaction in the Norwegian Sea. They all use XRD as a tool in their studies and their results go into great detail in the mineralogy of the Cenozoic mudstones.

In their study, Forsberg and Locat (2005) survey two wells with samples from the Kai and Brygge Formations. Based on their bulk XRD analysis, they interpret both of the formations to have high clay content and low feldspar content. The fine fraction analysis (Figure 2.6) shows that the Brygge Formation has high kaolinite content and notes an absence of chlorite. The Kai Formation has high smectite content and increasing chlorite content at shallower depths. SEM analyses done on the Kai Formation confirms the smectite content and reveals large amounts of siliceous and calcareous microfossils creating secondary porosity. An example of the SEM micrographs showing the clay content can be seen in Figure 2.7. They attempt to explain the difference in the mineralogy by the concept of weathering and denudation. The small amount of terrigenous material found in the Brygge Formation is mostly rich in kaolinite. The Kai Formation has a higher content of terrigenous and biogenic material with a significant amount of smectite. The increase in terrigenous material is explained by the initiation of the glaciation with an increase in denudation and deeper erosion of weathered rock. An explanation of the increase in smectite content is transport of sediments from the south and the erosion of basaltic igneous rocks.

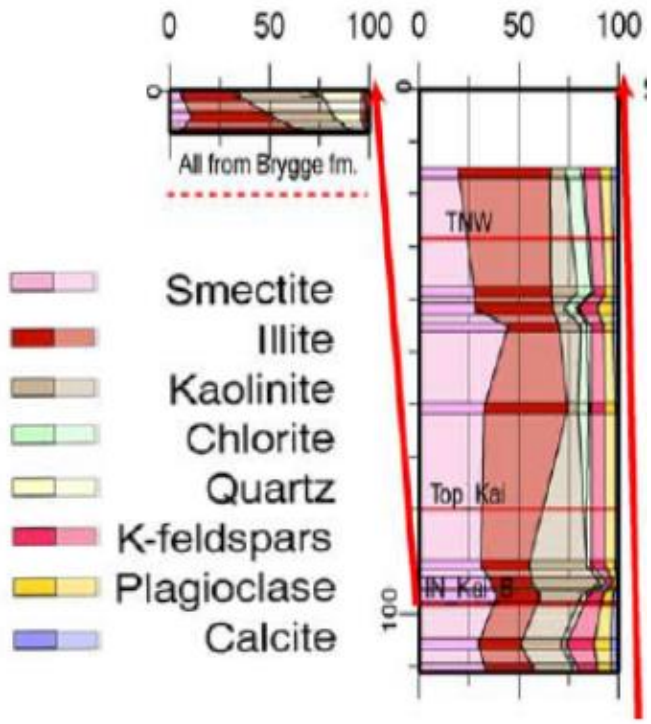

Figure 2.6 Example of fine fraction XRD results. Shows the XRD results for the fine fraction analysis of the samples from the Kai Formation and the Brygge Formation, modified from Forsberg and Locat (2005)

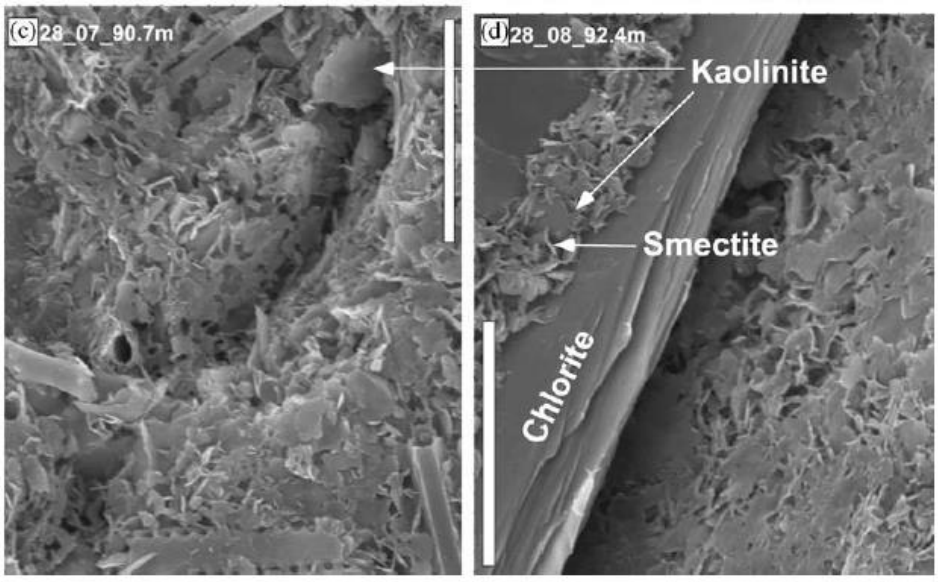

Figure 2.7 Example of SEM micrograph. Showing the clay content in a SEM micrograph from the Kai Formation. The different clay minerals present a clearly pointed out (Forsberg and Locat, 2005).

Peltonen et al. (2008) did an extensive study of the mudstones in the Norwegian Sea, with focus on the Møre and Vøring basins. To study the mineralogical changes vertically and regionally, 300 cuttings samples from five wells were analyzed by bulk (Figure 2.8) and fine (< 2μm) fraction (Figure 2.9) XRD. In addition SEM was used to determine feldspar composition. The results show significant changes in the mineralogy as a function of depth. To correlate the data, petrophysical logs were used to look at the effect of the mineralogy on the wireline logs. The mudstone on the logs appear homogenous, the mineralogical and geochemical data on the other hand, indicate great variations. The resulting XRD analysis confirms the domination of mudstones in the basins, with the exception of siliceous ooze in parts of the Brygge Formation. The mudstone consists of varying amounts of smectite, mixed layer clay, illite, kaolinite and chlorite. The non-clay fraction is composed of quartz and feldspar and minor siliceous ooze, pyrite and zeolite.

There is a clear trend in the smectite distribution, both regionally and vertically. The regional smectite distribution is associated with the volcanic ash from the opening of the Atlantic and the vertical is explained by the diagenetic smectite to illite reaction. The provenance of the smectite shows a clear link to the opening of the Atlantic due to the high content and large intervals in the south. The provenance studies of the feldspar indicate a different provenance area in the Cretaceous and the Tertiary.

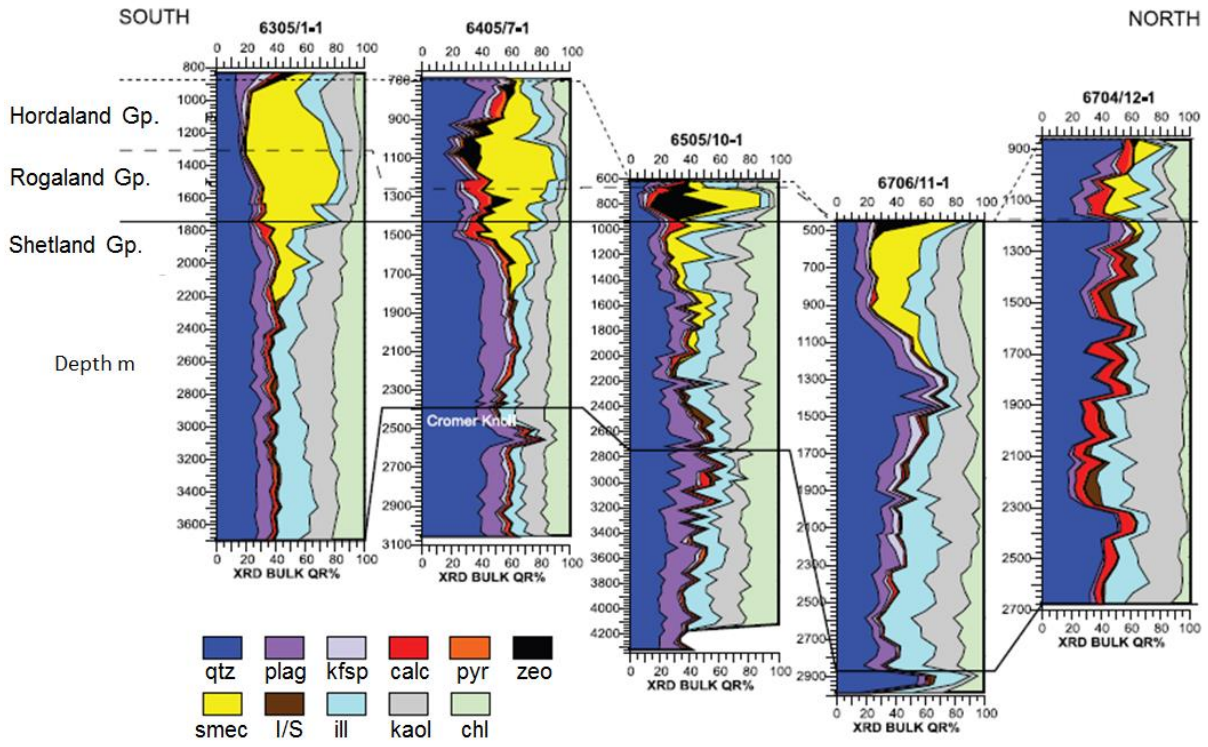

Figure 2.8 Results of the bulk XRD analysis from Peltonen et al. (2008) study of the Norwegian Sea.

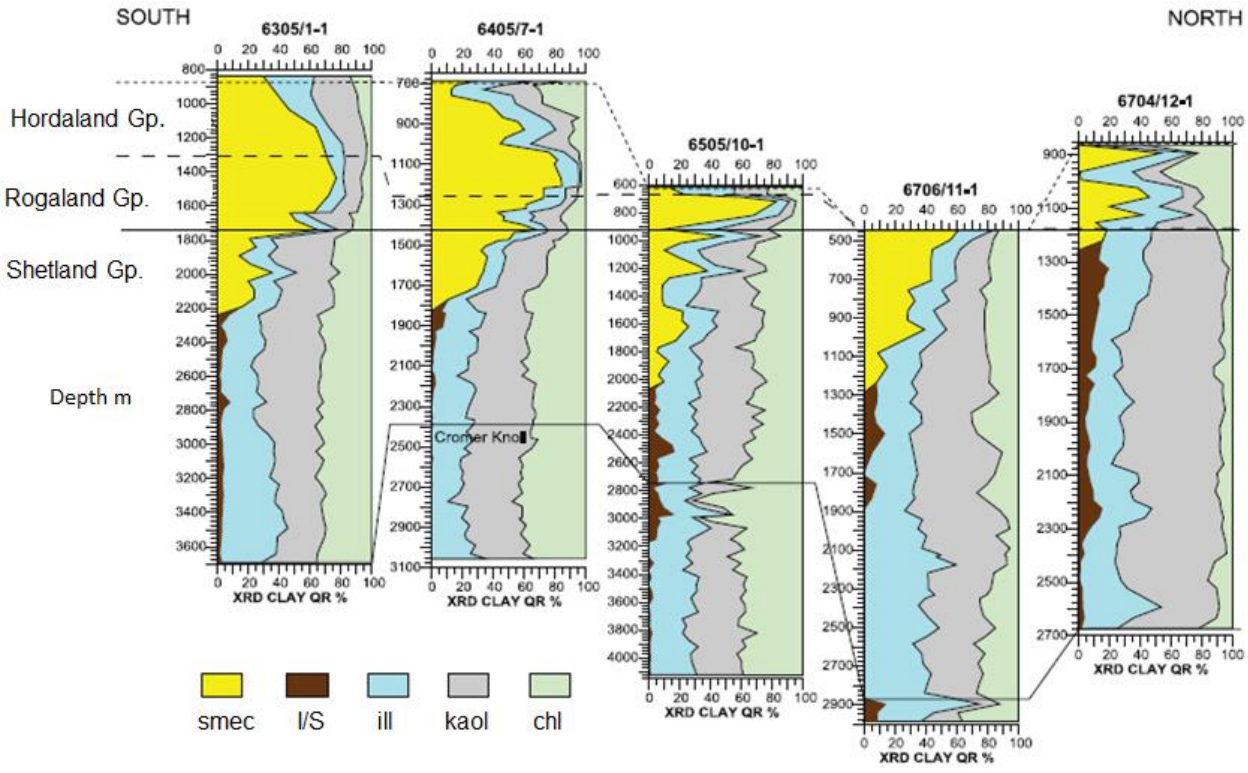

Figure 2.9 Results of the fine fraction XRD analysis modified from Peltonen et al. (2008) study of the Norwegian Sea.

Marcussen et al. (2009) have a similar study to Peltonen et al. (2008), with a different area of study, the North Sea. It is a study of the Cenozoic mudstones and how the properties changes vertically and laterally as a function of mineralogy. An attempt is made to investigate the effect of clay mineralogy on the compaction trends by integrating well logs and mineralogical data. Wireline logs from 42 wells were acquired, and in addition, mineralogical information from 6 wells was collected from the North Sea. Fine fraction XRD analysis (< 2μm) was done on 79 cuttings samples looking for smectite, illite, kaolinite and chlorite (Figure 2.10). Wireline logs and XRD information was collected from 6 wells in the Vøring Basin to have a basis for comparison with the fields in the Norwegian Sea.

The analysis of the wireline logs is based on the velocity, density and acoustic impedance trends. The results show a clear connection with the primary mineralogy and its effect on the compaction trends. An illustration is shown in Figure 2.11 of how the average velocity trends change through the groups investigated. To explain the trends Marcussen et al. (2009) look at the effect of temperature, provenance and overpressure. The temperature is linked to the geothermal gradient in the area and how it affects the stability of smectite. More information on the diagenesis of smectite can be found in chapter 3.4.3. The provenance is important for the primary mineralogy composition and Figure 3.4 shows the main sediment outbuilding directions in the area. Overpressure is common in smectite, with the expulsion of water, and can be seen as recognizable trends on the logs. The comparison with the Vøring Basin shows the same trends as in the North Sea, although a lower content of smectite is recorded. However the study indicates that only small amounts of smectite are necessary to dominate the log response. The conclusion is that the smectite content is the most important controlling factor for the velocity, bulk density and the compaction curves.

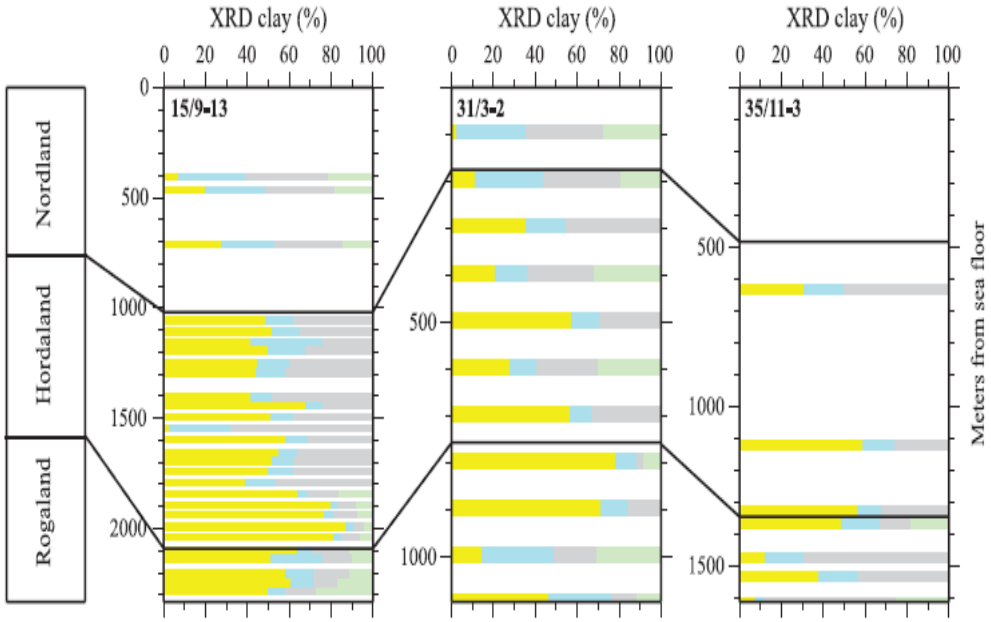

Figure 2.10 The XRD results from Marcussen et al. (2009). From left to right it might show the percentage of smectite (yellow), illite (blue), kaolinite (grey) and chlorite (green).

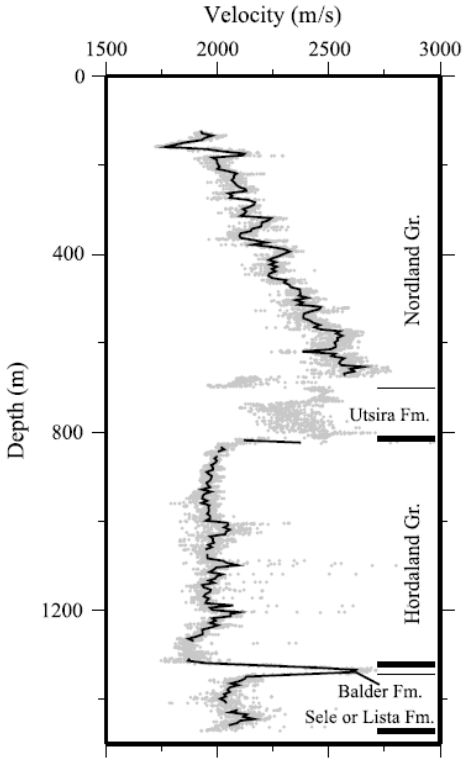

Figure 2.11 Velocity-depth curve. An illustration of the velocity trends through Nordland and Hordaland Group. The grey points are the original velocities and the black line is the average velocity for the well (Marcussen et al., 2009).

3 Theory

3.1 Geological history of the Cenozoic era

During the Cenozoic Era, continental drifting continued shaping and placing the continents into the configuration known today. The collision of India with Asia, and Africa with Europe, created one long mountain chain from the Pyrenees and the Alps in the west, to the Himalayans in the east (Martinsen and Nøttvedt, 2007). The orogeny created the great mountain chains, changing the ocean currents, the wind systems and ultimately the climate. Norway continued its drift from the southern hemisphere to its current place on the northern hemisphere, (Figure 3.1). Greenland and Norway started drifting apart around 55 Ma and the sea floor spreading created a deepening ocean between the two continents. The large scale volcanism at the new mid-ocean ridge controlled the tectonic and structural setting in the area. During the Cenozoic Era, the climate changed from warm and tropical in Cretaceous to a cooler and drier climate, ultimately leading to the glaciations at the transition to Quaternary (Martinsen and Nøttvedt, 2007). The geological events and resulting lithostratigraphy are summarized in Figure 3.2.

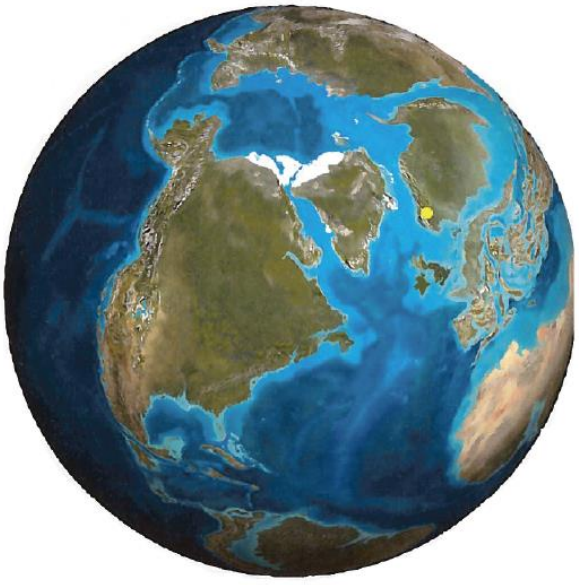

Figure 3.1 Plate configuration. Presentation of the plate configuration in the Cenozoic Era with the yellow dot showing the location of Norway (Martinsen and Nøttvedt, 2007) Illustration by R. Blakey.

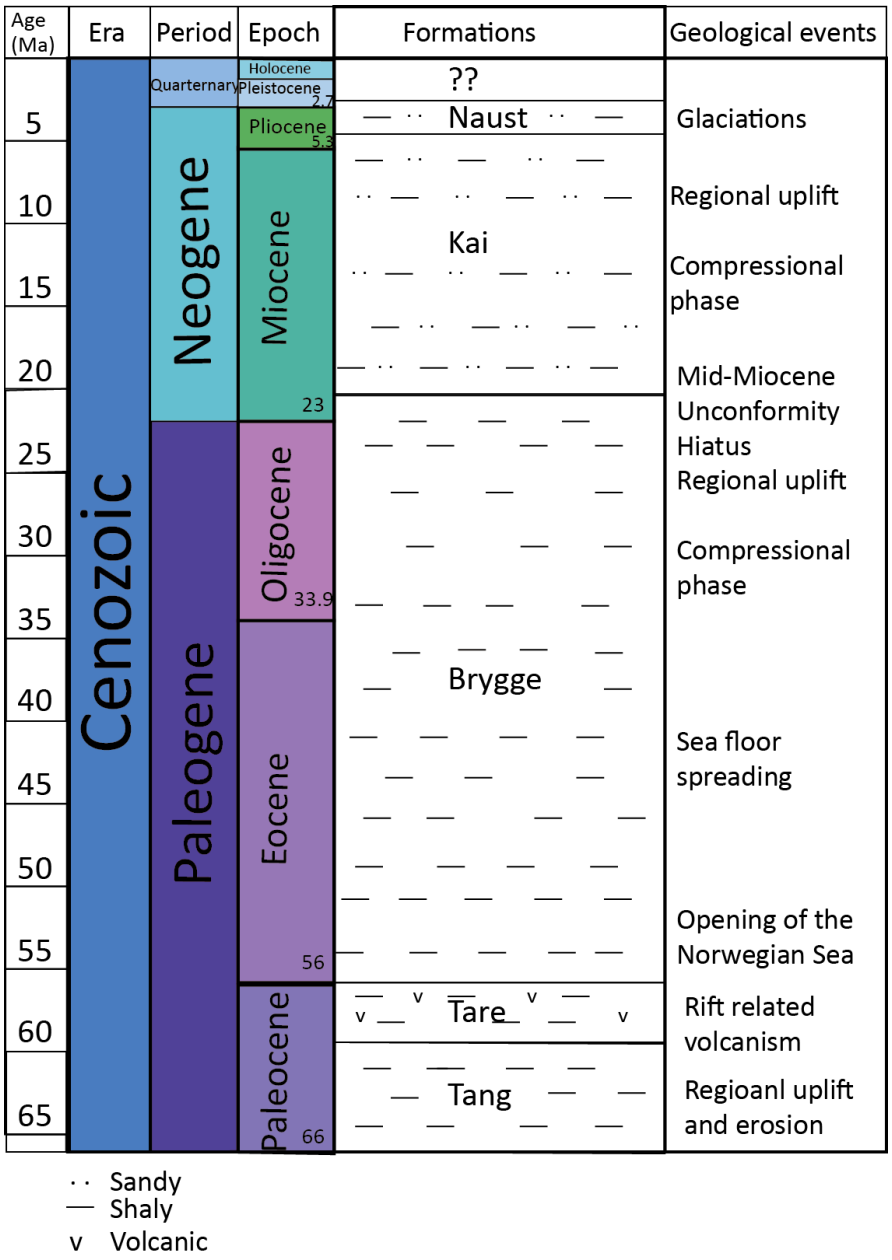

Figure 3.2 Lithostratigraphy and geological events. The figure shows a compilation of geological time scale, lithostratigraphy and geological events, modified from Dalland et al. (1988), Martinsen and Nøttvedt (2007) and Walker et al. (2012).

3.1.1 Paleocene (66 Ma – 56 Ma)

In Paleocene, the Norwegian coastline was fairly similar to the present day coastline, possibly slightly more eastward (Martinsen and Nøttvedt, 2007). The area experienced a regional uplift and subaerial exposure of the mainland area, resulting in increased sediment transport (Eidvin et al., 2007). The erosion of the Norwegian mainland transported large amounts of sediment out into the basin, through the old fault complexes along the coast. The fault complexes can be seen clearly on maps today as the fjords and valleys along the coast. These are part of the

old zones of weakness created by the Caledonian orogeny (Martinsen and Nøttvedt, 2007). The sediments consisted of a combination of sand, silt and clay, the latter being the dominant. Most of the sediments came from the eastern coast, but some of the sediments in the western part of the Møre-and Vøring basin might have been transported from the East Greenland before the sea floor spreading commenced. The clay-dominated formation deposited in early Paleocene is known as the Tang Formation. Towards the beginning of the sea floor spreading, the area experienced an increase in volcanism caused by the commencing of the rifting. The youngest formation in Paleocene, known as the Tare Formation, has a high content of volcanic constituents mixed in with the clay-dominated lithology. On the Trøndelag Platform the shallowest areas consist of thin sand and clay formations. In this area and that time period, the rivers on the mainland turned south and the sediment influx into the basin decreased (Martinsen and Nøttvedt, 2007)

3.1.2 Eocene (56 Ma – 33.9 Ma)

Eocene was a time of sea floor spreading between Norway and Greenland and as the two continents drifted further apart the newly formed sea floor cooled down and subsided. After the regional uplift in Paleocene, the area experienced subsidence, followed by the NW European Ypresian transgression of the Norwegian shelf and the mainland (Eidvin et al., 2007 , Chand et al., 2011 , Rasmussen et al., 2008). The sediment influx from mainland Norway decreased and only a thin clay dominated formation was deposited in the basin, known as the Brygge Formation (Martinsen and Nøttvedt, 2007). Eocene was also a period of global warming, possibly caused by the release of carbon and methane, connected to the volcanism of the continental breakup (Storey et al., 2007), in combination with the disappearance of the epicontinental sea between Norway and Greenland (Rasmussen et al., 2008 , Higgins and Schrag, 2006).

3.1.3 Oligocene (33.9 Ma – 23 Ma)

Oligocene was a period of tectonic activity, which resulted in compression and a regional uplift (Eidvin et al., 2007). The sea floor spreading continued and the ocean between the continents expanded. The thermal cooling caused the basin to subside further and the water depth continued to increase. With the greater water depths, less sediment was transported into the basin, and instead the cold nutrient rich water was the right environment for microorganisms to produce calcareous or siliceous clay known as ooze-deposits (Martinsen and Nøttvedt, 2007). These are formed when microorganism dominate a shallow sea, and when they die, they sink and form the ooze deposits. At the shelf area today, the Brygge

Formation consists mostly of clay, while deeper into Møre and Vøring Basins ooze-deposits are more common. The transition from Eocene to Oligocene also represents the shift from predominantly warm climate, to a colder and less tropical climate. The changes in the $\delta^{18}O$ isotope trend indicate a drop in sea level temperature from ~ 12 to ~ 4.5˚C (Rasmussen et al., 2008 , Zachos et al., 2001).

3.1.4 Miocene (23 Ma – 5.3 Ma)

The interval between Lower-Middle Eocene and Middle Miocene is defined by a marked hiatus. The hiatus is known as the Mid-Miocene Unconformity, which is defined as a period with no deposition, and not as a period of erosion (Eidvin et al., 2007). In Antarctica, the polar ice caps were rebuilt, causing a major sea level fall. Middle to Late Miocene was the second compressional phase recorded after the initiation of the sea floor spreading. Long wavelength buckling of the lithosphere caused uplift and doming of the lower Tertiary layers. The uplift of the land area caused a major regression, moving the coastline 50-150km westward of what it is today. Deltas were built out into the basins, transporting sediments from the Fennoscandinavian mainland (Løseth and Henriksen, 2005 , Rasmussen et al., 2008). The syn – tectonic Kai Formation was deposited in depressions and synclines related to the compressional structures, such as inversion domes and reactivated reverse faults. One example of a compressional dome is the Helland-Hansen Arch. Due to the regression; the Kai Formation is the most basinward of the Cenozoic formations. The Kai Formation and the proximal equivalent Molo Formation can be found above the unconformity. On the outer and middle margin, the Kai Formation was deposited as clay dominated formation. On the inner margin, coastal plains and deltas were built out from the Fennoscandinavian mainland, depositing large amounts of eroded sediments (Løseth and Henriksen, 2005 , Rasmussen et al., 2008). The Molo Formation was deposited as a sand dominated formation on the inner margin (Eidvin et al., 2007). On the shelf and slope of the Møre and Vøring Basins, the Kai Formation has high clay content with ooze sediments in the basinal parts.

3.1.5 Pliocene (5.3 Ma – 2.7 Ma)

After the deposition of the Kai and Molo Formations the area experienced cooling climate and onset of the glaciations. The first glaciations advanced in Late Pliocene, around 2.8Ma. Before 1.5Ma the glaciers did not extend beyond the mainland. Between 1.5Ma and 0.5Ma the glaciers advanced onto the shelf and after 0.5Ma the glaciers covered the shelf in three glacial periods until the glaciers retreated in Holocene (Eidvin et al., 2007). The Naust Formation was deposited in this glaciomarine environment during the last 2.8Ma years

(Chand et al., 2011). The Naust Formation is the youngest formation and is the shallowest, defined from 1342 mTVD to the sea bottom (Dalland et al., 1988).

3.2 Structural setting

The margin offshore mid-Norway can be divided into three parts as shown in Figure 3.3; the Møre Margin, the Vøring Margin and the Lofoten-Vesterålen Margin. The three margins have gone through the same structural evolution, giving them similar characteristics. On a large scale, the Mid-Norwegian margin has experienced an extended period of post-Caledonian extension (Faleide et al., 2008 , Stuevold and Eldholm, 1996). Prior to the continental breakup, the margin area was a part of an epicontinental sea between Greenland and the Fennoscandinavian landmasses. The evolution of the margin can be summarized as the following steps. (1) A period of extension and rifting on the Cretaceous-Paleocene transition, followed by (2) sea floor spreading and separation of the continents in Paleocene, and finally (3) subsidence and cooling of the newly formed margin (Eldholm et al., 2002 , Faleide et al., 2008).

The Cenozoic Era, was in general a period of regional uplift and even though the exact timing and mechanisms are highly debated, the cause is generally associated with the opening of the Norwegian Sea (Stuevold and Eldholm, 1996). On the Norwegian Continental Shelf, the Cenozoic stratigraphy is almost complete, making it possible to follow the uplift history. There is evidence of two separate uplift events during the Cenozoic Era. The first one is associated with the continental breakup. The second is characterized as a two-stage uplift during the middle of the era. According to Stuevold and Eldholm (1996), the two uplift events have two different mechanisms. The first represents a plate-boundary syn-rift uplift. The second is intraplate flexural deformation linked to heating from the Icelandic plume. The heat from the plume is assumed to be of a pulsing nature, and at the time of the second uplift, the heat from the plume increased.

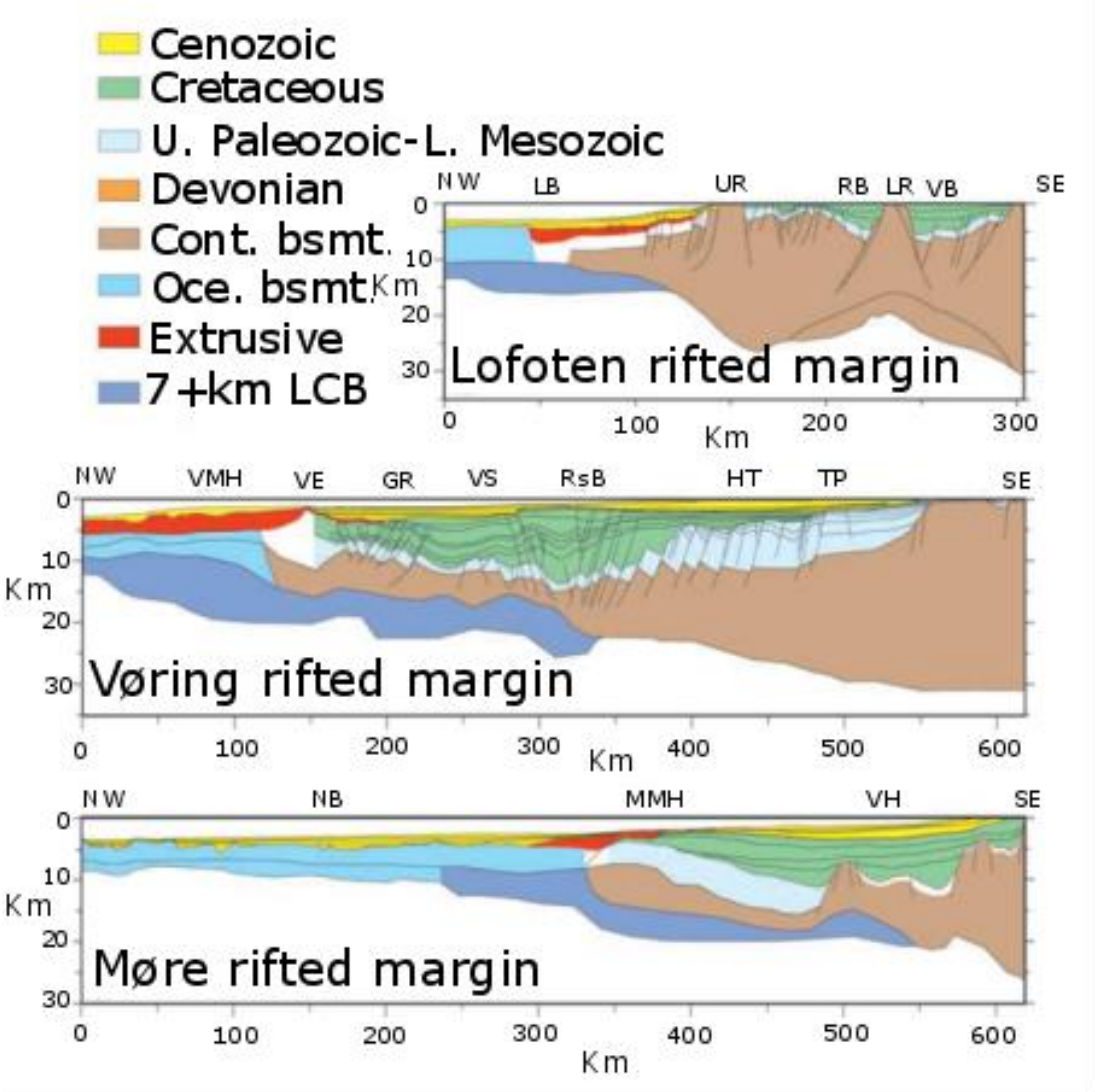

Figure 3.3 Cross sections of the Mid Norwegian Margin. Showing the Møre rifted margin, the Vøring rifted margin and the Lofoten rifted Margin U = Upper, L = Lower, Cont. = continental, Oce. = oceanic, bsmt = basement, LCB = lower crustal body, NB= Norway Basin, MMH= Møre Marginal High, VH= Vigra High, VMH = Vøring Marginal High, VE= Vøring Escarpment, GR= Gjallar Ridge, VS= Vigird Syncline, RsB= Rås Basin, HT= Halten Terrace, TP = Trømdelag Platform, LB= Lofoten Basin, UR= Utrøst Ridge, RB= Ribbain Basin, VB= Vestfjord Basin, modified from Faleide et al. (2008)

3.3 Provenance and sedimentation history

Earliest Paleocene was the beginning of the large clay deposits, which characterize the Cenozoic Era. The source area for the clay was most likely the erosion of the Shetland Platform. The volcanic platform emerging from the British Isles, past Greenland to the Baffin Isles, was the source for the ash and tuff layers occurring in the Paleocene and Eocene Brygge deposits. After the transition to Oligocene, the major source of sediment was the Fennoscandinavian landmass as shown in Figure 3.4. The erosion of Norway and the partly emerged Nordland Ridge transported sediments out into the basin. During Miocene the formation of the compressional domes controlled the sedimentation flow and the distal areas

were filled with mud and siliceous ooze (Marcussen et al., 2009 , Peltonen et al., 2008 , Rasmussen et al., 2008 , Stuevold and Eldholm, 1996) .

In their studies, Marcussen et al. (2009) and Peltonen et al. (2008) looked at the distribution of smectite in the North Sea and the Norwegian Sea. The source of the smectite is the ash and tuff layers deposited after the opening of the Atlantic. They notice a decreasing trend in the lateral distribution of smectite from south to north. The thickness of the smectite-rich layers and the abundance of smectite are highest in the south, closest to the volcanic source. Peltonen et al. (2008) however comments on the likelihood that the source of the terrestrial sediments is not the same as the smectite, but rather from the Fennoscandinavian landmass in the east.

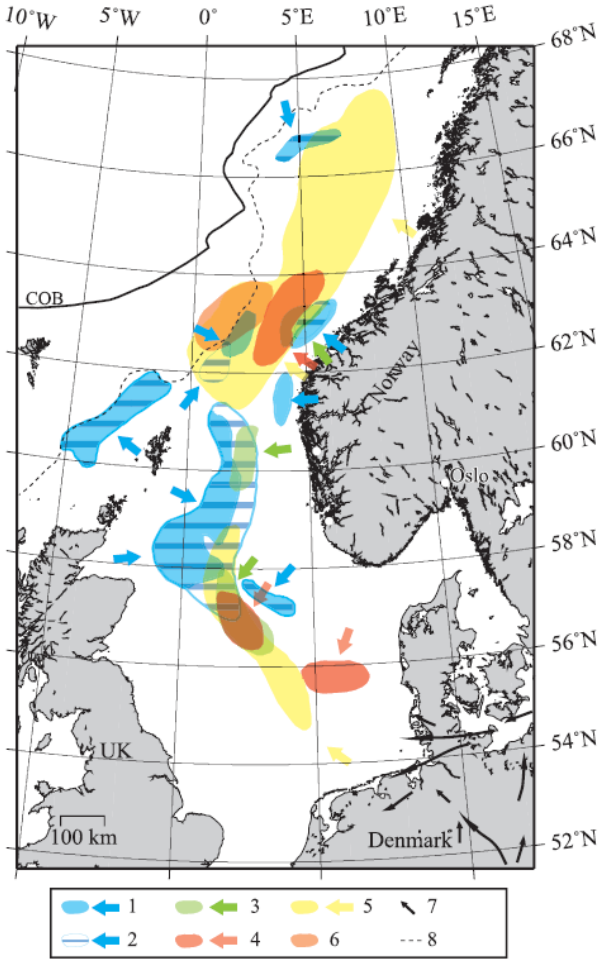

Figure 3.4 Sedimentary outbuilding directions. Main outbuilding directions and depocenters through time taken from references in Faleide et al. 2002 (1=Paleocene; 2=Eocene; 3=Oligocene; 4=Miocene; 5=Pliocene; 6=Pleistocene; 7=major river systems; 8=limits of inner flow) COB= continent – ocean boundary. (Marcussen et al., 2009)

3.4 Clay minerals and clay mineral properties

When using a shale formation as a hydraulic barrier, the shales have to have the necessary properties as described in chapter 1.3. The clay minerals in the shale determine the various properties and the behavior of the formation. The formations of interest to this thesis are defined as mainly claystone, interlayered with stringers of sandstone, limestone or siltstone. Even though they consist of various materials, claystone is the main component. A good understanding of the fundamental properties for shales and clay minerals is therefore necessary.

3.4.1 Definitions

Boggs (2009) uses a general definition of shales defining both shales and mudrocks as fine grained siliciclastic sedimentary rocks consisting mostly of particles smaller than 62 microns. Through time, shale has been used as a confusing term to describe both the broad group consisting of all fine grained siliciclastic rocks and also for the narrower group consisting of laminated clayey rocks. Boggs (2009), as a few others have done, attempts to introduce the term mudrocks for the broader group and restricting the use of shale to only the laminated clayey rocks. However, there is a general acceptance that shale and mudrocks mainly consist of hydrous aluminum silicates, classifying as phyllosilicates (layer structures) (Eslinger and Pevear, 1988 , Moore and Reynolds, 1989).

3.4.2 Formation and deposition

Clay minerals are abundant worldwide in the whole sedimentary sequence, constituting around 50% of all sedimentary rocks. They are also abundant in soils and hydrothermal alteration zones, they are however absent in igneous and most metamorphic rocks formed above 500˚C (Eslinger and Pevear, 1988). Deposition of clay occurs in most oceanic and continental settings e.g. from suspension in lakes and rivers, on deltas and tidal flats, below surface wave activity on the shelf and in deep marine environments (Boggs, 2009).

There are several different processes which form clay minerals, and they are often hard to distinguish. The processes have been summarized in Figure 3.5. The first process produces detrital (allogenic) clays, and is the mechanical and chemical breakdown of various pre-existing minerals, such as quartz, feldspar or clay minerals. There are two different types of chemical mechanisms; (1) neoformation, which is precipitation of clay from a solution, and (2) transformation, which is when the clay mineral inherits the silicate skeleton from another mineral. These two mechanisms are particularly hard to distinguish, but they can be

summarized as the following; chemical weathering, formation of authigenic minerals, formation of diagenetic minerals and hydrothermal alteration of clay minerals (Eslinger and Pevear, 1988).

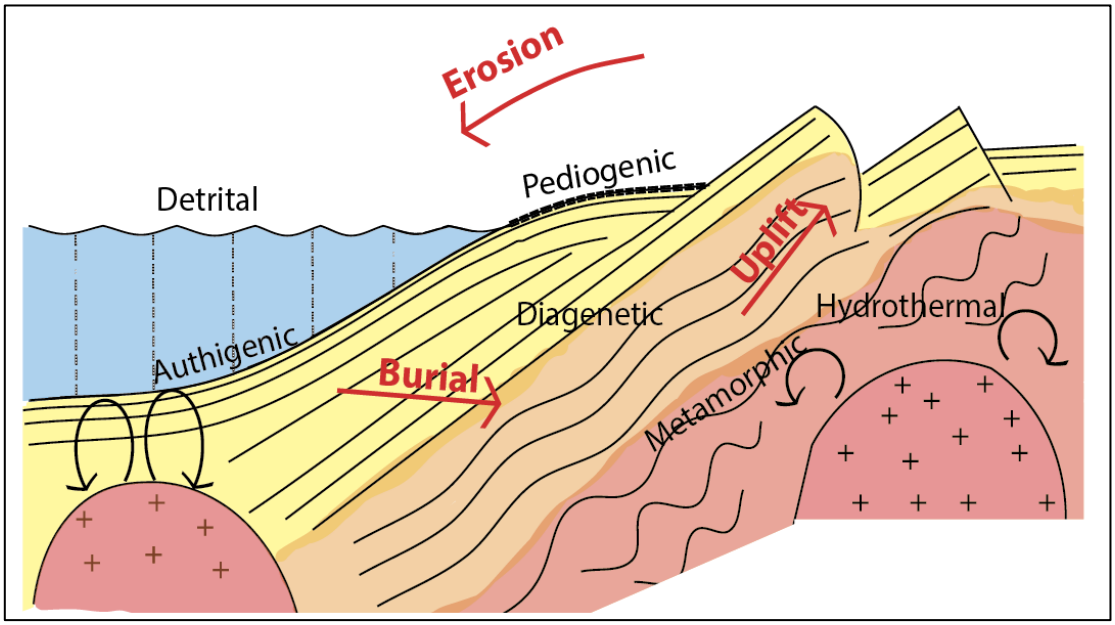

Figure 3.5 The clay cycle. The figure represent the clay cycle showing the location of the different processes modified from Eslinger and Pevear (1988).

3.4.3 Clay diagenesis

The definition of diagenesis according to Eslinger and Pevear (1988) (p. 5-1) is: "…all physical and chemical changes in sediments that take place after deposition and before metamorphism, excluding weathering at the earth's surface". For shale the main physical change is compaction, releasing water, and a main chemical change is the progressive reaction from smectite to illite. This reaction releases great amounts of water, silica and other ions, such as Mg and Fe. A common way to illustrate the diagenetic changes in clay formations is to use depth curves, for the physical changes; compaction vs depth (Figure 3.6) and for the chemical changes; mineralogy vs depth (Figure 3.7).

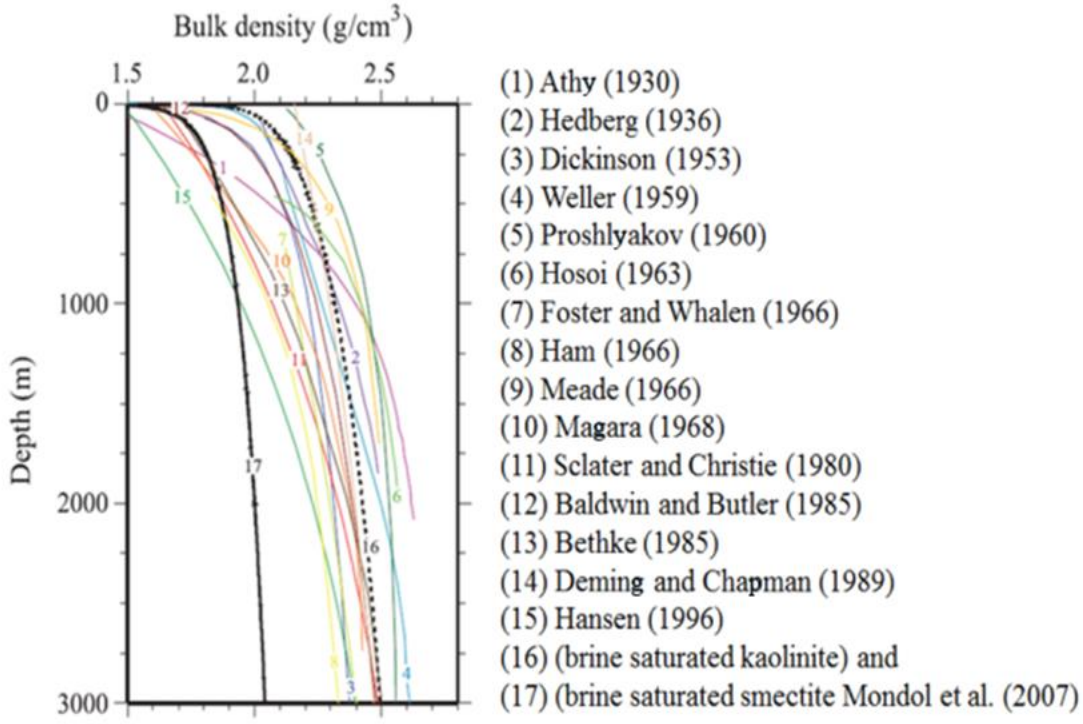

Figure 3.6 Compaction-depth curve. Compilation of published compaction curves, modified from Marcussen et al. (2009).

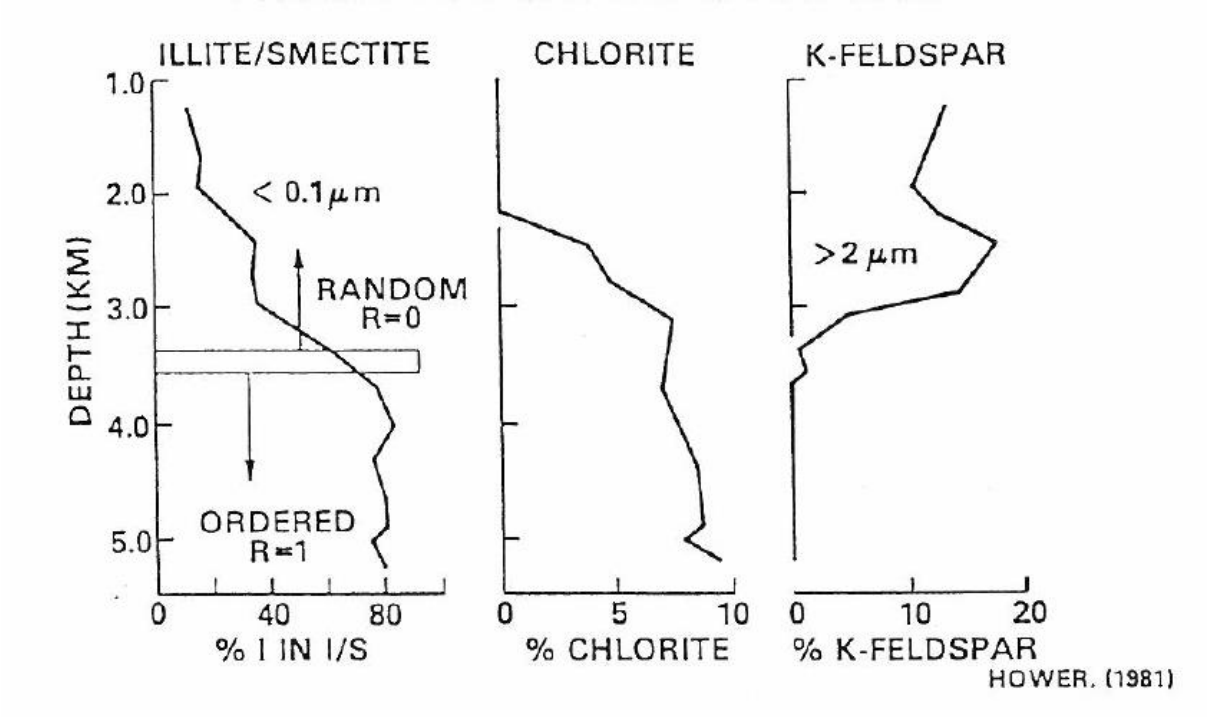

Figure 3.7 Mineralogy-depth curve. Examples of mineralogical changes with depth as a result of shale diagenesis (Eslinger and Pevear, 1988).

Mudstone compaction is dependent on the initial mineralogical composition, stress and temperature regime and burial history. The various compaction processes will affect the properties of shale and they determine how the shale behaves and how the petrophysical logs will respond. Usually the compaction-depth curves are based on simple exponential or linear curves, with the initial porosity separating the lithologies. In reality, the clay mineralogy has a major effect on the compaction curves for mudstone. In the study done by Marcussen et al. (2009), an attempt is made to correlate the mineralogical changes with the changes seen in the density and velocity curves as a function of depth (Figure 2.11). Their conclusion is that the smectite content is the most controlling factor, which explains the variations in the compaction of the Cenozoic North Sea mudstones.

The mineralogy vs depth curves show a distinct shift in the clay minerals with depth. In the youngest rocks there is a high abundance of smectite, mixed layer clay and kaolinite, while in the older rocks there is a higher abundance of illite and chlorite. This shift indicates that the smectite and kaolinite in the older rock have been diagenetically altered to illite and chlorite. The smectite-to-illite reaction occurs as a progressive change through mixed-layer illite/smectite (I/S) combinations.

The controlling factors for the reaction appear to be temperature, time and the fluid-rock chemistry. The temperature factor is important in the study done by Peltonen et al. (2008) of mineralogical control on mudstone compaction. At temperatures around 60-80˚C smectite dissolves and re-precipitates as illite and quartz according to the following reaction:

$$smectite + K^{+} \rightarrow illite + SiO_2 + H_2O$$

The transition has occurred at different temperatures in different areas, local variations in heating events, burial history and geothermal gradients are indicated. The area investigated in this thesis has a complex tectonic history with several heating, uplift and compressional phases. It is important to note that the regional and stratigraphic changes in mineralogy can also be explained by changes in provenance, sedimentation rate and especially important for this area, changes in volcanic activity. The mineralogical changes in the claystone are most likely a combination of diagenetic alteration and changes in the original mineral composition (Peltonen et al., 2008).

3.4.4 Characterization

Characterization of shale was for a long time very difficult only using petrographic microscopes due to the clay's fine-grained nature. With the development of x-ray methods and scanning electron microscopes the study of shales and mudrocks became easier (Boggs, 2009). The physical and chemical properties of clay minerals show great variation due to the differences in formation processes and mineral content. However, most clay minerals have similar properties when it comes to platy morphology and the perfect cleavage along (001) (Moore and Reynolds, 1989).

3.4.4.1 Clay mineral structure

Clay minerals are phyllosilicates or sheet silicates and they consist mostly of silica, aluminum, magnesium, iron and water (Bjørlykke, 2010). The main building block is the silica tetrahedron; SiO_4^{-4}, which links together to form the silicate sheets. There are two different sheets; the tetrahedral sheet and the octahedral sheet. The tetrahedral sheet (T) is built up of tetrahedron consisting of four oxygen atoms surrounding a smaller cation (Si^{4+}, Al^{3+} or Fe^{3+}) (Figure 3.8). The tetrahedral sheet has a negative charge, seen by the formula $Si_4O_{10}^{-4}$, and can therefore only exist in combination with cations and additional oxygen atoms in mineral structures. The octahedral sheet (O) is built up of cations surrounded by six oxygen or hydroxyl atoms, arranged as two closest-packed planes creating octahedral sites between the planes (Figure 3.9). The octahedral sites accommodates larger cations than the tetrahedral sheet and some of the common cations are; Al^{3+}, Mg^{2+}, Fe^{2+} or Fe^{3+} (Eslinger and Pevear, 1988 , Moore and Reynolds, 1989). When the cation is trivalent (Al^{3+}) only two out of three positions will be occupied in the octahedral sheet. The mineral is then called dioctahedral. If the cation is bivalent (Mg^{2+}), all three positions will be occupied and the mineral is called trioctahedral (Bjørlykke, 2010).

In nature, the phyllosilicates are a combination of the tetrahedral sheet and an octahedral sheet. There are two combinations of the sheets creating phyllosilicate structures; the 1:1 layer and the 2:1 layer (Moore and Reynolds, 1989) (see Figure 3.10). The 1:1 layer is the simplest one, and is a combination of one tetrahedral (T) sheet and one octahedral (O) sheet (T-O). The 2:1 layer is a combination of two tetrahedral sheets and one octahedral sheet (T-O-T). Both sheets can be either dioctahedral or trioctahedral (Eslinger and Pevear, 1988).

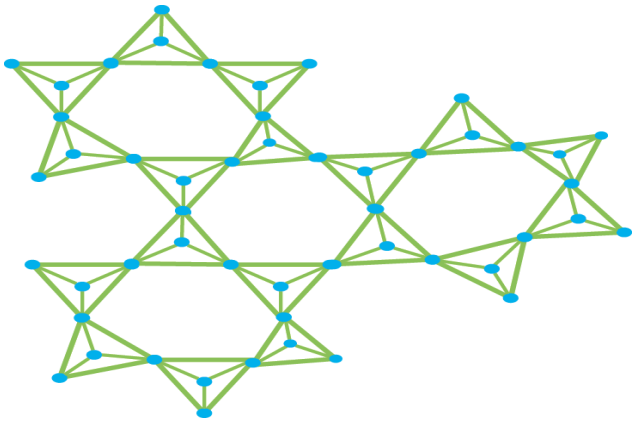

Figure 3.8 Tetrahedral sheet. Example of a tetrahedral sheet, showing the corner-linked tetrahedral and the hexagonal shape of the six-membered rings, modified Moore and Reynolds (1989).

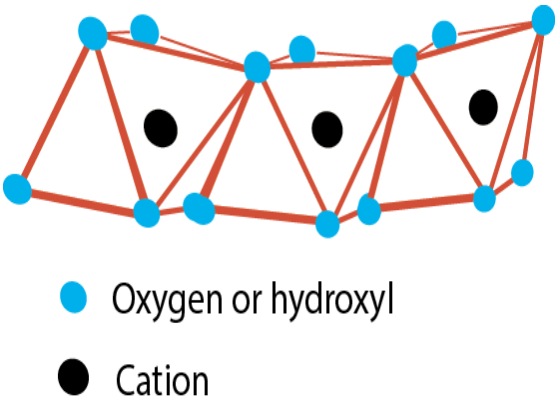

Figure 3.9 Octahedral sheet. Example of a octahedral sheet showing the edge-linked tetrahedra with the shared oxygen atoms or hydroxyls and the cation in the octahedral site, modified Eslinger and Pevear (1988)

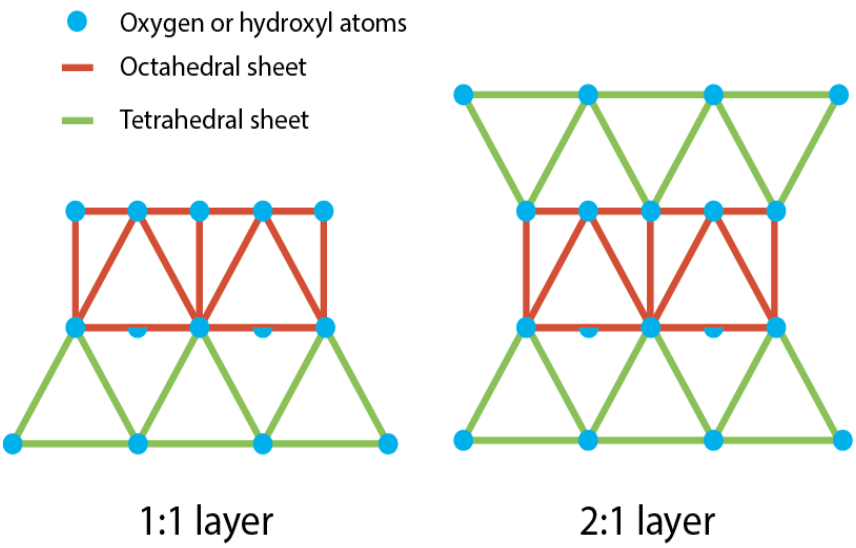

Figure 3.10 Clay layer structure (1:1 and 2:1). The figure shows an example of 1:1 layer (T-O) and 2:1 layer (T-O-T) structures for clay minerals, modified Moore and Reynolds (1989)

3.4.4.2 Physical features

Boggs (2009) describes both the large and small scale physical features for shales and the clay minerals. The large scale features are possible to identify either with petrographic microscope or with the naked eye. For the small scale features it is necessary to use scanning electron microscope or x-radiography methods. With these techniques it is possible to get a good view of the particle shapes and grain size of the clay minerals. Clay texture is dependent on the size of the clay particles, as it is defined as the relative proportions of clay, silt and sand. This

relationship varies greatly depending on sediments influx and transport. Since the clay minerals are very little altered by erosion and transport, their shape will to a high degree reflect the original shape of the particle. The clay fabric is the spatial relationship between the particles in the shale and is dependent on the shape of the clay minerals. With this in mind, it would be possible to use fabric, to some degree, as an environmental indicator. According to Wilson and Wilson (2014) the relationship can be described as either random or oriented and will affect the distribution of pores and voids. On a larger scale, a shale sedimentary structure is an important physical feature. There is a large number of possible features in shales; color banding, bioturbation, cementation, parallel stratification, massive bedding, trace fossils etc.

Wilson and Wilson (2014) argue in their article that all of these physical features affect the stability of shale. They point out that shales which usually are considered as homogenous and uniform, but should be seen as heterogeneous with great variations in their physical characteristics. They attempt to determine the effect of various properties on the shale instability.

3.4.4.3 Composition

Composition can be divided into two groups; mineralogical and chemical (Boggs, 2009). Mineralogical composition is a description of the common constituents of the rock. It varies depending on the depositional and diagenetic processes and mechanisms. The most common minerals in mudstone and shale are clay minerals, mica, quartz and feldspar. In addition there are various amounts of trace minerals; calcite, dolomite, iron oxides and siderite.

The chemical composition is defined as the relative abundance of the major chemical elements (presented as oxides) in clay minerals. Silica (SiO_2) is the most abundant with aluminium (Al_2O_3) coming second. Potassium oxide (K_2O) and magnesium oxide (MgO) are also important. This information helps in the classification of shale, by determining if it is, for example, high alumina shale or potassic shale.

3.4.4.4 Properties

Clay minerals are highly reactive due to their large surface area and their charged nature (Eslinger and Pevear, 1988). The charged nature determines the behavior of the shale when it comes to cation exchange capacity, hydration and swelling. The charge can be divided into structural charge, which is permanent and surface charge, which is pH-dependent. The structural charge occurs in the layer sheets and is due to ion substitution or structural imperfections and creates a negative charge. The surface charge is due to chemical reactions

occurring at the surface, such as hydrolysis breaking bonds between Si and O or Al and OH. The net charge at the surface can be either positive or negative depending on the pH. Low pH allows anion exchange and high pH allows cation exchange. The zero point of charge is the pH when the total net charge is 0. This determines at which pH cation or anion exchange occurs. The surface charge is also the basis for the theory of diffuse double layers. When clay is placed in, or exposed to, a solution, two electrically charged layers will be established to maintain equilibrium. A negatively charged layer at the surface and a positively charged diffuse layer make up the double layer. The thickness of this layer depends on surface charge and salinity of the solution (Eslinger and Pevear, 1988). In their study, Wilson and Wilson (2014) look at the importance of the diffuse double layer and the interaction between clay and water for shale instability. They propose an alternative explanation of swelling behaviour associated with the double layer. Swelling is when the "dry" clay adsorbs water and the water enters the interlayer spacing, hydrating the cations, increasing their radii and expands the interlayer space. When the hydrated cations reach their maximum expansion further swelling is called osmotic swelling and the distance might increase until complete dissociation occur. This depends on the layer charge and the interlayer cations. Swelling and hydration are often associated with shale instability.

3.4.5 Classification

Based on the characteristics above it is possible to classify the most important clay mineral groups.

- Illite consists of two tetrahedral layers and one octahedral layer bonded together to other packages by potassium as shown in Figure 3.11. Illite does not exhibit a swelling nature and it is relatively stable. According to Wilson and Wilson (2014) instability in illite might be associated with the diffuse double layer
- Smectite has the same structure as illite except the interlayer space is filled with water and exchangeable cations, shown in Figure 3.11. The water allows the smectite to swell from 14-17 Å, depending on the number of water layers. The volume expansion is commonly assumed as the reason for instability in smectite.
- Mixed layer (illite/smectite) clay has a composition intermediate between illite and smectite and will exhibit properties and stability problems similar to both minerals.
- Kaolinite is built up of only one tetrahedral and one octahedral layer, shown in Figure 3.11. The structure allows very little ionic substitution making kaolinite relatively stable at low temperatures. However, Wilson and Wilson (2014) found in

their studies that kaolinite sometimes exhibit stability problems, possibly linked to the clay/water interaction. Almon and Davies (1981) suggest kaolinite is responsible for problems associated with migration of fine material in reservoirs.

- Chlorite consists of two tetrahedral layers and two octahedral layers as seen in Figure 3.11. The stability problem caused by chlorite is linked to secondary precipitation of iron compounds (Almon and Davies, 1981).
- Vermiculite has similar structure to smectite and also has the same hydrated interlayer cations. Expansion of the hydrated layers result in swelling (Eslinger and Pevear, 1988).

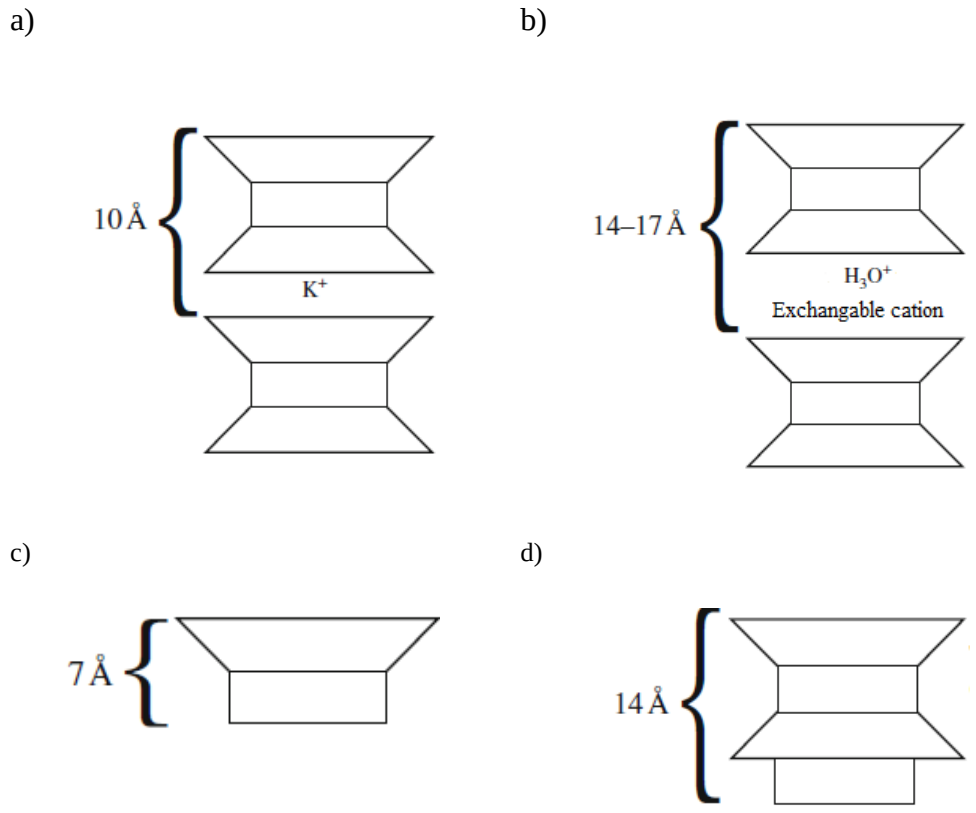

Figure 3.11 Clay minerals. Simplified illustration of common clay minerals; a) illite, b) smectite and vermiculite, c) kaolinite, d) chlorite, modified Bjørlykke (2010)

Important elements for the clay groups are summarized in Table 3.1.

Clay minerals	Important elements
Kaolinite	Al, Si, O, H
Smectite	Na, Mg, Ca, Al, Si, O, H
Illite	K, Al, Si, O, H
Chlorite	Mg, Fe, Al, Si, O, H

Table 3.1 Elements in clay minerals. List of the important elements in the various clay mineral groups (Almon and Davies, 1981)

The different clay minerals play different roles in shale instability. Almon and Davies (1981) summarize the different clay minerals role in formation damage, (Table 3.2).

Clay minerals	Potential effects
Kaolinite	Mobilization of fines
Smectite and vermiculite	Swelling
Illite	Microporosity
Chlorite	Iron precipitation
Mixed layer	Swelling

Table 3.2 Clay minerals in formation damage. List of the potential effects of different clay minerals in formation damage (Almon and Davies, 1981)

There is no generally accepted theory of what causes formation collapse, but as mentioned previously in chapter 1.3, the most likely mechanism is creep. When looking into transferability of the datasets concerning formation as a barrier, it is of great importance to know which clay minerals occur in which parts of the formation, and if this has any effect on its ability to act as a hydraulic seal. Being able to distinguish between the different clay minerals is therefore of the outmost importance. However, it is not within the scope of this thesis to determine which clay minerals that have the right barrier properties.

3.4.6 Difficulties and errors

Peltonen et al. (2008) points out a number of difficulties when it comes to the study of shale on the Norwegian Shelf. Shale and mudstones are often considered as homogenous and uniform, and are seldom analyzed by coring or with respect to geochemistry and mineralogy. Without these analyses, there is very little information to use in petrophysical and seismic correlation. Studies (Forsberg and Locat, 2005 , Marcussen et al., 2009 , Peltonen et al., 2008

, Wilson and Wilson, 2014) have shown that clay mineralogy is an important controlling factor, when it comes to the properties of shale.

In addition there are several possible difficulties and errors that might occur when attempting to identify clay minerals using XRD (Moore and Reynolds, 1989). When identifying the clay minerals it is important to remember that there are some non-clay minerals in the clay-sized fraction of the rock and not only clay minerals. In addition, the sample will most likely contain minerals which are not in the clay-size fraction. Most of the time it is necessary to compare and correlate the XRD information with information from other analytical techniques.

3.5 Datasets

Part of this thesis is to make an assessment of which datasets to use when transferring data between wells, fields and offset areas. With this in mind, it is necessary to know which datasets are available, and which ones are actually of interest. In the assessment of formation collapse, there are a few different types of datasets that are relevant; (1) petrophysical logs, (2) lithological descriptions and (3) mineralogical analyses.

3.5.1 Petrophysical logs

When comparing and correlating formations across great distances, petrophysical logs give a detailed view of the wells in the different areas. They provide information about lithology, porosity, pore geometry and permeability, all of great importance when distinguishing formations, zones and rock characteristics (Asquith and Krygowski, 2004). Logging is done to different extent for each well drilled on the Norwegian Continental Shelf. The information is easily stored and accessed when old wells are reviewed in preparation for new wells. Therefore, it is imperative to understand how and why the measurements have been taken, to ensure correct use of the data when correlations are needed. There are many different logging tools available today, compared to what they started out with. They started out with the wireline logging tools, which had to be lowered down into the hole after drilling. In the mid-80s the technique of measuring while drilling (MWD), directional drilling and data transfer to the surface, and logging while drilling (LWD), formation evaluation, were developed (Asquith and Krygowski, 2004). The logging tools can be divided into three categories based on the source for the logs; electrical, nuclear and acoustic or sonic.

3.5.1.1 Gamma Ray Log

The gamma ray (GR) tool is found in the array of logging instruments on the string. It measures the natural radioactivity in the rock, by recording the number of gamma rays emitted by the formations. The radioactive constituents are commonly uranium, thorium and potassium. The log can be used to differ between sandstone and shale. As shale has a higher content of radioactive material, it produces a higher gamma ray response than in sand. It is commonly used for correlating zones and determining shale volumes (Asquith and Krygowski, 2004). There are several possible uncertainties in the gamma ray measurements, associated with environmental effects in the borehole (e.g. borehole diameter, heavy or potassic mud or the size and configurations of the tool).

3.5.1.2 Sonic Log

The sonic log is based on acoustic measurements and records the interval transit time (DT, t or Δt) used by a compressional sound wave going through a formation. The unit for DT is microseconds per foot (µsec/ft.) and is a representation of the velocity of the sound wave. The logging tool consists of one or more transmitters, which send out the ultrasonic waves and one or more receivers, which detect the returning waves. The velocity through a formation is dependent on the lithology and porosity (Asquith and Krygowski, 2004). The cement bond log (CBL) and variable density log (VDL) are also acquired using a sonic tool. They are used to determine where there is good bonding between the casing and the formation or the cement, where there is fluid or where there is free pipe (Williams et al., 2009). This has been the method used to indicate intervals with formation collapse and to determine which intervals need to be tested.

3.5.1.3 Density Log

The density log measures the formations mass per unit in the form of grams per cubic centimeter (g/cm^3) and is represented by ρ. The tool uses a gamma ray source emitting gamma rays into the formation, which collide with electrons in the formation and lose energy. The returning gamma rays are recorded by a detector and are separated into two energy ranges. The highest energy range records the effect of Compton scattering and represents the electron density, associated with the formation bulk density. The Compton scattering effect is dependent on the porosity to a greater extent than lithology. The formation bulk density (ρ_b) can be used to determine porosity by using the density porosity formula. However, since the formation bulk density is dependent on the matrix density, porosity and the fluid in the pores, it is necessary to know both the density of the fluid and the density of the lithology matrix in

the formation. The lowest range records the effect of the Photoelectric effect (Pef) and is lithology-dependent. After its development in the 1970s the Photoelectric effect has been used by geologists to determine the lithology of the formation. For the purpose of this thesis, the density logs help distinguish between the different lithologies (Asquith and Krygowski, 2004).

3.5.1.4 Neutron Log

The neutron log records the porosity of the formation by measuring the concentration of hydrogen. Neutrons are sent into the formation from a chemical source in the tool. The neutrons collide with nuclei in the formation and loose energy. After losing enough energy the neutron is absorbed by a nucleus and a gamma ray is emitted and sent back to the tool. As the nucleus and hydrogen atoms are of almost of equal weight, the hydrogen atom is the most effective nucleus. The hydrogen atoms reside in the fluid in the pores of the formation and are therefore related to the porosity. The logging curve is however dependent on several variables; (1) different detector types, (2) variations in spacing between source and detector and (3) different lithology types. In addition it is important to be aware of the hydrocarbon effect and the shale effect and how they cause variations in the measurements (Asquith and Krygowski, 2004).

3.5.1.5 Resistivity Log

The resistivity log is based on sending a current through the formation and measuring the response. There are two types of tools used in the industry. The first tool uses electrodes to produce a current through the formation and it measures the resistivity of the formation. The second tool is called an induction tool and consists of a coil that sends a current through the formation. The tools receiver measures the conductivity of the formation. Often, they are combined to produce one single resistivity log. The log is used indirectly to measure porosity, indicate permeability, and maybe most importantly, distinguish between hydrocarbon bearing zones and water bearing zones. The resistivity of a formation is a function of the water saturation in the pores spaces. The matrix and hydrocarbons are nonconductive, meaning that the formation's aptitude for transmitting current is dependent of the water (Asquith and Krygowski, 2004). The environmental effects on the borehole for resistivity are often associated with the drilling fluids and the depth of invasion.

3.5.2 Lithological descriptions

The various petrophysical logs available can be considered one type of source for lithology data. The second source is the description of cuttings and cores. The best representation of the downhole lithology is using a combination of these two sources (Rider, 1986).

3.5.2.1 Cutting descriptions

The cuttings are the small pieces of rock that are broken of the formation while drilling and pumped out of the hole with the drilling mud. The mud is sent over the shale shaker, a metal sieve, to remove the cuttings and clean the mud. The cuttings are described by percentage of lithology type e.g. 90% sandstone (90% SST). By looking at the various cutting combinations, colors and fragments, the geologist has to make an estimate on the final lithology in the formation (Rider, 1986). On the way up the cuttings from deeper formations are mixed with cuttings from the shallower formations, it is therefore important to record the percentages and to note the influx of a new type of cuttings. By using a combination of the cutting description and the various logs it is possible for the geologists to correlate and identify formations across different fields and areas.

3.5.2.2 Core descriptions

There are two methods to obtain cores from a bore hole; (1) cutting the core while drilling using a core barrel and (2) core sampling after drilling, in which the sample is cut out from the bore hole . The first method gives the geologist a continuous, cylindrical sample of the subsurface lithology, which can be used to correlate the logs and cutting samples (Rider, 1986). The second method is based on a tool that takes samples by arranging the tool along the sidewall at intervals decided based on the logs. Samples from the core can be used for a wide range of tests, including visual and thin section examination, XRD analysis and SEM analysis.

3.5.3 Mineralogical analyses

Mineralogical testing is possible when a physical sample of the test is available in form of cuttings or core samples. With a rock sample available, there are several existing techniques to test both physical and chemical properties. For the purpose of this paper, considering the use of shale formation as a barrier, several techniques are of interest, but only x-ray diffraction (XRD) will be explained in greater detail. In addition, geomechanical testing and scanning electron microscope (SEM) are relevant when considering the properties of shale as hydraulic barriers, but will not be considered in this thesis.

3.5.3.1 X-ray Diffraction

X-ray diffraction (XRD) is a method to investigate the chemical and physical properties of various materials, and determine their structure and mineral phases. The technique is based on how x-rays interact with the electrons of atoms in mineral powder (Will, 2006). The atoms in the mineral lattice act as a diffraction grating, making the x-rays scatter in different ways depending on the structure of the lattice (Moore and Reynolds, 1989). When the X-rays interact with the electrons, there is a clear relationship between the spacing between the atoms (d), the wavelength of the x-rays (λ) and the angle between the incident x-ray and the crystal surface (Θ). This relationship is known as the Bragg Law, and the relationship can be represented by the following formula and Figure 3.12 (Moore and Reynolds, 1989):

$$2dsin\theta = n\lambda$$

How the x-rays are scattered depend on the structure of the atom lattice, and the diffracted x-rays are recorded by the detector as a unique pattern for the different clay minerals (Figure 3.13) (Moore and Reynolds, 1989). The pattern shows intensity peaks for the different 2Θ-positions, thus indicating the mineral phase of the sample (Röser, 2007 , Will, 2006). The peaks for the sample in question are compared to published values from various literature. The character of the peak for clay minerals shows distinct and recognizable features such as; the position of the peak, the intensity, the shape and the breadth. The position of the peak is dependent on the Bragg law and for clay minerals the resulting 2Θ peaks are commonly less than 40˚ (Moore and Reynolds, 1989). The breadth allows the viewer to determine if the peaks are due to clay minerals and which are due to other non-clay minerals. Non-clay minerals generally have a sharp, thin peak, while clay minerals, with their decreasing size produces broader, more diffuse peaks (Moore and Reynolds, 1989)

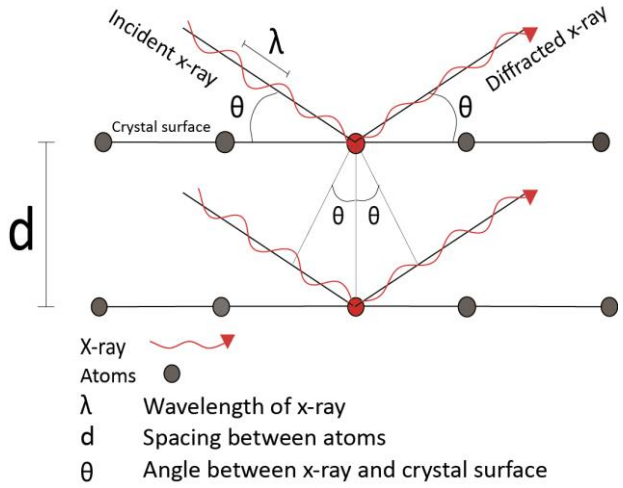

Figure 3.12 Bragg Law. The figure shows the Bragg Law and the relationship between the wavelength λ, the d-spacing and the angle between the incident x-ray and the plane of atoms.

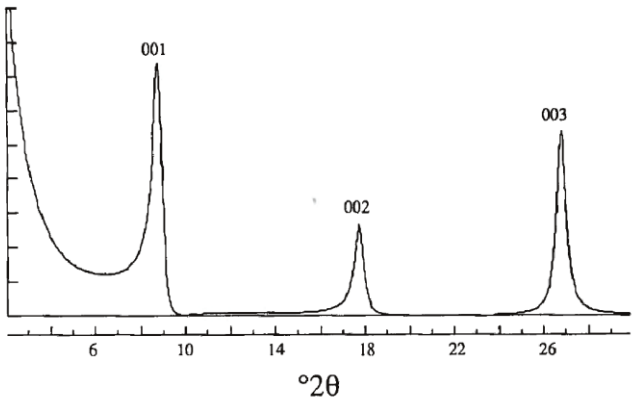

Figure 3.13 Diffraction pattern for illite. Example of a diffraction pattern for illite showing the intensity peaks for 2Θ (Moore and Reynolds, 1989).

In order to gain a complete dataset for the reference well 0, additional mineralogical information was necessary and a XRD analysis was requested. The samples were collected from the confirmed interval in the Kai Formation on the Heidrun Field in well 0.2 to supplement the reference well (chapter 4.2.1 and 5.3.1). The analysis was done using a Bruker X-ray Diffractor D8 Advance at the Department of Geology and Mineral Resources Engineering, NTNU. The diffractograms were recorded from 3-65˚, 2θ, and each step taking 0,009/sec. The identification was done using the Diffrac EVA software, using the search and match tool based on the PDF-4+ database. The quantification was based on the Rietveld method using the Topas software. The samples were unwashed and even though the well was drilled with water based mud, gloves and other precautions were still recommended. The geologists offshore noted the presence of cement and mud in the samples; however it was assumed the percentage was less than 5%, and that it would be of little consequence. The samples were prepared for both bulk analysis and fine fraction (6µm) analysis.

For the bulk analysis part of the samples were put in petri dishes and set to dry at 60˚C overnight. The morning after the samples were not completely dried and they were grinded to smaller pieces and left to dry another night. When they were completely dry, large grains were discovered and it was necessary to crush the samples using an agate micronizing mill. The samples were left to dry for an hour at 105˚C, and when all the ethanol had evaporated; the powder was pressed into a Standard Bruker PNMA XRD Sample Holder and readied for XRD analysis.

For the fine fraction analysis another part of the sample was put into a beaker with 200ml of de-ionized water. The clay samples were disintegrated, stirred and poured into settling cylinders. Separation was done on all samples according to Stokes' law, leaving only the particles < 6μm to be used in the analysis. The water in each sample was filtrated out using a vacuum pump and the layer on the Millipore filter was transferred onto glass plates and air dried; two glass plates for each sample. One was put in an exicator with ethylene glycol and left at 60 ˚C for approximately 24 hours. The samples were mounted for XRD analysis. Presence of smectite is identified in the samples by the shift in the glycolated line, as the peak position is shifted to a higher spacing. Quantification of the fine fraction is not suitable due to the amorphous nature of the samples and difficulty in knowing the difference between the size of the fine fraction samples and the original sample.

4 Dataset collection

4.1 Dataset collection

In the next part, the datasets will be presented for each well. For the different datasets, it is easiest to take note of the trends and patterns and compare these, instead of going into detail for each specific depth. This is true, especially for the petrophysical logs (Appendix B) which will in general show the two formations as claystone, but the trends might reveal other increasing or decreasing properties, such as sand or clay content. For the cuttings and core descriptions, it is important to keep in mind that they are a product of different geologists' interpretation of the rock content, and can only be used as an indication of the lithology. The cuttings (Appendix C) show the lithology, but not how the lithological layers extend or their origin. The x-ray diffraction data (Appendix D) will be the best indication of clay type, the problem is however, that there are only a limited number of samples tested. In addition, it might not always have been the same purpose for the testing. It is at this point, that the challenge of transferability of datasets becomes apparent, and the importance of a having good method to compare the data. An overview of all the available datasets in each well is shown in Figure 4.1.

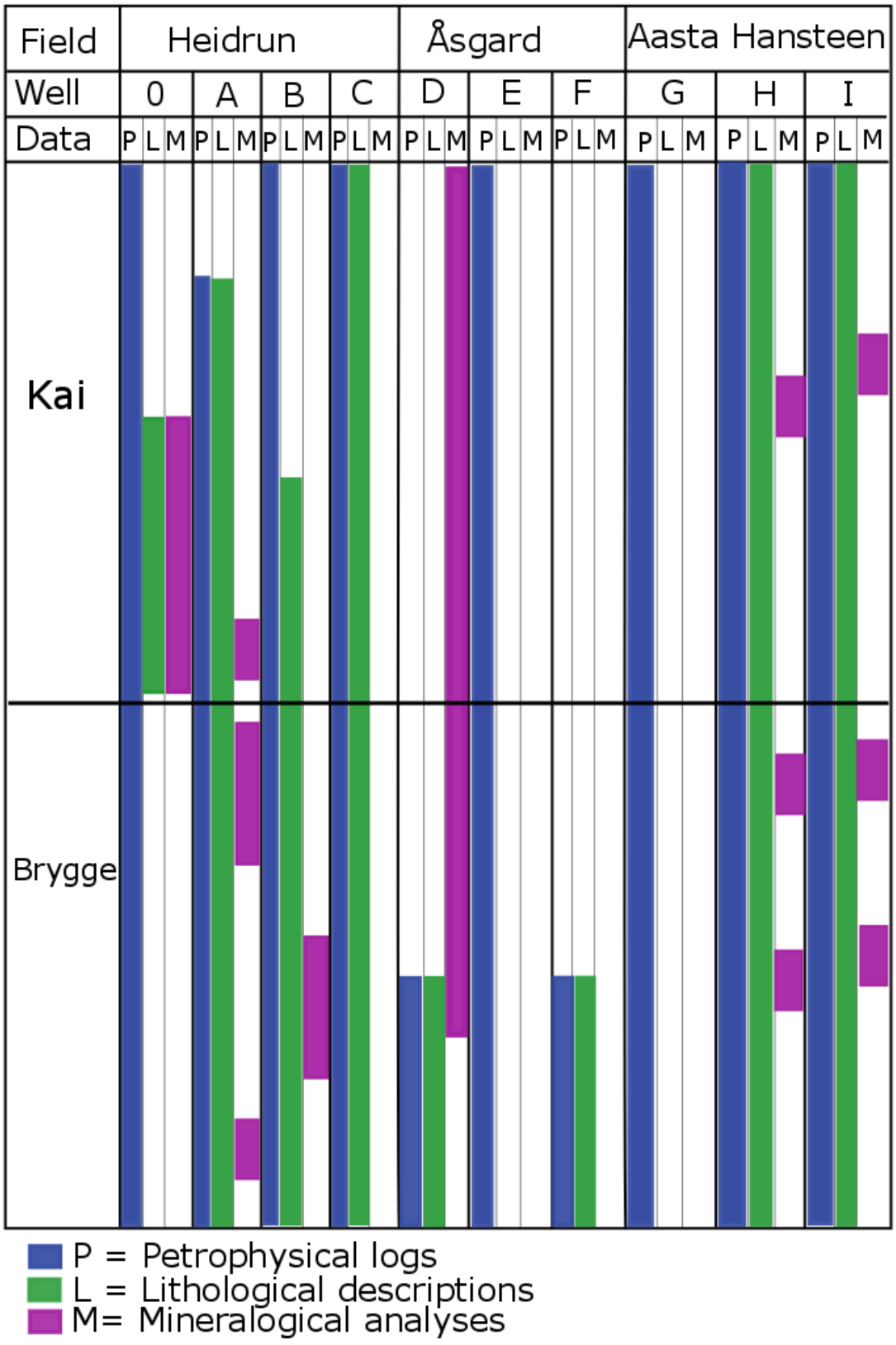

Figure 4.1 Overview of the dataset distribution within the wells and the fields. The formations and placement of the datasets are not to scale and are based on estimation.

4.2 Heidrun datasets

All the wells drilled on Heidrun have water depths of 345m and the RKB-MSL distance is 74,2m. The distance between well A and well B is approximately 10m, the distance between well C and well A and B is approximately 2500m.

4.2.1 Well 0

The well chosen as the reference well for the comparison is located on the Heidrun field and is a production well. During plug and abandonment of the well, to fulfill the requirements for barrier elements, the use of the Kai Formation as a barrier was a good option. The bond logs revealed that an interval in the middle of the formation showed good bonding to the annulus. The formation was qualified by pressure testing (FIT, XLOT) the interval at two depths; 1662,8 mTVD MSL and 1700,8 mTVD MSL. The results from the logs and the tests confirmed that there was no fluid connection in the tested interval and sufficient strength to withstand the applied pressure, thus confirming the Kai Formation as a hydraulic barrier on the Heidrun Field. The logs and properties from the interval used as a barrier will be the basis for the other wells.

The datasets available from well 0 is a petrophysical log (Appendix B), consisting of gamma ray (GR) and resistivity (Rt), and the report confirming the Kai Formation as a barrier. In addition, the formation tops for the Kai, Brygge and Tare formation are known, as shown in Table 4.1.

Formation Top	Depth mTVD MSL
Kai	1440,8
Brygge	1783,2
Tare	1930,5

Table 4.1 Formation tops in well 0 for the Kai, Brygge and Tare Formations.

After looking through the data, and discussing with the supervisors at Statoil, it became necessary to collect more data to have a better basis for comparison. The reference well 0 above has a sidetrack with more available information. The sidetrack will be referred to as well 0.2 to avoid confusion. In addition it was decided to correlate the confirmed interval across to the sidetrack and acquire cuttings for the corresponding interval, to be used for XRD analysis. The available datasets for well 0.2 is a petrophysical log consisting of gamma ray (GR), resistivity (Rt), density (RHOB) and neutron (NPHI) and the cuttings descriptions for

the interval. This additional information will give a more complete picture of the confirmed interval and the reference well.

A request was sent to Weatherford for cutting samples, and nine samples were sent from the interval of interest, seen in Table 4.2.

Depth (mMD)	Depth mTVD MSL	Sample location
1810	1655	Above confirmed interval
1820	1664	Above confirmed interval
1840	1684	In confirmed interval
1850	1694	In confirmed interval
1860	1704	In confirmed interval
1870	1714	In confirmed interval
1880	1723	In confirmed interval
1920	1762	Below, near base Kai
1940	1781	Below, near base Kai

Table 4.2 Overview of sample depths and location in relation to the confirmed interval in the Kai Formation. Samples are taken from well 0.2 on the Heidrun Field.

4.2.2 Well A

Well A is a production well and there is a variety of datasets available. Access has been granted to two logs; the completion log and a petrophysical evaluation log. The completion log consists of gamma ray (GR), caliper (Cali), resistivity (Rt), sonic (Dt), neutron (NPHI) and density (RHOB) for the Kai and Brygge Formations. In addition, there is a lithological description of the cuttings. The petrophysical evaluation has a more detailed view of the same curves, with the exception of the neutron curve. With the higher level of detail it is easier to correlate with the other wells and to see possible changes in the trends.

There are also two reports available for well A; the first concerning borehole stability and the second is a rockmechanical and petrophysical evaluation. The rockmechanical aspect will not be reviewed in this study. The reports are based on samples taken from three 1m long cores from three different depths in the Brygge Formation; 2312.2 mMD (1897.2 mTVD MSL), 2322.7 mMD (1905.2 mTVD MSL) and 2339.5 mMD (1918.1 mTVD MSL). From these samples a variety of petrophysical analyses were made:

- Visual examination of the cores and thin section
- XRD – and SEM – analysis
- Shale property evaluation – cation exchange capacity, water content, porosity, bulk density, specific surface area, etc.

The formation tops have also been picked, shown in Table 4.3.

Formation Top	Depth mTVD MSL
Kai	1455.0
Brygge	1806.1
Tare	1944.6

Table 4.3 Formation tops from well A for the Kai, Brygge and Tare Formation

4.2.3 Well B

Well B is a production well and the datasets granted access to, consist of a petrophysical evaluation log and a core analysis report. Similarly to well A, the log has a high level of detail, however, the upper section of the Kai Formation, only have the gamma ray (GR) and the resistivity (Rt) curves. About halfway through the Kai Formation and into the Brygge Formation more curves becomes available; caliper (Cali), photoelectric effect (Pef), density (RHOB), neutron (NPHI) and sonic (Dt). The core analysis report is based on samples taken from the Brygge and Tang Formation, and makes a comparison of these two formations. However for this thesis only the Brygge Formation will be examined. During drilling, 21 meter of core was collected and six samples from different depths in the interval were collected. These samples are described by visual examination and thin section examination, in addition to XRD-analysis. The result is a detailed description of the facies in the formations. Cutting descriptions and the formations tops (Table 4.4) are also available for well B.

Formation Top	Depth mTVD MSL
Kai	1427,8
Brygge	1786,2
Tare	1931,1

Table 4.4 Formation tops from well B for the Kai, Brygge and Tare Formation

4.2.4 Well C

Well C is an exploration well and will be used as a supplementary well. All the datasets are taken from NPD. The datasets available are a completion log and a completion report. The log consists of gamma ray (GR), resistivity (Rt) and sonic (Dt) curves. There is also a detailed cutting description on the log and the completion log provides the formation tops (Table 4.5). There is no available geochemical or petrological information from well C, so it will mostly be used as comparison for the logs and the cutting descriptions.

Formation Top	Depth mTVD MSL
Kai	1458
Brygge	1881
Tare	1984

Table 4.5 Formation tops from well C for the Kai, Brygge and Tare Formation

4.3 Åsgard datasets

The distance between Well D and Well F is approximately 17 km and the Åsgard Field has water depths between 240 and 300m.

4.3.1 Well D

Well D is a production well on the Åsgard Field and it has very poor coverage for the Kai and Brygge Formations. The completion log shows only the lower part of the Brygge Formation and consists of gamma ray (GR), resistivity (Rt) and cuttings description. What makes this well interesting is the incredible coverage of XRD analysis through the upper part of the well. A total of 40 samples in the interval between 620 and 2152m have been analyzed. The only formation top available from the data is the Tare Formation as seen in Table 4.6.

Formation Top	Depth mTVD MSL
Tare	2159,90

Table 4.6 Formation tops from well D for the Tare Formation

Due to the lack of information it was necessary to use an exploration well nearby as a supplementary well to estimate the formation tops for the Kai and Brygge Formations and to have a second completion log to consider.

4.3.2 Well E

Well E is an exploration well and will be used as a supplementary well for well D since the distance is only about 1km between the two wells. All the data available are found at the NPD fact pages. Available data are the completion log consisting of gamma ray (GR) and resistivity (Rt) and the formation tops shown in Table 4.7.

Formation Top	Depth mTVD MSL
Kai	1462
Brygge	1899
Tare	2192

Table 4.7 Formation tops for well E for the Kai, Brygge and Tare Formations

4.3.3 Well F

Well F is also a production well and similarly to well D the coverage of the Kai and Brygge Formations is very poor. The completion log shows only the lower part of the Brygge Formation and consists of gamma ray (GR), resistivity (Rt) and cuttings description. The XRD report from well F on the other hand, has extremely poor quality and will be hard to use in the comparison. The formation tops are available and can be seen in Table 4.8.

Formation Top	Depth mTVD MSL
Kai	1471,29
Brygge	1935,5
Tare	2206,7

Table 4.8 Formation tops from well F for the Kai, Brygge and Tare Formations

4.4 Aasta Hansteen datasets

All the wells on the Aasta Hansteen field are exploration wells. They have been drilled with a triangular distribution to cover all the possible prospects in the area. The distance between the wells is less than 10 km. The water depth is 1247.5m and the KB elevation is 23.5m.

4.4.1 Well G

Well G is an exploration well; however the upper part of the well is not as well covered as the other two wells. The available data is a completion log consisting of only gamma ray and a bad quality sonic log for the Kai and Brygge Formation. There is also done a stability report for all of the wells on Aasta Hansteen. In addition the formation tops are known, see Table 4.9

Formation Top	Depth mTVD MSL
Kai	2010
Brygge	2059
Tare	2151

Table 4.9 Formation tops from well G for the Kai, Brygge and Tare Formations

4.4.2 Well H

Well H is also an exploration well with the same datasets as well G, however the coverage of the Kai and Brygge Formation is better. The completion log consists of gamma ray (GR), resistivity (Rt), sonic (Dt), density (RHOB) and neutron (NPHI) and cuttings descriptions. The stability report is based on three samples from well H, one in the Kai Formation and two in the Brygge Formation. They are all investigated using XRD. The only problem is that two of the samples are taken in the ooze interval and might not be representative for the shale formation. The formation tops can be seen in Table 4.10.

Formation Top	Depth mTVD MSL
Kai	2096
Brygge	2188
Tare	2356,5

Table 4.10 Formation tops from well H for the Kai, Brygge and Tare Formations

4.4.3 Well I

Well I is also an exploration well and has the same datasets as well H and G, but the coverage is not as good as in well H. The completion log consists of gamma ray (GR), density (RHOB) and cuttings descriptions. In the stability report there are three samples analyzed; one sample from the Kai Formation, in the ooze interval, and two samples in the Brygge Formation, outside the ooze. The samples are investigated using XRD. The formation tops can be seen in Table 4.11.

Formation Top	Depth mTVD RKB
Kai	2045
Brygge	2072,5
Tare	2165,5

Table 4.11 Formation tops from well I for the Kai, Brygge and Tare Formations

5 Results

5.1 Petrophysical logs

This will be a comparison of the trends seen in the petrophysical logs (Appendix B) and an attempt will be made to correlate the formations across the fields. An overview of the formation tops and thickness can be seen in Figure 5.1.

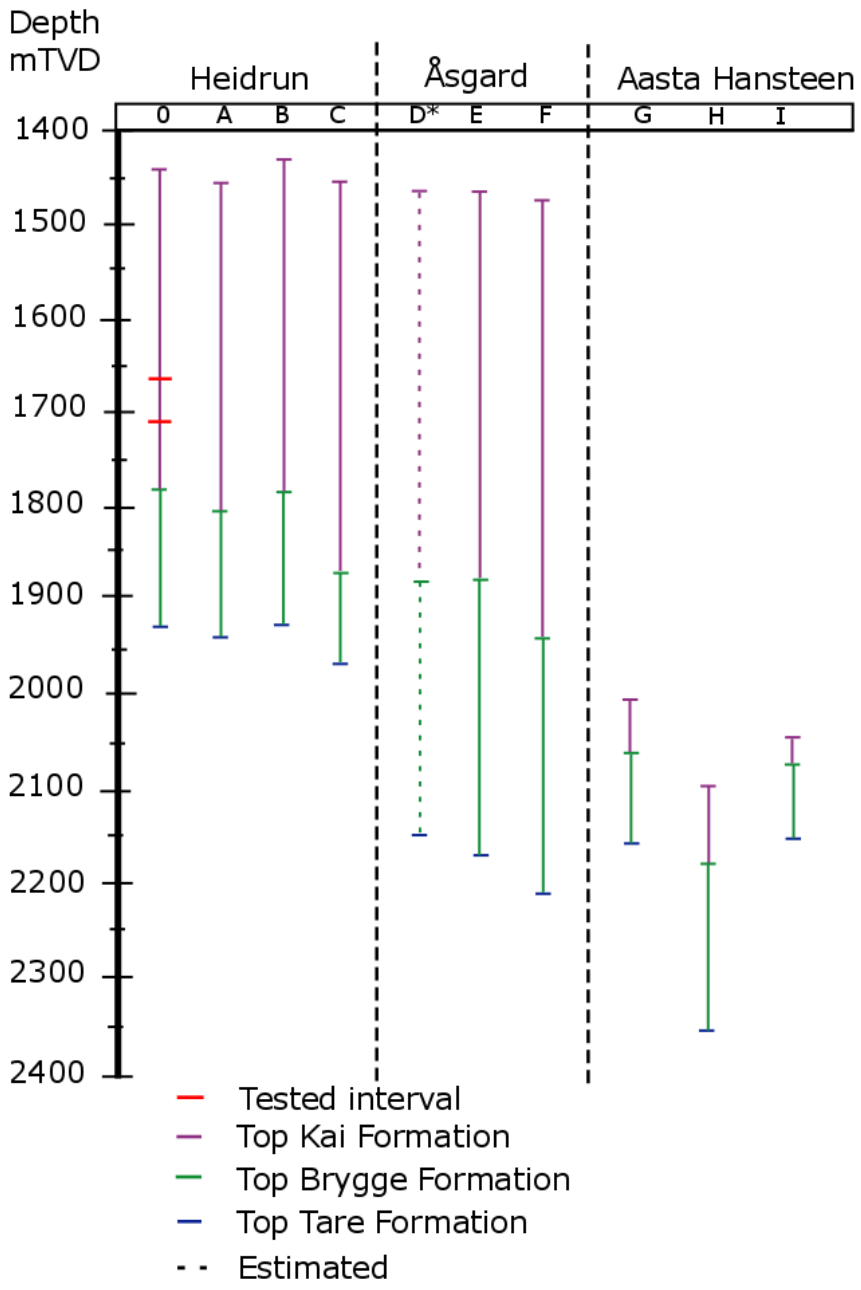

Figure 5.1 Overview of the formation tops. The formations tops for all the wells and the thickness of the intervals for each formation. The interval in well D* is an estimate based on well E, which is the closest well.

5.1.1 Heidrun Field

Well 0

The two petrophysical logs for the reference well (well 0 and 0.2) show similar trends through the two formations. In the reference well, the logging curves (GR, RHOB, NPHI and Rt) are stable through the Kai Formation (Figure 5.2) the only indication of anything other than claystone are peaks indicating calcite stringers (Figure 5.3). The Brygge Formation shows greater variations in the log responses. At the transition between the two formations, the gamma ray and the resistivity show a decreasing trend from the Kai Formation to the Brygge Formation. The resistivity decreases from the range 1-10 ohmm to < 1ohmm. There is also a higher number calcite peaks throughout the Brygge Formation. The general assumption can be made, that the Brygge Formation is a less homogenous claystone than the Kai Formation. Well 0.2 has the same log response for the gamma ray and the resistivity curves as well 0. The additional density and neutron information supports the indications of a homogenous claystone in the Kai Formation and a more varied lithology in the Brygge Formation. In well 0.2 the density-neutron separation indicates porosity in the upper part of the Brygge Formation. The decrease in gamma ray, density and resistivity might be an indication of either siliceous or calcareous ooze. Another possibility is silty or sandy intervals. Where the gamma ray, density and resistivity increase there is most likely a higher content of clay.

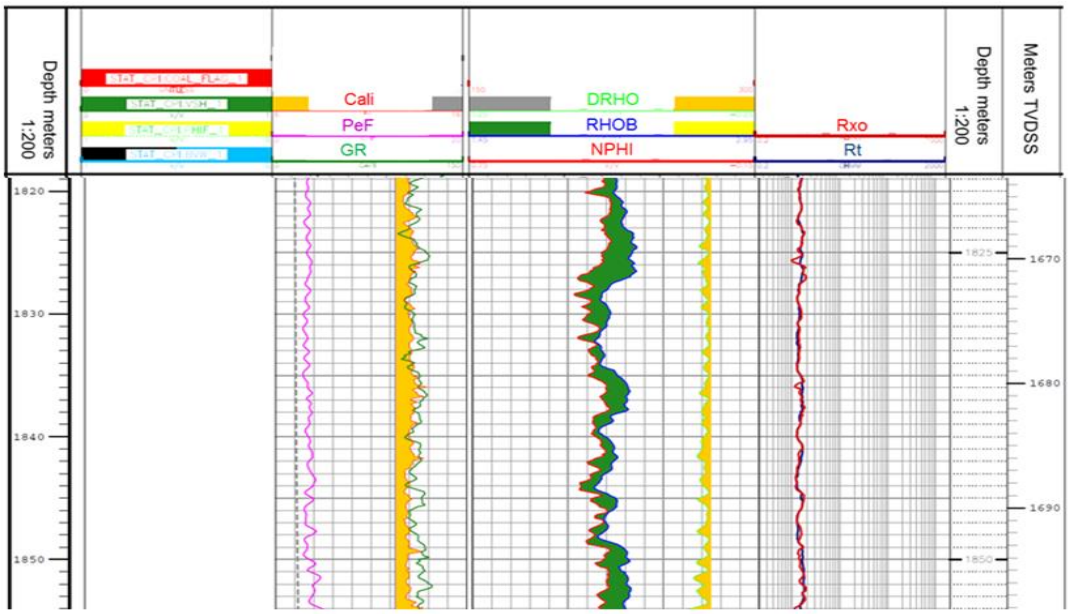

Figure 5.2 Log from the Kai Formation Example of log interval (well 0.2, the sidetrack to well 0) from the Kai Formation representing the stable logging curves through the formation. The curves represented are; gamma ray (GR), density (RHOB), neutron (NPHI) and resistivity (Rt). The log shows the interval between 1670-1700 mTVD.

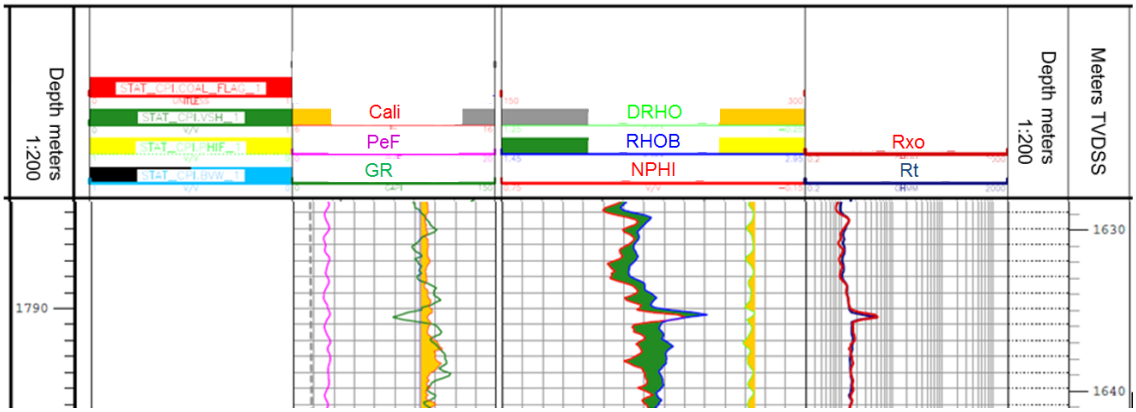

Figure 5.3 Example of calcite stringer. An example of a calcite stringer from well 0.2, the log response indicating the calcite, is the sharp decrease in the gamma ray (GR) (green line to the left), the increase in neutron (NPHI) and density (RHOB) (red and blue line filled with green in the middle) and the peak in the resistivity (Rt) (blue and red line to the right).

The formation tops for the four wells on the Heidrun Field show that the formations have approximately the same depth and thickness, which can be seen in Figure 5.1. This makes it easy to compare and correlate the logging curves. Correlating the confirmed interval in the Kai Formation across the Heidrun Field was relatively easy due to the close proximity of the wells. Using the correlation software Stratworks, a correlation panel was made, as shown in Figure 5.4. The correlation panel shows that the top of the confirmed interval consistently lies approximately 120m above the top of the Brygge Formation. There is no clear trend in the interval, but the range of the GR and Rt values can be seen in Table 5.1. Well C deviates slightly from the other wells, but the reason is the difference in the logs and the resolution (Appendix B).

Well	GR (A.P.I)	Rt (ohmm)
0	120 – 135	1 – 10
A	80 – 120	1 – 10
B	75 – 90	1 – 10
C	40-55	1 – 2

Table 5.1 Range of values in confirmed interval. The range of values for the Heidrun wells through the confirmed interval, correlated across the field. GR = gamma ray, Rt = resistivity

The specific values are of little interest as they are dependent on the parameters explained in chapter 3.5.1 about borehole effects. However, the range of the values shows the same

variations. Overall, the correlation of the confirmed interval in the Kai Formation shows a similar, homogenous claystone across the Heidrun Field.

All the remaining wells on the Heidrun Field appear to have the same log signature through the Kai and the Brygge Formation. The Kai Formation has stable log responses without any significant increase or decrease. The Brygge Formation consistently shows great variations in its log responses, but the same patterns can be seen in all the wells; a decrease in GR, Rt and density with depth; the resistivity decreases to < 1 ohm. In addition, a corresponding decrease in the sonic in all the wells indicating the transition into the ooze interval. In the middle part of the Brygge Formation there are similar indications of high content of limestone and in the lower part of higher clay content.

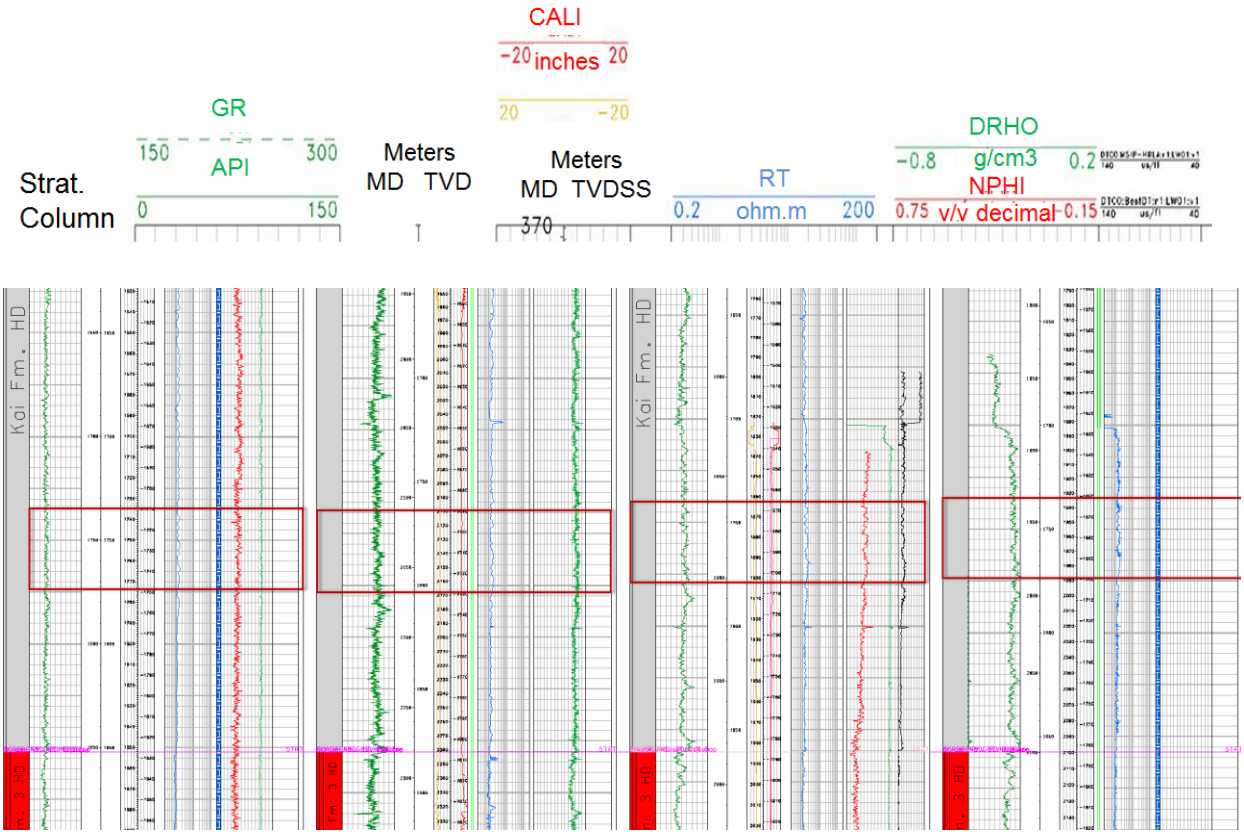

Figure 5.4 Correlation panel for the Heidrun Field drawn in the Stratworks software by Anniken Berge at Statoil. The correlation panel shows how the confirmed interval in well 0 can be correlated across the Heidrun field. From left to right: well C, well A, well B and well 0. The legend shown above is the same for all the wells in the figure.

5.1.2 Åsgard Field

The available formations tops on the Åsgard Field are limited compared to the information from the Heidrun Field, however it is possible to assume that formations in well D and well E have similar depths and thickness due to their close proximity (Figure 5.1). Well F, on the other hand, is further west and the base of the Brygge Formation is slightly deeper than in the other wells. The thickness of the Kai Formation is similar on the Åsgard Field and on the Heidrun Field, which will make it possible to correlate the confirmed interval across the two fields. The Brygge Formation on the other hand has a thicker interval and the base is deeper in the Åsgard Field, which makes sense considering the sedimentary succession in Figure 2.5, since the base of the Brygge Formation is located further west into the basin.

A possible reason for the small data coverage on the Åsgard Field is that the wells with XRD information were side-tracks, meaning they were kicked off at a point down in the well, and not at the sea bottom, and that the logging was mostly done in the reservoir. When comparing well E to the reference well 0, it is possible to see similar trends through the Kai and Brygge Formation. The GR and Rt are stable and relatively high through the Kai Formation, but at the transition to the Brygge Formation they both show the characteristic decreasing trend. The latter also have indications of higher content of limestone. In well D and F it is difficult to actually see any trends, based only the short log interval. It can be noticed, however, that the resistivity is below 1 in both wells (D and F) in the lower part of the Brygge Formation.

5.1.3 Aasta Hansteen Field

The formation tops for the Aasta Hansteen Field are in general much deeper, and the thickness of the formations thinner, than for the other two fields (Figure 5.1). The depth of the formations can partly be explained by the water depths on the Aasta Hansteen, which are approximately 1270m and partly by the deeper and narrower configuration of the basins further north (Figure 3.3). Within the field, the depths and sediment thickness for well G and I are fairly similar. The formations in well H are much deeper than in the other two wells. The difference in the formation tops depths, is the first indication of the difficulty in correlating the two formations across to the Halten Terrace.

The log from well G only has a good GR curve, the sonic log is not continuous and there are no additional curves. The GR does not show any clear trends in either of the two formations, in fact they look quite similar. A possible trend is that the Kai Formation appears to have slightly higher GR, than the upper part of the Brygge Formation. A second possible trend is a

slight increase in GR down through the Brygge Formation, but without any additional information this does not give any good lithological indications. Well H and I have better resolution logs than well G, giving more information for the formations. Compared to well 0 these two wells have relatively different log responses. The GR through the Kai Formation is more varied and have several intervals with much lower GR, indicating sandy or silty areas. Since there are no corresponding shifts in the resistivity, it is more likely sand than limestone. The resistivity is on average lower in these wells than in well 0. The Brygge Formation shows great variation in the GR curve in both well H and I, more similar to the response in the reference well. Although the resistivity is low in most of the formation, there are intervals with a higher resistivity, unlike the response seen in the reference well. In well H, the sonic shows a clear decrease at the transition between the Kai and Brygge Formations. A second transition occurs in the middle of the Brygge Formation, where the sonic suddenly increases greatly. In general, the log response on the Aasta Hansteen Field is hard to compare with the reference well, and even though there might be similarities, it is not possible to correlate the confirmed interval across to the Aasta Hansteen Field.

5.1.4 Petrophysical summary

The petrophysical logs appear to have many of the same log responses through the two formations on the Heidrun Field and the Åsgard Field. The Aasta Hansteen Field, on the other hand, has quite different log response. On the Halten Terrace, the Kai Formation looks like it is a homogenous claystone on both fields, while the Brygge Formation indicates several intervals with different lithologies. The formations on the Aasta Hansteen Field are thinner and show indications of different lithologies than on the Halten Terrace.

5.2 Lithological descriptions

The lithological descriptions are mostly done by geologists offshore and are commonly a part of the completion logs. In a few wells there have also been done core analyses, giving a more detailed description of the lithology. A summary of the lithological description for the different wells can be seen in Figure 5.5.

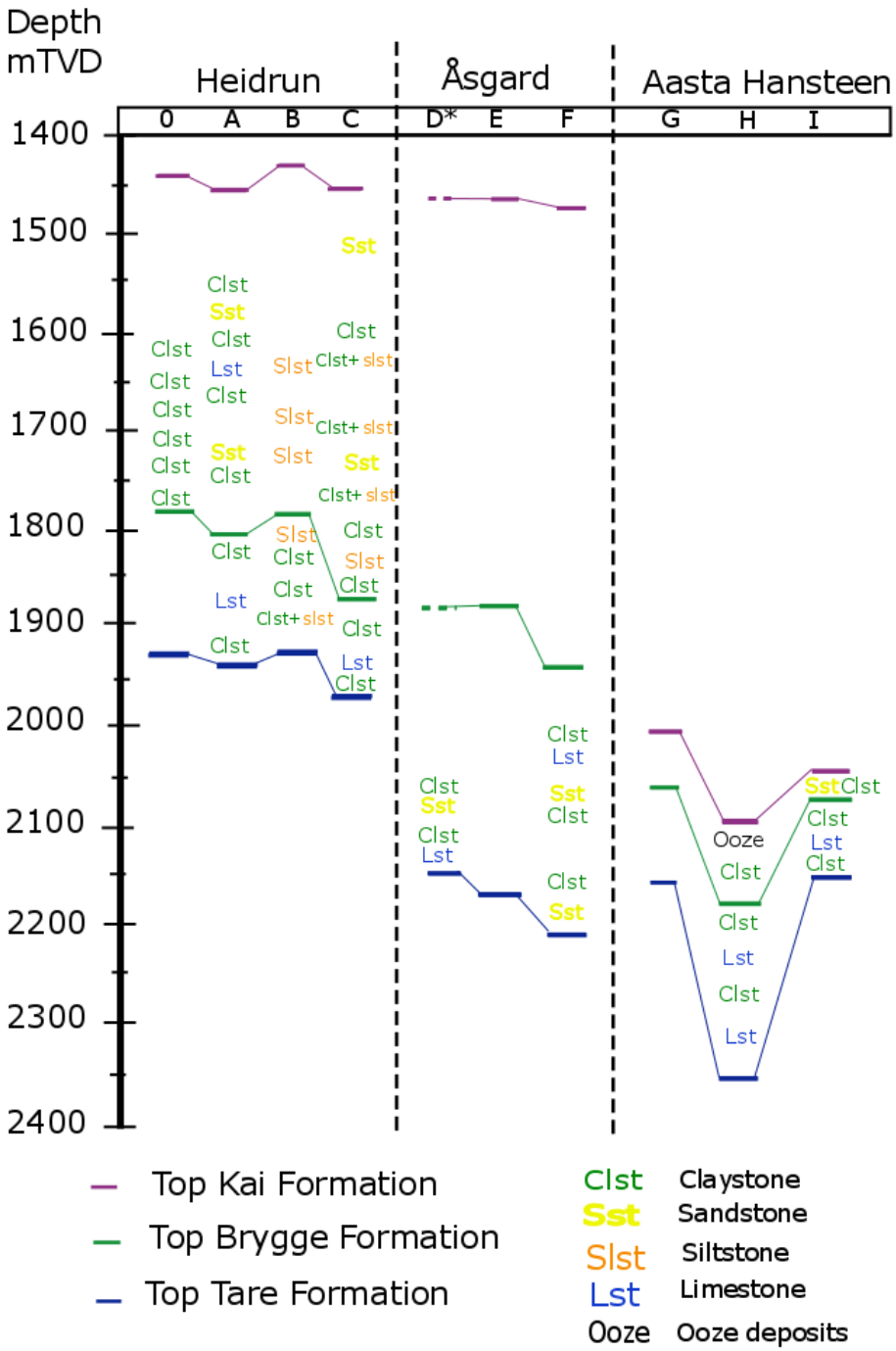

Figure 5.5 Overview of the lithological descriptions. An overview of the lithological descriptions based on the cuttings or cores for the different wells.

5.2.1 Heidrun Field

Well 0

The additional data from well 0.2 contained cuttings descriptions from the confirmed interval and one can assume well 0 and well 0.2 have the same lithology, due to the close proximity. The lithological information from well 0 is summarised in Figure 5.5 and is dominated by claystone throughout the interval. The detailed descriptions are of a 100% claystone, with traces of calcareous material, glauconite or silt. In addition, the geologist comments on traces of cement and abundant mud additives. The last part is important to remember during the XRD analysis of the cuttings.

On Figure 5.5, the overview of the cuttings descriptions can be seen for well A, B and C. In these wells, the Kai Formation seems to have a higher content of silt and sand, than in the reference well. However, the distinction between siltstone and claystone is marginal and may depend on the geologist observing the cuttings. The Brygge Formation has a higher content of limestone. Well B shows a slight deviation from this trend with more silt in the Brygge Formation. Well A and B have additional information concerning lithology in the form of core descriptions.

The three cores samples in well A have all been described as shale with varying shades of grey. Examination of thin sections showed that the three shale samples contained different amounts of silt grains, consisting of feldspar and quartz, and traces of glauconite, pyrite and microfossils (Table 5.2). The stability report contains a more detailed description of the three depths; all the cuttings, taken at 10m intervals were investigated using XRD and SEM.

Depth mTVD	Rock type	Visual description	Thin section
1823	Shale	Medium grey/beige	Silt, pyrite, glauconite, microfossil
1831	Marl (shale)	Pale greenish grey	Pyrite, glauconite, microfossil
1843,9	Shale	Dark grey, faintly greenish	Pyrite, microfossil, gypsum

Table 5.2 Summary of the lithological information from well A based on the visual description and the thin sections. The information is found in the lithological reports provided by the Heidrun Field (Statoil).

The cores taken in well B have been investigated with respect to facies and depositional environment. The interpretation proved difficult to due to the fine grained nature of the clay mineral and therefore thin sections, XRD and SEM were collected to do the analysis. An

overview of the depths tested and interpreted can be seen in Table 5.3 and the descriptions can be seen in Table 5.4.

Depth mMD	Depth mTVD	Facies number	Facies name
2059,60	1860,5	B3	Streaky mudstone
2060,60	1861,5	B1	Diatom – radiolarian wackestone
2065,90	1866,1	B4	Organic rich mudstone
2072,24	1874,1	B3	Streaky mudstone
2076,48	1877,5	B3	Streaky mudstone
2076,90	1877,1	B6	Recrystallized diatom – radiolarian wackestone

Table 5.3 Overview of lithological descriptions from well B. An overview of the depths interpreted using thin section, XRD and SEM to determine facies and depositional environment. The information is taken from the core report done for well B, provided by the Heidrun Field (Statoil).

Formation	Facies	Facies name	Description	Bioclasts	Bio nr	Trace fossils
Brygge	B1	Diatom – radiolarian wackestone	Carbonate limestone, Wackestone	Radiolarian Diatoms	3-6	Zoophycos, Planolites, Thalassinoides, Chondrites
	B2	Highly bioturbated green mudstone	Clay rich mudstone, Silt-bearing, clay-rich mudstone and silt-dominated mudstone	No thin sec	5-6	Zoophycos, Chondrites
	B3	Streaky mudstone	Clay-rich mudstone to siltstone Green to black	Radiolarian Diatoms Ooids	5-6	Zoophycos (most abun), Chondrites, Planolites, Phycosiphon
	B4	Organic rich mudstone	Clay-rich mudstone to siltstone High TOC	Radiolarian Diatoms	0-5	Chondrites
	B5	Rippled siltstone	Siltstone and silt-dominated mudstone	No thin sec	1-3	
	B6	Recrystallized diatom-radiolarian-wackestone	Carbonate limestone Wackestone	Radiolarian Diatoms	2-5	Planolites, Thalassinoides,

Table 5.4 Summary of the facies interpreted in well B. The table is taken form the core description report for well B, modified from the Heidrun Field (Statoil) report.

5.2.2 Åsgard Field

The overview in Figure 5.5 is not complete for the Åsgard Field. The reason is most likely that both well D and F are side-tracks and data from those well paths have not been made available. There were no cuttings available for the reference well E either. Nonetheless, according to the few cuttings descriptions available it seems that the lower part of the Brygge Formation has a higher content of sand in addition to the limestone, compared to the Heidrun Field.

5.2.3 Aasta Hansteen Field

The Aasta Hansteen Field shows a distinctly different lithology than the other two fields. The main difference is the presence of the ooze deposits and a higher content of limestone. However, based on well I there might be a similar trend to the other two fields in the high sand content in the Kai Formation and the limestone content in the Brygge Formation. However it is difficult to prove or disprove these trends based on the available information.

5.2.4 Lithological summary

The lithological results are relatively varied, there are however a few similarities across the fields in the two formations. The Kai Formation consistently consists of claystone with high sand and silt content, except on the Aasta Hansteen Field, where there are indications of ooze deposits in addition. The Brygge Formation appears to be less homogenous, in all the fields, with indications of ooze intervals and higher content of limestone.

5.3 Mineralogical analysis

The mineralogical analysis is based on information from x-ray diffraction (Appendix D). The samples are taken from either cuttings or cores and an overview of samples depths can be seen in Figure 5.6.

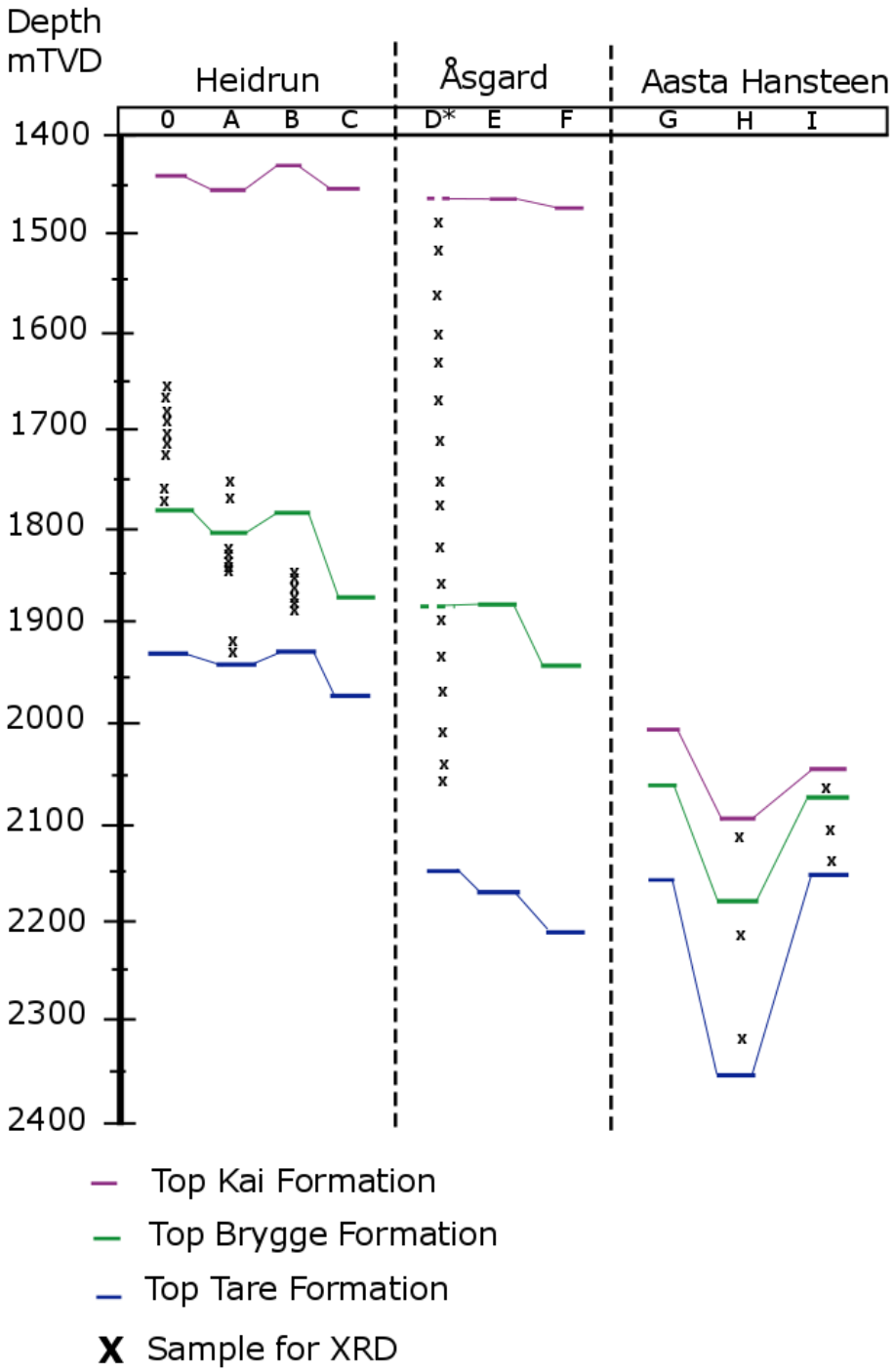

Figure 5.6 Overview of the sample depths from all the wells with XRD analysis.

5.3.1 Heidrun Field

The Heidrun Field is the one best covered for the mineralogical analysis. Well A and B have detailed reports with XRD analyses. In addition to the reports, the cuttings from well 0 have been analyzed to give a better basis for comparison in the Kai Formation.

Well 0

The results from the XRD analysis done on the cuttings from well 0.2 are shown in Figure 5.7 and in Table 5.5. They summarize the whole rock mineralogy and show a relatively homogenous shale formation. The fine fraction analysis did not provide sufficient evidence for the presence of swelling clays in the tested interval. The samples have been analyzed with respect to quartz, feldspar, plagioclase, chlorite, kaolinite, mica/illite, calcite, amphibole and barite. The non-clay fraction is quite significant covering more than 50% of the weight percentage. The amount of barite is also quite high, which was expected since it is one of the additives in the mud and was noted in the cuttings description. The clay content is dominated by mica/illite, with chlorite coming second. The remaining percentages are covered by sylvite, pyrite and dolomite, but they have been disregarded in this thesis. There are no clear trends in the mineral content, except maybe a slight decrease in the clay amount with increasing depth.

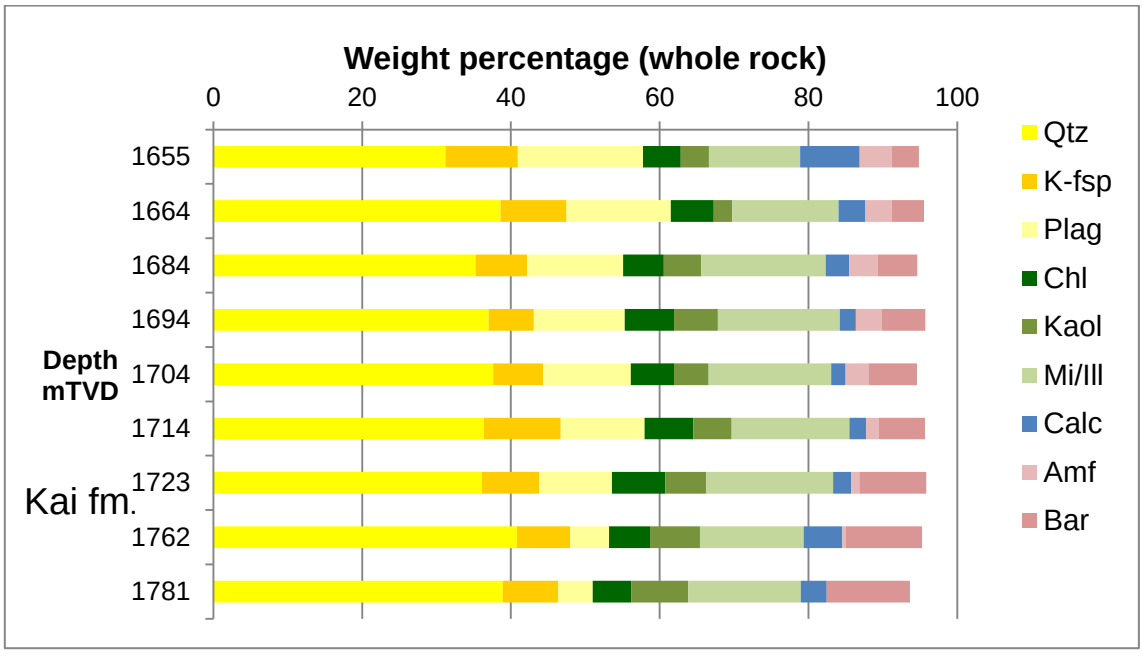

Figure 5.7 Mineralogy in reference well. The mineralogical summary from the whole rock fraction XRD analysis of the samples from well 0.2. The results show the same content and amount of the minerals found in the samples throughout the analysed interval.

Formation	Depth mTVD	Depth mMD	Qtz	Fsp	Plag	Chl	Kaol	Mi/Ill	Calc	Dol	Amph	Syl	Pyr	Bar
Kai	1655	1810	31,2	9,71	16,84	5,1	3,79	12,25	8,01	0,39	4,35	2,99	1,76	3,62
Kai	1664	1820	38,6	8,85	14,06	5,74	2,52	14,28	3,61	0,17	3,55	2,62	1,68	4,33
Kai	1684	1840	35,23	6,96	12,9	5,47	5,02	16,73	3,16	0,57	3,89	3,51	1,27	5,29
Kai	1694	1850	37,03	6,05	12,21	6,62	5,91	16,4	2,14	0,25	3,51	2,64	1,43	5,83
Kai	1704	1860	37,63	6,71	11,8	5,81	4,64	16,48	1,94	0,37	3,12	3,47	1,56	6,47
Kai	1714	1870	36,37	10,34	11,26	6,56	5,16	15,83	2,25	0	1,67	2,69	1,66	6,22
Kai	1723	1880	36,12	7,7	9,77	7,16	5,51	17,04	2,42	0,08	1,14	2,57	1,52	8,97
Kai	1762	1920	40,8	7,17	5,23	5,5	6,7	13,95	5,2	0,03	0,47	2,53	2,18	10,27
Kai	1781	1940	38,91	7,42	4,67	5,16	7,66	15,14	3,48	0,38	0	3,32	2,67	11,19

Table 5.5 Summary of the semi-quantification of the whole rock fraction XRD analysis of the samples taken from well 0.2. Qtz = quartz, Fsp = feldspar, Plag = plagioclase, Chl = chlorite, Kaol = kaolinite, Mi/Ill = mica/illite, Calc = calcite, Dol = dolomite, Amph = amphibole, Syl = sylvite, Pyr = pyrite, Bar = barite.

Fine fraction

The fine fraction XRD analysis of the sample was done in an attempt to establish the presence of swelling clay by the shift in peak positions of the red (glycolated) line. The diffractograms (Appendix A) shows that there are only two depths that have any indication of swelling clays; 1870mMD and 1880mMD (Figure 5.8). It is difficult, however, to determine if this is evidence of swelling clays or not. There is no indication of swelling in any of the other diffractograms, seen by the almost perfect alignment of the red and the black lines. The samples have been analyzed with respect to many of the same minerals as the bulk samples; muscovite, calcite, illite, chlorite, plagioclase, feldspar, pyrite, amphibole, quartz and barite.

1870 mMD (1714 mTVD)

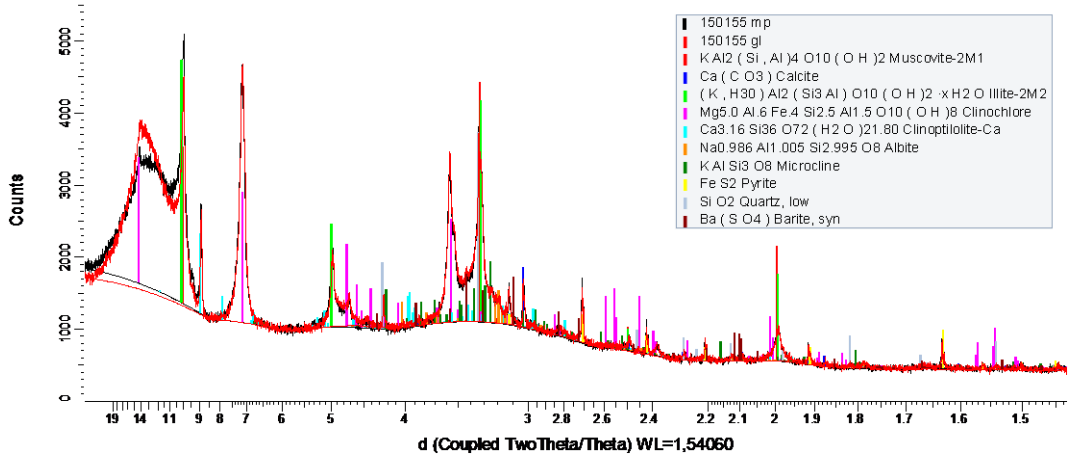

1880 mMD (1723 mTVD)

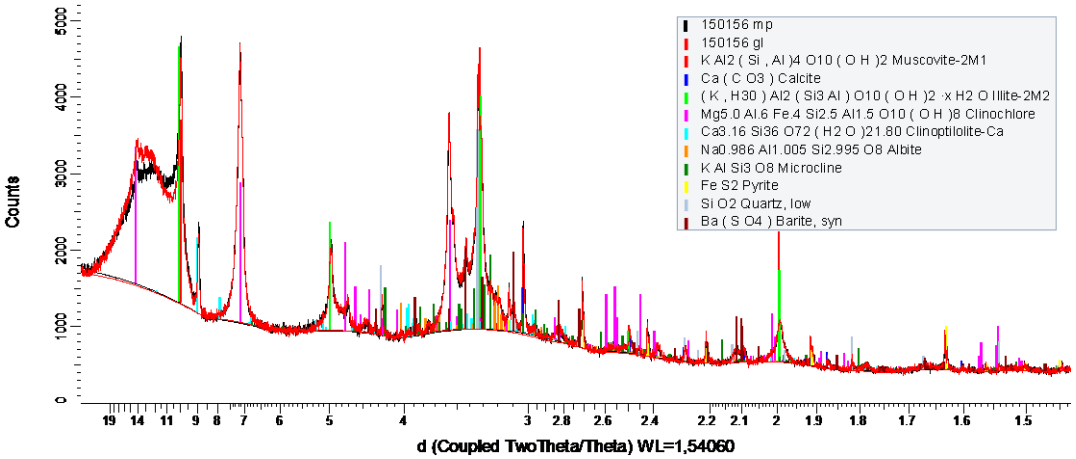

Figure 5.8 Diffractograms from fine fraction XRD analysis. Two of the diffractograms from the fine fraction XRD analysis of the samples from well 0.2. A shift in the red line indicates presence of swelling clay. The only two depths that show any indication of swelling are shown.

Well A

In well A both cuttings and cores have been analyzed by XRD. The location of the samples can be seen in Figure 5.6, with two cuttings samples from the Kai Formation and the remaining cuttings samples from the Brygge Formation, the core samples are from the Brygge Formation. All the available XRD information from well A has been summarized in Figure 5.9 and Figure 5.10. The first figure shows the results from the whole rock fraction including both cuttings and core samples. The second figure is the fine fraction, consisting of the core samples as the fine fraction of the cuttings was not analyzed. Looking at the results there are two apparent trends through the bulk samples; a clear decrease in the quartz content and a corresponding increase in the smectite content with depth. The same trends can be seen in the fine fraction as well, but it is not as clear with so few samples. The amount of calcite is usually quite small, except in in the sample at 1834 mTVD, which is most likely, a calcite stringer. Another interesting depth is 1846 mTVD; where there is both a cutting sample and a core sample. Theoretically, these two samples should have had the same mineralogy; however, the content is relatively different between the two. The clay content in the cutting sample at 1846 mTVD has no indication of smectite, while the core sample is dominated by smectite.

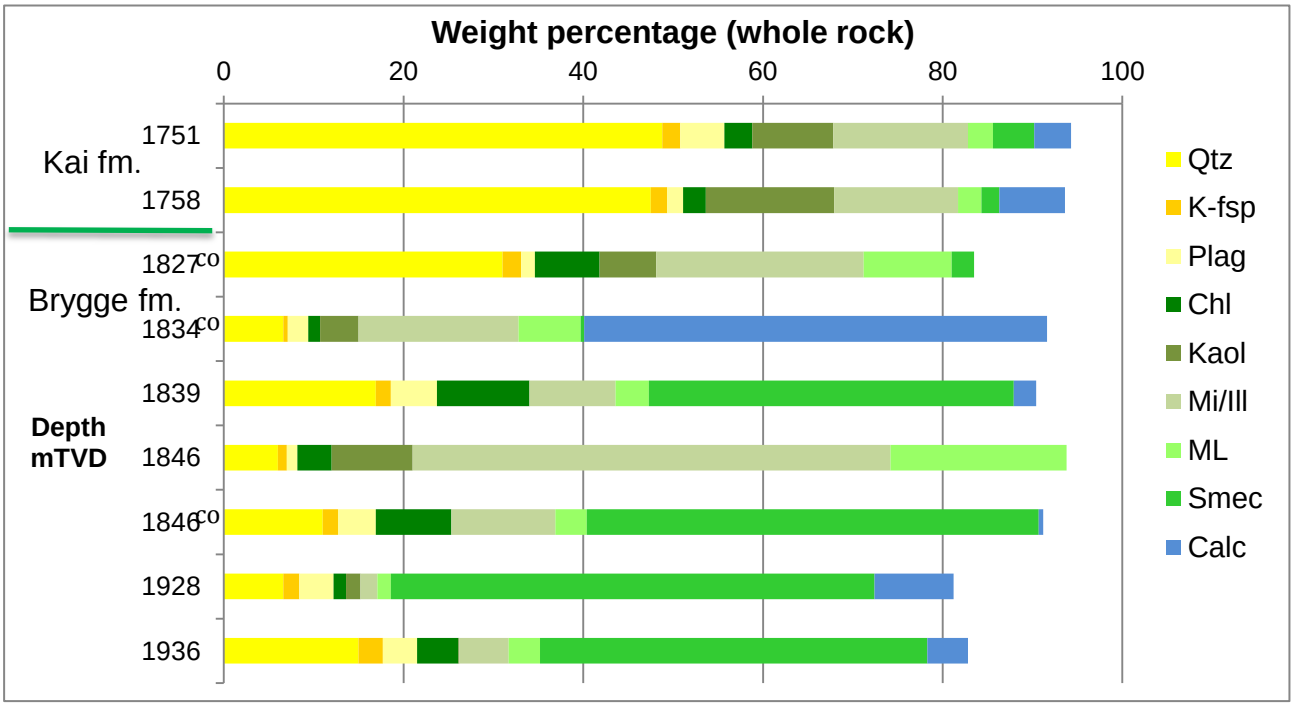

Figure 5.9 Mineralogy well A (whole rock).Summary of all the whole rock XRD analysis from well A including both core samples and cuttings. The Kai Formation has high content on non-clay material, kaolinite and mica/illite. The Brygge Formation has higher content calcite and smectite. Co = core sample

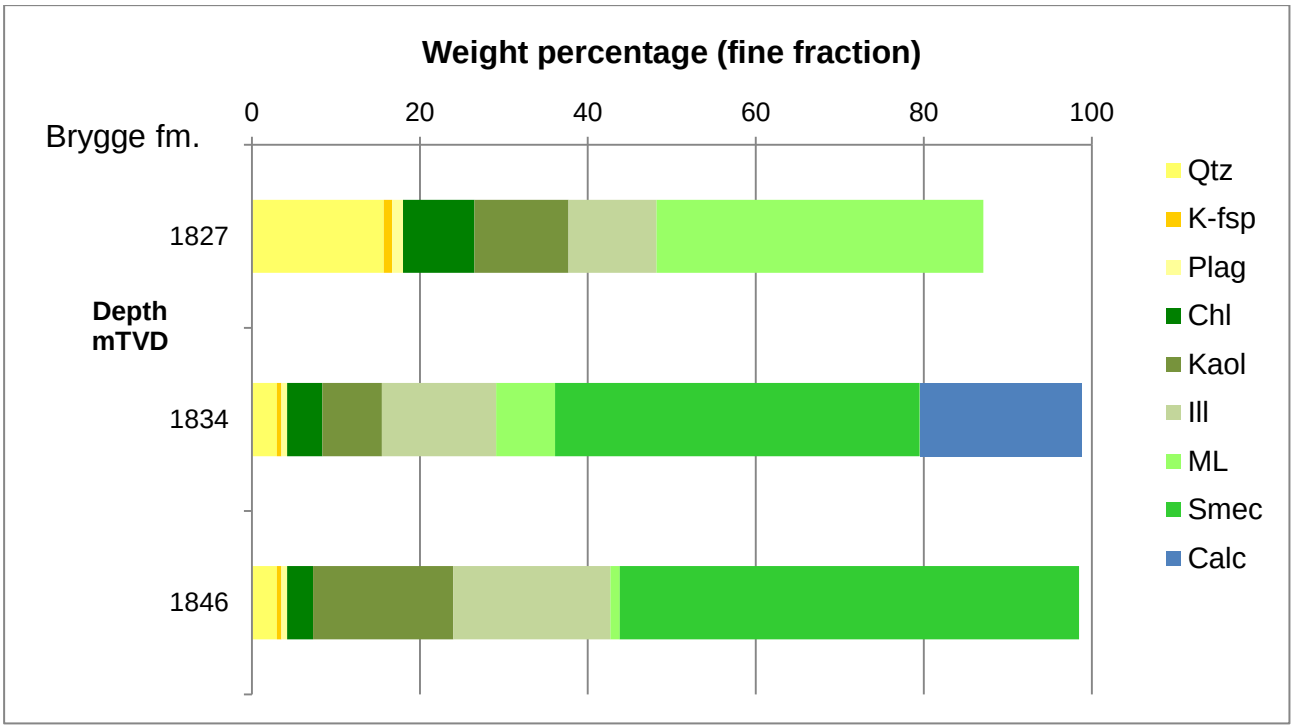

Figure 5.10 Mineralogy well A (fine fraction). Summary of the fine fraction XRD analysis from well A based only on the core samples, as no fine fraction analysis was done on the cutting samples. All the samples are from the Brygge Formation and confirm the high amount of smectite and mixed layer clay.

Well B

All the samples from well B are taken in the Brygge Formation, as can be seen on Figure 5.6, and they are all based on the core samples. The samples are used to describe the facies and the depositional environment as described in the lithology section. Dissimilar to the other XRD analyses in this thesis; the samples contain chert and quartz as the non-clay material and not kalifeldspar and plagioclase as the other wells do. The samples were taken from a short interval of about 20 meters and the mineralogy varies greatly. The samples from 1861 mTVD and 1878 mTVD have high content of calcite, indicating calcite stringers. The trends in the clay content are easier to see in the fine fraction analysis (Figure 5.12), which shows the fine fraction for well B and one can see the change from the smectite dominated samples in the upper part, through the increase in illite and into the mixed layer clay dominated samples in the lower part.

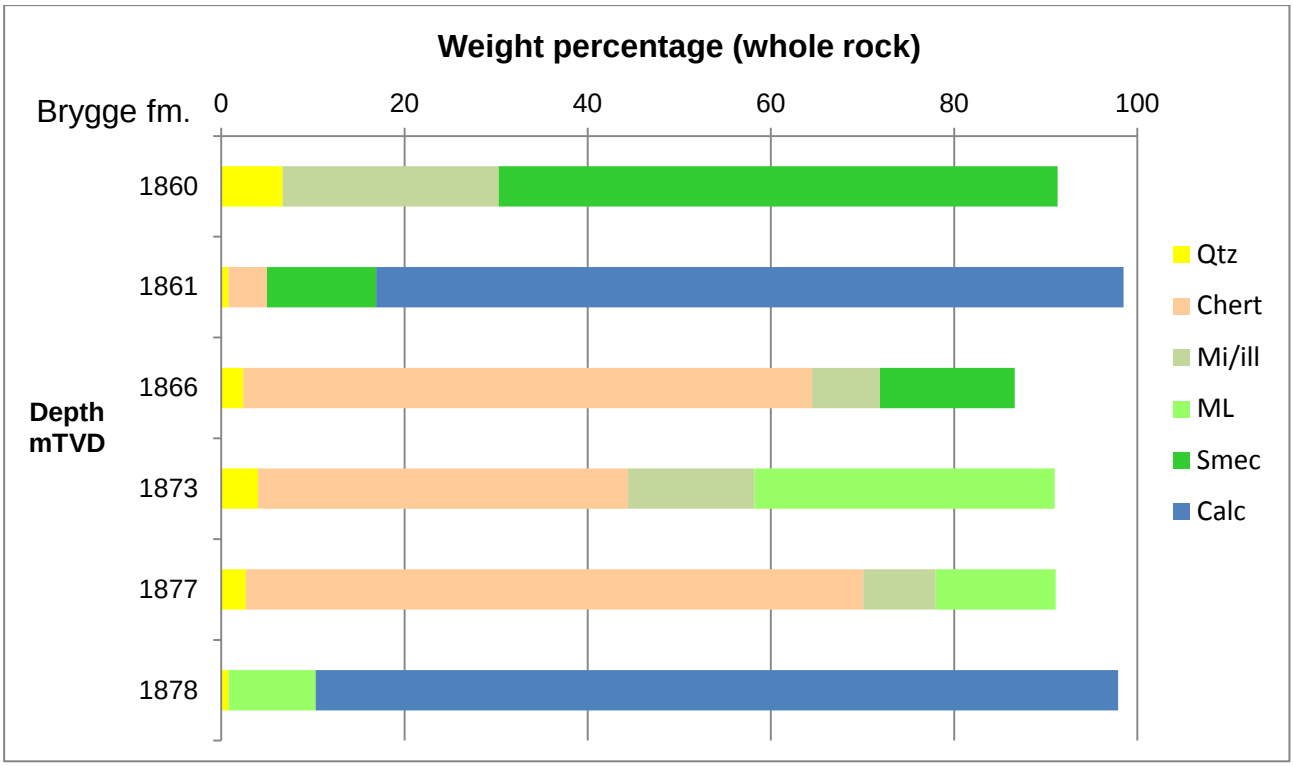

Figure 5.11 Mineralogy well B (whole rock). Summary of the whole rock fraction XRD analysis for well B. All the samples are from the Brygge Formation and in the whole rock fraction there is a high amount of chert, calcite and smectite.

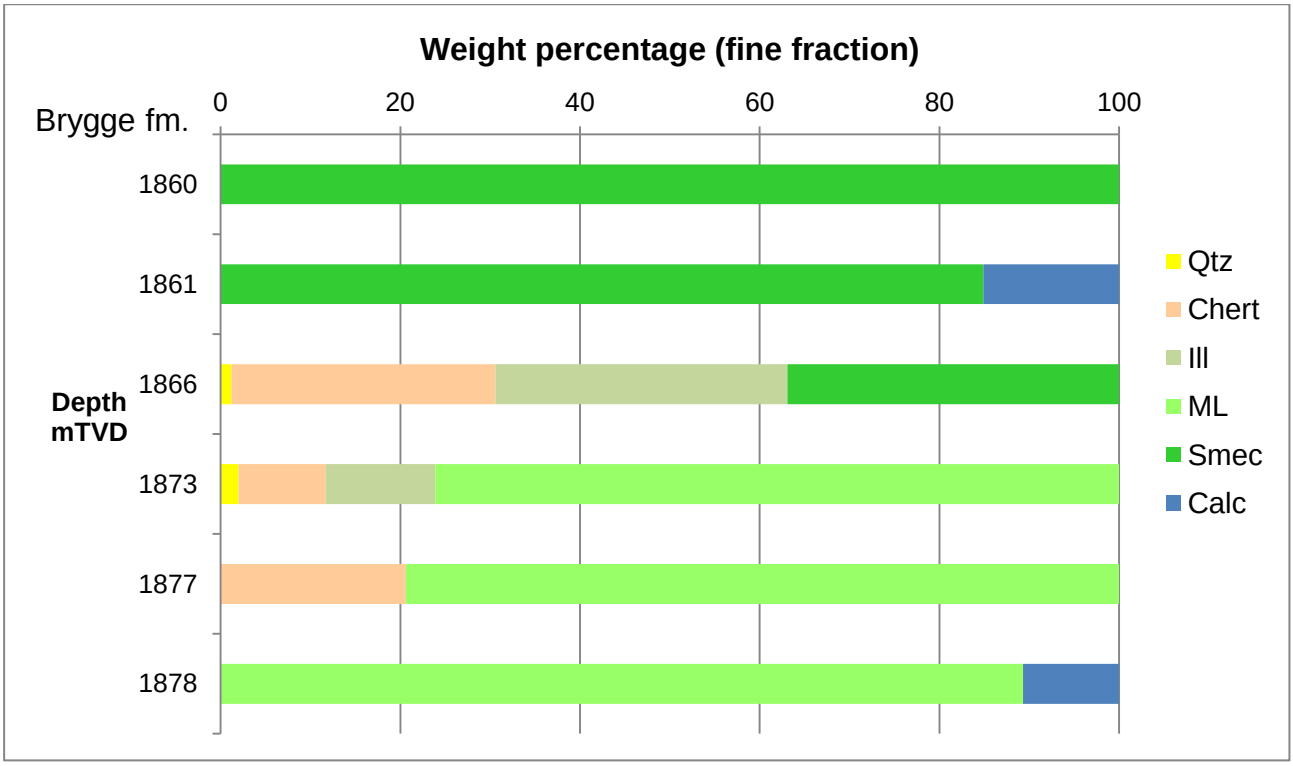

Figure 5.12 Mineralogy well B (fine fraction). Summary for the fine fraction XRD analysis for well B. All the samples are from the Brygge Formation, and the clay content is dominated by smectite and mixed layer clay.

5.3.2 Åsgard

For the Åsgard Field, both well D and F had reports containing XRD analyses, however, it was only well D that had a report possible to use. When looking through the XRD report for well F it quickly became apparent that it was not possible to gain any information from the XRD report due to the poor quality of the figures and tables. Well D had the most extensive set of samples analysed from all the fields.

Well D

The XRD analysis for well D was based on cuttings taken at approximately 40 m intervals and gives a relatively complete picture of both the Kai and the Brygge Formations. The only section missing is the lower part of the Brygge Formation. The samples have been analysed with respect to the same suit of minerals as well A. Figure 5.13 and Figure 5.14 show how easy it is to see clear trends when a large number of samples have been analysed at consequent intervals. In Figure 5.13 the changes in the non-clay fraction is apparent with the decrease in quartz, kalifeldspar and plagioclase with depth. The changes in the clay fraction are seen clearly in Figure 5.14 with the change from a mica/illite dominated Kai Formation and into the smectite dominated Brygge Formation.

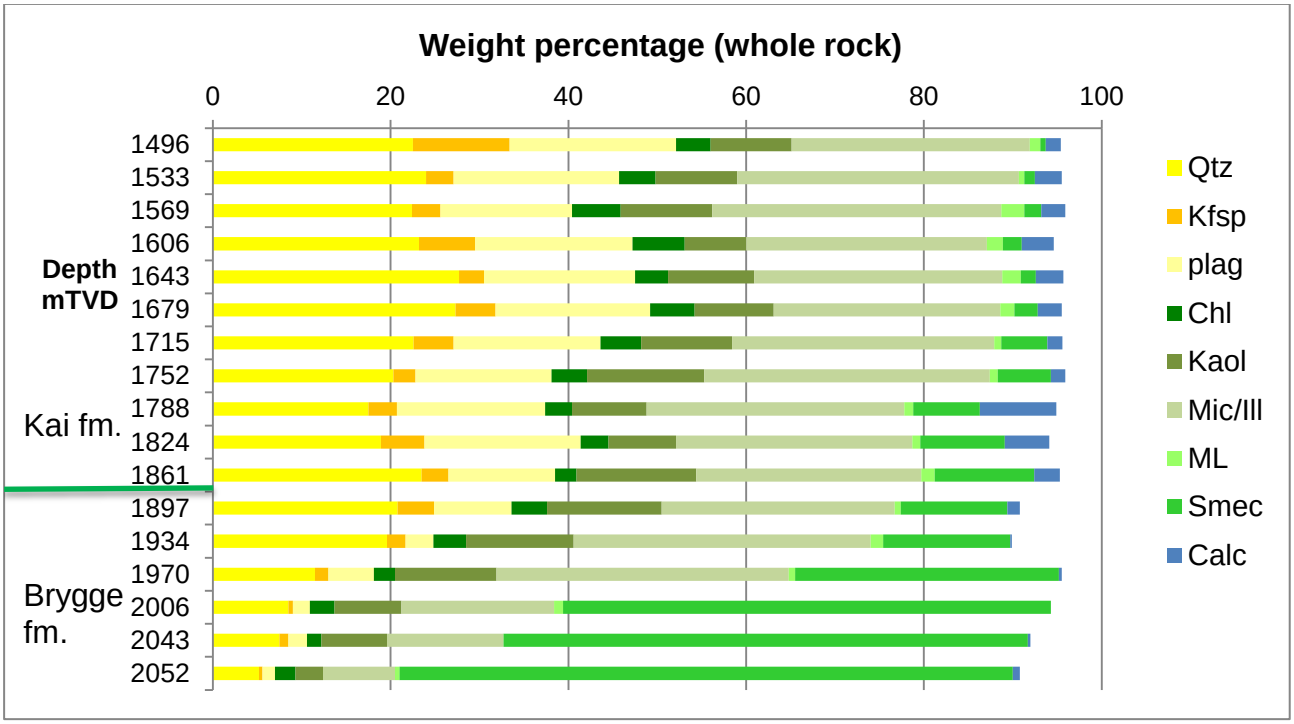

Figure 5.13 Mineralogy well D (whole rock). Summary of the whole rock fraction XRD analysis for well D. The samples from the Kai Formation have high content of non-clay material, mica/illite and kaolinite. The samples from the Brygge Formation have high content of smectite. There is a clear decreasing trend in the non-clay material and the mica/illite content.

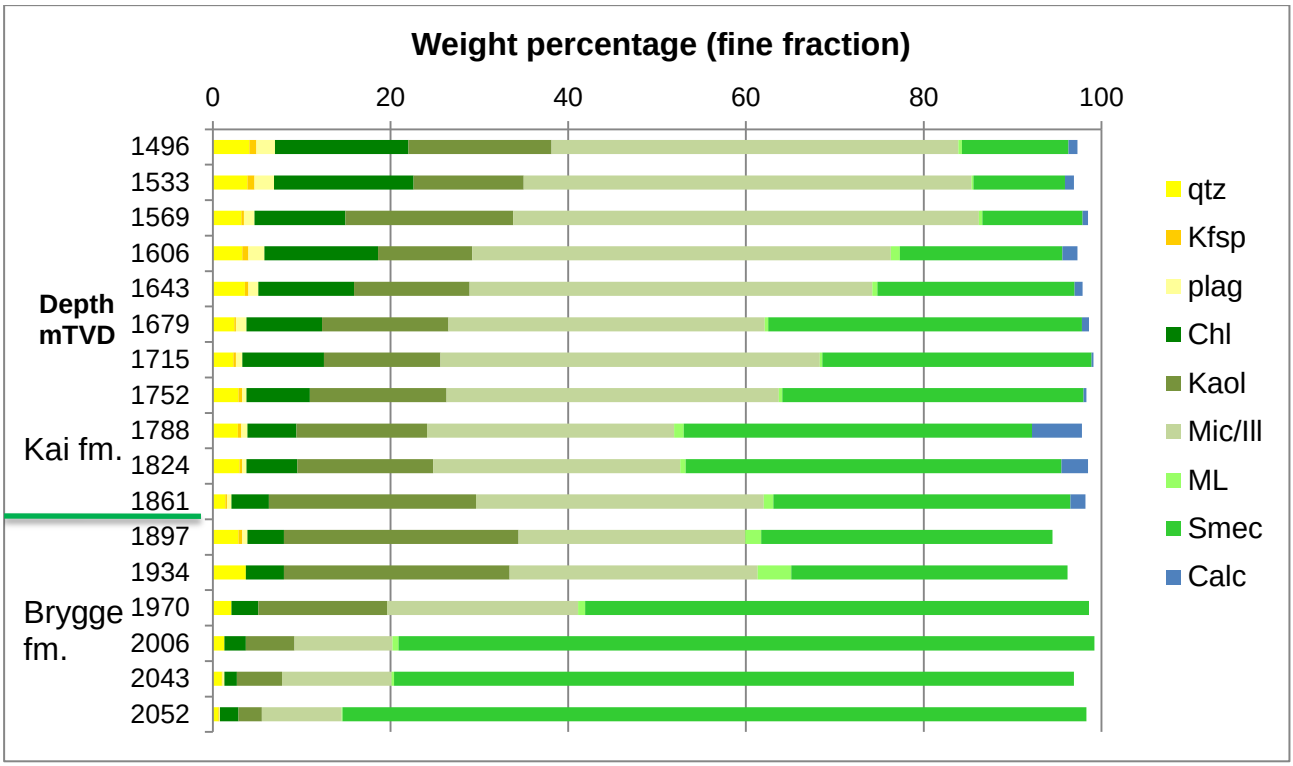

Figure 5.14 Mineralogy well D (fine fraction). Summary of the fine fraction XRD analysis for well D. The trends seen in the whole rock fraction analysis are confirmed in the fine fraction analysis. A clear decrease in mica/illite and kaolinite, and an increase in smectite with increasing depth.

5.3.3 Aasta Hansteen

The report from the Aasta Hansteen Field provided XRD information for all the three wells; however after looking closer at the formation tops it was noticed that the XRD analysis in well G was not located within the interval for the two formations. Apparently a few years ago, after the XRD analysis was completed, a revision of the formation tops was done and the tops in well G was altered enough, so the samples were no longer in the Kai and the Brygge Formations. Therefore, only well H and I are represented below.

Well H

The samples have been taken from three depths in well H; 2116 mTVD in the Kai Formation and 2216 mTVD and 2365 mTVD in the Brygge Formation. There are two samples from 2216 mTVD; the upper from the pale grey cuttings and the lower from the medium grey cuttings. The results from these two samples illustrate the differences in the mineralogy at one depth and how the colour might help to distinguish between the mineralogy. In addition to the usual suit of minerals analysed, vermiculite and pyrite have been added to analysis. At 2365 mTVD in the bulk analysis, the low weight percentage is explained by relatively high

amounts of opal and clinoptilolite (zeolite), which have not been taken into account. The mineralogy shows relatively low amount of non-clay constituents, the clay fraction, however, is dominant and varies a great deal. The sample from the Kai Formation (2116 mTVD) has the highest quartz content and the clay consists of vermiculite, mica/illite and kaolinite. The samples from 2216 mTVD have the same combination, with a slightly higher amount of the vermiculite. The sample from lower Brygge (2365 mTVD), the clay content is lower and the vermiculite is replace by smectite. Smectite and vermiculite are both swelling clays, and might show similar response on the logs and the lithology.

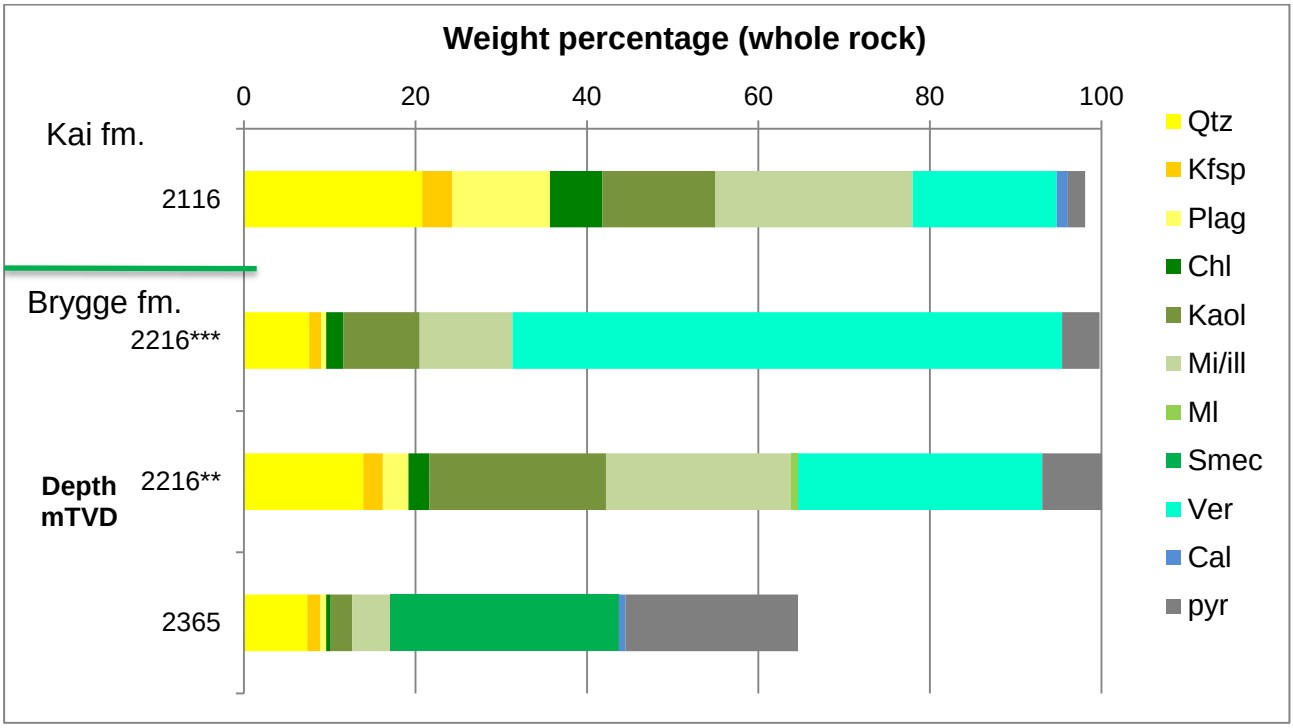

Figure 5.15 Mineralogy well H (whole rock). Summary of the whole rock fraction XRD analysis for well H. The sample from the Kai Formation has high content of non-clay material, kaolinite and mica/illite. The samples from the Brygge Formation have a higher content of the swelling clays; smectite and vermiculite. ** = medium grey cuttings, *** = pale grey cuttings

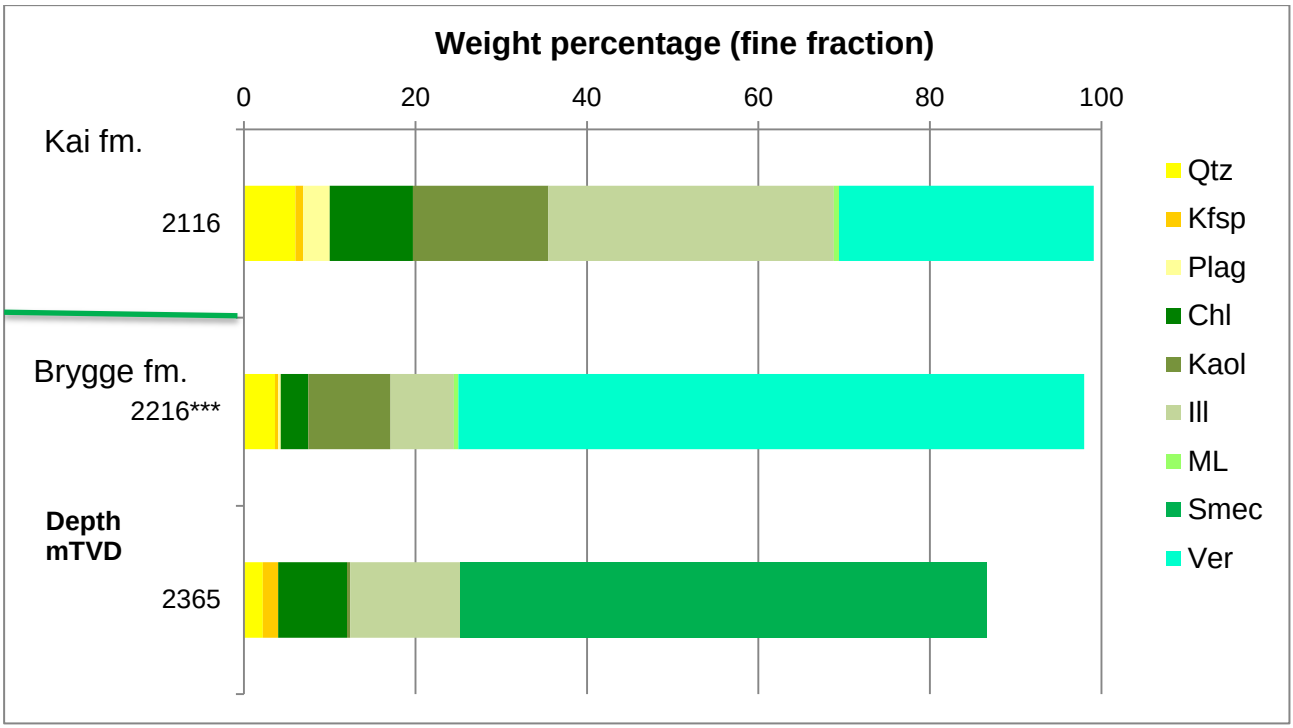

Figure 5.16 Mineralogy well H (fine fraction). Summary of the fine fraction XRD analysis for well H. The fine fraction analysis confirms the results from the whole rock fraction; a clear increase of swelling clays with depth. *** = pale grey cuttings

Well I

Similarly to well H, there are three samples from well I; one from the Kai Formation (2077 mTVD) and two from the Brygge Formation (2127 mTVD and 2157 mTVD). There are two samples taken from 2157 mTVD based on the cuttings colour. If disregarding the pale grey cuttings sample from 2157 mTVD, the other three samples look very similar, with approximately the same amount of the minerals and the same combination. The non-clay content is relatively similar in the whole rock fraction, maybe a slightly higher content of plagioclase. The clay content has a relatively high kaolinite and illite content, but there is still a significant amount of smectite. The pale grey cuttings from 2157 mTVD are dominated by smectite. The mineralogy between well H and I appear to be relatively different, except that the two samples from the Kai Formation are similar when it comes to non-clay content and the clay type distribution.

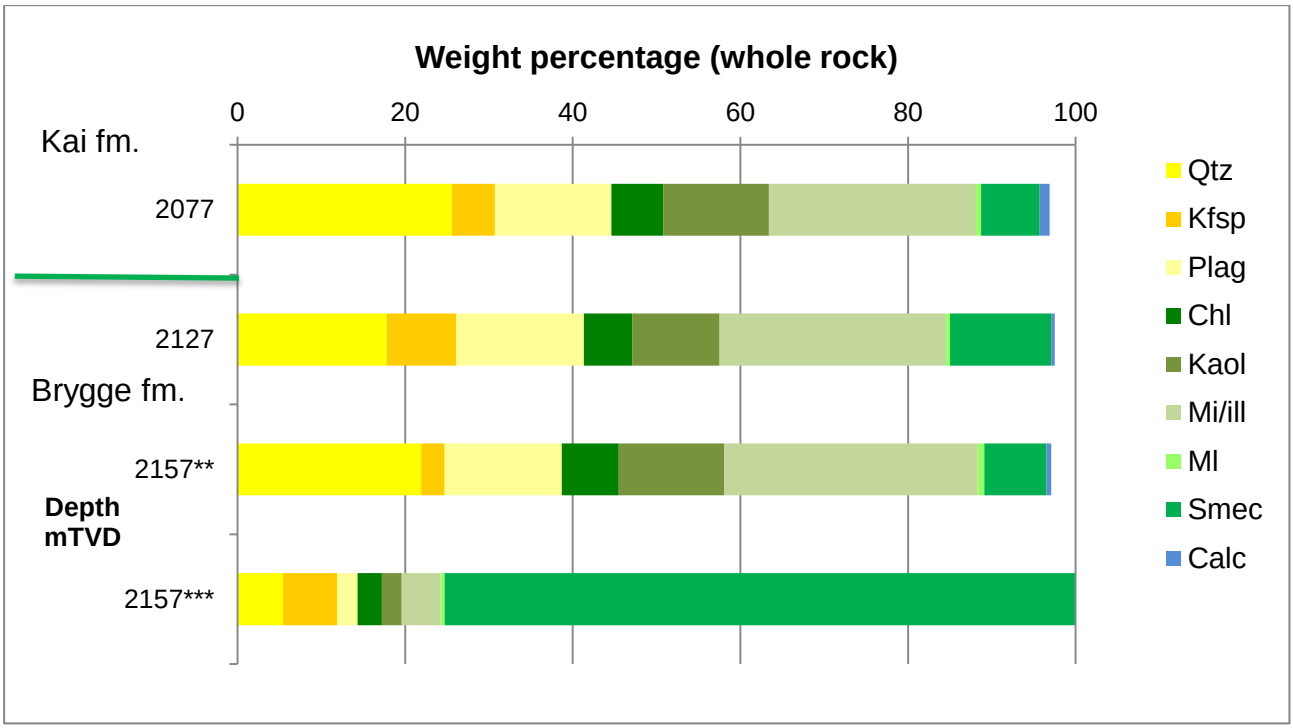

Figure 5.17 Mineralogy well I (whole rock). Summary of the whole rock XRD analysis for well I. All the samples, except the 2357*** have similar mineral distribution, with a high content of non-clay material, mica/illite and kaolinite. ** = medium grey cuttings, *** = pale grey cuttings

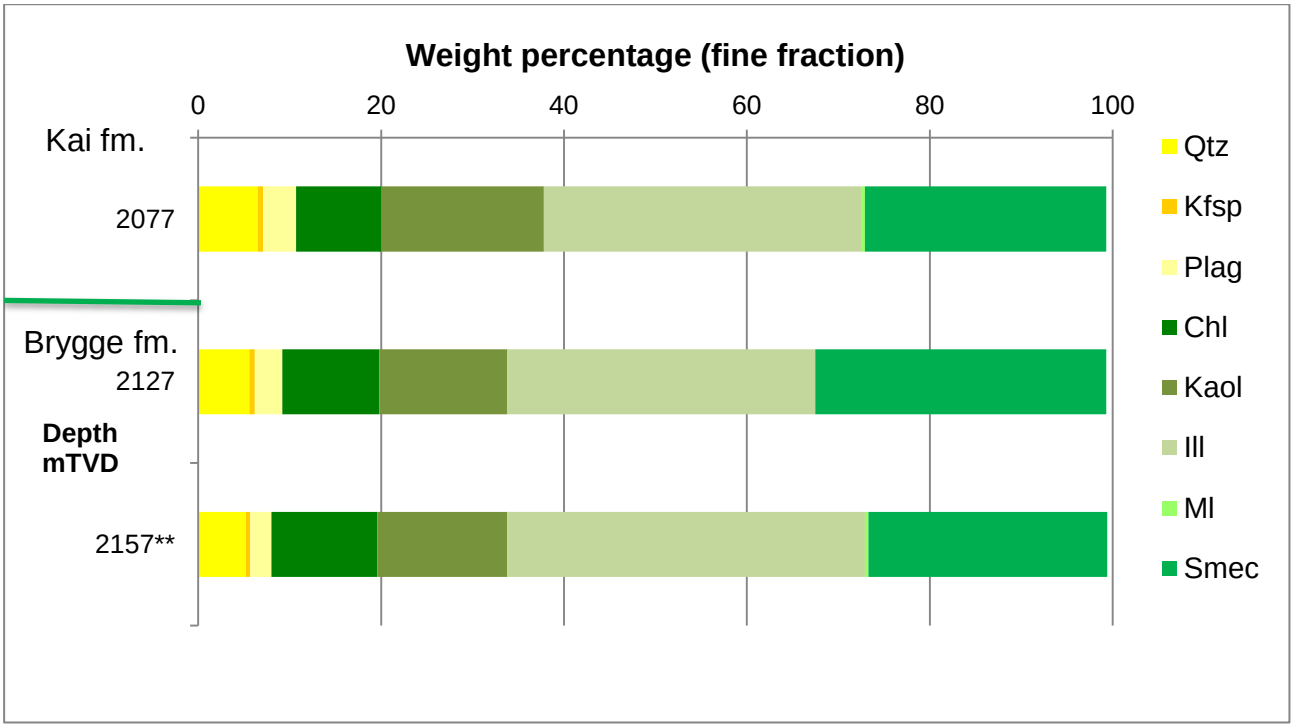

Figure 5.18 Mineralogy well I (fine fraction). Summary of the fine fraction XRD analysis for well I. The fine fraction analysis shows the same results as the whole rock fraction; a similar distribution of the mineralogical content. ** = medium grey cuttings,

5.3.4 Mineralogical summary

Although there are many differences between the wells within the fields and between the fields, there are a few trends that are recurring. In the Kai Formation there is high content of the non-clay material; quartz, kalifeldspar and plagioclase. The clay content dominantly consists of illite, kaolinite and chlorite. At the transition to the Brygge Formation, the non-clay material content decreases significantly and the clay content becomes increasingly smectite-rich. These trends are shown in Figure 5.6 as sector charts representing the common minerals in the two formations.

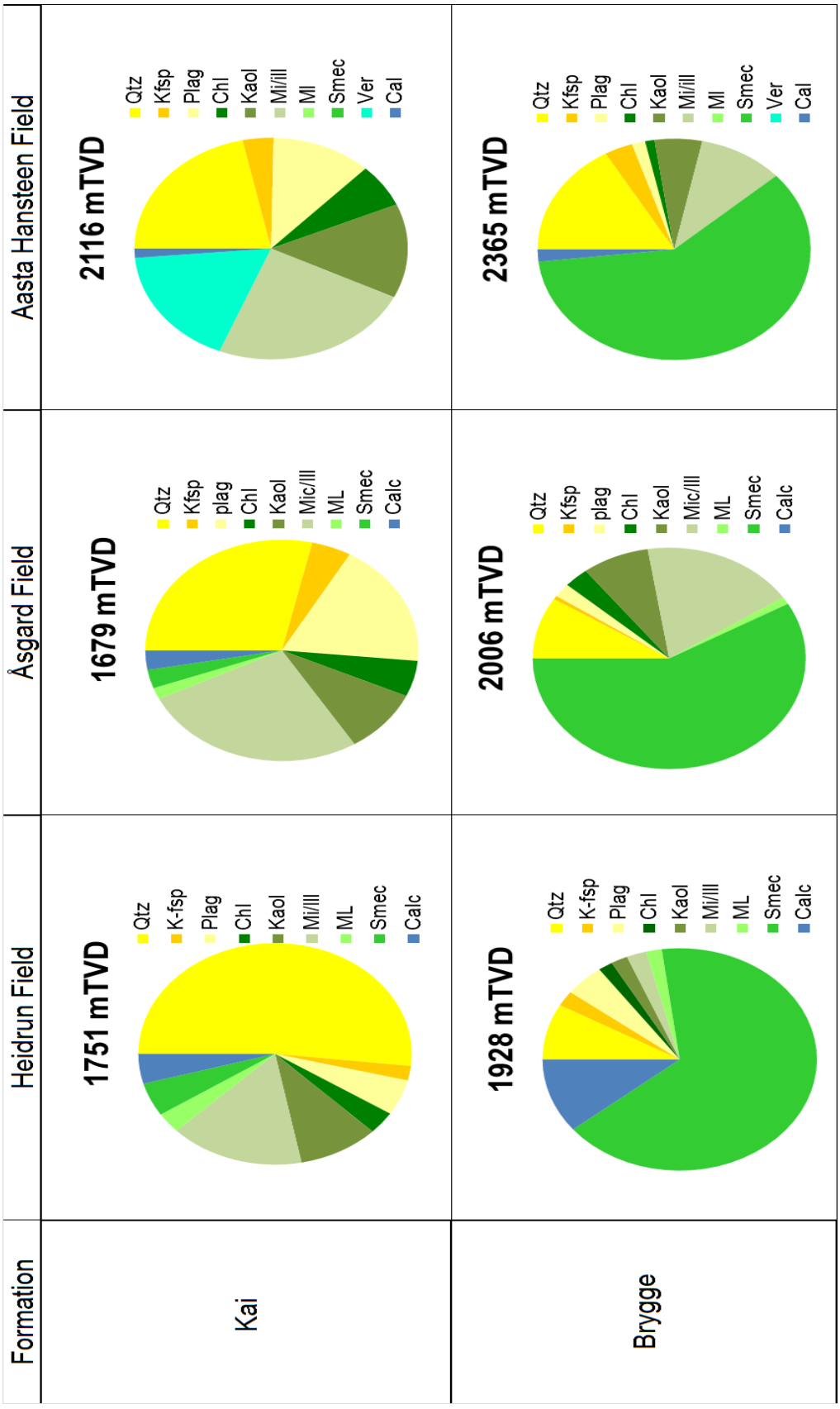

Figure 5.19 Table 5.6 Compilation of mineralogy for the formations. Compilation of representative depths from the Kai and Brygge Formations for each field. Samples from well A was chosen from the Heidrun Field, samples from well D from the Åsgard Field and samples from the Aasta Hansteen Field are taken from well H.

6 Discussion

The question of transferability is not easily answered since the answer is a complex combination of datasets, estimations and assumptions. Taking a step back and looking at the larger picture, the question of transferability has been investigated by doing an analysis of the datasets associated with the use of shale formations as hydraulic barriers; the hierarchy of the investigation can be seen in Figure 6.1. The discussion will follow this hierarchy by starting with a comparison of the datasets, followed by analysis of the use of shale formations as barrier and finally based on the results an assessment of the question of transferability.

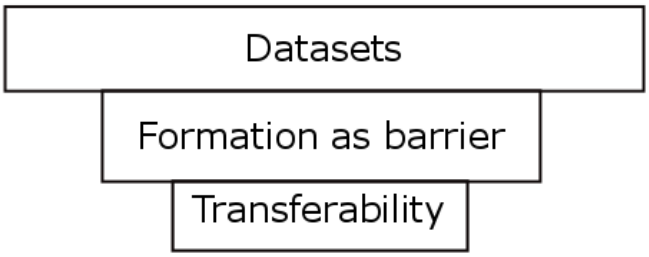

Figure 6.1 Hierarchy of discussion. An illustration of the hierarchy for the categories covered in this thesis

6.1 Correlation and comparison of the results

With the results in mind, it is now possible to see some clear trends in the datasets. After the addition of data from well 0.2, the reference well became a good basis for comparison. The petrophysical logs indicated a relatively homogenous clay formation through the Kai Formation with a few calcite stringers. This was confirmed by the cuttings descriptions and XRD results from well 0.2. The cuttings were described as 100% claystone with minor trace-minerals. The XRD results from the Kai Formation showed claystone with significant amounts of non-clay materials, and the clay content consisting of mica/illite, chlorite and kaolinite, in decreasing order. The fine fraction analysis was done in an attempt to establish the presence of swelling clay. There was, however no clear evidence of swelling and thus not possible to prove any swelling clay. The problem with this kind of evaluation is the possibility that, the clay has changed after being exposed outside the borehole and that it would be difficult to establish any evidence. The question of shale instability in the borehole and in the laboratory is discussed by Wilson and Wilson (2014). They discuss the effect of exposing the clay outside the borehole, and the possible corruption of the clay. They question whether this

gives the correct results in laboratory testing. In the interval analyzed, an assumption can be made based on the fine fraction analysis, that there is no or very little swelling clay in the Kai Formation. In the logs from the reference well, the Brygge Formation shows greater variation than the Kai Formation. The log response in the upper part indicates higher porosity and is often associated with siliceous ooze, often observed in the formation. In the lower part of the Brygge Formation, the log response indicates higher content of clay and possibly more calcite stringers, in any case, a more claystone dominated interval. This information is the basis for the reference well, and this is what will be correlated and compared with the other wells and fields.

The wells on the Heidrun Field all have similar log responses, lithological and mineralogical descriptions. Well A, B and C all show similar log responses compared to well 0; the relatively homogenous claystone through the Kai Formation, and then similar trends into the Brygge Formation, indicating siliceous ooze in the upper part and higher clay content in lower part. The lithology through the Kai Formation in well A, B and C, varies slightly from well 0, with indication of more sand and silt content (Figure 5.5). These are most likely local variations; it is not however, possible to determine if these are regional variations. The mineralogical description gives a more detailed analysis of the clay content. The two samples taken from the Kai Formation in well A are quite similar to the samples from well 0 with respect to low smectite content and significant mica/illite content, in addition to high non-clay content. However to confirm this, more samples from the Kai Formation should be examined. There are no XRD results from the Brygge Formation in the reference well, but well A and B on the other hand are quite well covered, and with the relatively short distance between the wells on the Heidrun Field, it should be possible to extrapolate the results between the wells; especially with the similarity in the logs responses in mind. In well A the core samples have been taken from three strategic depths in the Brygge Formation; at 1827 mTVD in the siliceous ooze deposits, at 1834 mTVD in an apparent calcite stringer and at 1846 mTVD in a claystone interval. With these samples it was possible to see what the mineralogy of these distinctive log responses looked like. The ooze sample had a significant amount of non-clay material, and the clay content was dominated by mica/illite and mixed layer clay, but nothing else to indicate the ooze deposit. The calcite stringer, on the other hand, had dominating calcite content, confirming the presence of a calcite stringer. The clay interval had very little non-clay material and close to 60% smectite. Combining the core samples and the cuttings samples, as have been done in Figure 5.9, it is possible to see the trends in clay content with

increasing depth in well A. At the transition to the Brygge Formation, there is a clear decrease in the kaolinite and mica/illite content and a corresponding increase in smectite content. The results in well B are harder to correlate since the analysis of the core was done with a different purpose; to establish the facies and depositional environment. Nonetheless, in the fine fraction analysis in Figure 5.12 a trend can be seen going from smectite dominated clay content to mixed layer clay content. This trend makes sense diagenetically, when considering the transition from smectite to illite. The problem is that the same change cannot be seen in well A, even though one could assume they would have similar diagenetic changes. It is possible that this is a local phenomenon due to differences in burial or temperature history. The most likely case is however, that the interval is not thick enough to see any diagenetic changes. In any case, there seems to be highest content of smectite and mixed layer clay in the Brygge Formation and highest content of kaolinite, chlorite and illite in the Kai Formation.

The Åsgard Field has, in general, little information compared to the Heidrun Field; still, it is possible to see the same trends on the logs. Well E, the exploration well used to supplement well D, has a log response through the Kai Formation indicating a moderately homogenous claystone. The Brygge Formation also shows similar trends to the reference well, with the general decrease in the log responses (GR, Rt). The lower part of the formation is also represented in well D and F, both showing the same variations in gamma ray and low resistivity, as seen in the reference well. When the resistivity goes below 1 as it does in the Brygge Formation, it is an indication of water in the formation. Usually this might indicate better porosity, in the case of shale however, it might also indicate water expelled from smectite during diagenesis. It is difficult to see any patterns in the lithological descriptions, except it seems to be the same variations between claystone and limestone as in the Heidrun Field. On the other hand, the Brygge Formation on the Åsgard Field seems to have a higher sand content than on the Heidrun Field. Without more data it is not possible to confirm whether this is a regional pattern or due to local variations. The base of the Brygge Formation on the Åsgard Field is located deeper than it is on the Heidrun Field and, since Åsgard is in general further west than Heidrun, there might be some sedimentary differences due to longer transport. The mineralogical analysis within the Åsgard Field is hard to compare since the results from well F are not possible to use. The results from well D, on the other hand, have an incredible coverage of both the Kai and Brygge Formation. The only reason the results from well F are discussed in this thesis, is as an example of the difficulty in finding good results from the overburden claystones. Well D is the well where it is easiest to see the

changes in mineralogy with depth. The upper nine samples through the Kai Formation have high amount of non-clay material and the clay content is dominated by mica/illite and kaolinite. At the transition to the Brygge Formation there is a clear increase in smectite and decrease in the non-clay content and the mica/illite content. The lower samples from the Brygge Formation are almost completely dominated by smectite in the fine fraction analysis. This is the same trend as seen on the Heidrun Field, with a kaolinite and illite dominated Kai Formation and a smectite dominated Brygge Formation.

The Aasta Hansteen Field is very different compared to the other two fields. First of all the water depth is greater and the formations are much deeper and thinner. The log responses are also quite different from those in the Heidrun and Åsgard Fields, in addition to being different within the field. The Kai Formation is extremely thin on the Aasta Hansteen Field, and the log response shows great variations. Instead of a homogenous claystone, there are indications of several sand intervals, which can be seen on both well H and I. Well G logs are of so poor resolution that it is difficult to see any trends. The Brygge Formation has an even more erratic log response, indicating intervals of claystone, limestone and sandstone. Based only on the logs it is not possible to correlate or compare the formations with the reference well, other than to say they are very different. Lithologically, the only similarities between the Aasta Hansteen Field and the other fields is possibly a higher sand content in the Kai Formation and higher calcite content in the Brygge Formation, but only based on this, it is not possible to draw any conclusions concerning the lithology. The mineralogical analysis on the Aasta Hansteen Field was presented in one report, the goal being to examine the ooze deposits, and not the clay formations. The ooze deposits have not been examined, only the clay content as this was the focus in this thesis. This is another example of the difficulty in obtaining good material for comparison between the fields. The XRD results from well H, shows that the sample from the Kai Formation is dominated by kaolinite and mica/illite and the samples from the Brygge Formation are dominated by vermiculite and smectite. This show that even though the log responses and the lithology might be very different from the Heidrun and Åsgard Fields, the mineralogy appear to be somewhat similar. Well I does not show the same transition between the Kai and Brygge Formation, but appear to have the same mineralogy through both formations, with high amount of mica/illite and kaolinite, but also a significant amount of smectite. The result from well I does not follow the same trend as the Heidrun well, and based on the mineralogy, one could almost think all the samples were taken from the Kai Formation.

6.2 Regional and vertical variations

This summary of the results shows there are several variations both regionally and vertically. The regional differences are commonly associated with changes in provenance and sediment influx. According to Marcussen et al. (2009) and Peltonen et al. (2008), the vertical changes are often associated with diagenetic alteration, burial and temperature history.

The regional variations in the area must be looked at from two perspective scales; the variations between the Heidrun Field and the Åsgard Field, within the Halten Terrace, and the variations between the Halten Terrace and the Aasta Hansteen Field. Within the Halten Terrace, there seems to be relatively little variation between the Heidrun and Åsgard Fields, their logs correspond well, the lithology corresponds relatively well and the mineralogy in well A and well D follow the same trends. A slight difference between the two is the depth of the formation tops, but it is unlikely enough to see changes due to diagenesis. The Kai Formation can be correlated across the area relatively well, as can be seen on Figure 5.1. The base of Brygge, however, is slightly deeper on the Åsgard Field. This is explained by the outbuilding sequence of the formations on the Mid-Norwegian Margin as illustrated on Figure 2.5. The variations between the Halten Terrace and the Aasta Hansteen Field are much greater and can be seen by the formation tops, the logs and the lithology. The mineralogy on the other hand is more similar than expected. According to both Marcussen et al. (2009) and Peltonen et al. (2008), there is a clear decreasing trend in the smectite content and amount from south to north, seen in both the North Sea and in the Vøring Basin. The reason being the southernmost areas were closest to the discharge of volcanism during the opening of the Atlantic. Thus one might expect very little to no smectite on the Aasta Hansteen Field. The XRD analyses from both well H and I contain swelling clays in the form of smectite and vermiculite, with the highest amount being in the Brygge Formation. However, based only on these six samples, it is difficult to see if this is just local or applies to the whole area. The other major differences between the Halten Terrace and the Aasta Hansteen Field, is the thickness and depth of the formations. The thinner and deeper intervals of the formations are linked to the fact that the basins further north are narrower and deeper (Figure 3.3), and the main sediment influx was further south than the Nyk High and the Aasta Hansteen Field. Another theory discussed by Peltonen et al. (2008) is that there might be a regional difference in the amount of kaolinite and non-clay material with closer proximity to the source of terrestrial sediments, i.e. the uplifted Norwegian mainland. With this theory in mind a comparison of the non-clay material and kaolinite in the Heidrun Field and the Åsgard field

did not give any conclusive results. It is possible that the two fields are too close to show any major differences in the sediments output from source. The Aasta Hansteen Field, on the other hand, has in general less non-clay material, but the presence of the ooze deposits is a testament to the great distance from the sediment source and the water depth.

The vertical variations can also clearly be seen through the two formations. The logs show the transition between the two formations and several variations within the formations. The homogenous claystone in the Kai Formation can be seen across both the Heidrun and Åsgard Fields, with the noticeable calcite stringers. The vertical transition into the Brygge Formation is marked by the beginning of the siliceous ooze, which is evident across the two fields on the Halten Terrace. The increasing clay content with depth can also be correlated across the logs on the Halten Terrace. The same transition is not observable on the Aasta Hansteen Field; neither are the variations in the lithology the same as they are on the Halten Terrace. The lithology on the Halten Terrace goes from a claystone with sand and silt domination in the Kai Formation to the limestone dominated Brygge Formation. The vertical variations in lithology between the two formations are most likely associated with the depositional environment. According to Dalland et al. (1988), both formations were deposited in marine environment, but the Kai Formation was deposited during a time with great variations in the water depth, depositing sand. The marine environment during the deposition of the Brygge Formation was possibly better for the formation of limestone. It is also important to remember that the Kai Formation was deposited as a result of uplift and regression on top of the mid-Miocene unconformity, so the transition between the two formations is not only lithological but also a separation in time.

There are two types of changes that occur in claystone with depth; compaction and diagenesis. Peltonen et al. (2008) discuss both topics in their study of the mudstones in the Norwegian Sea. On the topic of compaction, the results show that the smectite content will have great effect on the mudstone compaction trend and the resulting log responses. Overpressure is often a result from the expulsion of water from smectite and often gives unexpected log responses, if one is not aware of the smectite content. In the discussion of mudstone diagenesis, the smectite to illite reaction is the main topic. The stability of smectite is associated with the changes in temperature, and at temperatures around 60-80˚C, smectite becomes unstable. This, however, does not explain the vertical variations seen in the results from Heidrun and Åsgard. In the mineralogical results, it is the oldest Brygge Formation which has the highest amount of smectite and the overlying Kai Formation has the highest

amount of illite, which is the opposite of what is expected by diagenetic changes. So the vertical variations cannot be explained by diagenetic alterations. In the study of the North Sea, Marcussen et al. (2009) points out that, at depths around 2km (base of the Brygge Formation), the temperature is approximately 70˚C, and since the formations in question range from 1,4km to 2km, very little diagenetic change would have occurred through the formations. The only possible sign of any diagenetic alterations might be seen in well B, Figure 5.12, in which there is a transition from dominating smectite content to dominating mixed layer clay content. As mentioned this is unlikely, if you take the short sampling interval into account and the shallow depth. The explanation for the variations is more likely linked to the sedimentary source. The smectite content in the Brygge Formation is a result of erosion of the volcanic basalts in the south. The relatively high content of illite and kaolinite in the Kai Formation is due to the erosion and transport of sediments from the uplifted Norwegian mainland.

According to both Marcussen et al. (2009) and Peltonen et al. (2008) it is the clay content that has the most significant effect on the physical properties in a formation, and then especially the smectite content. Illite and kaolinite are relatively stable clay minerals, and even though there have been some recent discussions on the matter by Wilson and Wilson (2014), they are easier to predict than smectite. Swelling clays (smectite and vermiculite), on the other hand, are highly unstable both when it comes to swelling behavior and diagenetic alteration. The effect on logs is not easy to predict due to the relatively high porosity and the possibility of overpressure, and Marcussen et al. (2009) observe that only 5% smectite is enough to affect the logs. From the mineralogical results, it appear that the clay in the Kai Formation, consisting mostly of illite, kaolinite and chlorite, would have a more stable behavior than the smectite and mixed layer clay dominated Brygge Formation.

6.3 Shale formation as a barrier

From the discussion above it is clear that the Kai Formation appears to be the most stable and homogenous of the two clays formation. The interval is already confirmed as a hydraulic barrier in well 0 and according to the log and the lithology, is dominated by claystone with traces of pyrite, calcite and other non-clay material. The XRD results show that the clay content consists mostly of mica/illite, kaolinite and chlorite. There was no or very little evidence of swelling clays. Across the Heidrun Field it appears that the same interval has the same log response, lithology (with only minor differences) and the same mineralogy. It is for this reason the Kai Formation has been confirmed as a hydraulic barrier across the Heidrun Field. The Brygge Formation has not been confirmed as a barrier in any of the fields, and with

the great variations within the formation it will probably be difficult to find a good interval to use as barrier. The only possible interval might be in the lower part of the Brygge Formation, where it might be a better claystone. The only problem then would be if the smectite-rich claystone is suitable for a barrier or not, when considering the instability of the smectite. Other than that it appears that the datasets from the Brygge Formation are fairly similar across the Heidrun Field. And if the Brygge Formation was ever to be confirmed as a barrier, it would probably be possible to correlate the confirmed interval across the Heidrun Field.

The Åsgard Field is relatively easy to correlate across from the Heidrun Field, however due to the limited amount of information; especially in the Kai Formation it is difficult to draw any conclusion. However, based on the little information available, the Kai Formation appear to have similar depth and interval across the two fields, and the logs appear to be fairly consequent. The best source of information is the XRD analysis in well D and the mineralogy appear to be corresponding when considering the clay type and content. The Kai Formation appears to have the same stable suite of minerals consisting of mica/illite, kaolinite and chlorite on both fields. Based only on this information, there is a possibility that the Kai Formation would show the same barrier properties as it did on the Heidrun Field, but without more information from the logs, the lithology and mineralogy it is not possible to draw any conclusions. The Brygge Formation on the Åsgard Field has a thicker interval and the base is located deeper, than on the Heidrun Field. At the same time, the logs, the lithology and the mineralogy match the results from the Heidrun field, but it is still the same case as above, without more information it is not possible to draw any conclusions concerning the direct transferability of the results from the Heidrun Field.

The Aasta Hansteen Field has a better coverage of information, than the Åsgard Field, but already from the starting point, looking at the formation tops it was evident that correlating the formations across this distance would not be possible. The logs and the lithology gave very little indications of any similarities between the Aasta Hansteen Field and the Halten Terrace. The Kai Formation was too thin and the indications of ooze intervals did not match the Kai Formation on the Halten Terrace. The only possible similarity to be found was the mineralogy. The same suit of minerals was found in the Kai Formation on the Aasta Hansteen Field consisting of the stable minerals, while in the Brygge Formation there was a higher content of the swelling clays. The rest of the information from the Brygge Formation did not, however, give any good indications for the transferability of data between the two areas.

6.4 Transferability

The question of transferability of datasets between fields is extremely complex and intricate. However, based on the results and the discussion above, the resulting method seems to be viable for these kinds of datasets. In the end the method can be summarized as the following steps:

1. Determine the topic for investigation
2. Collect all available information for a suitable number of fields and wells
3. Organize the information in a logical manner and determine if more information is needed
4. If so, do the necessary tests or laboratory work to add the missing information
5. Compare and correlate the information to give a complete picture
6. Draw conclusions

This method is a general workflow, which also works for other type topics and investigations. The main challenge is often to simplify the material, without taking away all the details and data points that will make it possible to correlate between the formations.

Another challenge with these kinds of datasets is all the possible sources of errors and mistakes that can be made. First off, when considering petrophysical logs there are a certain amount of errors linked to the logging and measuring downhole, in addition to the possible errors during interpretation. Secondly, all the lithological descriptions are done by various geologists, all with their own set of references when it comes to interpretation. Finally, the XRD analyses are often done by different laboratories and different interpreters, and the identification of minerals based on the diffractograms requires lots of experience. These are just a few examples of the possible sources of errors in this kind of project. However, one cannot take all this into account; otherwise it would not be possible to draw any conclusions.

The feasibility of transferability is highly dependent on the amount of data one has available. Working at a company where all the data is available at all times and where one has access to software like Stratworks, will make correlations easier. As a student, working with a limited amount of data, and having to wait for access to be granted by partners, it becomes a relatively time consuming process. However, the literature research necessary for the fundamental understanding of the formations and topics covered in this thesis, takes a significant amount of time. And if you consider the hourly cost of an employee, in addition to the necessary tests and laboratory work if there is any missing information, the cost becomes

considerable. It then raises the question; which is most cost efficient, the transferability of data or just doing the necessary conventional tests without doing any research beforehand? This thesis will not go into the exact costs of the different methods, so the question still remains.

6.5 Further work

This thesis has been limited to a few sets of data; petrophysical logs, lithological descriptions and mineralogical analyses. The mineralogical analysis was based on XRD information from the reports. The reports also contained SEM information which was not used in this thesis, but might have been a good supplement in an extended project. To obtain a complete picture, a much larger set of data is necessary, in addition to adding more fields and formations. This thesis has not taken into account datasets related to rock-mechanical aspects, such as strength and pressure tests, or geochemical aspects, such as carbon content. Another possible approach is to use geoseismic data to correlate the formations on a larger scale. To obtain a complete picture of the formations it would be necessary to add datasets concerning these aspects. In order for this project to be completely scientific and falsifiable, all the previous logs, lithological descriptions and mineralogical analyses, should have been taken again to investigate if the same results were obtainable. However, this is not feasible and will never be prioritized in the economic situation today.

The probably most important, although, challenging question, concerning using formation as a barrier is; what is the exact cause for the properties found in the intervals where formation collapse or creep is observed? Is it linked to the amount of smectite, or possibly to the absence of smectite? Why do some intervals, in the same formation, experience creep, while others do not? Is it linked to the strength and brittleness or to the ductile nature of the claystone? All of these questions need to be answered before one can develop an optimized method for transferability of datasets associated with the use of shale formation as barrier.

7 Conclusion

Considering the transferability of datasets associated with the use of shale formations as barrier and the method used to find the results, a statement can be made for the chosen fields.

- Transferability of datasets within the Heidrun Field is easily done due to the close proximity of the wells and the available information. The Kai Formation has already been confirmed as a barrier and the results from this thesis support this confirmation. The Brygge Formation has not been confirmed as a barrier and due to the great variations within the formation it might be difficult to find a good interval. However, if a good interval is confirmed, transferability of datasets across the Heidrun Field should be feasible.
- Transferring the datasets from the Heidrun Field to the Åsgard Field proved possible, even with the limited information available. The similarities between the Kai Formation in the two fields make it possible to correlate the datasets, and transferability should be feasible. The Brygge Formation is slightly different on the Åsgard Field, but there are enough similarities to correlate across the two fields, making transferability of datasets viable. However, without a confirmed interval in the Brygge Formation, no conclusive statements can be made.
- Transferability between the Halten Terrace and Aasta Hansteen proved difficult due to the long distance and the major difference between the formations. It was not possible to correlate either the Kai Formation or the Brygge Formation across the areas, and transferability of datasets is not suitable under the circumstances.

Some general remarks can be made for the two formations. The Kai Formation is a homogenous claystone with varying amounts of sand. The mineralogy consists of high amount of non-clay material; quartz, kalifeldspar and plagioclase and the clay content is dominated by illite, kaolinite and chlorite. These minerals are considered relatively stable and make up the barrier interval in the Kai Formation. The Brygge Formation is less homogenous with a higher content of limestone. There are indications of several lithological intervals consisting of ooze deposits, calcite stringer and shale. The mineralogy is dominated by clay which is rich in smectite and mixed-layer clay.

The method for transferring datasets, is in itself viable, and can be used for other similar projects. However, it is a general approach, and further work is necessary to optimize the datasets and amount of data. The feasibility of transferring datasets between fields is dependent on previous knowledge of the area, the available data and the opportunity to do more tests and gather more samples if necessary. The vertical differences can best be examined with samples taken at consequent intervals covering the formations. The regional differences can best be examined by comparing the distribution of the content in the samples over a large area. Comparing the costs and amount of work in this kind of project with conventional testing (strength and pressure tests) during drilling, it will probably be less expensive and more efficient to do the conventional testing of the intervals in questions, rather than initiate a transferability of data project.

8 References

ALMON, W. R. & DAVIES, D. K. 1981. Formation damage and the crystal chemistry of clays. *Short course in clays and the resource geologist: Montreal, Mineralogical Association of Canada,* 7**,** 81-102.

ASQUITH, G. B. & KRYGOWSKI, D. 2004. *Basic well log analysis,* Tulsa, Okla., American Association of Petroleum Geologists.

BERNDT, C., BUENZ, S. & MIENERT, J. 2003. Polygonal fault systems on the mid-Norwegian margin; a long-term source for fluid flow. *Geological Society Special Publications,* 216**,** 283-290.

BJØRLYKKE, K. 2010. Sedimentary Geochemistry *In:* BJORLYKKE, K. (ed.) *Petroleum geoscience: From sedimentary environments to rock physics.* Springer Science & Business Media.

BLYSTAD, P., FÆRSETH, R., LARSEN, B., SKOGSEID, J. & TØRUDBAKKEN, B. 1995. Structural elements of the Norwegian continental margin between 62 and 69 N. *Norwegian Petroleum Directorate Bulletin,* 8**,** 45.

BOGGS, S. 2009. Mudstones and shales. *In:* BOGGS, S. (ed.) *Petrology of sedimentary rocks.* 2nd ed.: Cambridge University Press.

CHAND, S., RISE, L., KNIES, J., HAFLIDASON, H., HJELSTUEN, B. O. & BØE, R. 2011. Stratigraphic development of the south Vøring margin (Mid-Norway) since early Cenozoic time and its influence on subsurface fluid flow. *Marine and Petroleum Geology,* 28**,** 1350-1363.

DALLAND, A., WORSLEY, D. & OFSTAD, K. 1988. *A Lithostratigraphic Scheme for the Mesozoic and Cenozoic and Succession Offshore Mid-and Northern Norway*, Oljedirektoratet.

EIDVIN, T., BUGGE, T. & SMELROR, M. 2007. The Molo Formation, deposited by coastal progradation on the inner Mid-Norwegion continental shelf, coeval with the Kai Formation to the west and the Utsira Formation in the North Sea. *Norsk Geologisk Tidsskrift,* 87**,** 75.

ELDHOLM, O., TSIKALAS, F. & FALEIDE, J. 2002. Continental margin off Norway 62–75° N: Palaeogene tectono-magmatic segmentation and sedimentation. *Geological Society, London, Special Publications,* 197**,** 39-68.

ESLINGER, E. & PEVEAR, D. 1988. *Clay minerals for petroleum geologists and engineers,* Tulsa, Okla., SEPM.

FALEIDE, J. I., TSIKALAS, F., BREIVIK, A. J., MJELDE, R., RITZMANN, O., ENGEN, O., WILSON, J. & ELDHOLM, O. 2008. Structure and evolution of the continental margin off Norway and the Barents Sea. *Episodes,* 31**,** 82-91.

FORSBERG, C. F. & LOCAT, J. 2005. Mineralogical and microstructural development of the sediments on the mid-Norwegian margin. *Marine and Petroleum Geology,* 22**,** 109-122.

HIGGINS, J. A. & SCHRAG, D. P. 2006. Beyond methane: Towards a theory for the Paleocene-Eocene Thermal Maximum. *Earth and Planetary Science Letters,* 245**,** 523-37.

JACKSON, J. S., ARTHUR, T., OLSON, R. C. & TOWER, D. B. 2006. The Heidrun Field, offshore mid-Norway. *Abstracts: Annual Meeting - American Association of Petroleum Geologists,* 15**,** 52.

LIVERSIDGE, D., TAOUTAOU, S. & AGARWAL, S. Permanent plug and abandonment solution for the North Sea. SPE Asia Pacific Oil & Gas Conference and Exhibition, 2006. Society of Petroleum Engineers.

LØSETH, H. & HENRIKSEN, S. A Middle to Late Miocene compression phase along the Norwegian passive margin. Geological Society, London, Petroleum Geology Conference series, 2005. Geological Society of London, 845-859.

MARCUSSEN, O., THYBERG, B. I., PELTONEN, C., JAHREN, J., BJORLYKKE, K. & FALEIDE, J. I. 2009. Physical properties of Cenozoic mudstones from the northern North Sea; impact of clay mineralogy on compaction trends. *AAPG Bulletin,* 93**,** 127-150.

MARTINSEN, O. & NØTTVEDT, A. 2007. Av hav stiger landet; Paleogene og neogene (kenozoikum), kontinentene av i dag formes; 66-2,7 Ma. *In:* RAMBERG, I. B., BRYHNI, I. & NØTTVEDT, A. (eds.) *Landet blir til; Norges geologi.* 2 ed. Trondheim: Norsk Geologisk Forening.

MOORE, D. M. & REYNOLDS, R. C. 1989. *X-ray Diffraction and the Identification and Analysis of Clay Minerals*, Oxford university press Oxford.

PELTONEN, C., MARCUSSEN, O., BJORLYKKE, K. & JAHREN, J. 2008. Mineralogical control on mudstone compaction; a study of Late Cretaceous to early Tertiary mudstones of the Voring and More Basins, Norwegian Sea. *Petroleum Geoscience,* 14**,** 127-138.

RASMUSSEN, E. S., HEILMANN-CLAUSEN, C., WAAGSTEIN, R. & EIDVIN, T. 2008. The Tertiary of Norden. *Episodes,* 31**,** 66-72.

RIDER, M. H. 1986. Lithology reconstruction from logs. *In:* RIDER, M. H. (ed.) *The geological interpretation of well logs.* BlackieJohn Wiley and Sons, Glasgow, United KingdomNew York, NY, United States.

RÖSER, G. 2007. *Petrography, physical properties, and geotechnical behavior of modern sediments, Southern Chile Trench.* Universitätsbibliothek Freiburg.

STOREY, M., DUNCAN, R. A. & SWISHER, C. C., III 2007. Paleocene-Eocene Thermal Maximum and the opening of the Northeast Atlantic. *Science,* 316**,** 587-589.

STUEVOLD, L. M. & ELDHOLM, O. 1996. Cenozoic uplift of Fennoscandia inferred from a study of the mid-Norwegian margin. *Global and Planetary Change,* 12**,** 359-386.

THE NORWEGIAN PETROLEUM DIRECTORATE. 2014a. *NPD Fact Maps* [Online]. Available: http://gis.npd.no/factmaps/html_20/ [Accessed 24.11 2014].

THE NORWEGIAN PETROLEUM DIRECTORATE. 2014b. *NPD Fact Pages 6507/7-2* [Online]. Available: http://factpages.npd.no/ReportServer?/FactPages/PageView/wellbore_exploration&rs:Command=Render&rc:Toolbar=false&rc:Parameters=f&NpdId=464&IpAddress=78.91.31.139&CultureCode=nb-no [Accessed 21.10 2014].

THE NORWEGIAN PETROLEUM DIRECTORATE. 2014c. *NPD Fact Pages Fields* [Online]. Available: http://factpages.npd.no/factpages/Default.aspx?culture=no [Accessed 14.11 2014].

THE STANDARDS ORGANISATION IN NORWAY (NORSOK) 2004. Standard D-010. *Well integrity in drilling and well operation (rev. 3, August 2004)* Lysaker: The Norwegian Oil Industry Association (OLF) and Federation of Norwegian Manufactering Industries (TBL).

TORSOY, T. THE åSGARD FIELD–NORWAY'S BIGGEST OFFSHORE CHALLENGE TO DATE. 16th World Petroleum Congress, 2000. World Petroleum Congress.

WALKER, J. D., GEISSMAN, J. W., BOWRING, S. A. & BABCOCK, L. E. 2012. GSA Geologial Time Scale v. 4.0: Geological Society of America. v. 4.0 ed.: Geological Society of America.

WHITLEY, P. K. 1992. The geology of Heidrun; a giant oil and gas field on the mid-Norwegian shelf. *AAPG Memoir,* 54**,** 383-406.

WILL, G. 2006. *Powder diffraction; the Rietveld method and the two-stage method*, Springer-Verlag Berlin Heidelberg, Berlin, Federal Republic of Germany.

WILLIAMS, S., CARLSEN, T., CONSTABLE, K. & GULDAHL, A. Identification and qualification of shale annular barriers using wireline logs during plug and abandonment operations. SPE/IADC Drilling Conference and Exhibition 2009, March 17, 2009 - March 19, 2009, 2009 Amsterdam, Netherlands. Society of Petroleum Engineers (SPE), 342-356.

WILSON, M. J. & WILSON, L. 2014. Clay mineralogy and shale instability; an alternative conceptual analysis. *Clay Minerals,* 49**,** 127-145.

ZACHOS, J., PAGANI, M., SLOAN, L., THOMAS, E. & BILLUPS, K. 2001. Trends, rhythms, and aberrations in global climate 65 Ma to present. *Science,* 292**,** 686-93.

Appendix

Appendix A: Diffractograms of the XRD analysis of the reference well

Appendix B: Petrophysical logs

Appendix C: Cuttings descriptions

Appendix D: Mineralogical analyses

Appendix A

- Diffractograms for whole rock fraction XRD analysis from well 0.2
- Diffractograms for fine fraction XRD analysis from well 0.2

Whole rock fraction XRD results from well 0.2 (Heidrun Field)

Heidrun Field, well 0.2, Kai Formation (1810mMD)

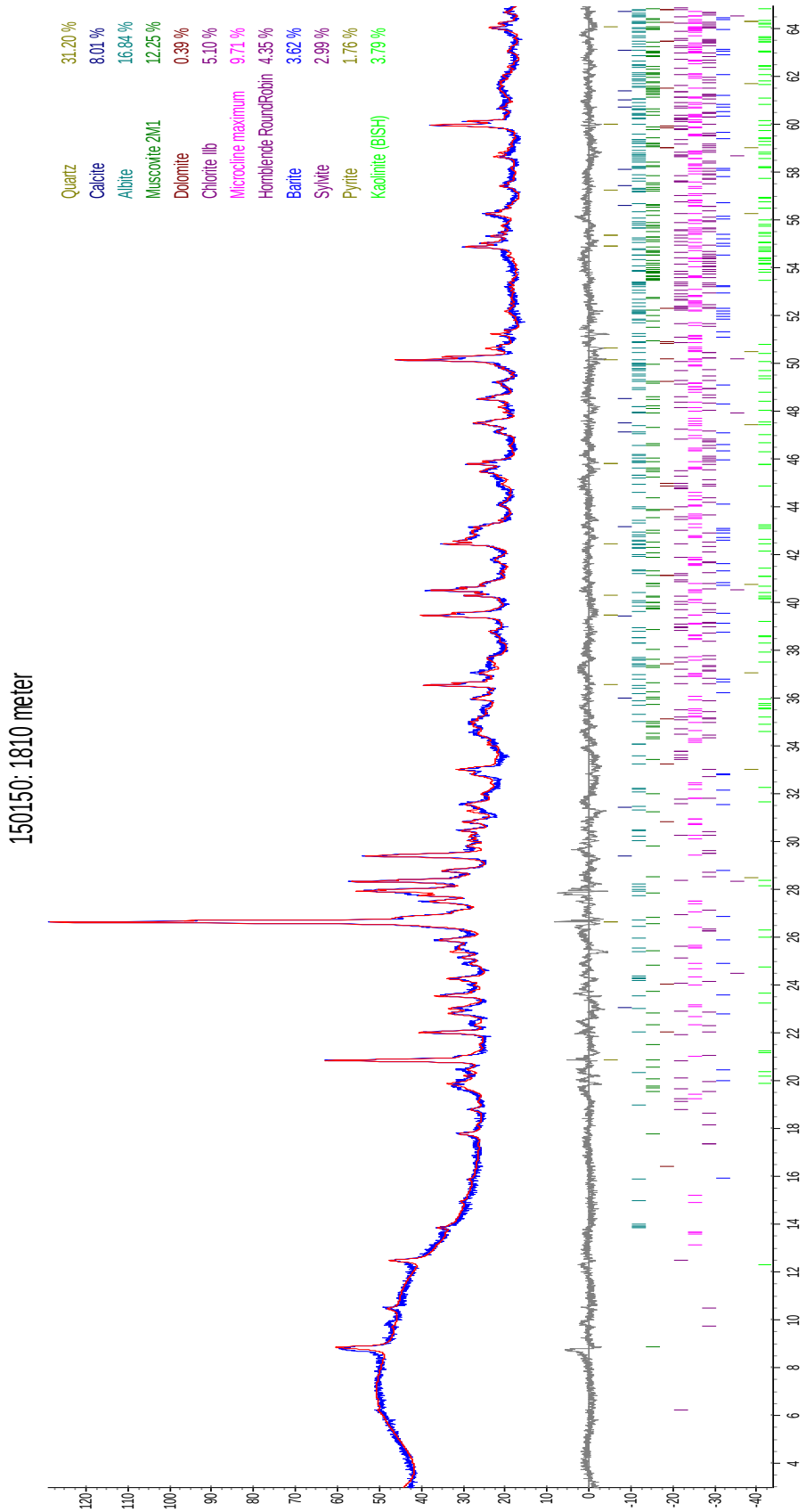

Heidrun Field, well 0.2, Kai Formation (1820mMD)

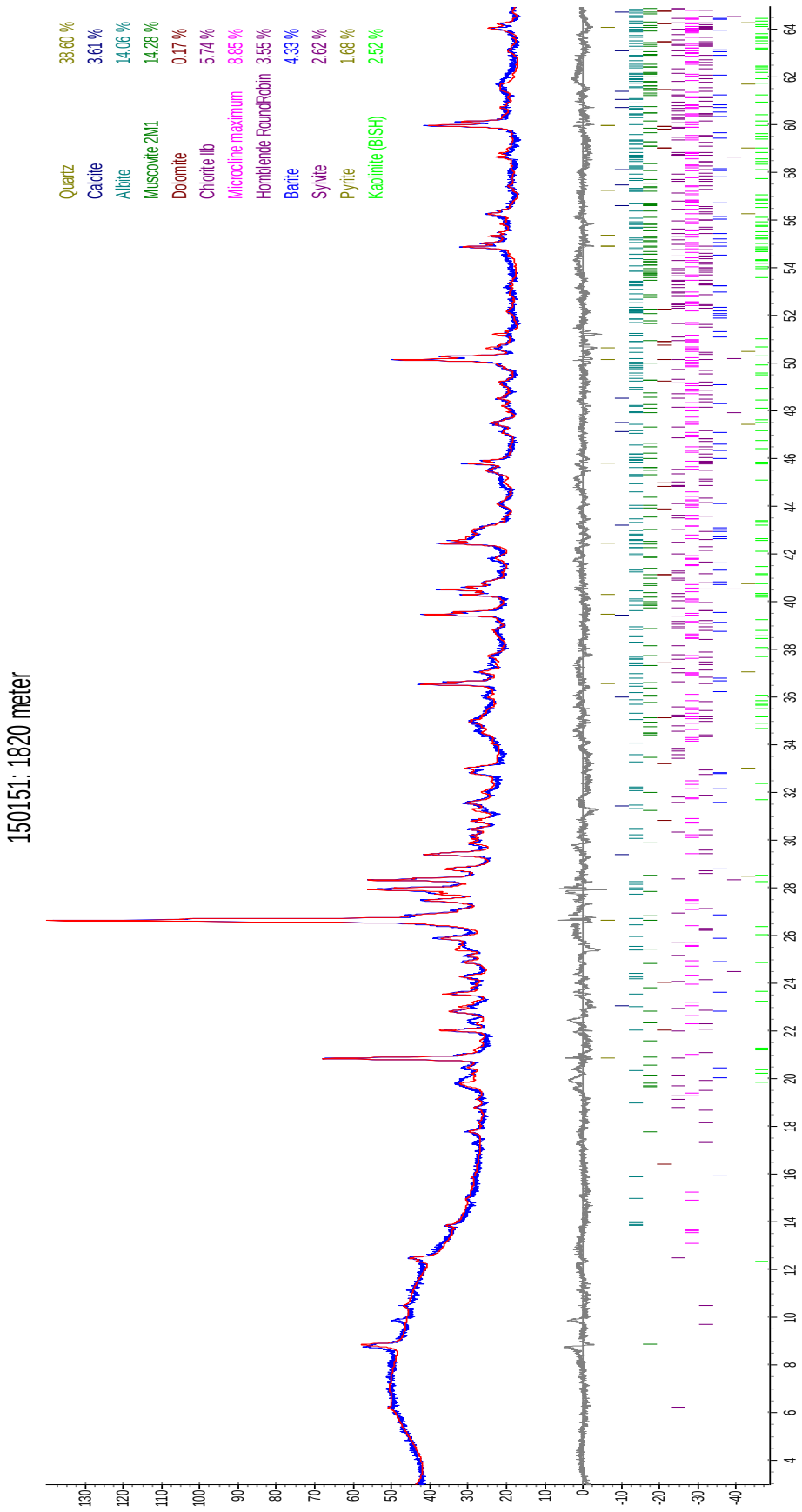

Heidrun Field, well 0.2, Kai Formation (1840mMD)

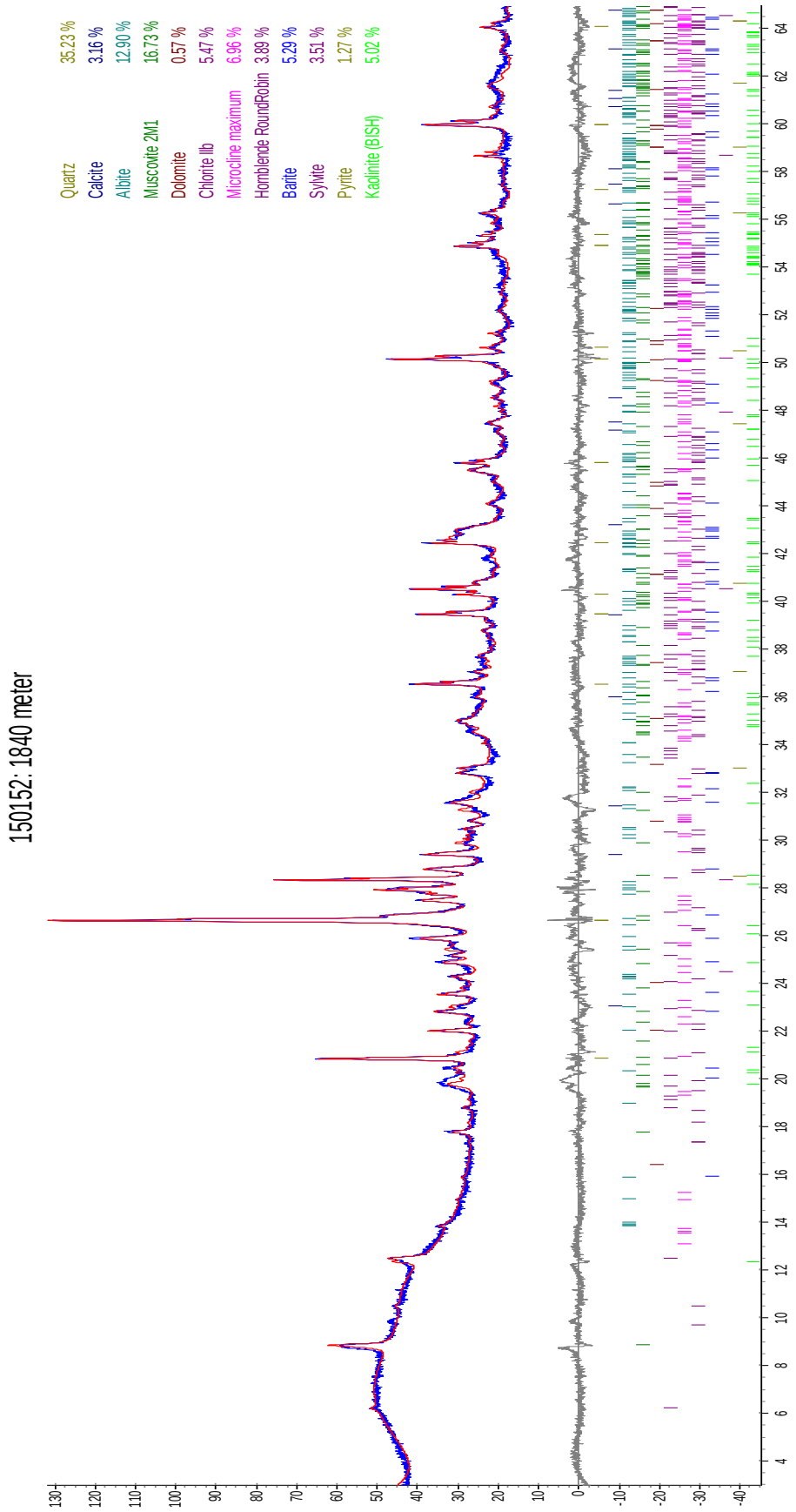

Heidrun Field, well 0.2, Kai Formation (1850mMD)

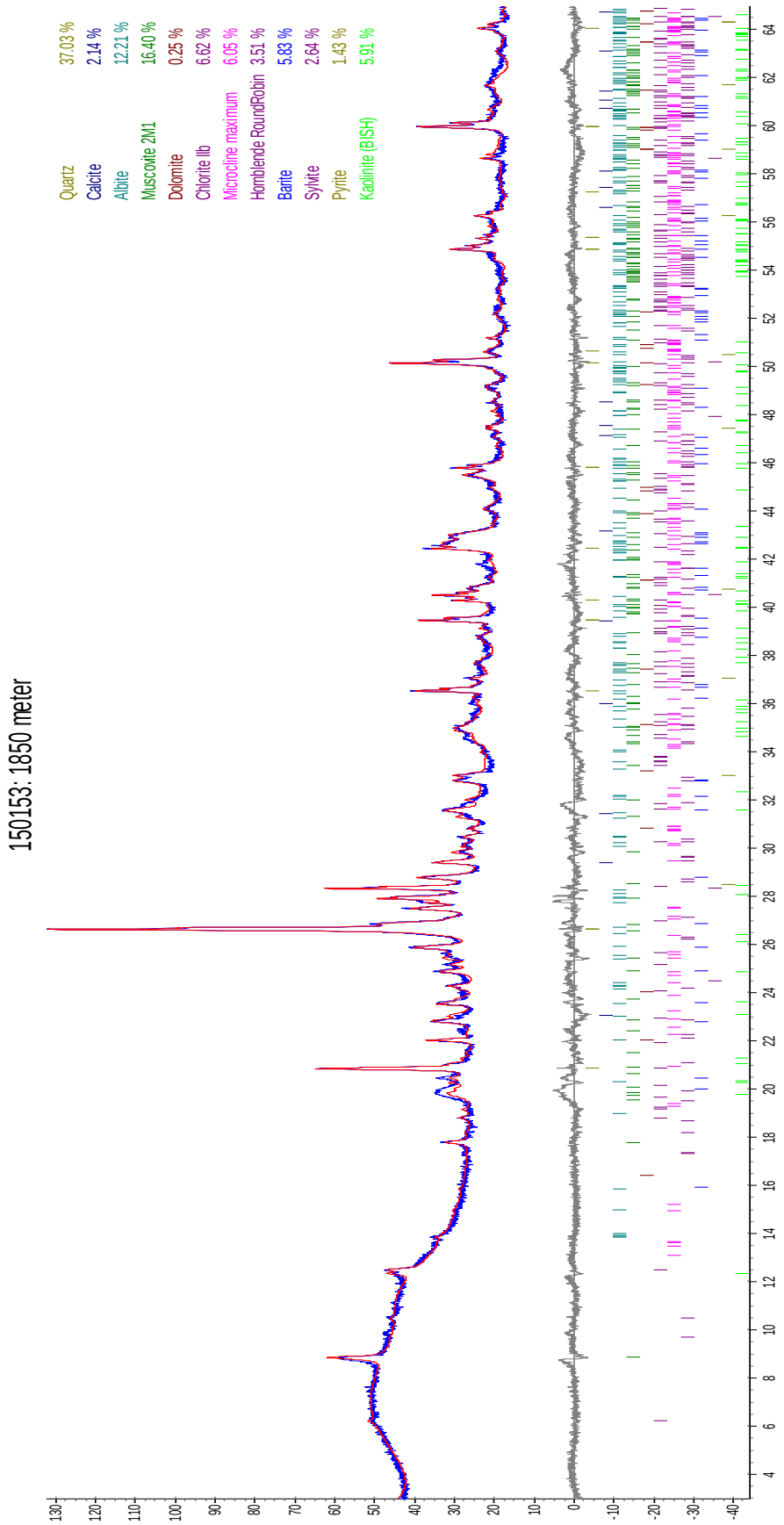

Heidrun Field, well 0.2, Kai Formation (1860mMD)

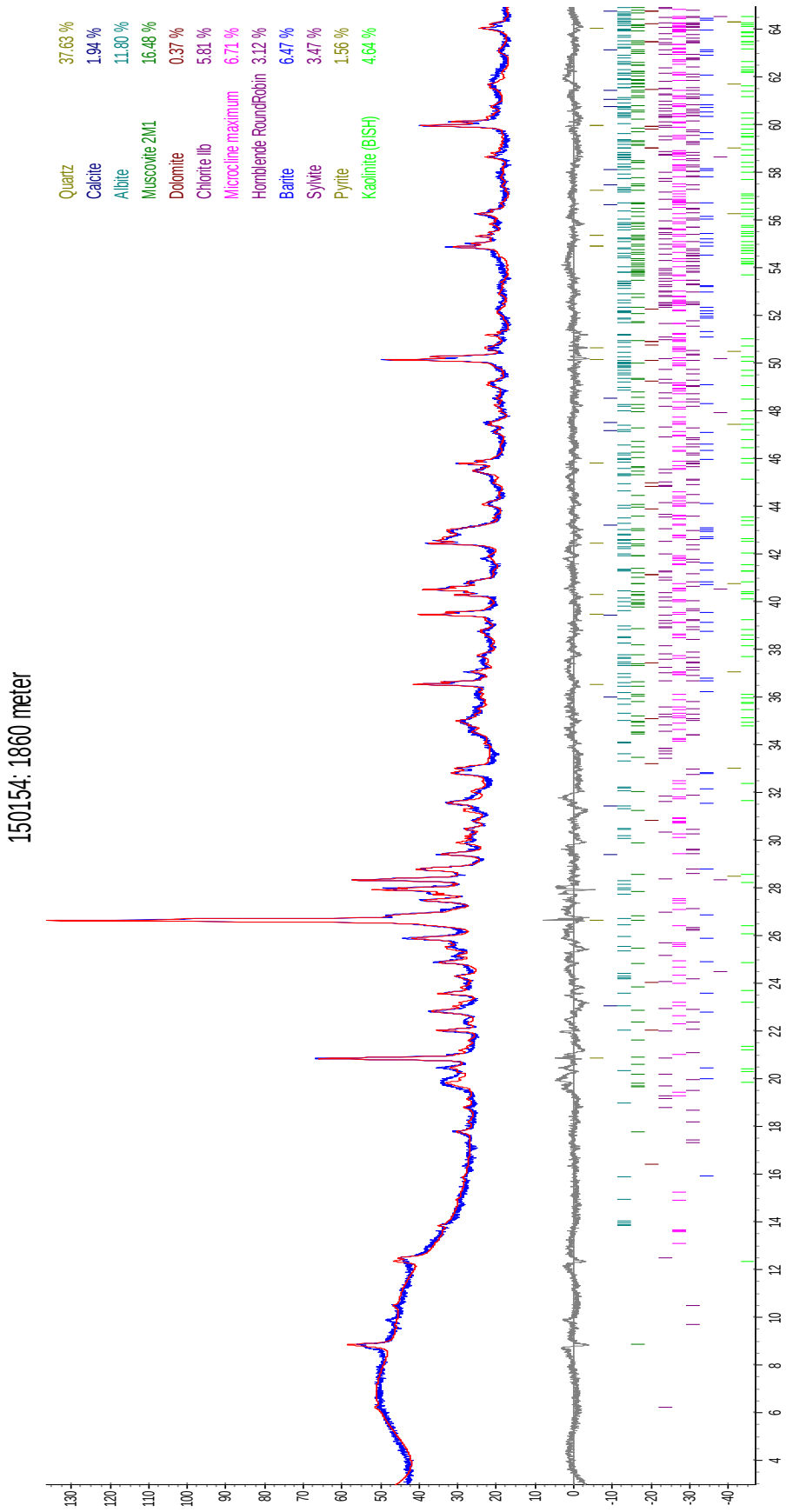

Heidrun Field, well 0.2, Kai Formation (1870mMD)

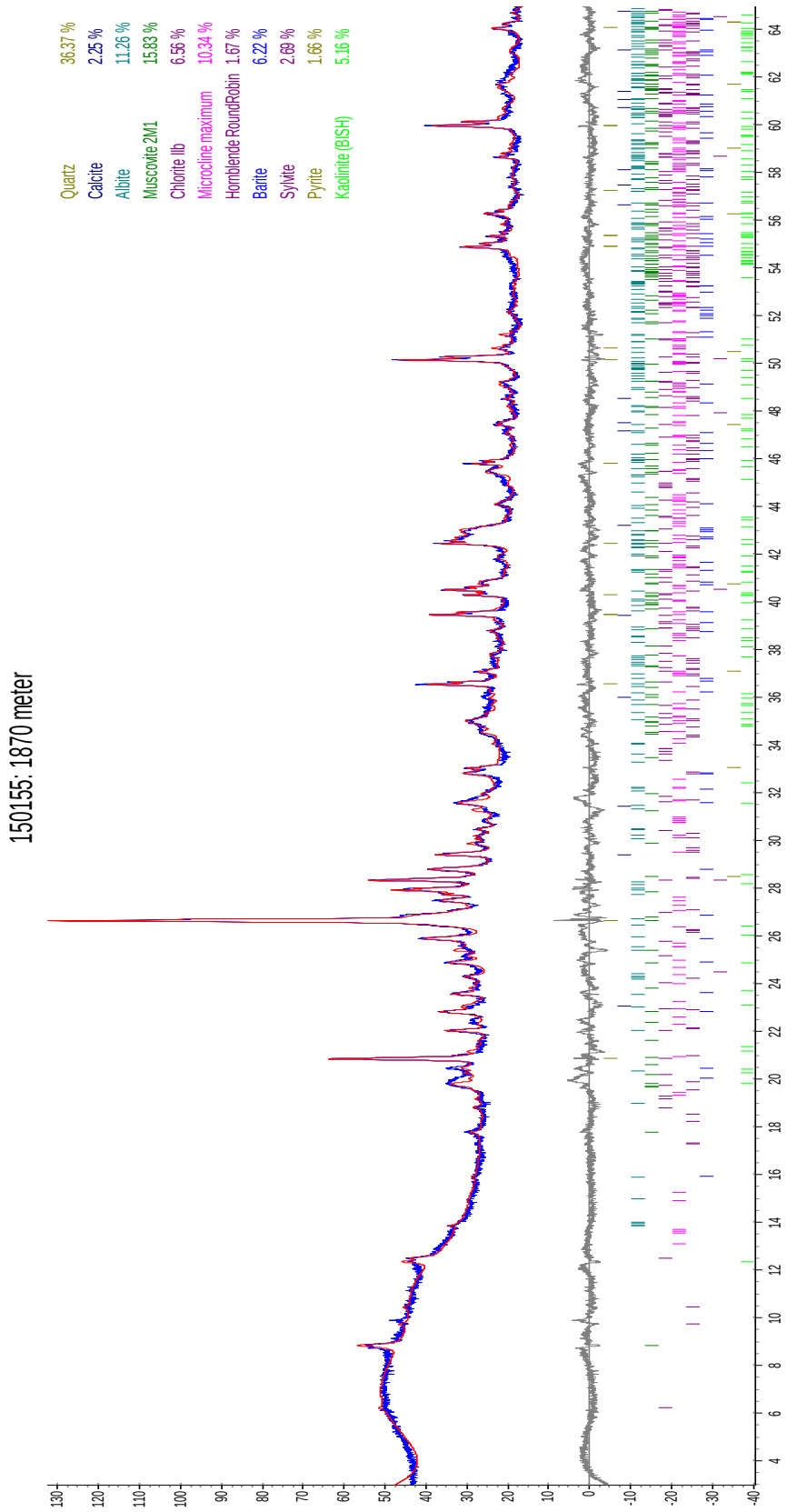

Heidrun Field, well 0.2, Kai Formation (1880mMD)

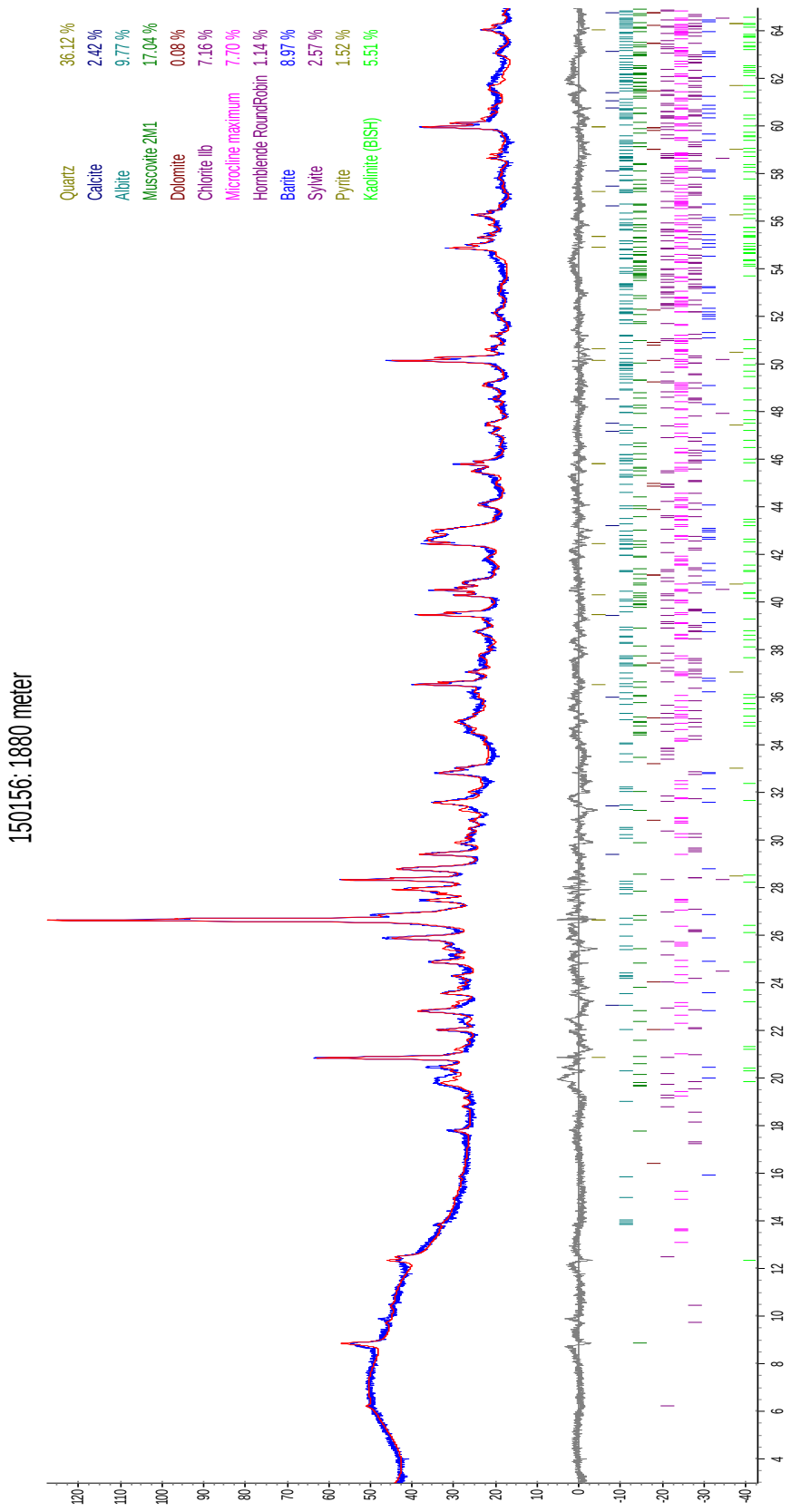

Heidrun Field, well 0.2, Kai Formation (1920mMD)

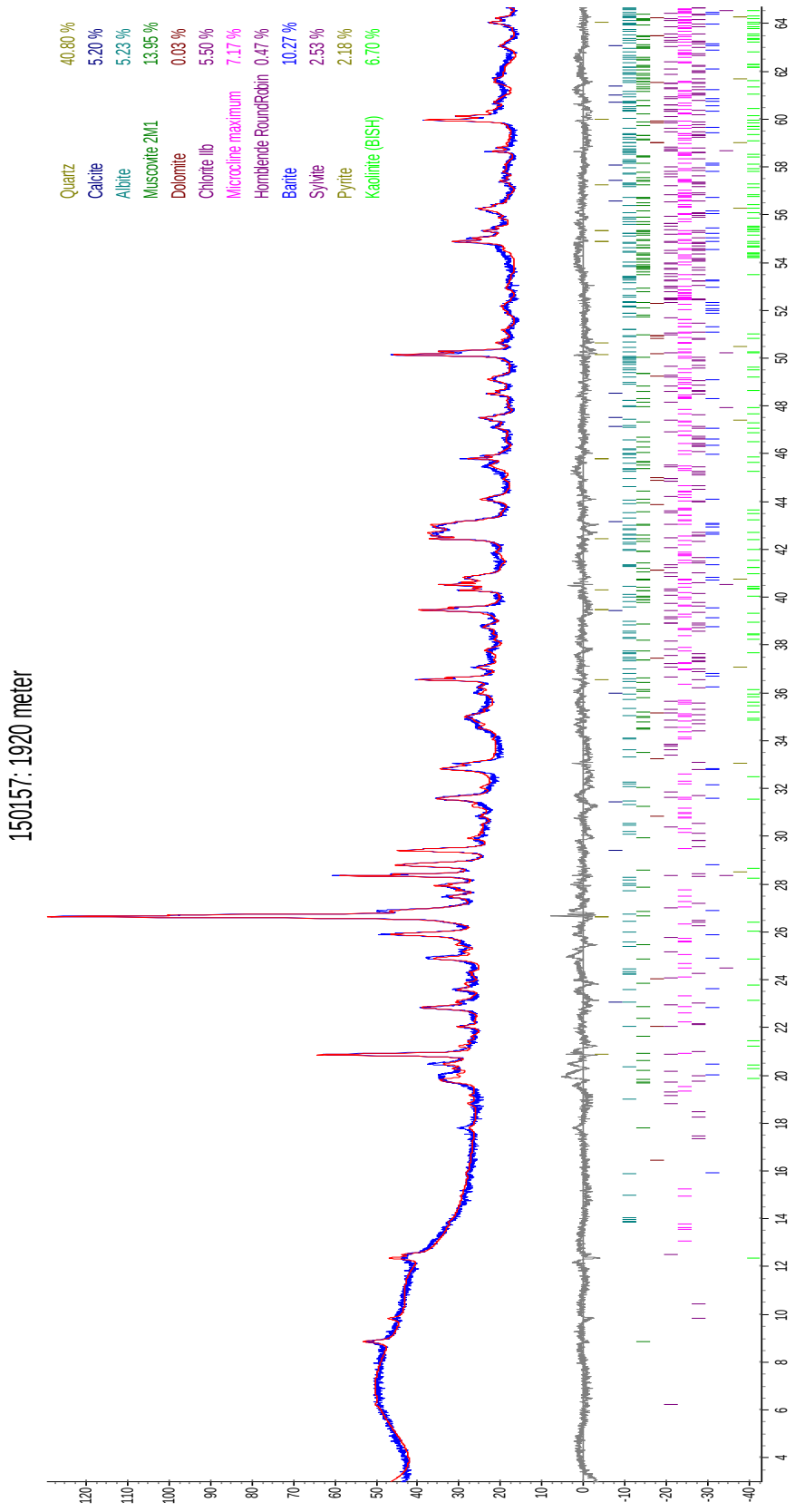

Heidrun Field, well 0.2, Kai Formation (1940mMD)

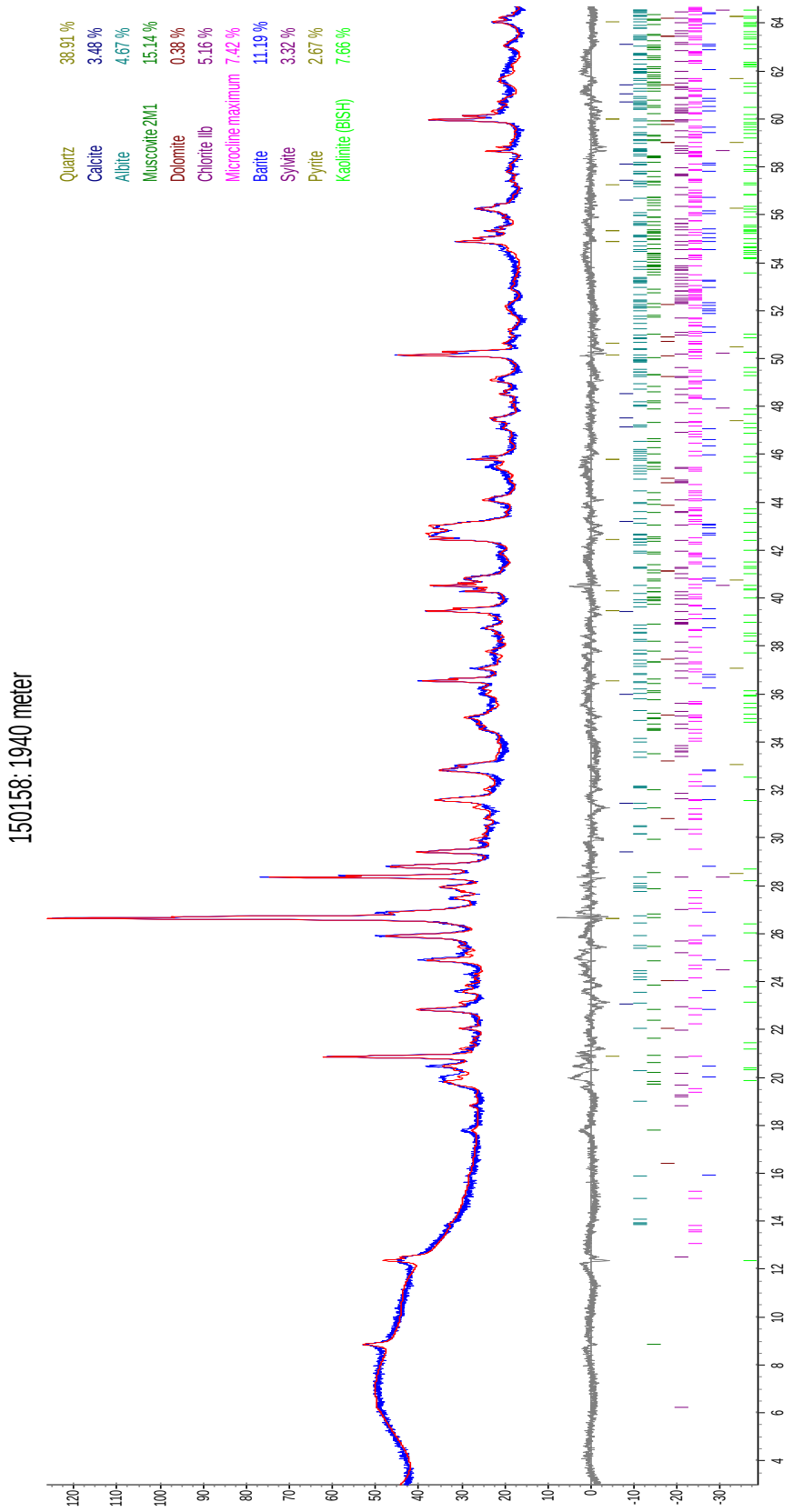

Fine fraction XRD results from well 0.2 (Heidrun Field)

150150: Heidrun Field, well 0.2, Kai Formation (1810 mMD), < 6 µm

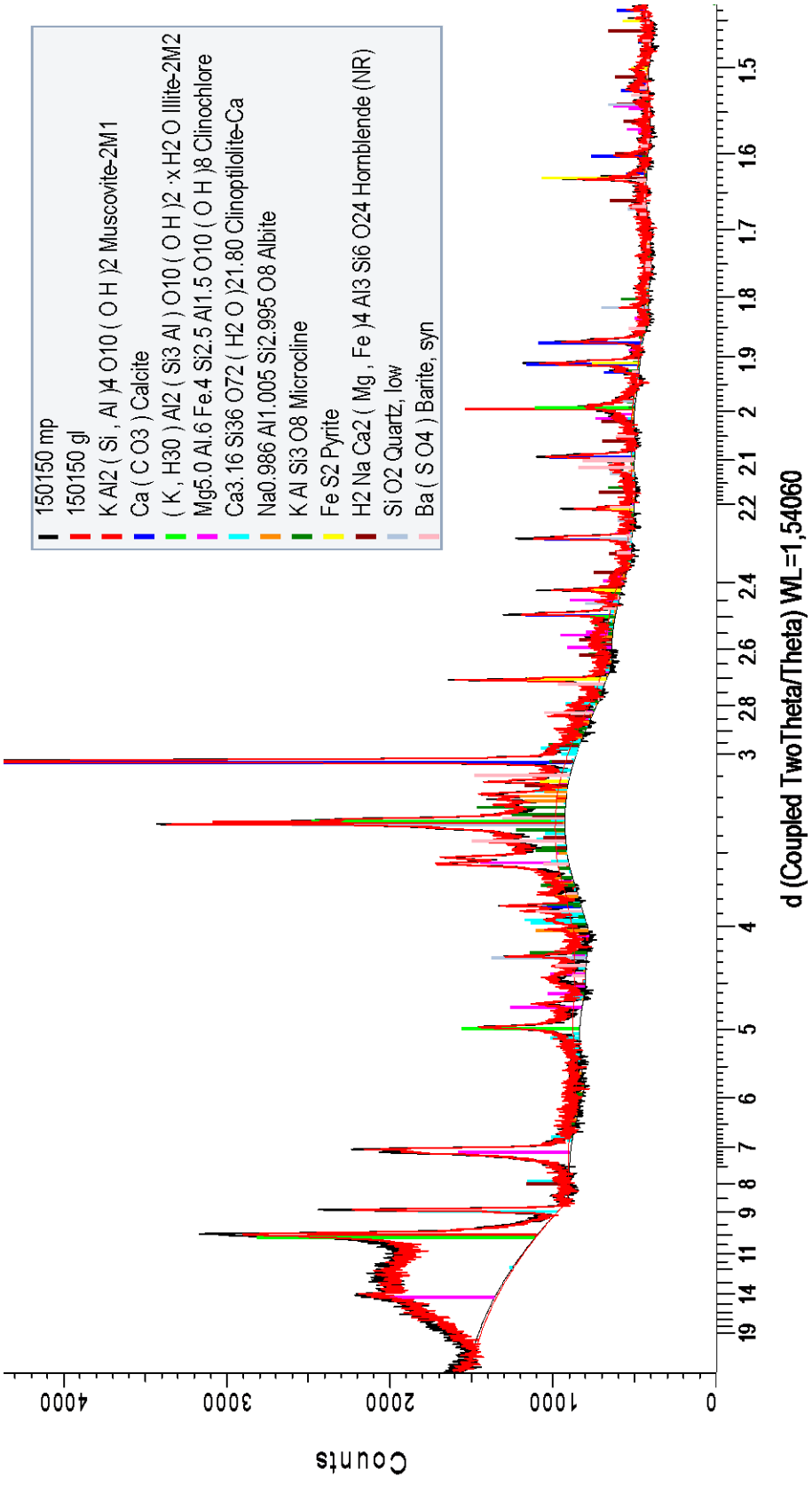

150151: Heidrun Field, well 0.2, Kai Formation (1820 mMD), < 6 µm

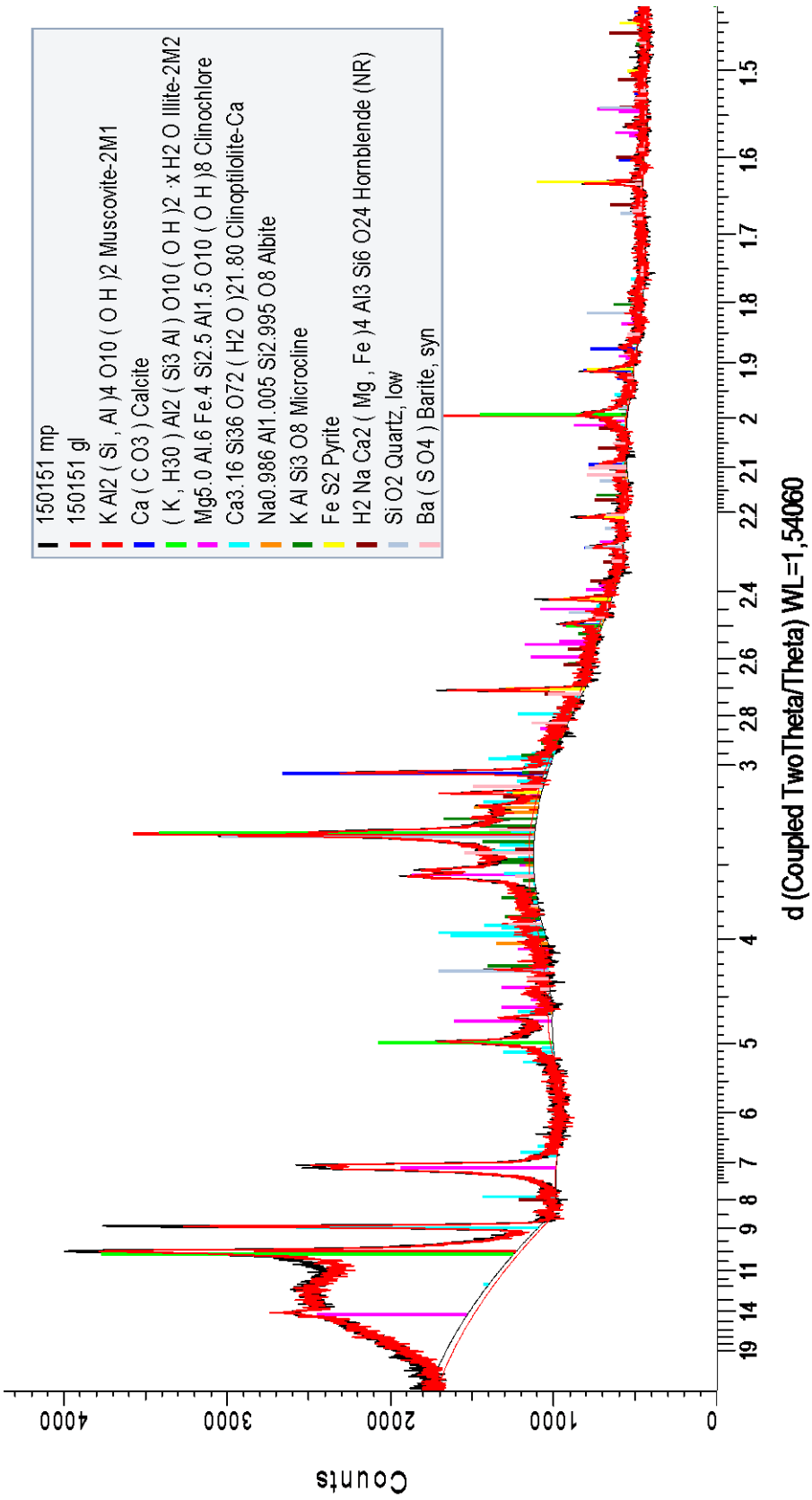

150152: Heidrun Field, well 0.2, Kai Formation (1840 mMD), < 6 µm

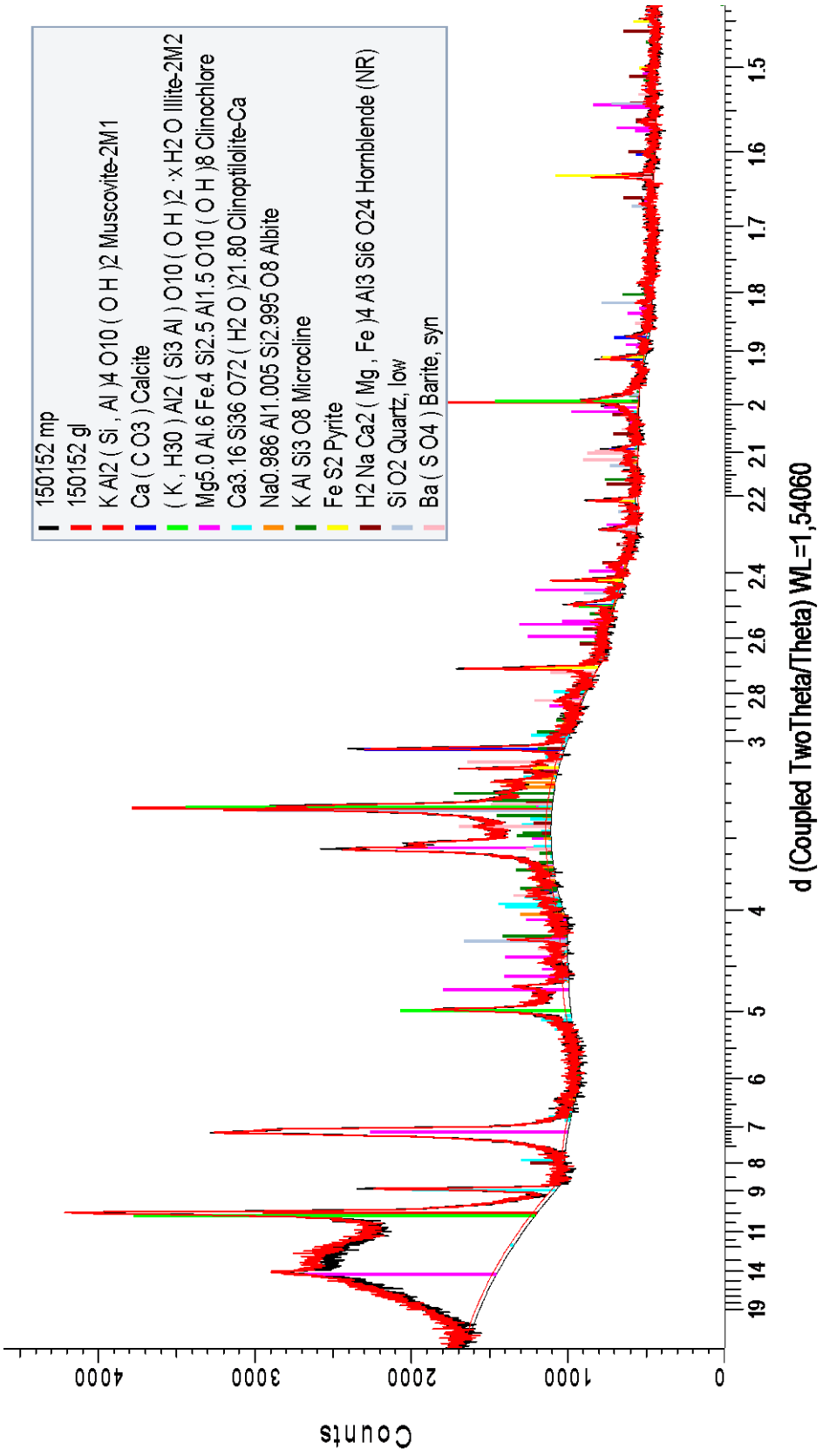

150153: Heidrun Field, well 0.2, Kai Formation (1850 mMD), < 6 µm

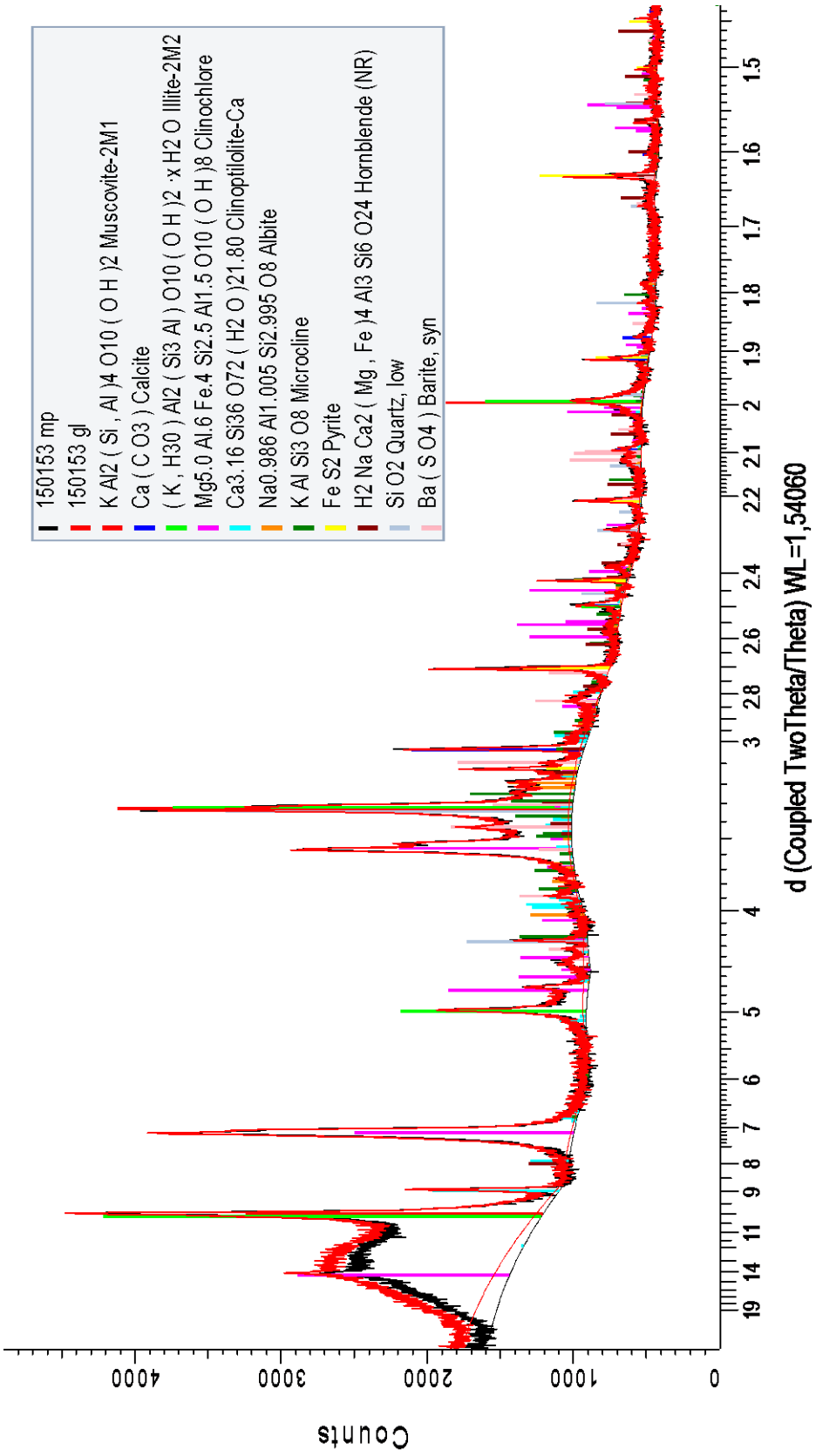

150154: Heidrun Field, well 0.2, Kai Formation (1860 mMD), < 6 µm

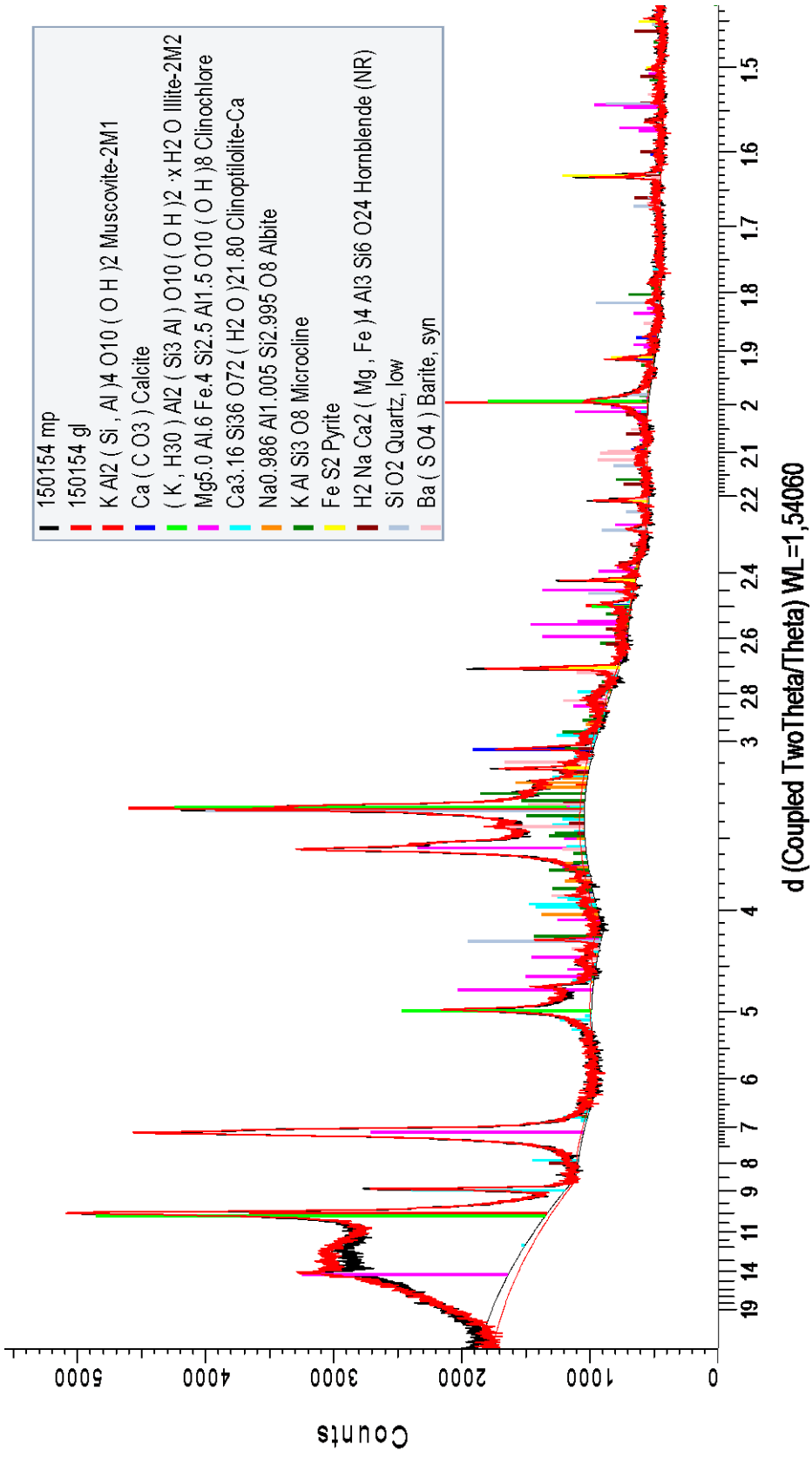

150155: 1870 meter, < 6 µm

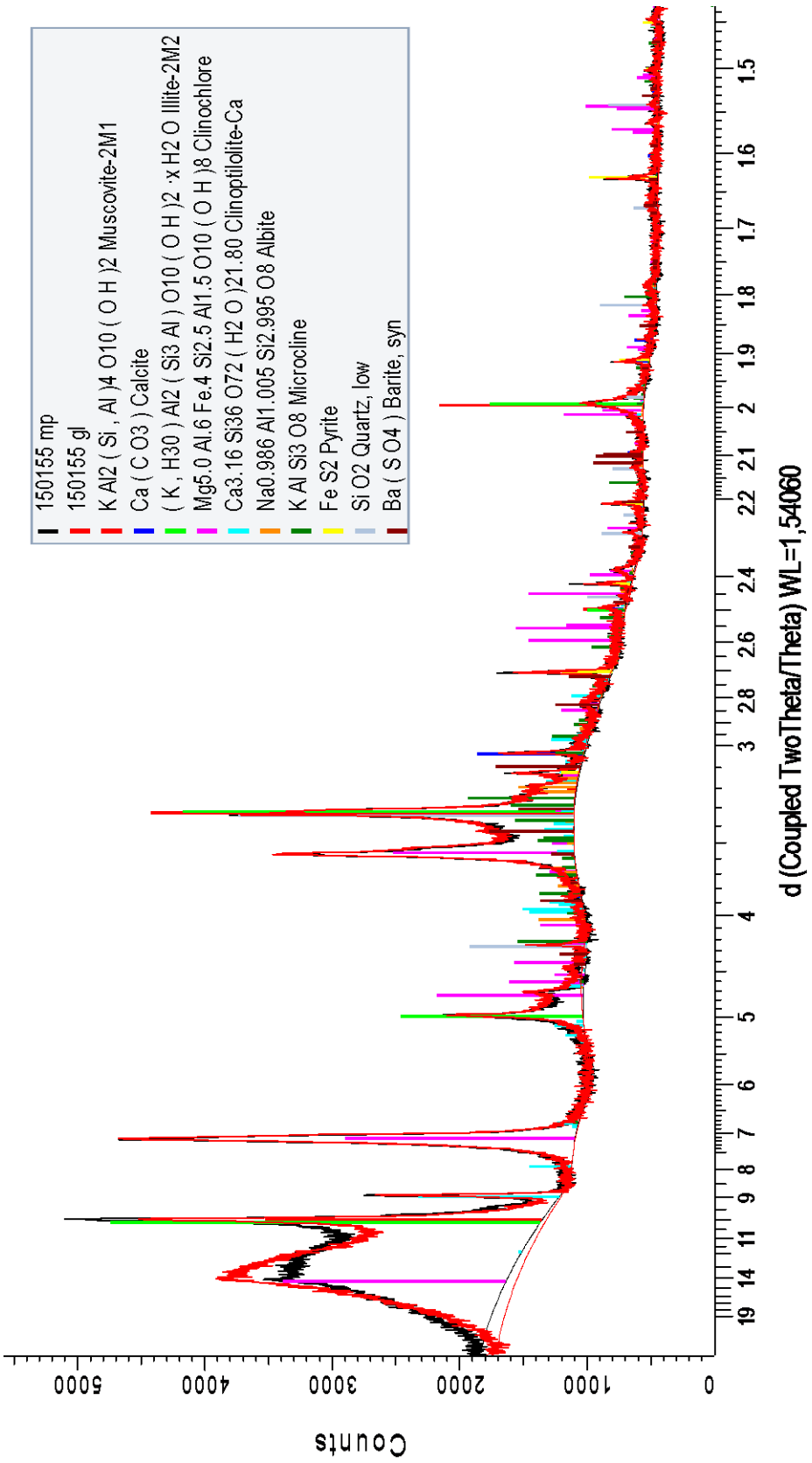

150156: Heidrun Field, well 0.2, Kai Formation (1880 mMD), < 6 µm

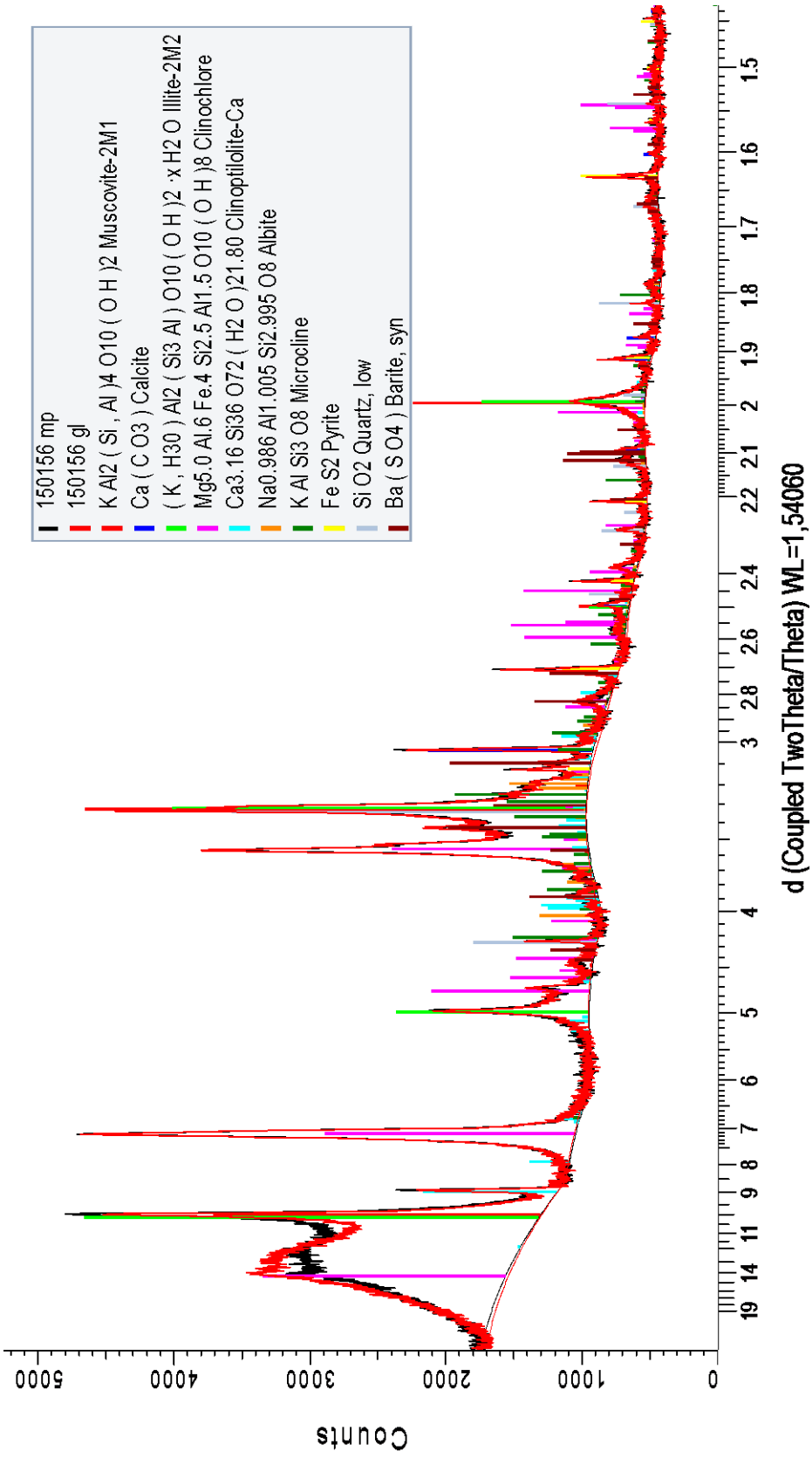

150157: Heidrun Field, well 0.2, Kai Formation (1920 mMD), < 6 µm

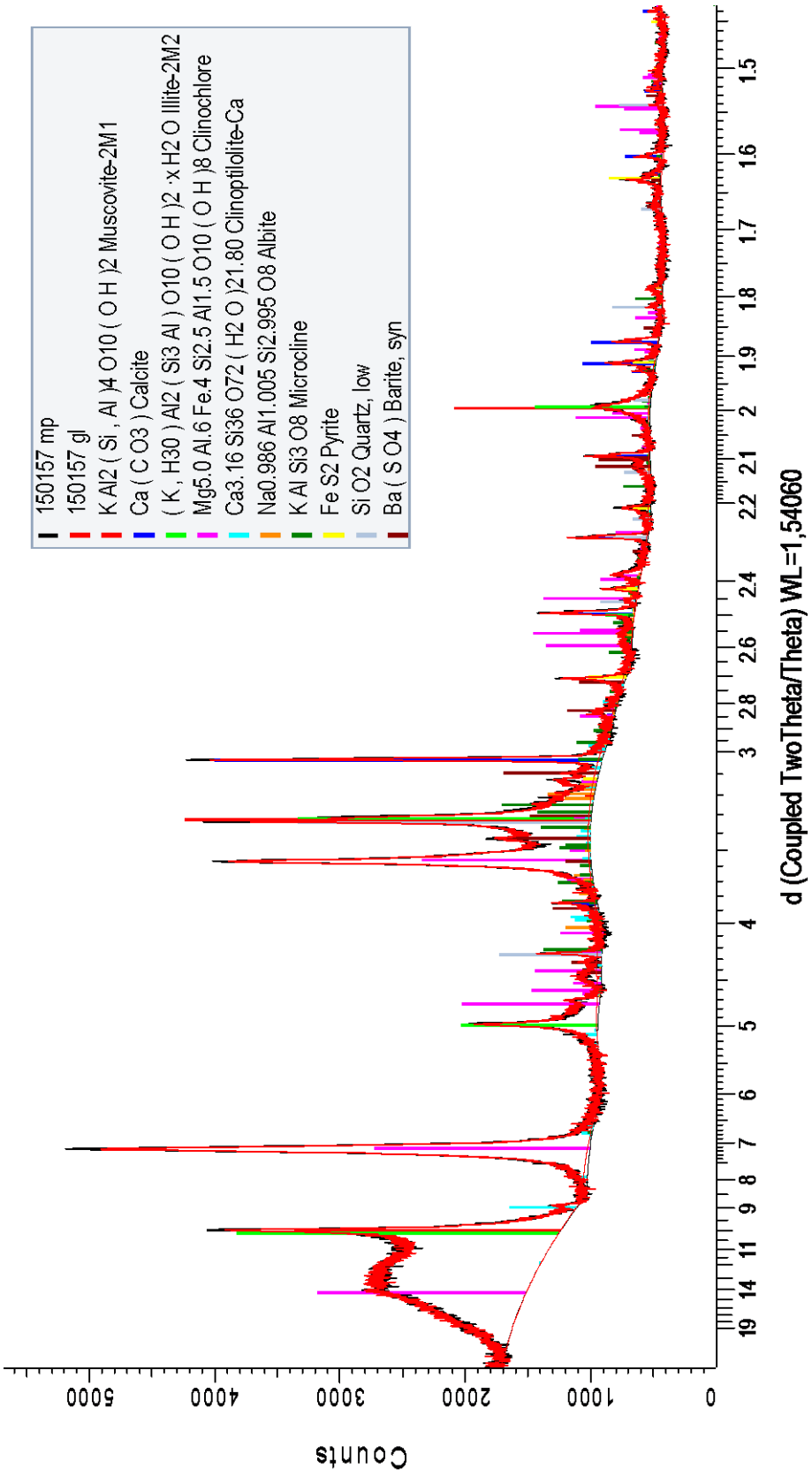

150158: Heidrun Field, well 0.2, Kai Formation (1940 mMD), < 6 µm

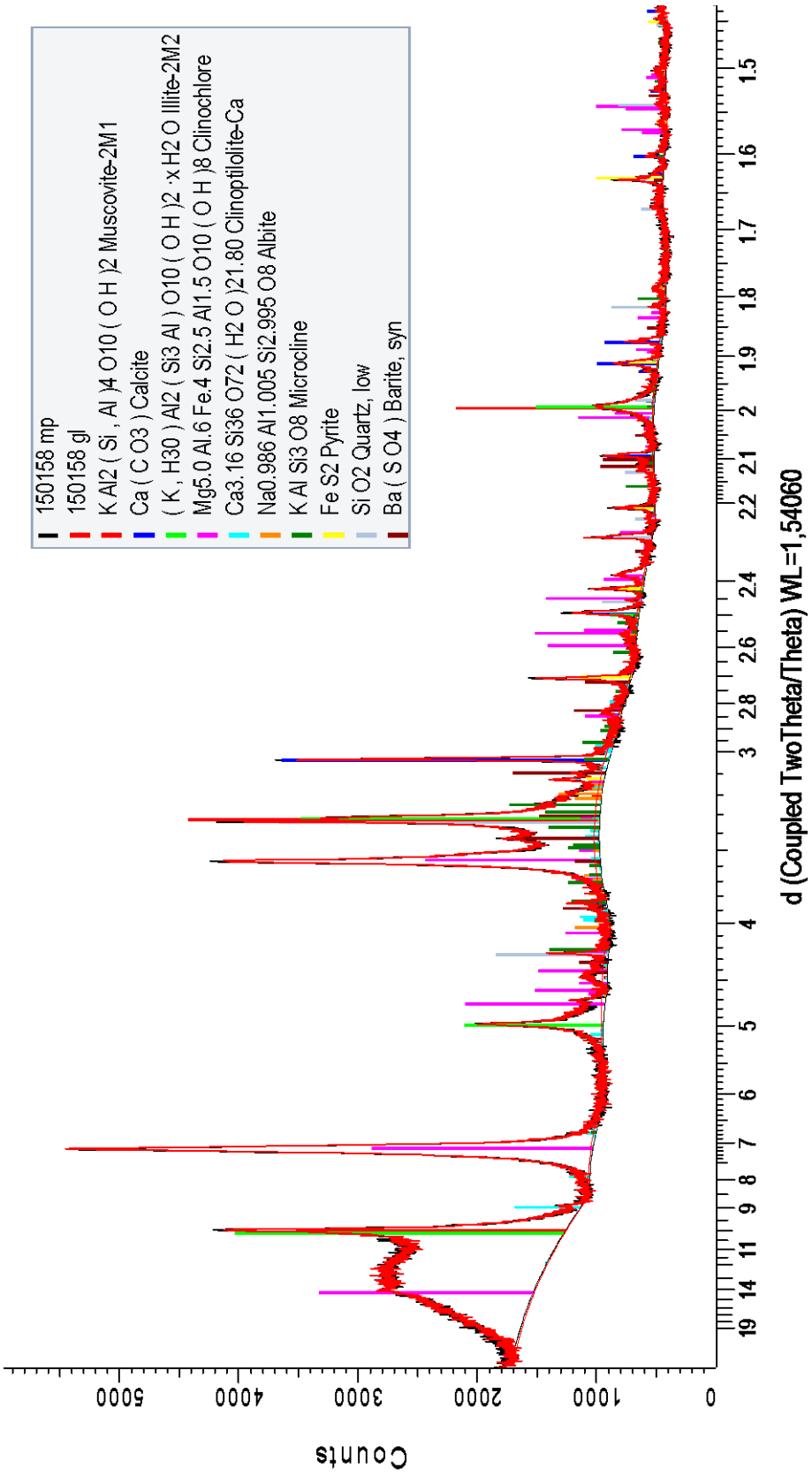

Appendix B

Petrophysical logs from:

- Well A
- Well B
- Well C (also include cuttings description)
- Well D (also include cuttings description)
- Well E
- Well F (also include cuttings description)
- Well G
- Well H (also include cuttings description)
- Well I (also include cuttings description)

Heidrun Field: Well 0

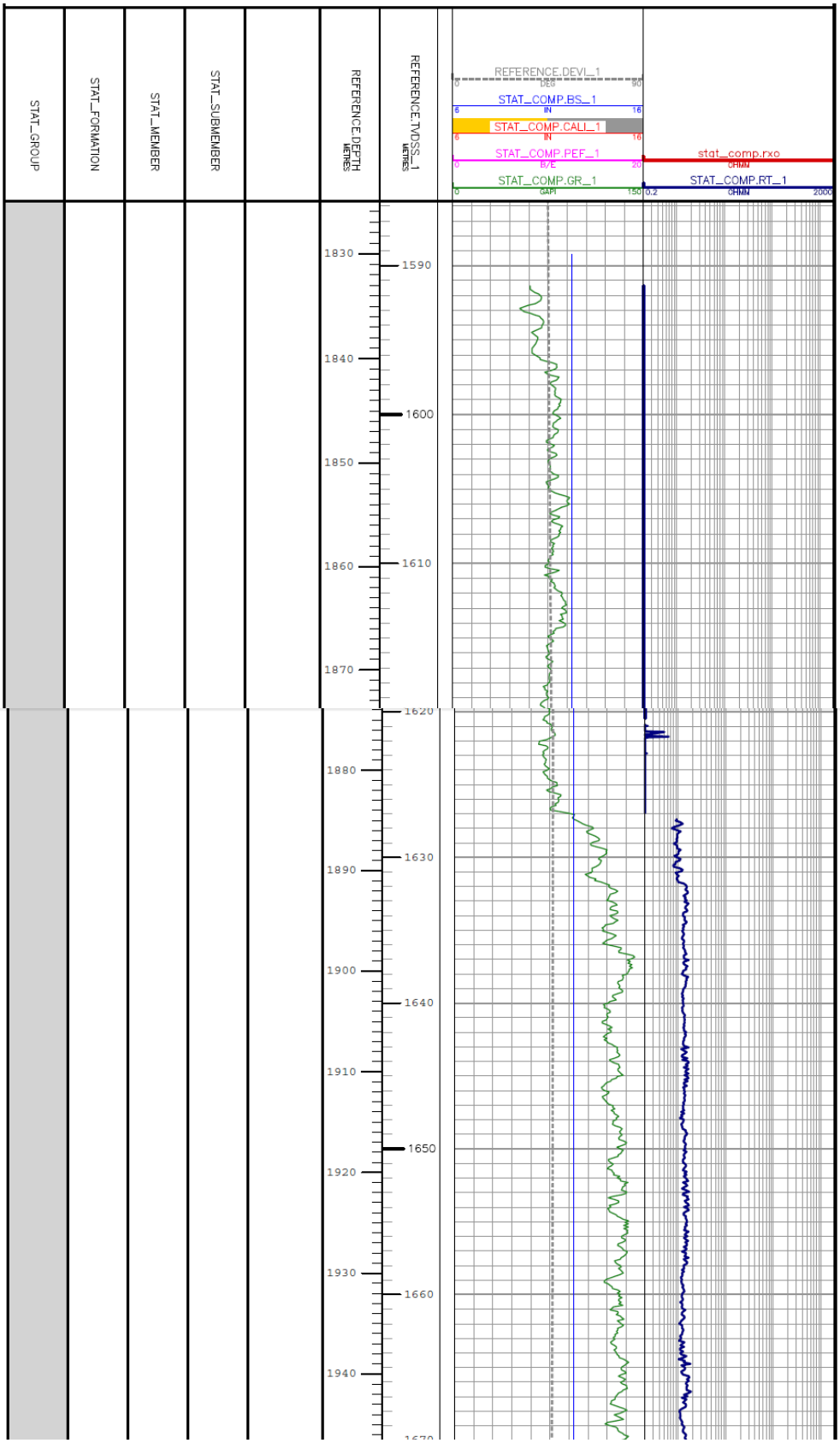

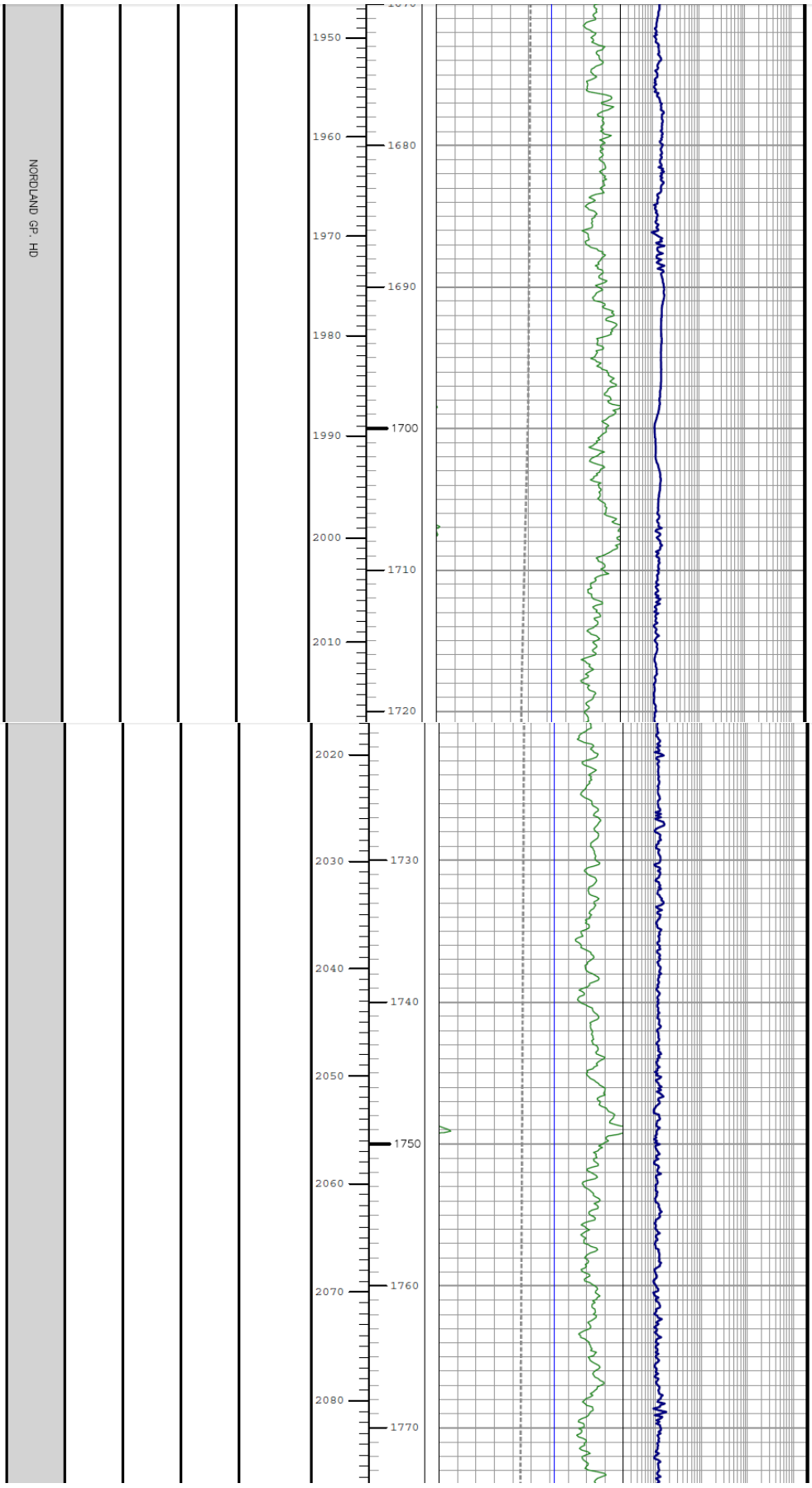
NORDLAND GP. HD
1950
1960
1970
1980
1990
2000
2010
1680
1690
1700
1710
1720
2020
2030
2040
2050
2060
2070
2080
1730
1740
1750
1760
1770

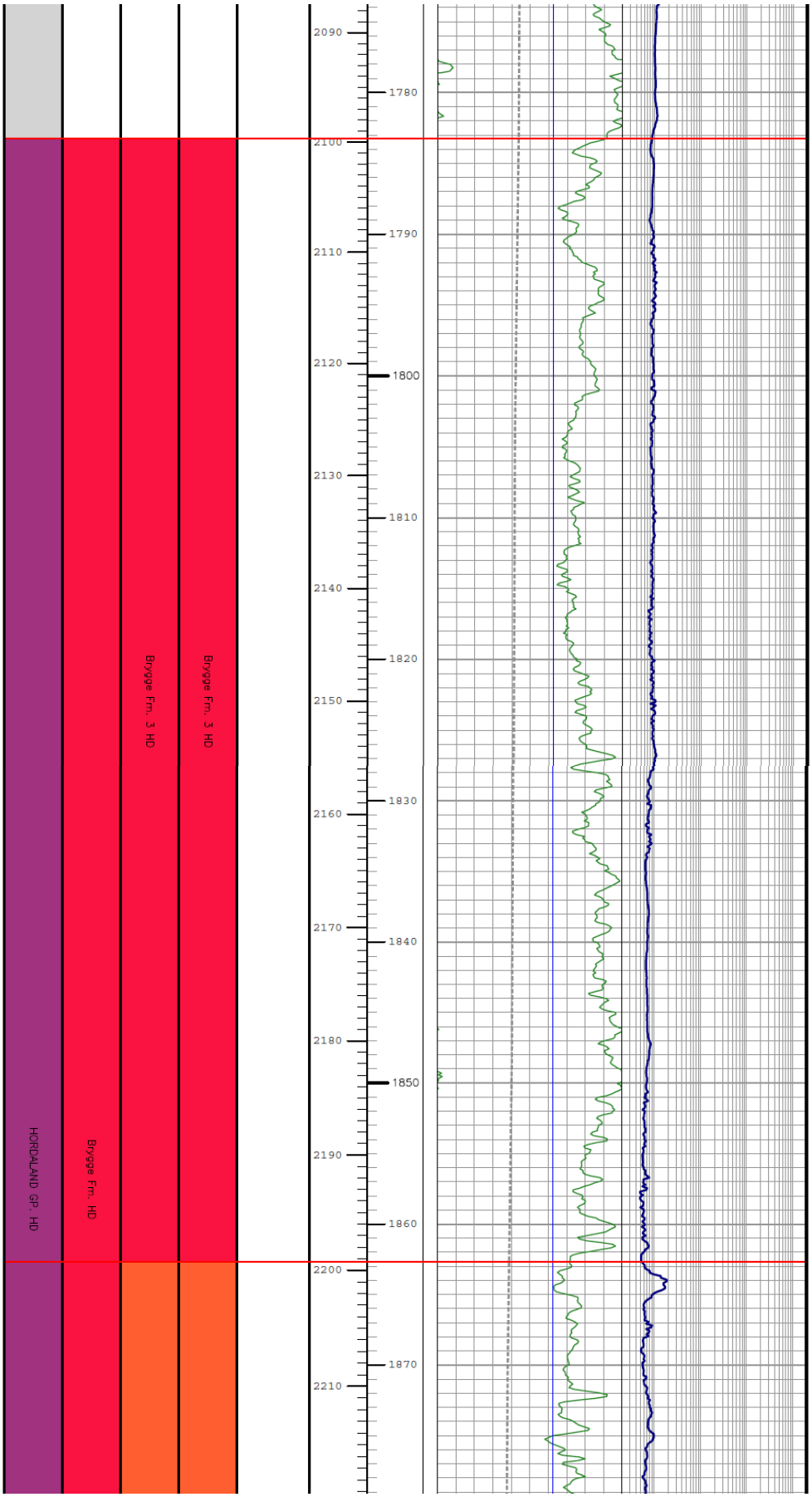
HORDALAND GP. HD
Brygge Fm. HD
Brygge Fm. 3 HD
Brygge Fm. 3 HD
2090
2100
2110
2120
2130
2140
2150
2160
2170
2180
2190
2200
2210
1780
1790
1800
1810
1820
1830
1840
1850
1860
1870

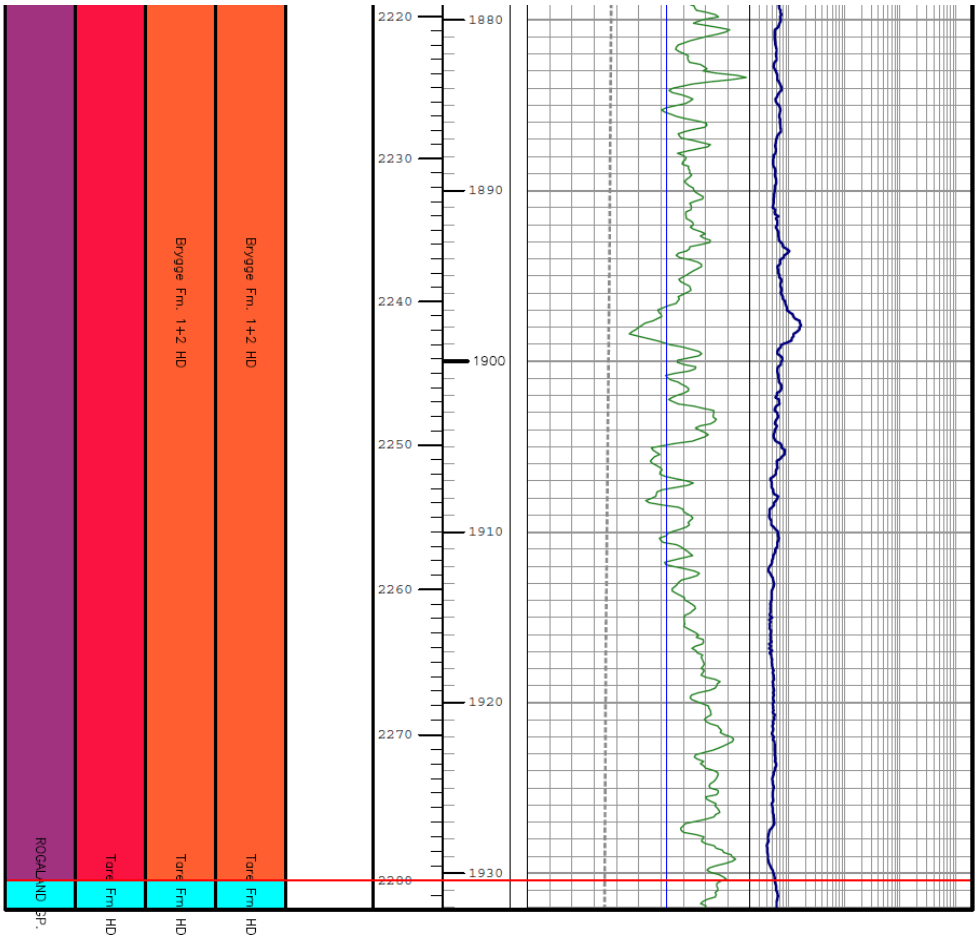
ROGALAND GP.
Tare Fm HD
Tare Fm HD
Tare Fm HD
Brygge Fm. 1+2 HD
Brygge Fm. 1+2 HD
2220
2230
2240
2250
2260
2270
2280
1880
1890
1900
1910
1920
1930

Heidrun Field: Well 0.2

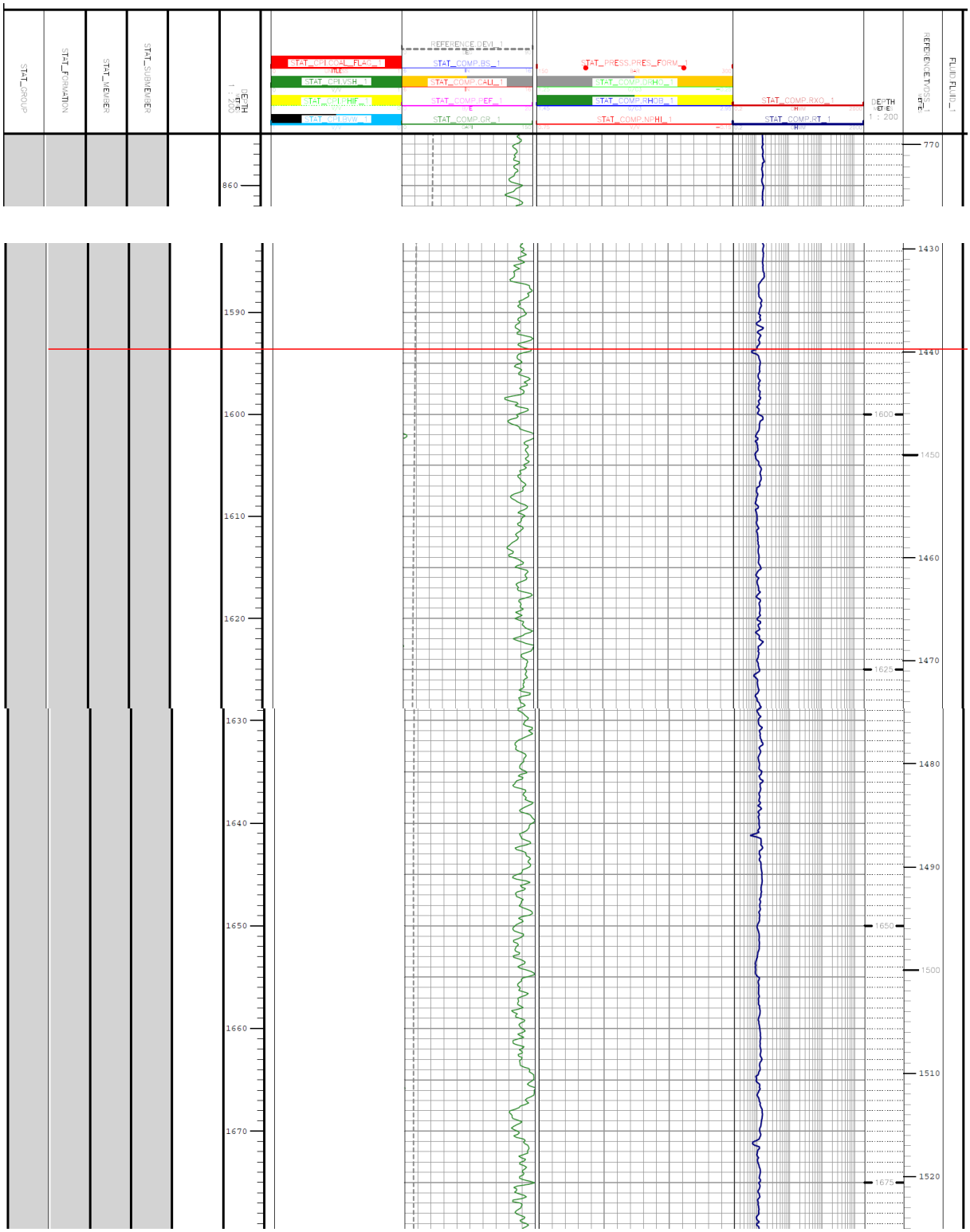

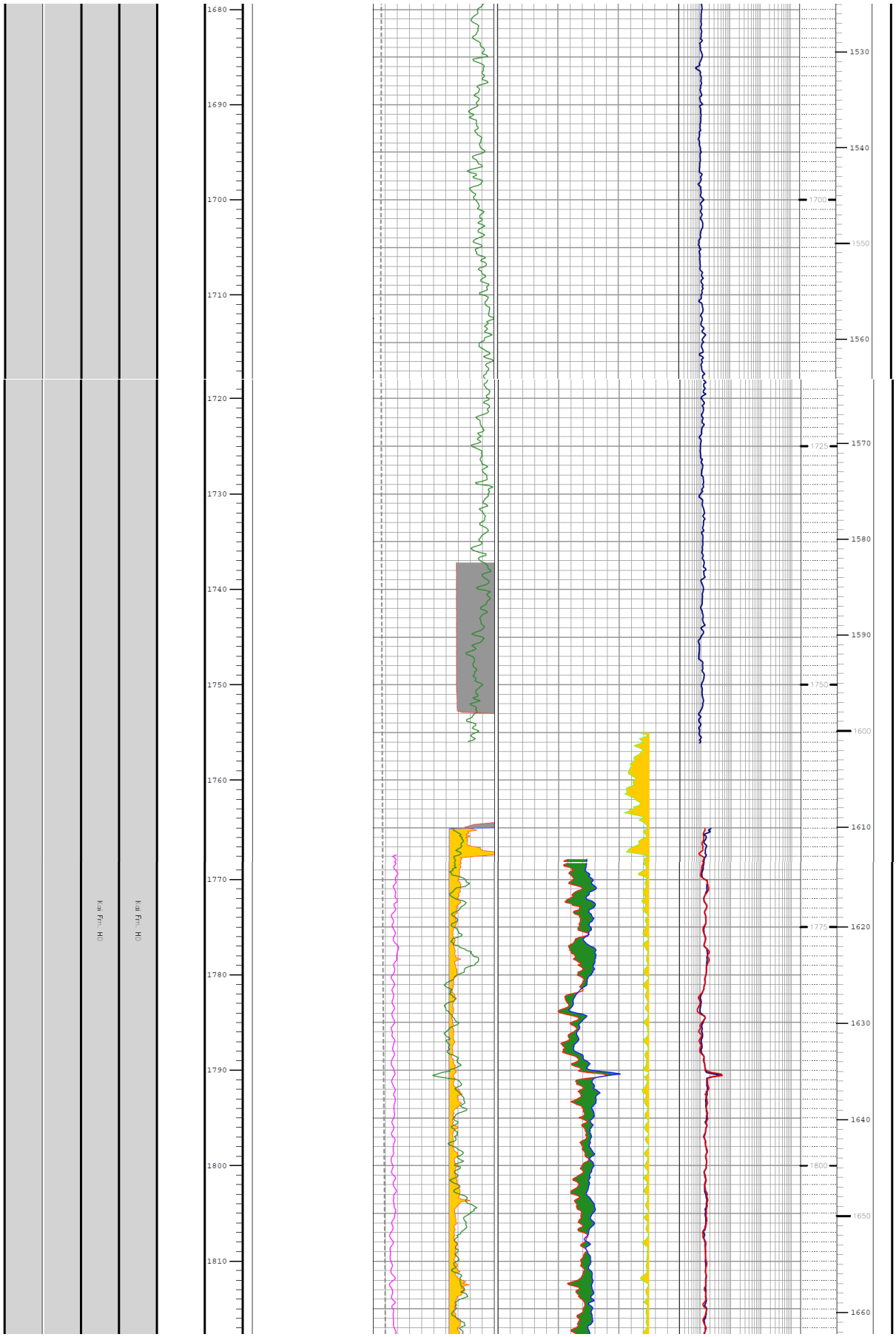
1680
1690
1700
1710
1720
1730
1740
1750
1760
1770
1780
1790
1800
1810
1530
1540
1700
1550
1560
1725
1570
1580
1590
1750
1600
1610
1775
1620
1630
1640
1800
1650
1660

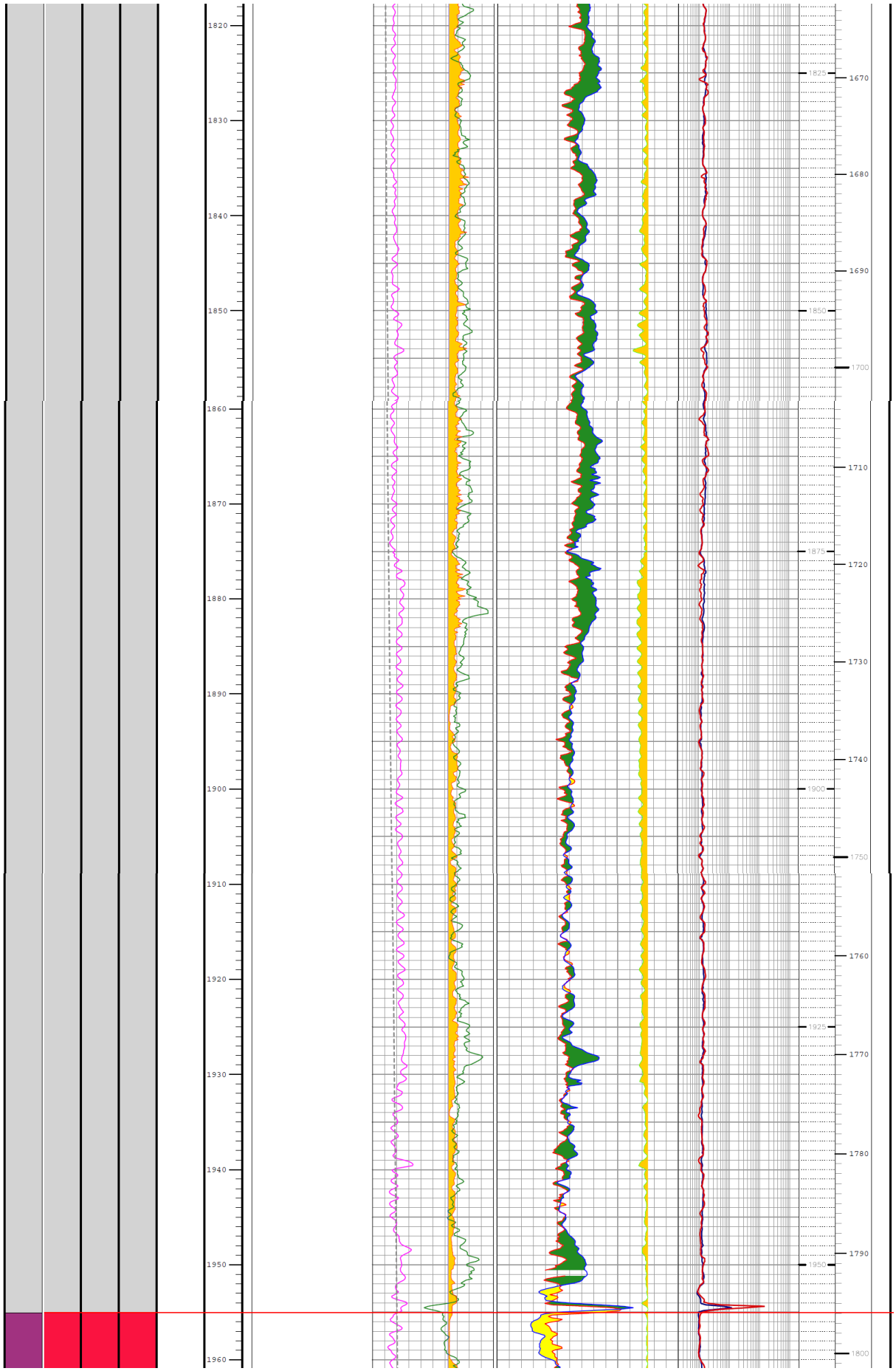
1820
1830
1840
1850
1860
1870
1880
1890
1900
1910
1920
1930
1940
1950
1960
1825
1850
1875
1900
1925
1950
1670
1680
1690
1700
1710
1720
1730
1740
1750
1760
1770
1780
1790
1800

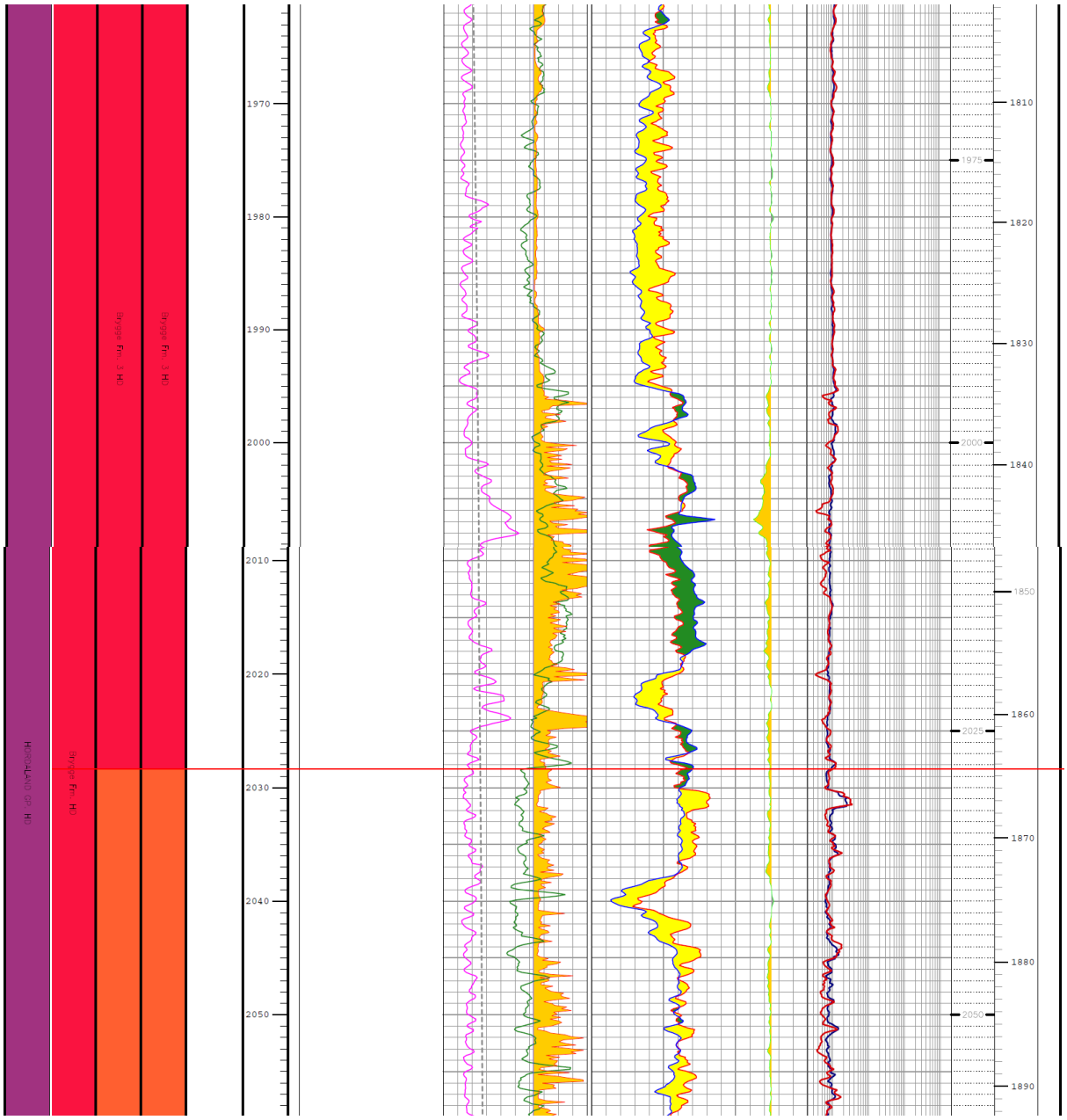
Brygge Fm. 3 HD
Brygge Fm. 2 HD
Brygge Fm. 1 HD
HORDALAND GP HD
1970
1980
1990
2000
2010
2020
2030
2040
2050
1810
1820
1830
1840
1850
1860
1870
1880
1890
1975
2000
2025
2050

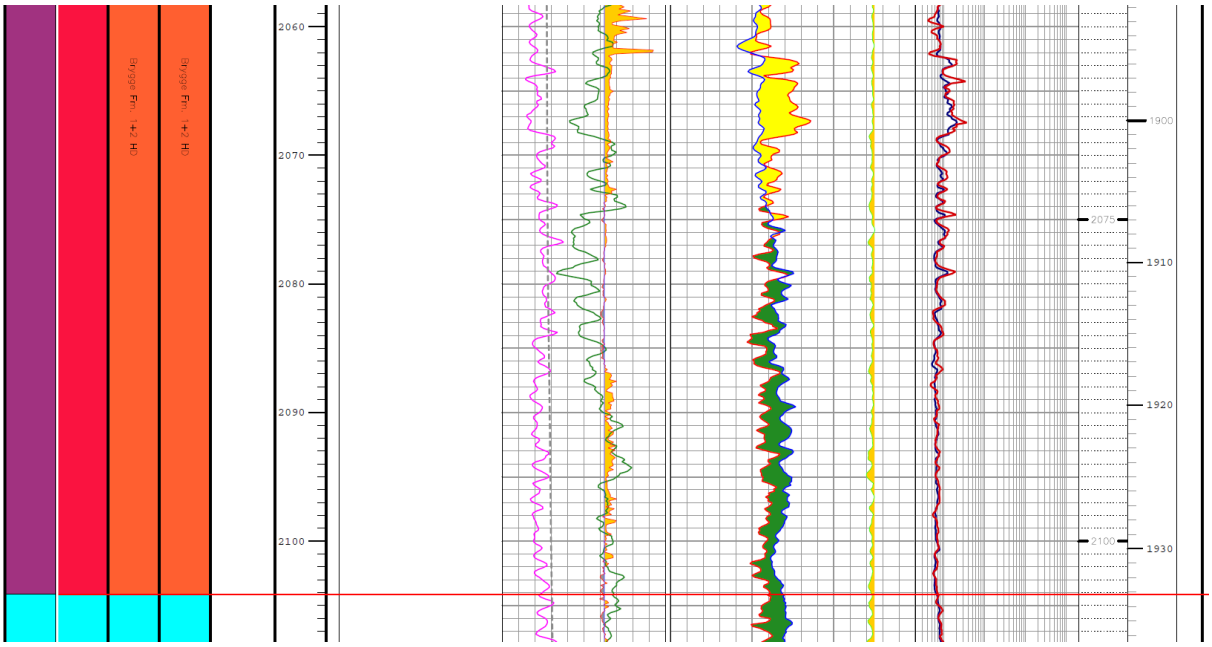
Brygge Fm. 1+2 HD
Brygge Fm. 1+2 HD
2060
2070
2080
2090
2100
1900
2075
1910
1920
2100
1930

Heidrun Field: Well A

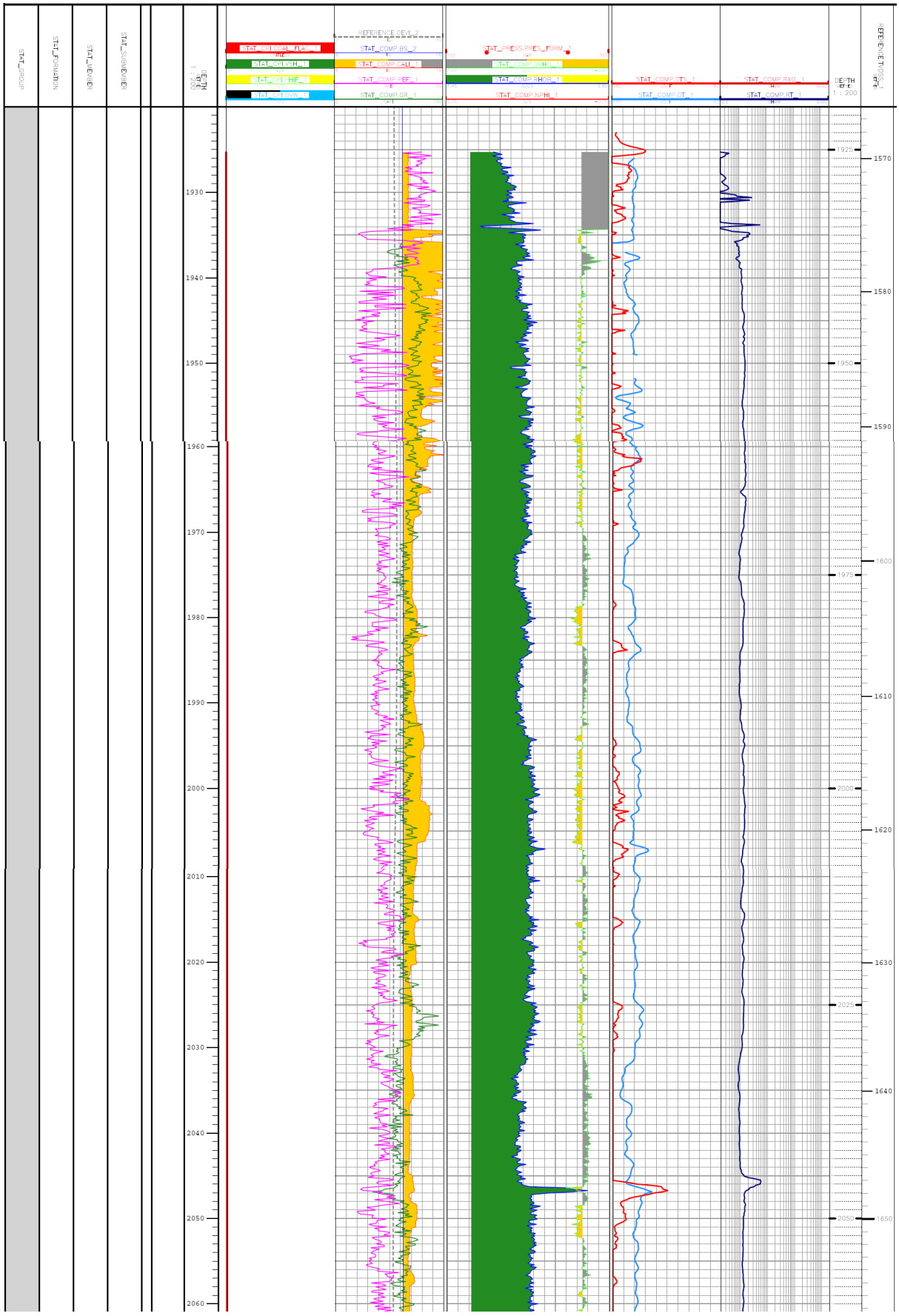

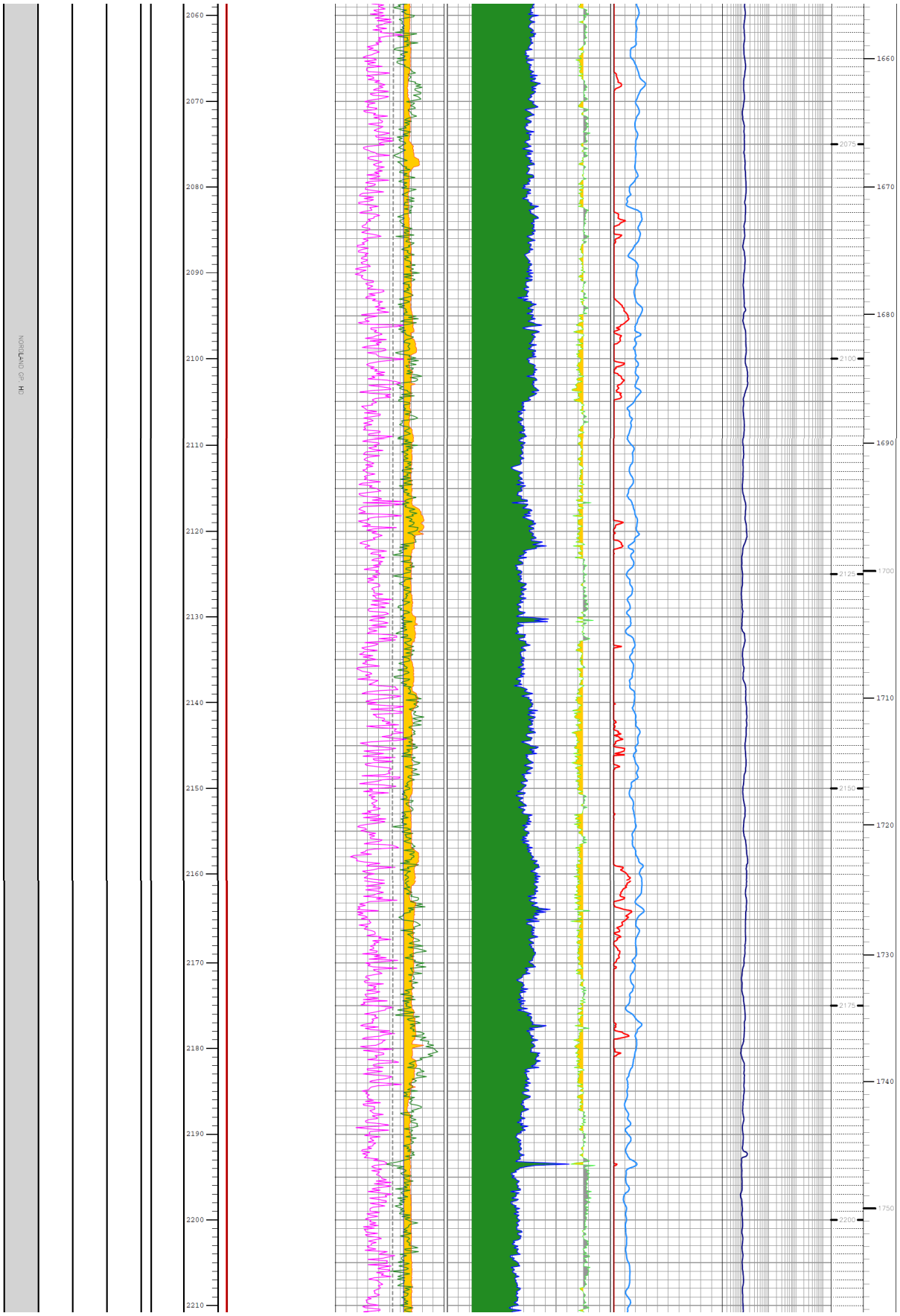
GR
NORMALIZED
2060
2070
2080
2090
2100
2110
2120
2130
2140
2150
2160
2170
2180
2190
2200
2210
1660
1670
1680
1690
1700
1710
1720
1730
1740
1750
2075
2100
2125
2150
2175
2200

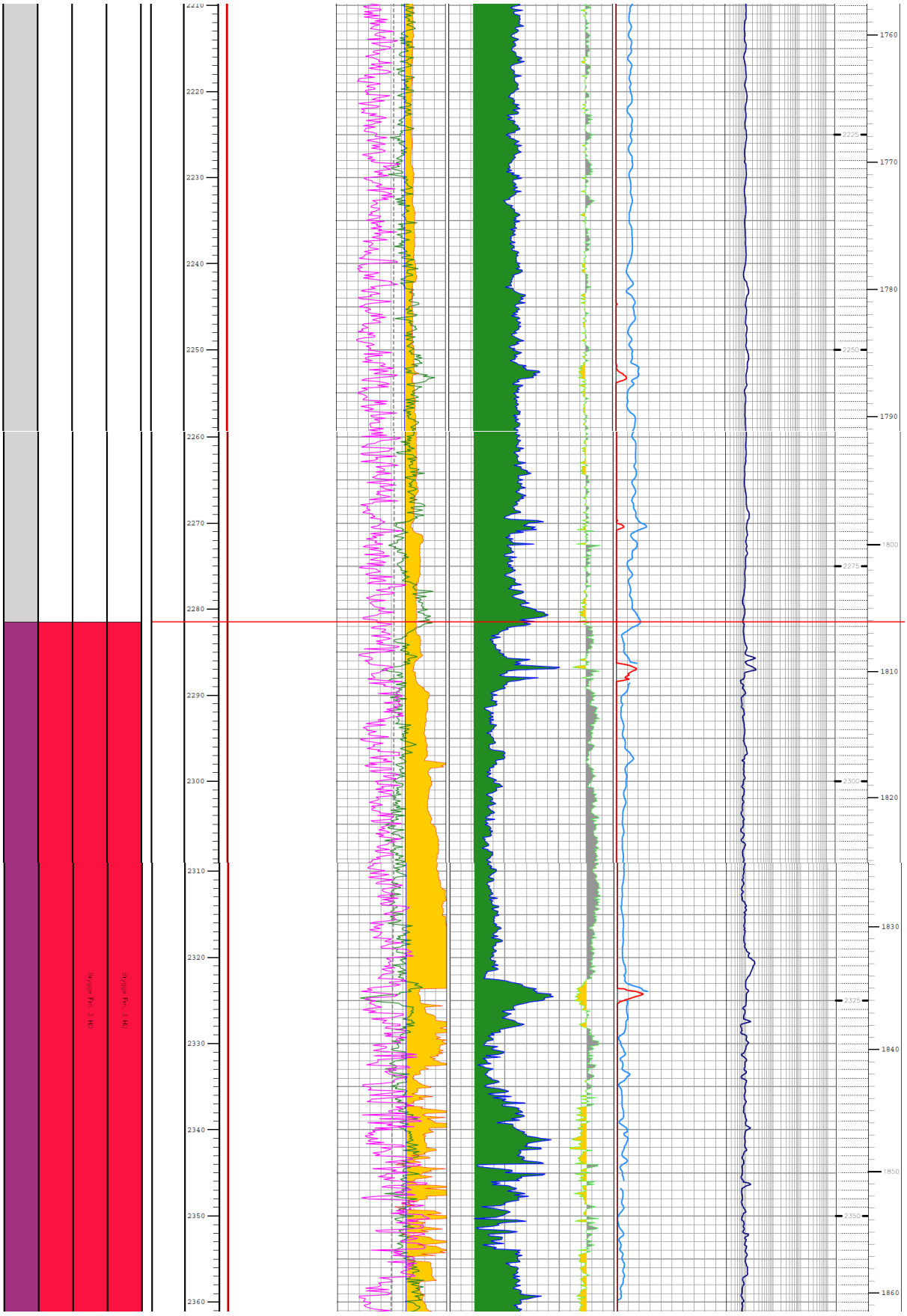
2210
2220
2230
2240
2250
2260
2270
2280
2290
2300
2310
2320
2330
2340
2350
2360
1760
1770
1780
1790
1800
1810
1820
1830
1840
1850
1860
2225
2250
2275
2300
2325
2350

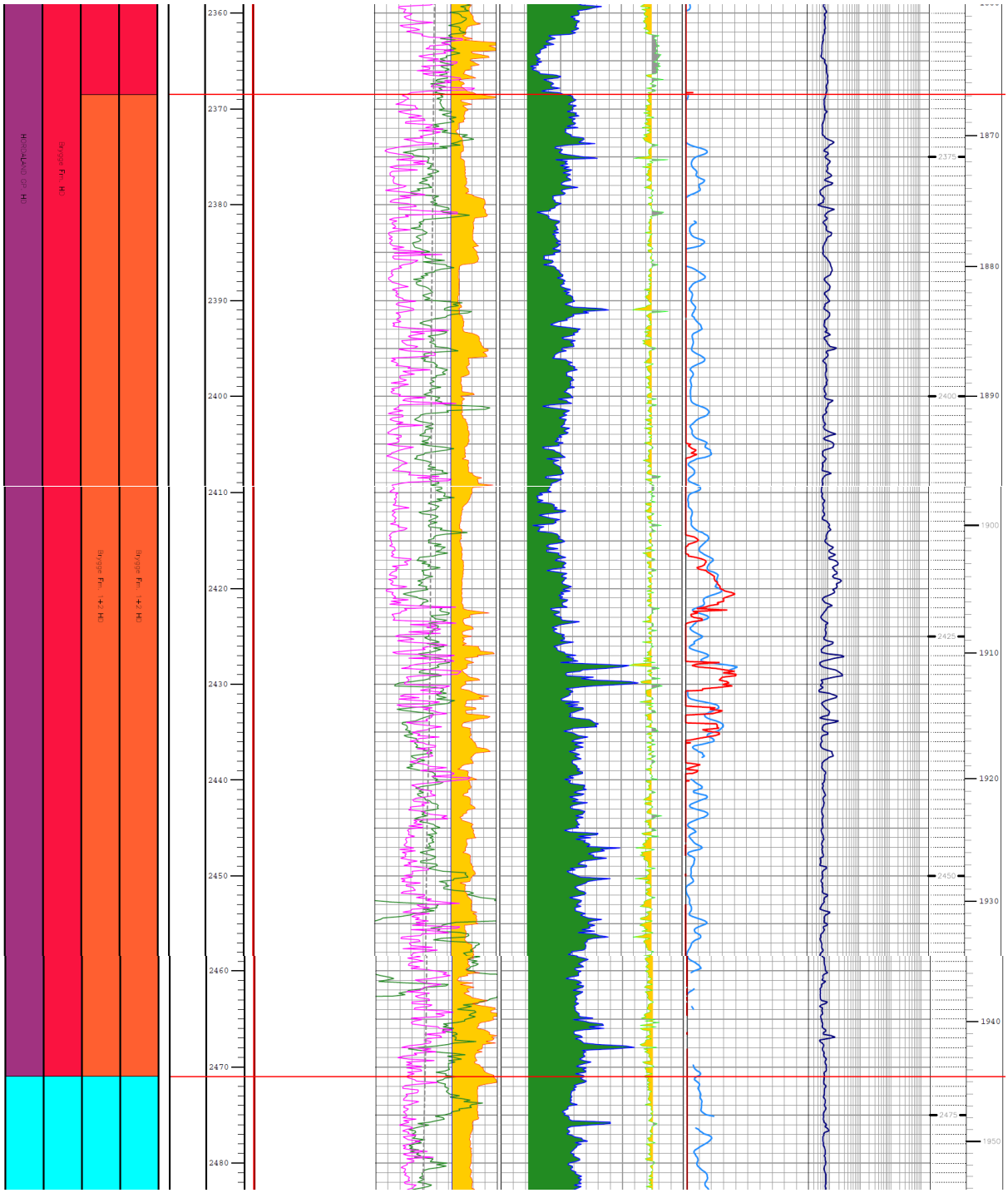
Bridge Fm. HD
Bridge Fm. +2 HD
2360
2370
2380
2390
2400
2410
2420
2430
2440
2450
2460
2470
2480
1870
1880
1890
1900
1910
1920
1930
1940
1950
2375
2400
2425
2450
2475

Heidrun Field: Well B

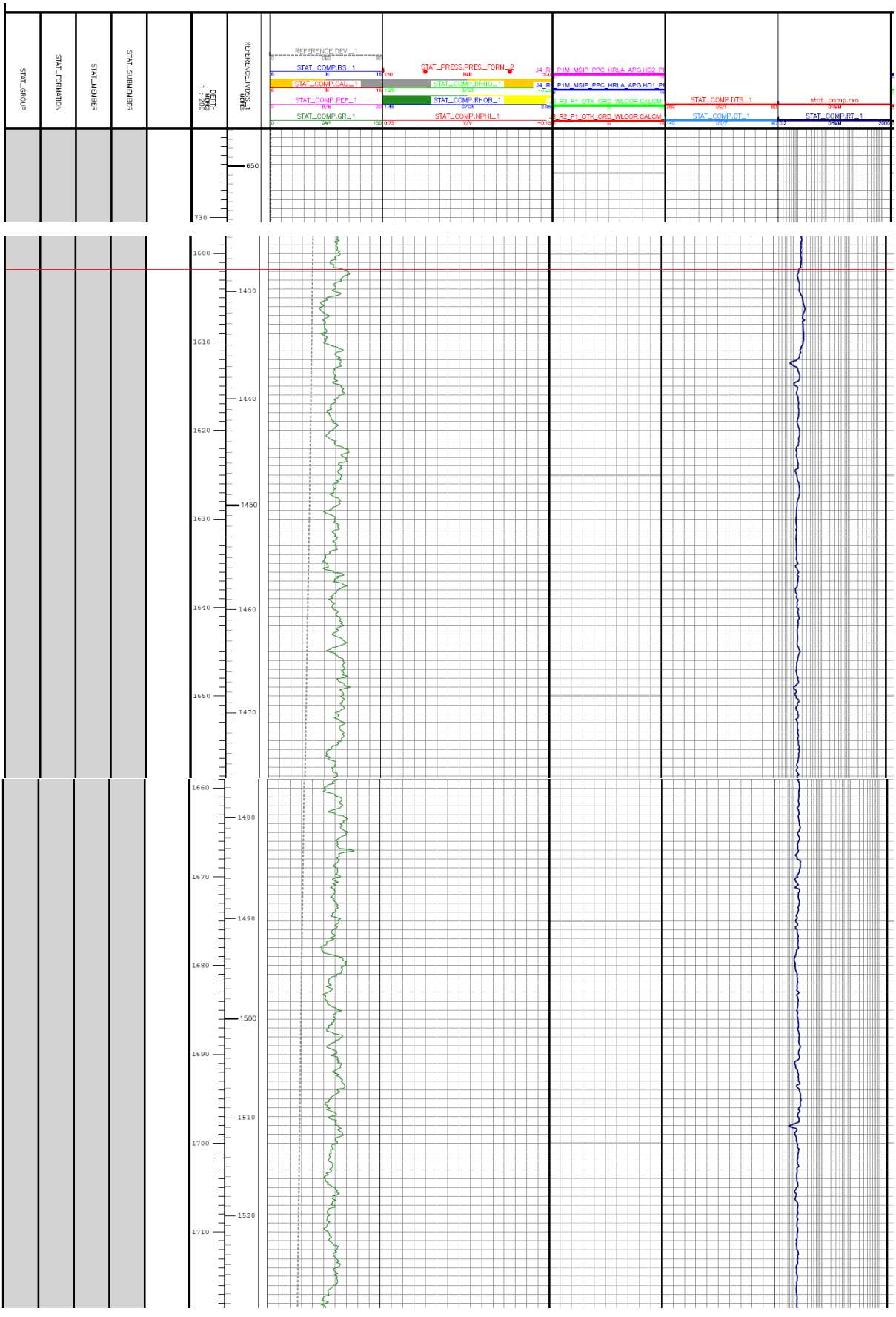

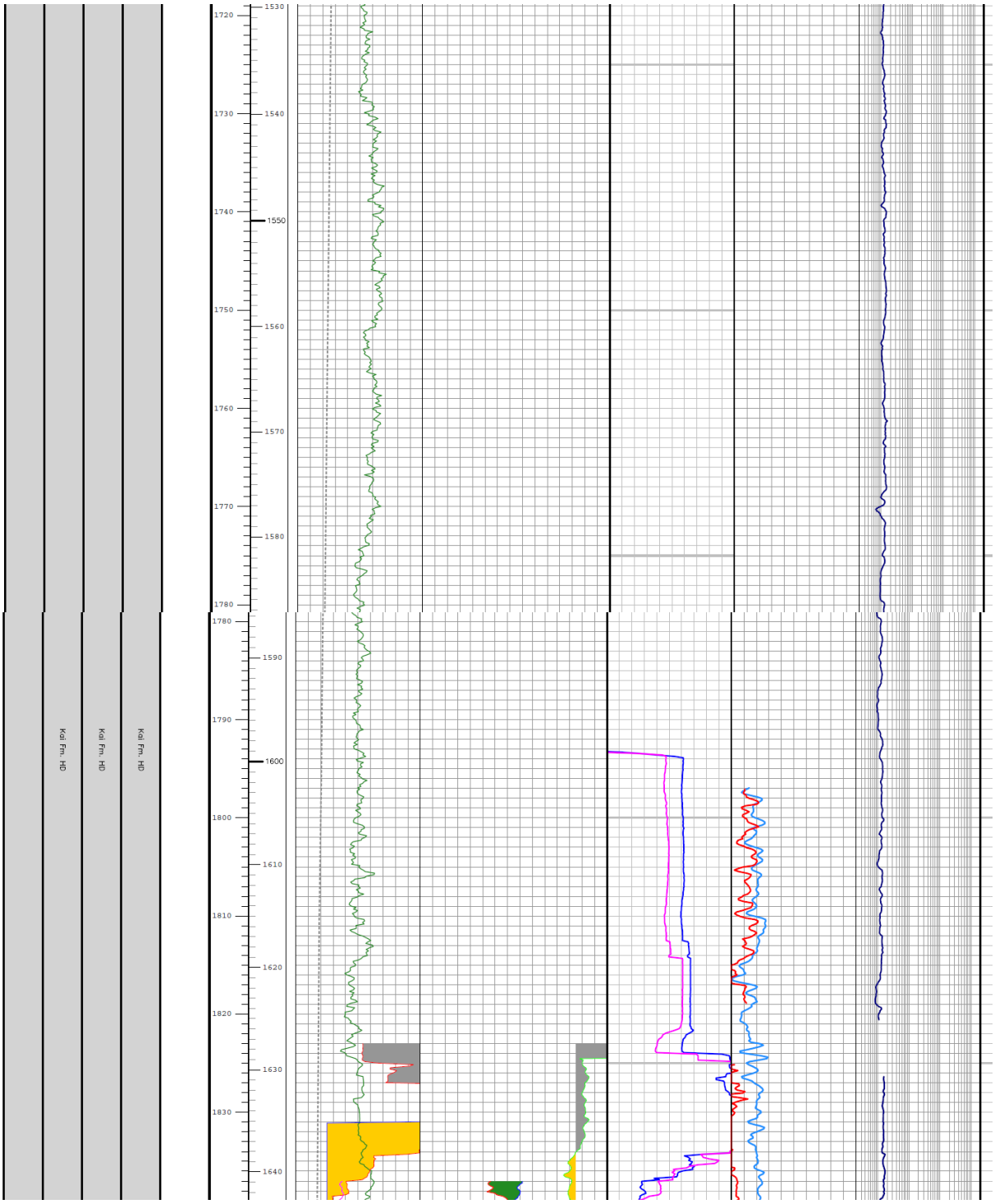
Kai Fm. HD
Kai Fm. HD
Kai Fm. HD
1720
1730
1740
1750
1760
1770
1780
1530
1540
1550
1560
1570
1580
1780
1790
1800
1810
1820
1830
1590
1600
1610
1620
1630
1640

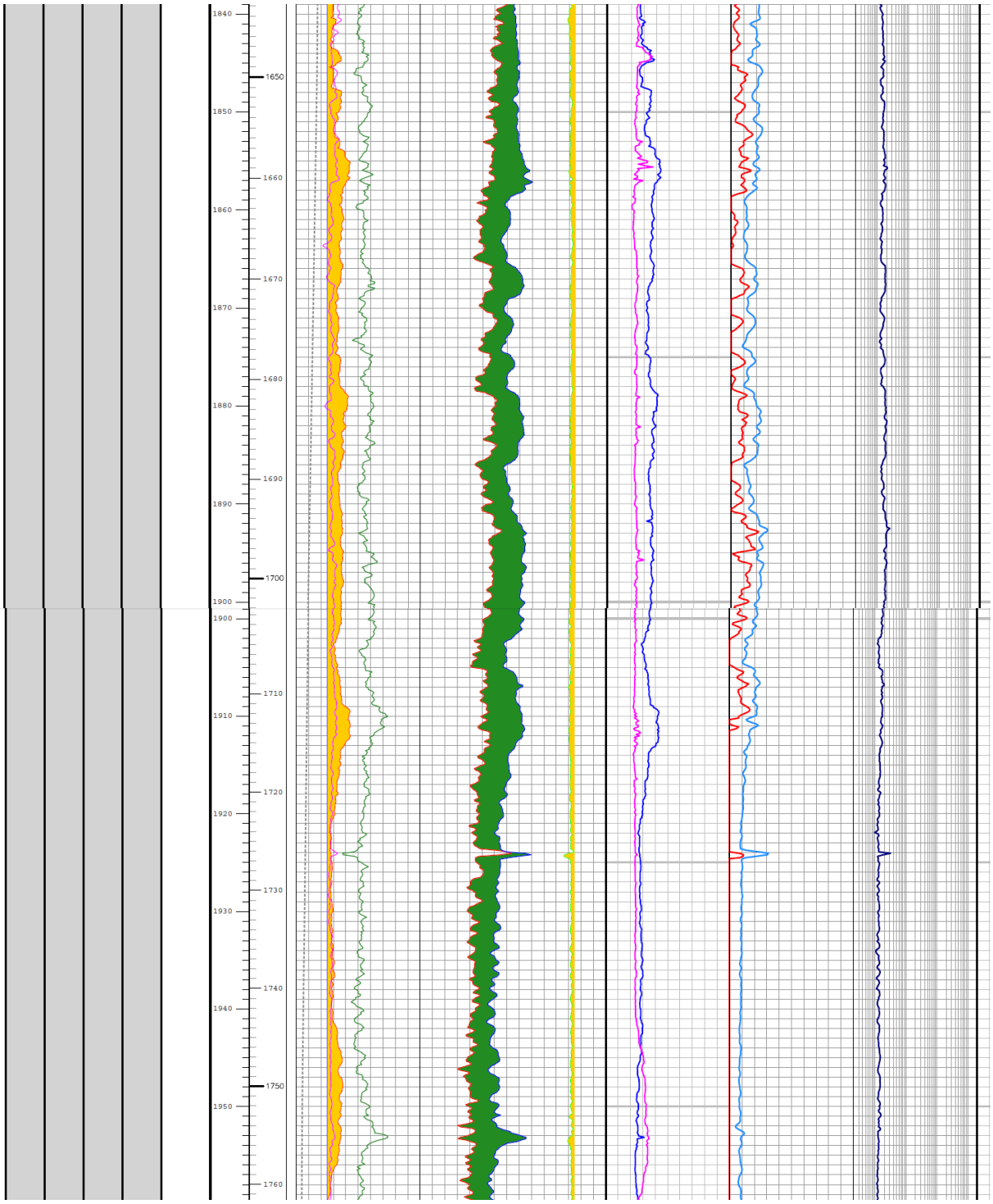
1840
1850
1860
1870
1880
1890
1900
1910
1920
1930
1940
1950
1650
1660
1670
1680
1690
1700
1710
1720
1730
1740
1750
1760

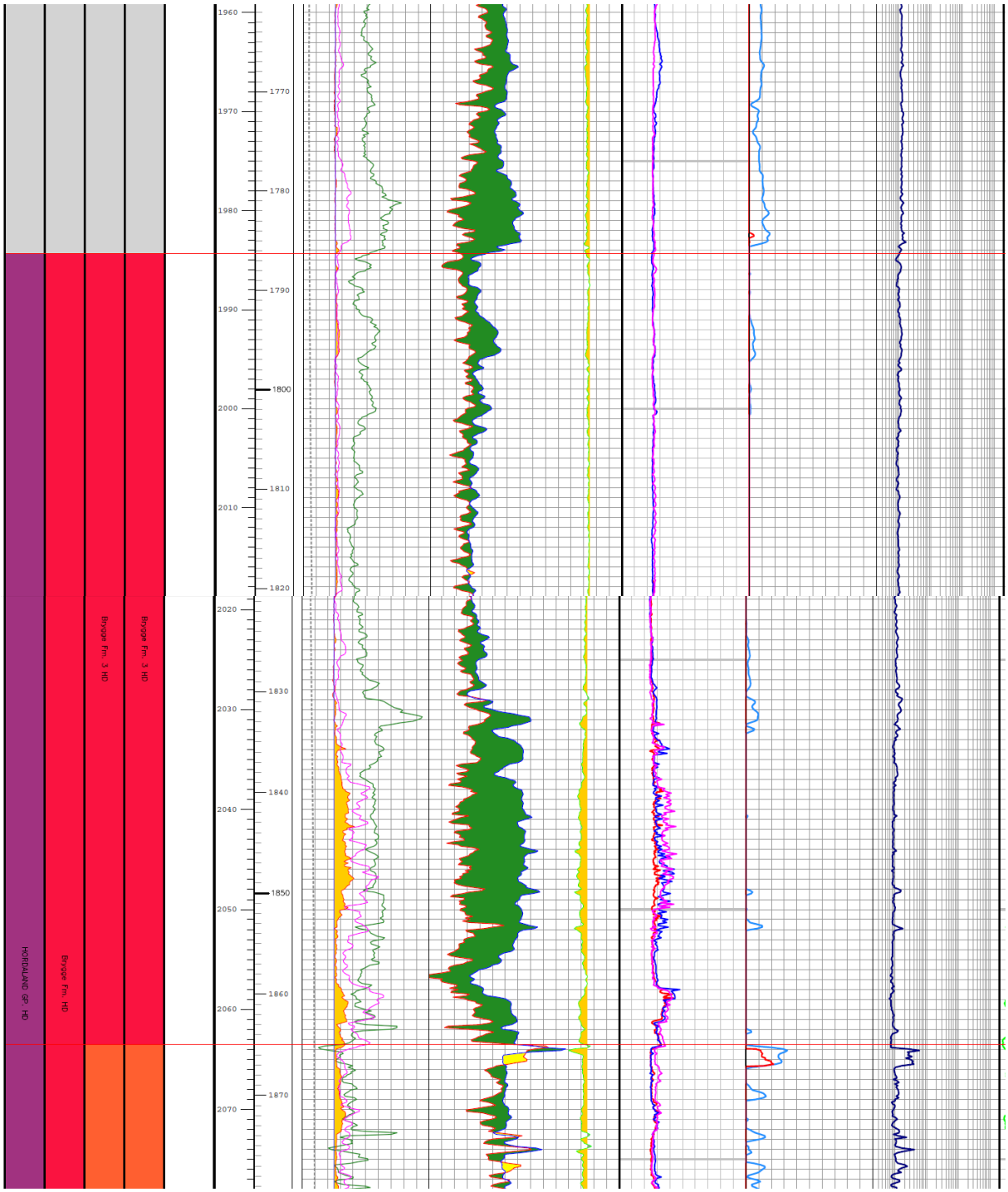
HORDALAND GP. HD
Brygge Fm. HD
Brygge Fm. 3 HD
Brygge Fm. 3 HD
1960
1970
1980
1990
2000
2010
2020
2030
2040
2050
2060
2070
1770
1780
1790
1800
1810
1820
1830
1840
1850
1860
1870

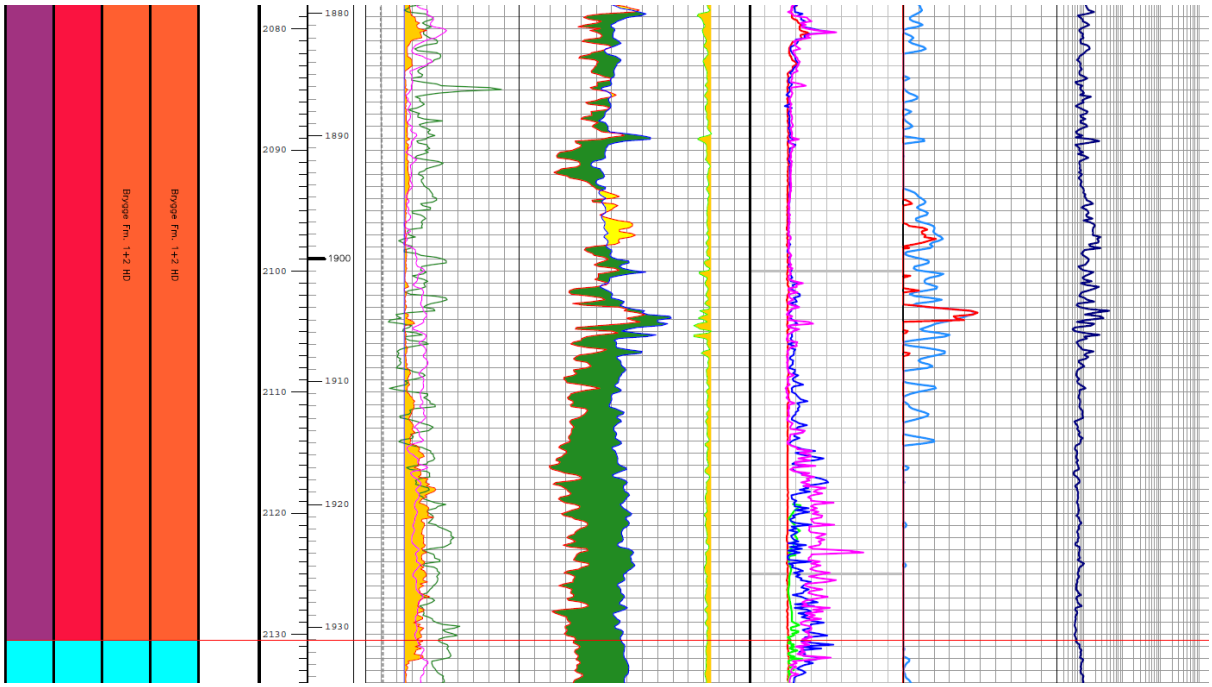
Brygge Fm. 1+2 HD
Brygge Fm. 1+2 HD
2080
2090
2100
2110
2120
2130
1880
1890
1900
1910
1920
1930

Heidrun Field: Well C

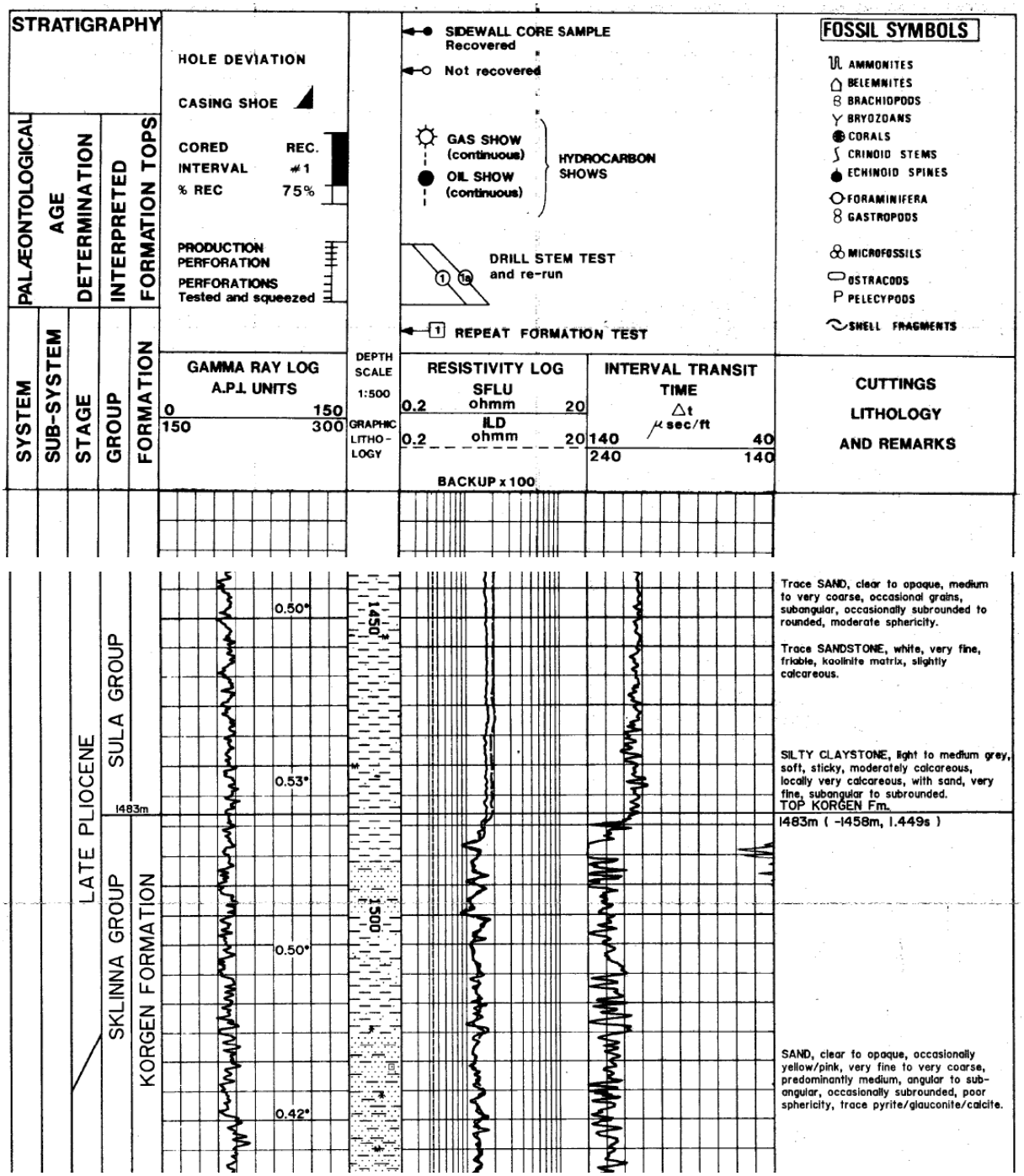

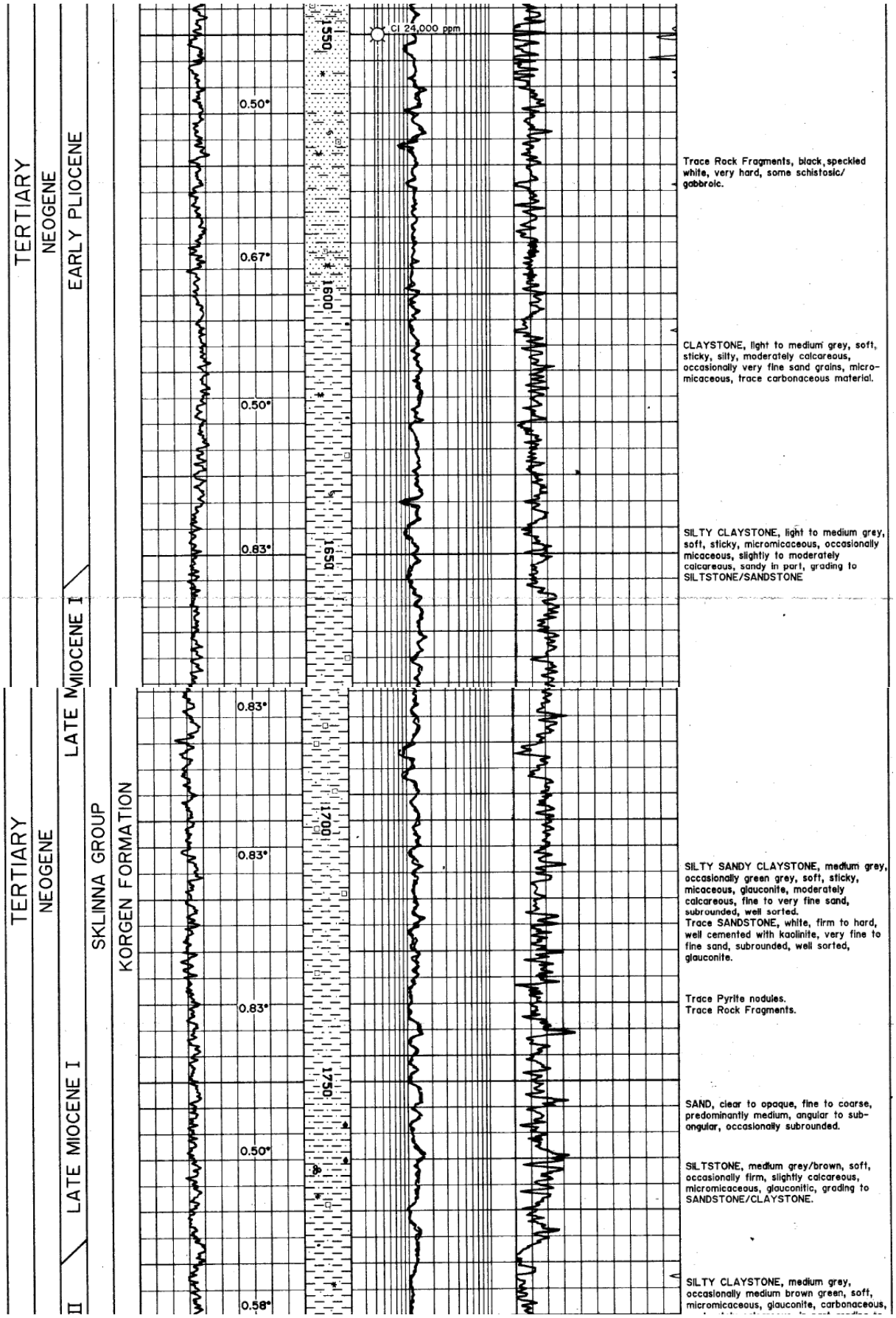
TERTIARY
NEOGENE
EARLY PLIOCENE
MIOCENE I
Cl 24,000 ppm
1550
1600
1650
1700
1750
0.50°
0.67°
0.50°
0.83°
0.83°
0.83°
0.83°
0.50°
0.58°
Trace Rock Fragments, black, speckled white, very hard, some schistosic/ gabbroic.
CLAYSTONE, light to medium grey, soft, sticky, silty, moderately calcareous, occasionally very fine sand grains, micro-micaceous, trace carbonaceous material.
SILTY CLAYSTONE, light to medium grey, soft, sticky, micromicaceous, occasionally micaceous, slightly to moderately calcareous, sandy in part, grading to SILTSTONE/SANDSTONE
TERTIARY
NEOGENE
LATE MIOCENE I
II
SKLINNA GROUP
KORGEN FORMATION
SILTY SANDY CLAYSTONE, medium grey, occasionally green grey, soft, sticky, micaceous, glauconite, moderately calcareous, fine to very fine sand, subrounded, well sorted.
Trace SANDSTONE, white, firm to hard, well cemented with kaolinite, very fine to fine sand, subrounded, well sorted, glauconite.
Trace Pyrite nodules.
Trace Rock Fragments.
SAND, clear to opaque, fine to coarse, predominantly medium, angular to sub-angular, occasionally subrounded.
SILTSTONE, medium grey/brown, soft, occasionally firm, slightly calcareous, micromicaceous, glauconitic, grading to SANDSTONE/CLAYSTONE.
SILTY CLAYSTONE, medium grey, occasionally medium brown green, soft, micromicaceous, glauconite, carbonaceous,

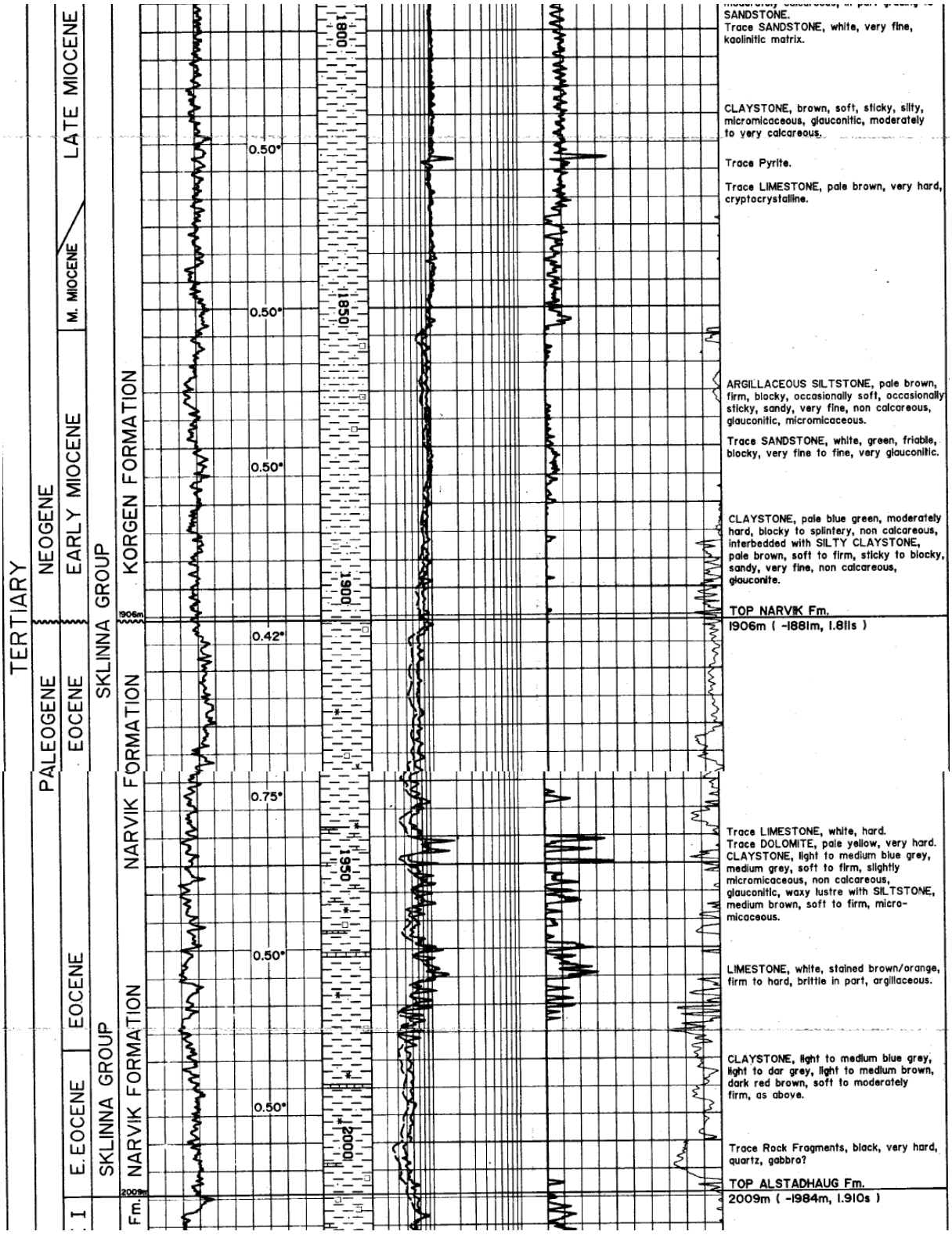
TERTIARY
PALEOGENE
NEOGENE
EOCENE
EARLY MIOCENE
M. MIOCENE
LATE MIOCENE
SKLINNA GROUP
KORGEN FORMATION
NARVIK FORMATION
1906m
E. EOCENE
EOCENE
SKLINNA GROUP
NARVIK FORMATION
Fm.
2009m
1800
1850
1900
1950
2000
0.50°
0.50°
0.50°
0.42°
0.75°
0.50°
0.50°
SANDSTONE.
Trace SANDSTONE, white, very fine, kaolinitic matrix.
CLAYSTONE, brown, soft, sticky, silty, micromicaceous, glauconitic, moderately to very calcareous.
Trace Pyrite.
Trace LIMESTONE, pale brown, very hard, cryptacrystalline.
ARGILLACEOUS SILTSTONE, pale brown, firm, blocky, occasionally soft, occasionally sticky, sandy, very fine, non calcareous, glauconitic, micromicaceous.
Trace SANDSTONE, white, green, friable, blocky, very fine to fine, very glauconitic.
CLAYSTONE, pale blue green, moderately hard, blocky to splintery, non calcareous, interbedded with SILTY CLAYSTONE, pale brown, soft to firm, sticky to blocky, sandy, very fine, non calcareous, glauconite.
TOP NARVIK Fm.
1906m (-1881m, 1.81ls)
Trace LIMESTONE, white, hard.
Trace DOLOMITE, pale yellow, very hard.
CLAYSTONE, light to medium blue grey, medium grey, soft to firm, slightly micromicaceous, non calcareous, glauconitic, waxy lustre with SILTSTONE, medium brown, soft to firm, micro-micaceous.
LIMESTONE, white, stained brown/orange, firm to hard, brittle in part, argillaceous.
CLAYSTONE, light to medium blue grey, light to dar grey, light to medium brown, dark red brown, soft to moderately firm, as above.
Trace Rock Fragments, black, very hard, quartz, gabbro?
TOP ALSTADHAUG Fm.
2009m (-1984m, 1.910s)

Åsgard Field: Well D

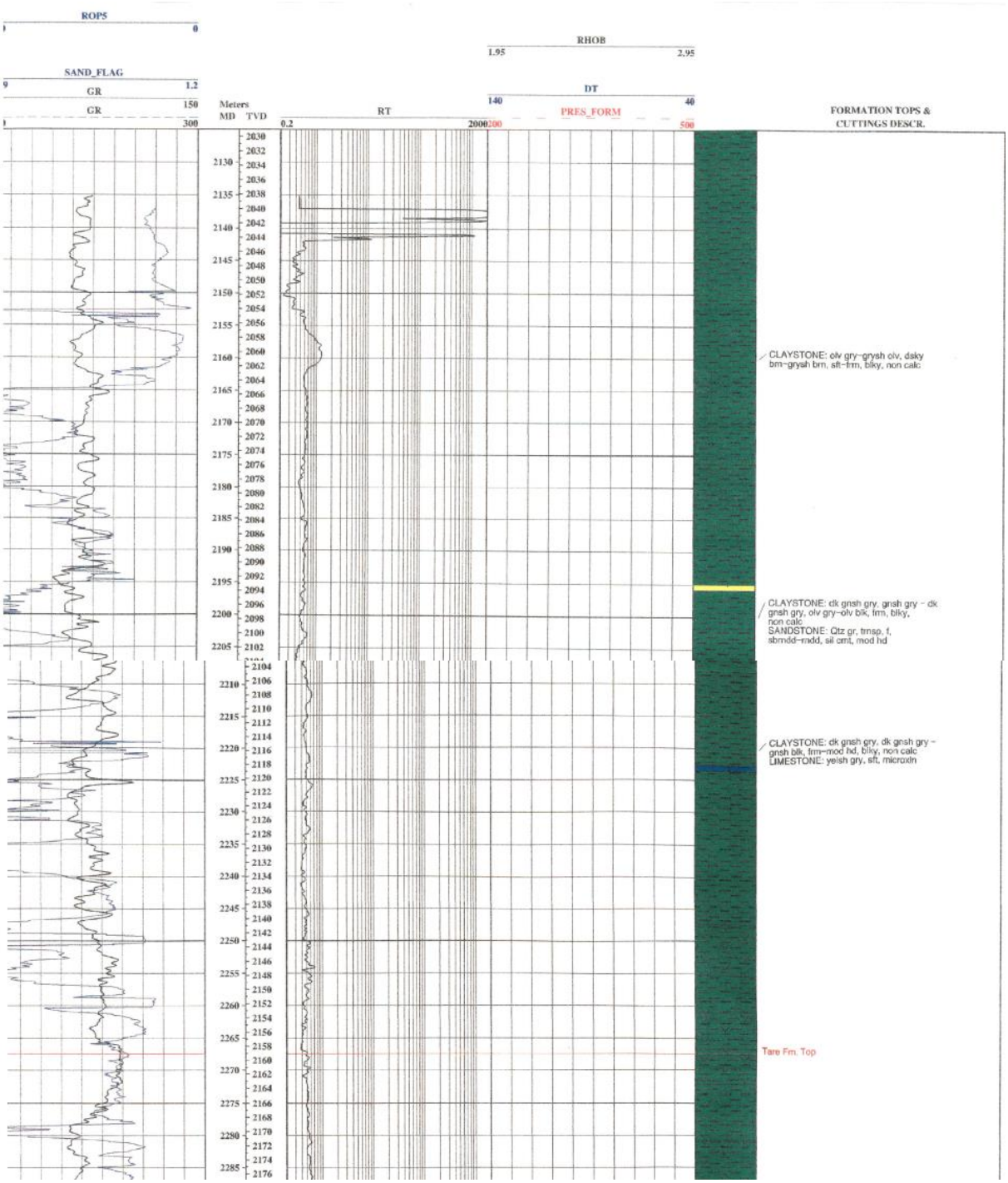

Åsgard Field: Well E

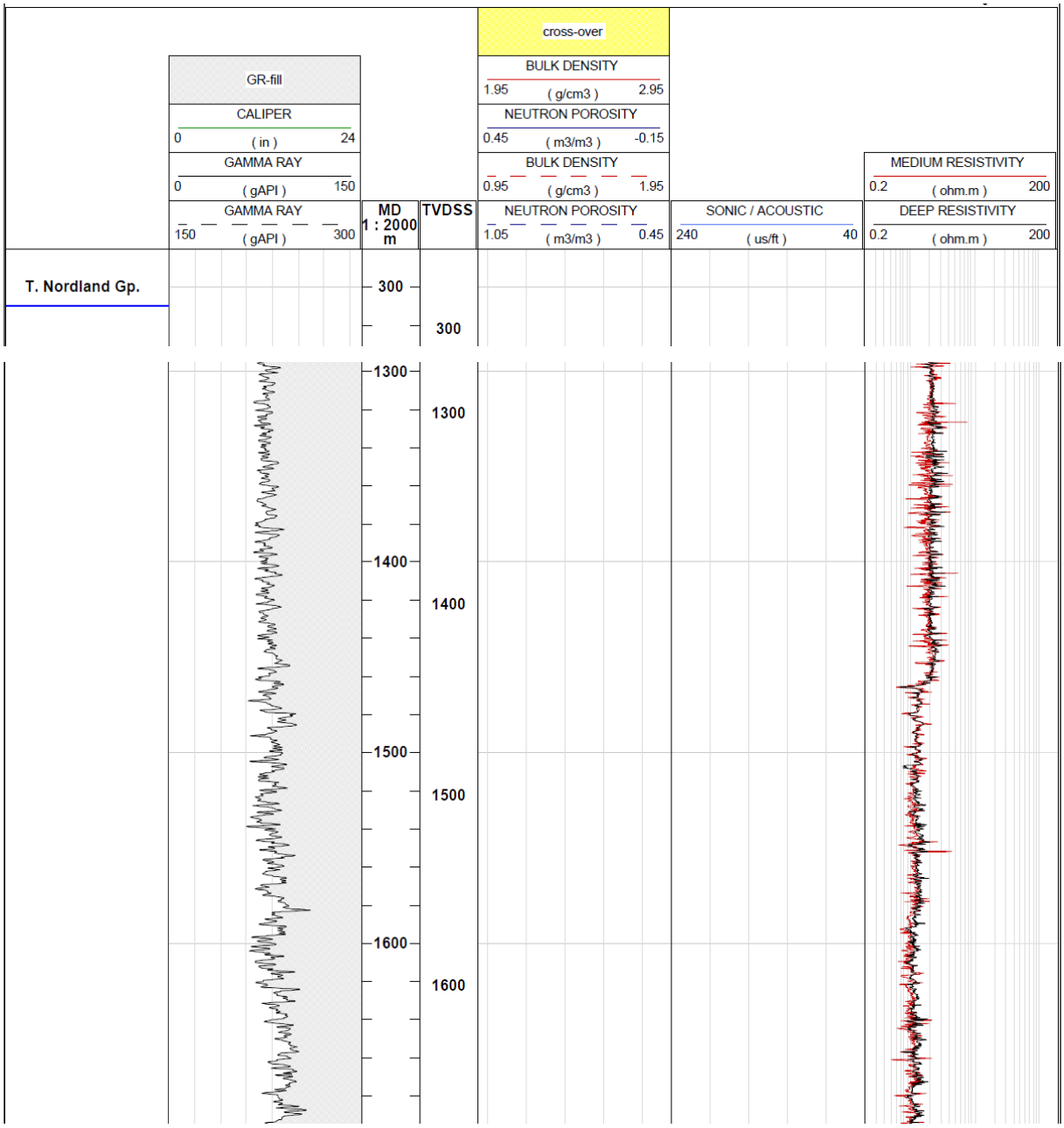

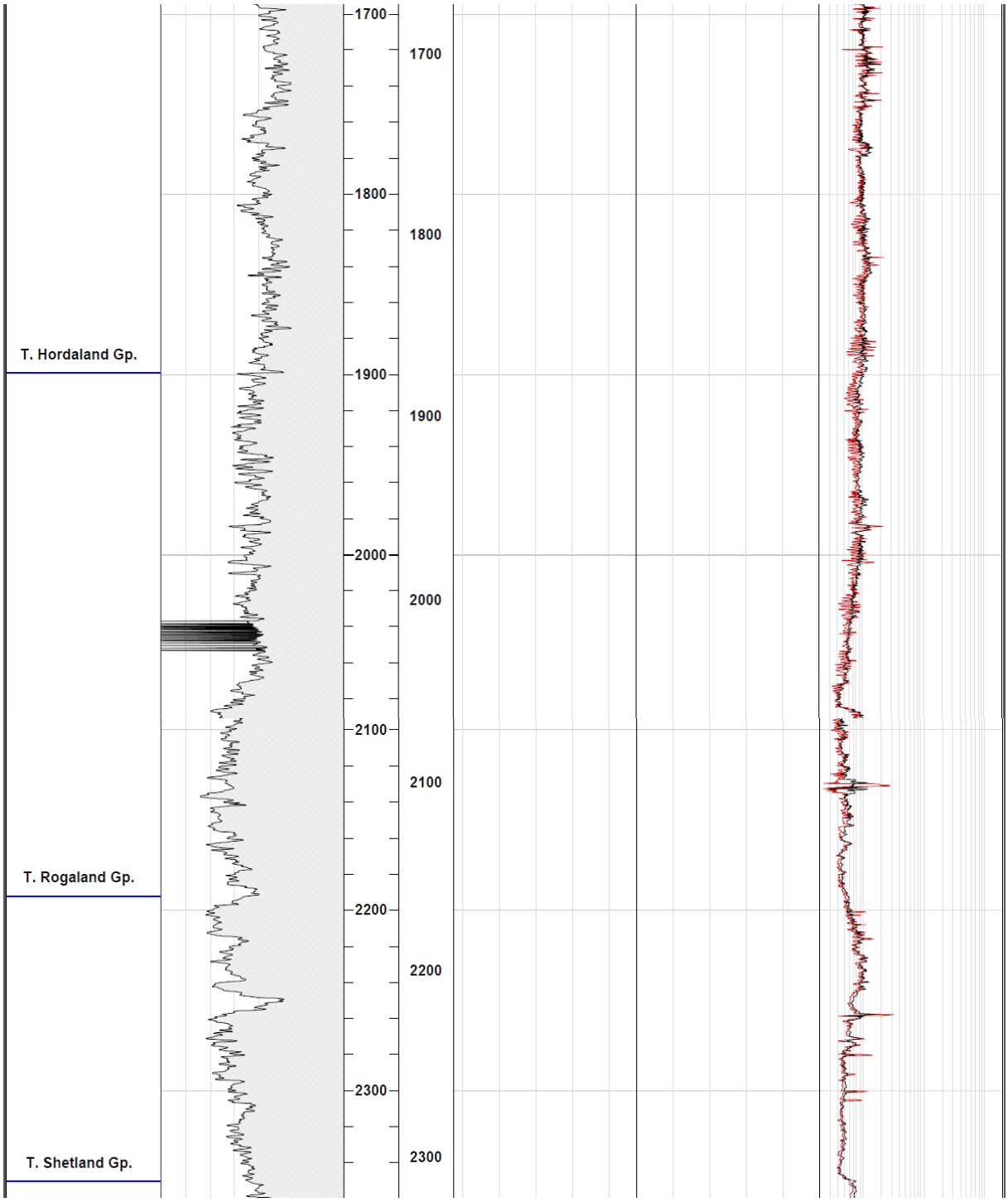
T. Hordaland Gp.
T. Rogaland Gp.
T. Shetland Gp.
1700
1800
1900
2000
2100
2200
2300

Åsgard Field: Well F

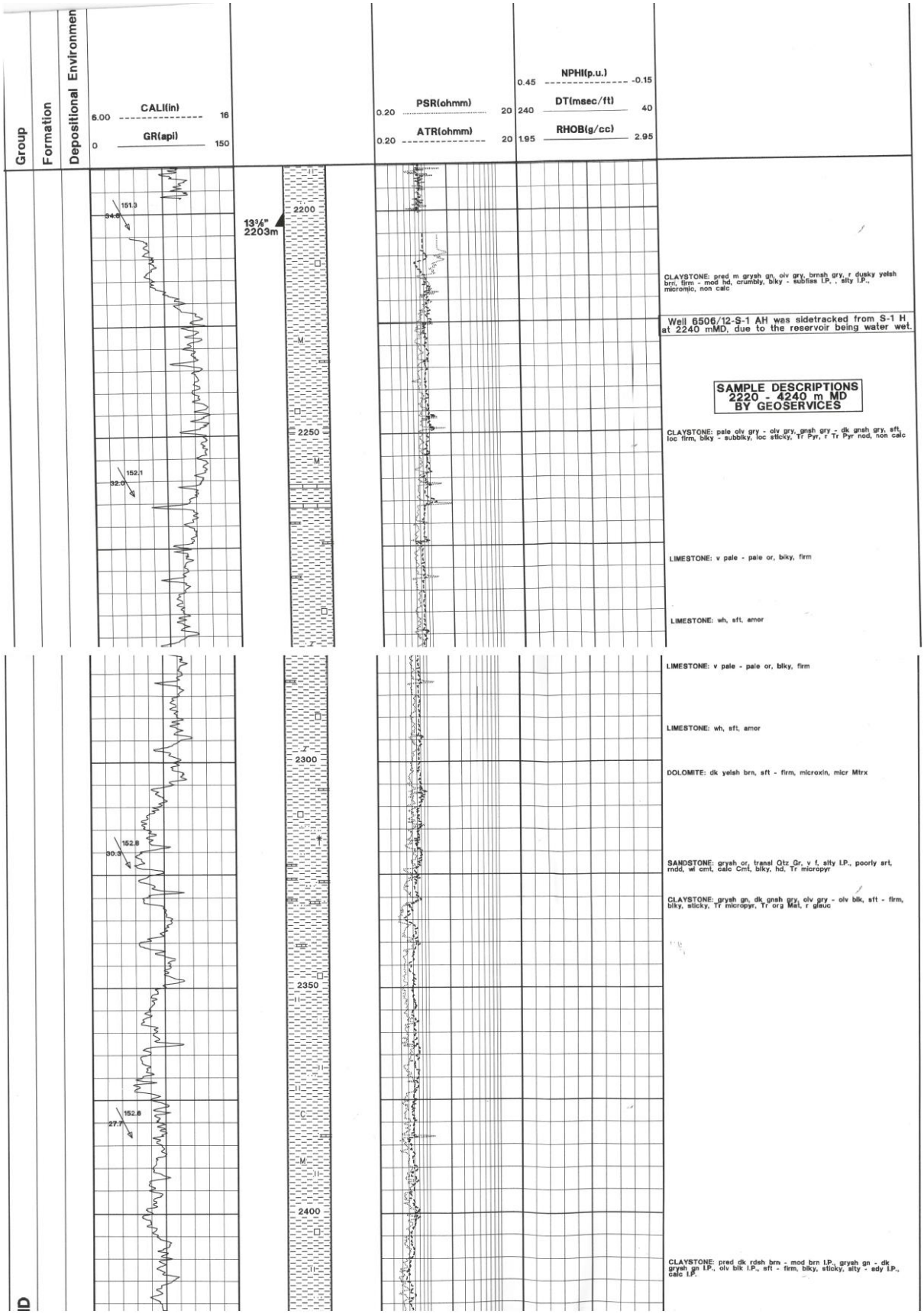

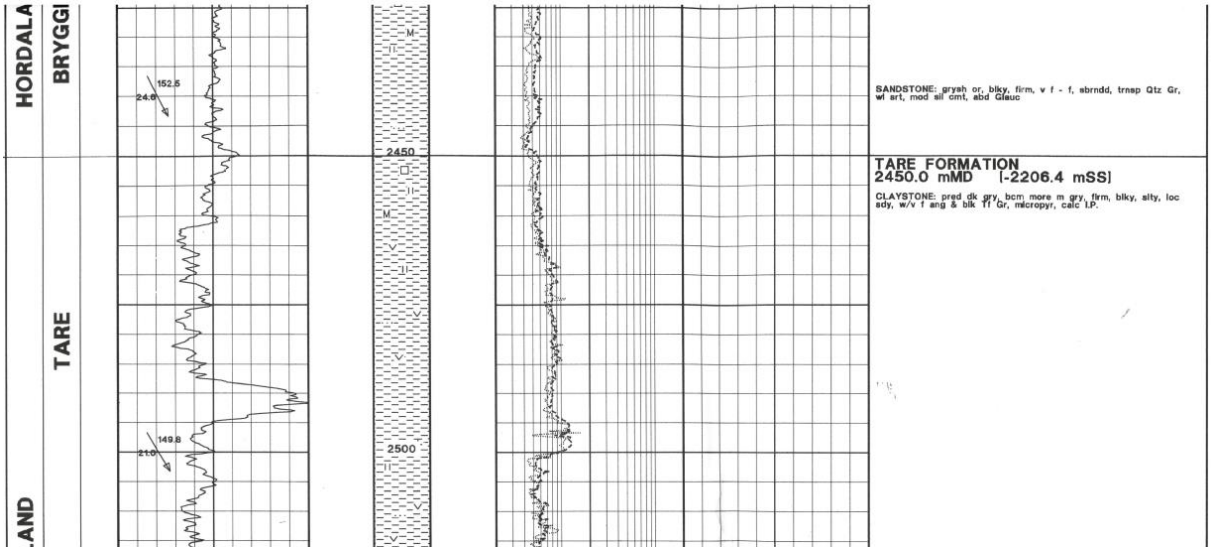
HORDALA
BRYGGI
TARE
.AND
152.5
24.0
149.8
21.0
2450
2500
SANDSTONE: gryish or, blky, firm, v f - f, sbrndd, trnsp Qtz Gr, wl srt, mod sil cmt, abd Glauc
TARE FORMATION
2450.0 mMD [-2206.4 mSS]
CLAYSTONE: pred dk gry, bcm more m gry, firm, blky, silty, loc sdy, w/v f ang & blk ft Gr, micropyr, calc I.P.

Aasta Hansteen Field: Well G

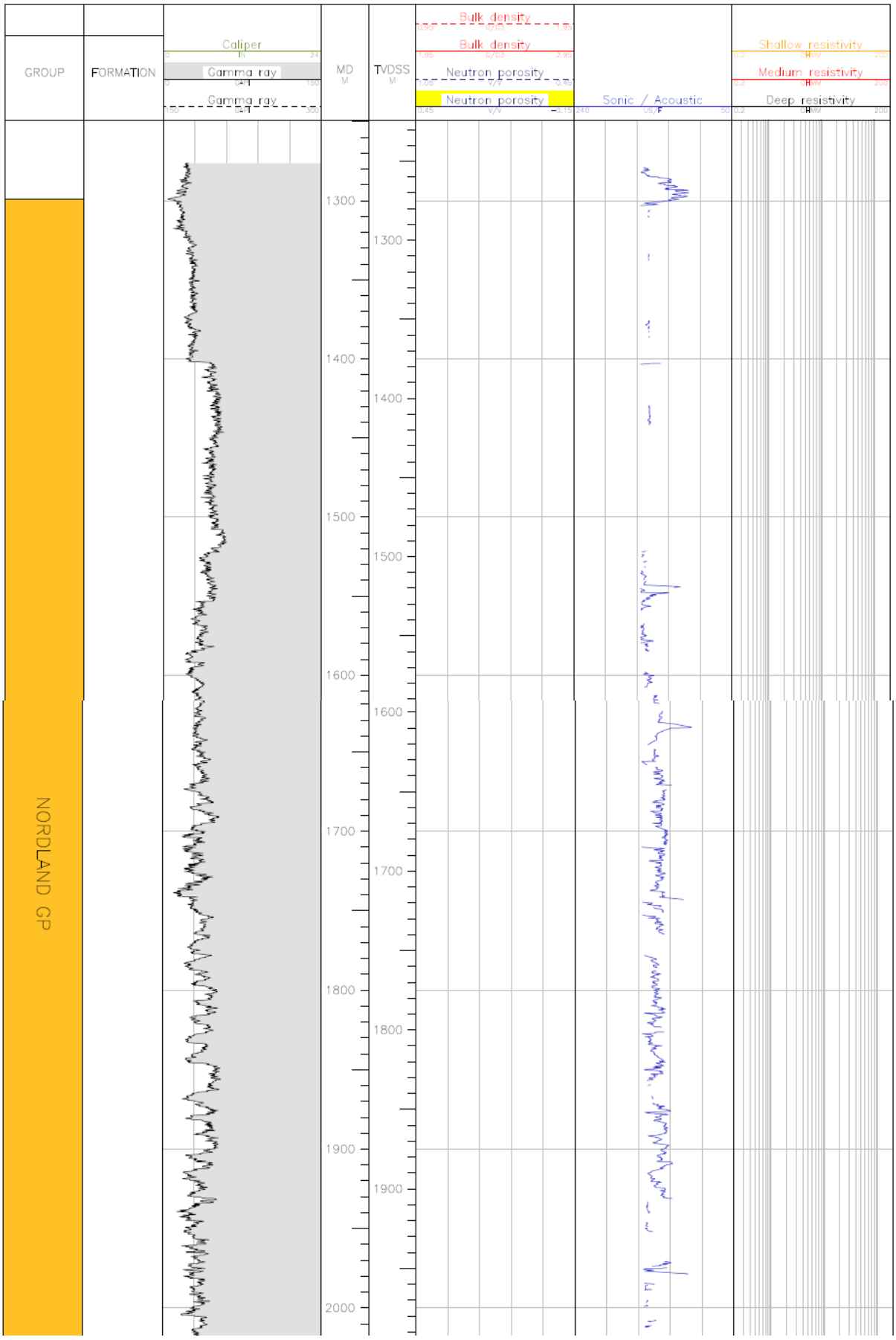

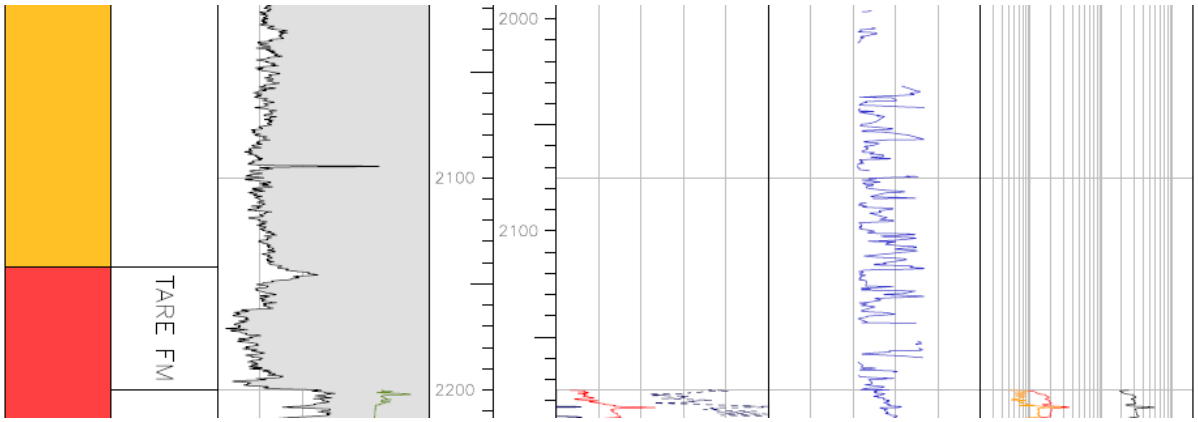
TARE FM
2000
2100
2100
2200

Aasta Hansteen Field: Well H

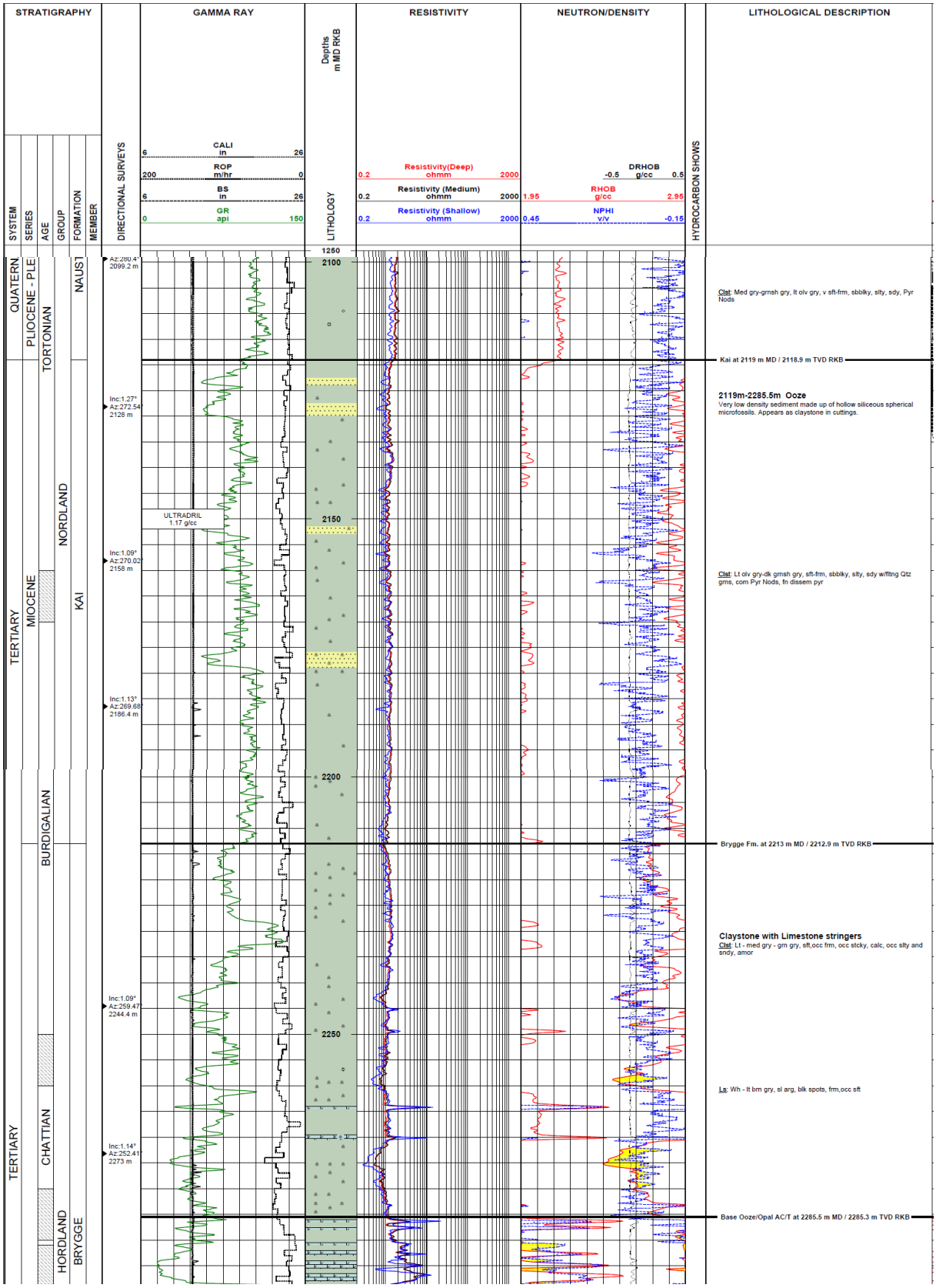

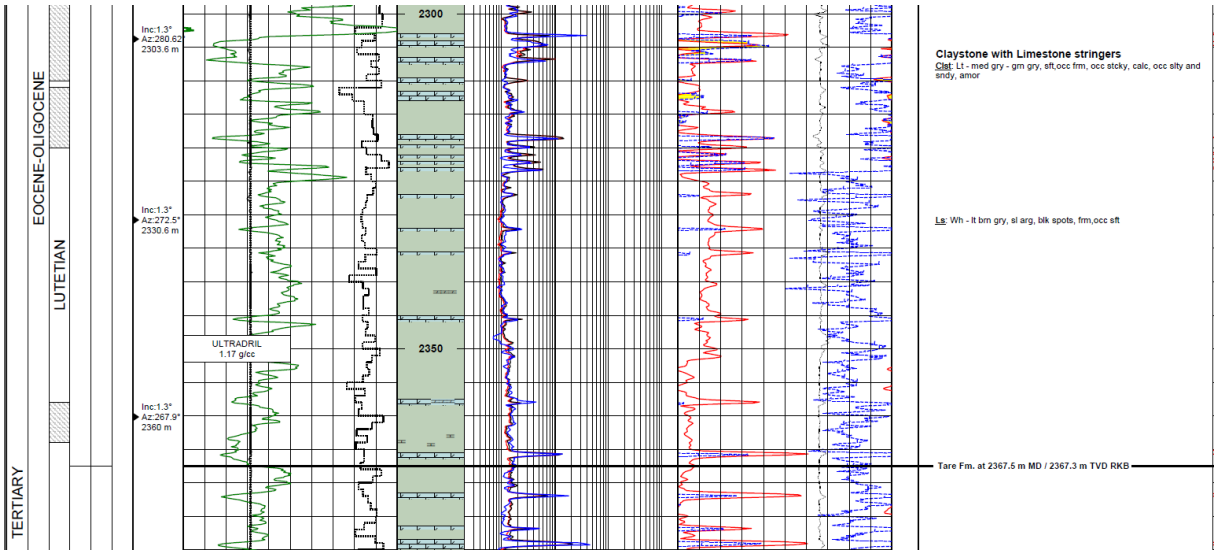
TERTIARY
EOCENE-OLIGOCENE
LUTETIAN
Inc:1.3°
Az:280.62°
2303.6 m
Inc:1.3°
Az:272.5°
2330.6 m
Inc:1.3°
Az:267.9°
2360 m
ULTRADRIL
1.17 g/cc
2300
2350
Claystone with Limestone stringers
Clst: Lt - med gry - grn gry, sft,occ frm, occ sticky, calc, occ slty and sndy, amor
Ls: Wh - lt brn gry, sl arg, blk spots, frm,occ sft
Tare Fm. at 2367.5 m MD / 2367.3 m TVD RKB

Aasta Hansteen Field: Well I

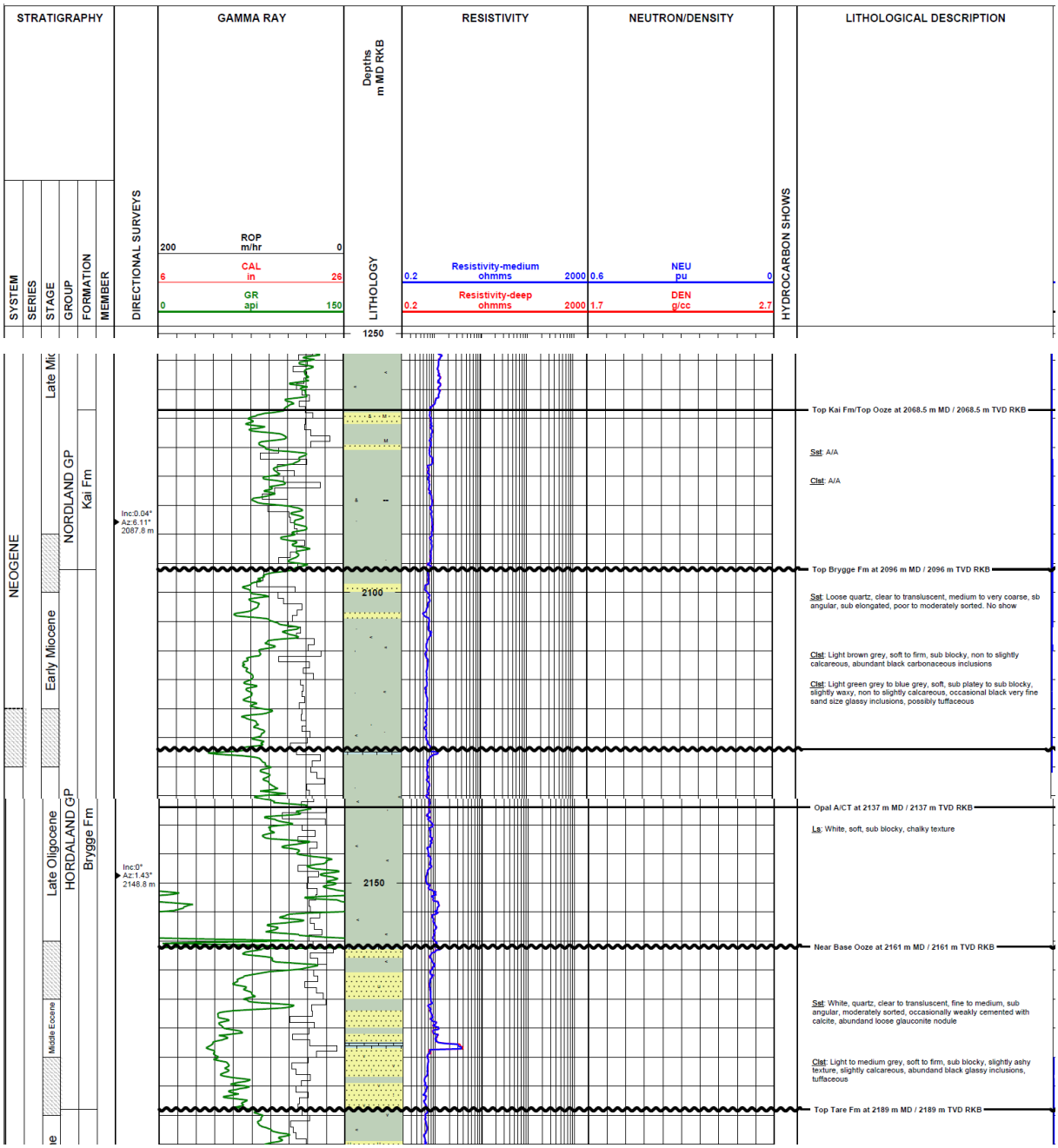

Appendix C

Cuttings descriptions from:

- Well 0.2
- Well A
- Well B

Heidrun Field: Well 0.2

1770			Sample mainly cmt, Bar carb and Steal seal	abd mud add, cmt
1780	100	CLST	Med gry, sft-frm, blky, v calc	abd mud add, cmt
1790	100	CLST	Med gry-dk gnsh gry, sft, amor, sl slty, v calc, Tr glauc	abd mud add, cmt
1800	100	CLST	a/a, Glauc	abd mud add, cmt
1810	100	CLST	a/a	abd mud add, cmt
1820	100	CLST	Olv gry-brn gry, mod hd, sbblky-sbrndd, ea, sl calc, v slty	abd mud add, Tr cmt
1830	100	CLST	a/a, sft-frm	abd mud add, Tr cmt
1840	100	CLST	Olv gry, else a/a	abd mud add, Tr cmt
1850	100	CLST	a/a, i.p. amor	abd mud add, Tr cmt
1860	100	CLST	a/a	abd mud add, Tr cmt
1870	100	CLST	Dk gnsh gry, else a/a	abd mud add, Tr cmt
1880	100	CLST	a/a	abd mud add, Tr cmt
1890	100	CLST	a/a, Tr glauc	abd mud add, Tr cmt
1900	100	CLST	a/a, v slty	abd mud add, Tr cmt
1910	100	CLST	a/a, v slty, calc	abd mud add, Tr cmt
1920	100	CLST	a/a, sly calc	abd mud add, Tr cmt
1930	100	CLST	a/a, brn gry	abd mud add, Tr cmt
1940	100	CLST	a/a	Tr mud add, Tr cmt

Heidrun Field: Well A

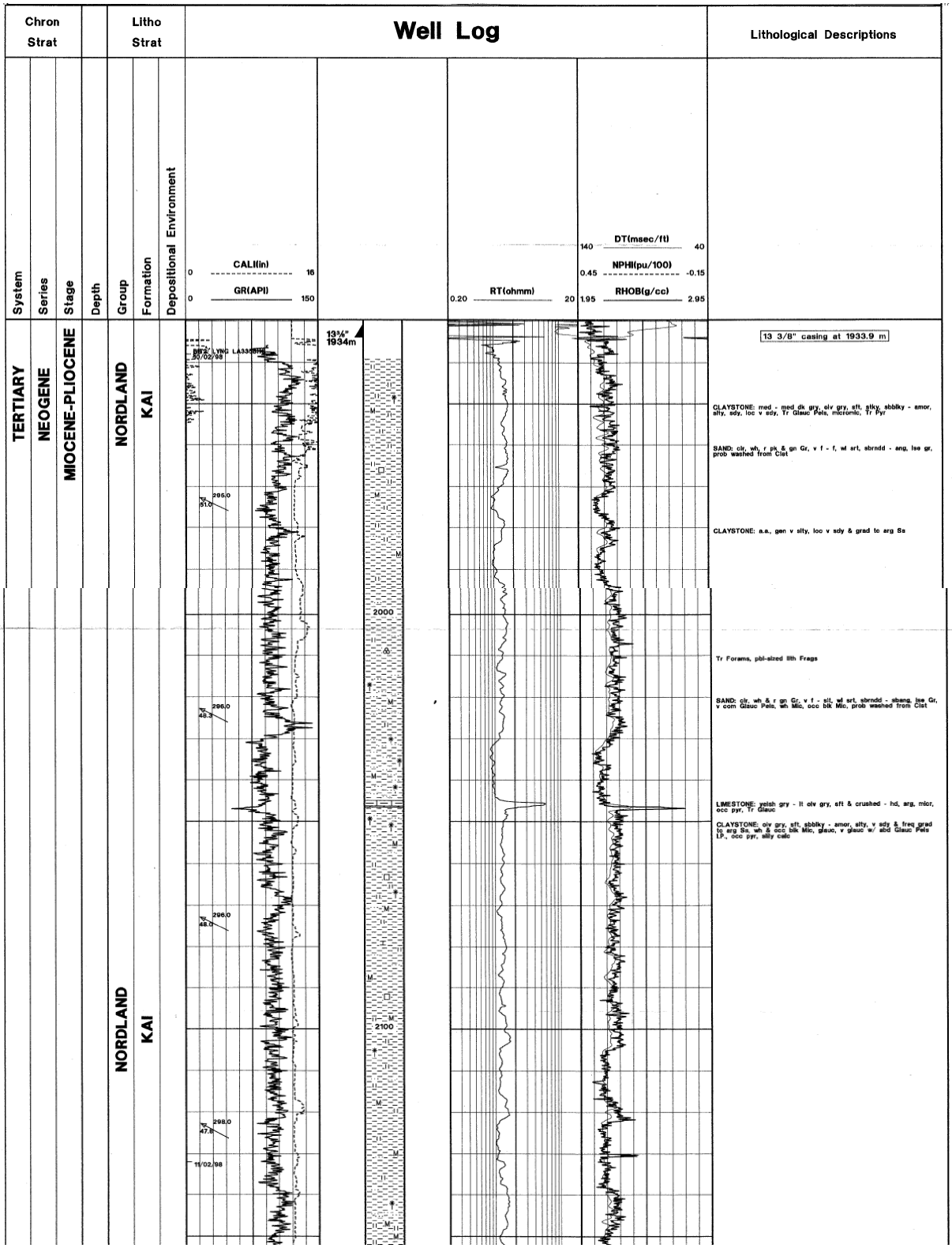

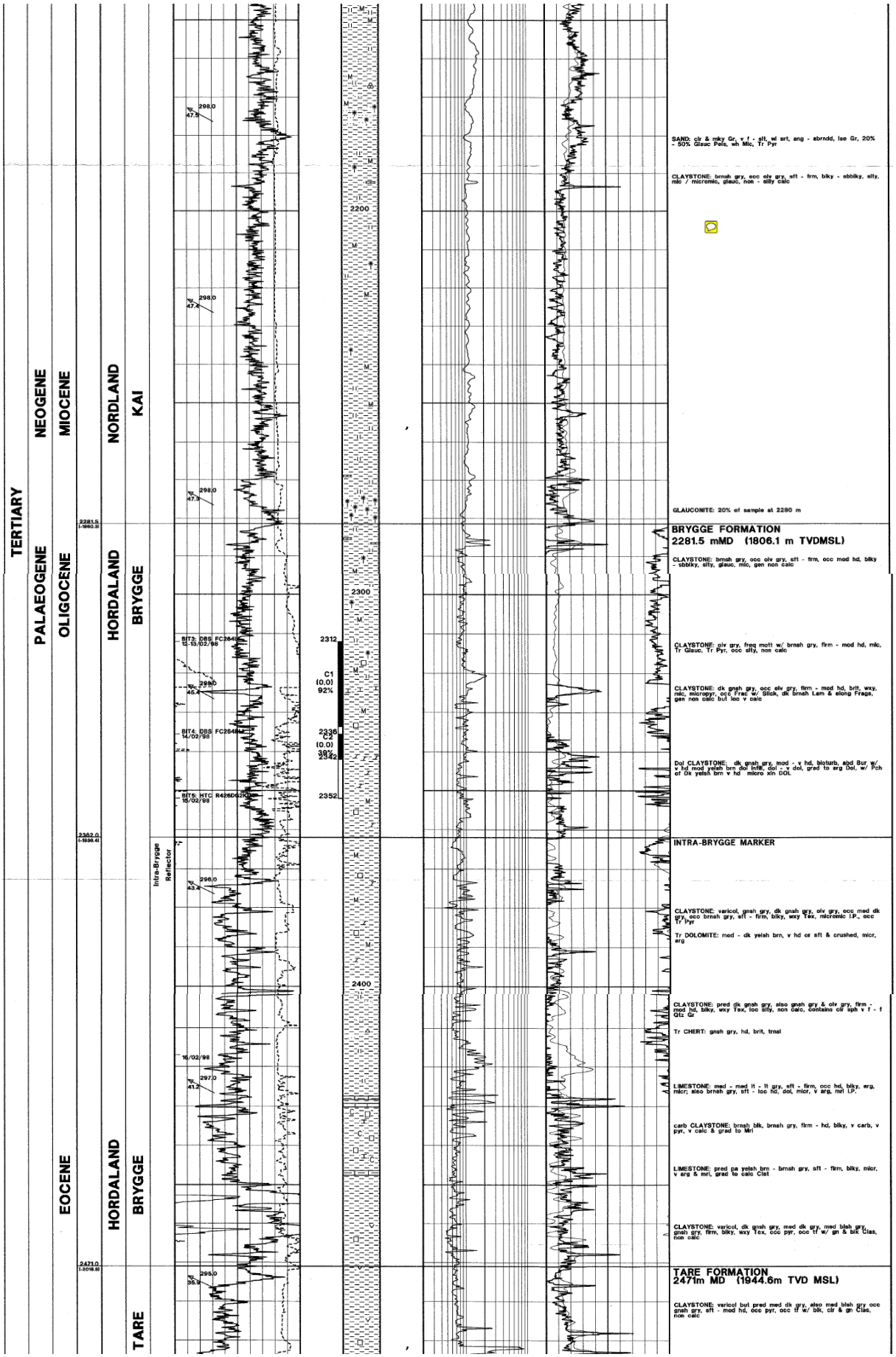
TERTIARY
PALAEOGENE
NEOGENE
EOCENE
OLIGOCENE
MIOCENE
HORDALAND
NORDLAND
HORDALAND
BRYGGE
KAI
BRYGGE
TARE
Intra-Brygge Reflector
2281.5 (-1960.3)
2302.0 (-1938.4)
2471.0 (-2018.8)
2312
2336
2342
2352
C1 (0.0) 92%
C2 (0.0) 98%
BIT3, DBS FC264 C, 13/02/98
BIT4, DBS FC264M2, 14/02/98
BIT5, HTC R426D62K2, 15/02/98
16/02/98
SAND: clr & mky Gr, v f - slt, wl srt, ang - sbrndd, lse Gr, 20% - 50% Glauc Pels, wh Mic, Tr Pyr
CLAYSTONE: brnsh gry, occ olv gry, sft - frm, blky - sbblky, silty, mic / micromic, glauc, non - silty calc
GLAUCONITE: 20% of sample at 2280 m
BRYGGE FORMATION
2281.5 mMD (1806.1 m TVDMSL)
CLAYSTONE: brnsh gry, occ olv gry, sft - frm, occ mod hd, blky - sbblky, silty, glauc, mic, gen non calc
CLAYSTONE: olv gry, freq mott w/ brnsh gry, frm - mod hd, mic, Tr Glauc, Tr Pyr, occ silty, non calc
CLAYSTONE: dk gnsh gry, occ olv gry, firm - mod hd, brit, wxy, mic, micropyr, occ Frac w/ Slick, dk brnsh Lam & elong Frags, gen non calc but loc v calc
Dol CLAYSTONE: dk gnsh gry, mod - v hd, bioturb, sbd Bst w/ v hd mod yelsh brn dol intst, dol - v dol, grad to arg Dol, w/ Pch of Dk yelsh brn v hd micro xln DOL
INTRA-BRYGGE MARKER
CLAYSTONE: varicol, gnsh gry, dk gnsh gry, olv gry, occ mod dk gry, occ brnsh gry, sft - firm, blky, wxy Tex, micromic I.P., occ Tr pyr
Tr DOLOMITE: mod - dk yelsh brn, v hd or sft & crushed, micr, arg
CLAYSTONE: pred dk gnsh gry, also gnsh gry & olv gry, firm - mod hd, blky, wxy Tex, loc slty, non calc, contains clr sph v f - f Qtz Gr
Tr CHERT: gnsh gry, hd, brit, trnal
LIMESTONE: med - med lt - lt gry, sft - firm, occ hd, blky, arg, micr; also brnsh gry, sft - loc hd, dol, micr, v arg, mrl I.P.
carb CLAYSTONE: brnsh blk, brnsh gry, firm - hd, blky, v carb, v pyr, v calc & grad to Mrl
LIMESTONE: pred pa yelsh brn - brnsh gry, sft - firm, blky, micr, v arg & mrl, grad to calc Clst
CLAYSTONE: varicol, dk gnsh gry, med dk gry, med blsh gry, gnsh gry, firm, blky, wxy Tex, occ pyr, occ lt w/ gn & blk Clas, non calc
TARE FORMATION
2471m MD (1944.6m TVD MSL)
CLAYSTONE: varicol but pred med dk gry, also med blsh gry occ gnsh gry, sft - mod hd, occ pyr, occ lt w/ blk, clr & gn Clas, non calc

Heidrun Field: Well B

1840	100	Sltst	lt olv gry – grnsh gry, amor-sbblky, sft-frm, Tr glauc, r pyr, Tr calc, r mica
	r	Sst	Clr trnsl Qtz, sil cmt w/calc Xln, n.v.p
1850	100	Sltst	a.a.
1860	100	Sltst	a.a., r kao Mtrx
1870			Spl a.a
1880	100	Sltst	a.a., Tr kao Mtrx, Tr calc cmt
1895	100	Sltst	a.a., r kao Mtrx, Tr mica
1900			Spl a.a
1910	100	Sltst	a.a., r kao Mtrx, Tr mica, abd glauc
1920	100	Sltst	a.a., Tr glauc, r mica, r calc cmt
1930	100	Sltst	a.a., Tr glauc, r mica, r pyr, Tr kao Mtrx
1940	100	Sltst	a.a., Tr Glauc, r Mica
1950	100	Sltst	Lt olv gry-gn gry, sbblky-amor, sft-frm, Tr glauc, Tr pyr, slily calc, v f sdy
1960			Spl a.a
1970	100	Sltst	V glauc I.P, else a.a
1980			Spl a.a
1990			Spl a.a
2000	100	Sltst	Bcm lt brn, else a.a
2010			Spl a.a
2020	100	Sltst	Lt olv gry-lt brn gry, sbblky, pred frm, r sft, Tr glauc, r pyr, non calc, r v f sdy
2030			Spl a.a
2035	10	Sltst	Lt brn gry-lt olv gry, sbblky, frm, Tr glauc, r pyr, occ v f sdy
	90	Clst	Lt olv gry-gn gry, sbblky, frm, non calc, r slty
2040	Tr	Sltst	Also Glauc Nod, else a.a
	100	Clst	a.a

2045	100	Clst	Lt olv gry-gn gry, sbblky, frm, non calc, r slty, Tr glauc Nod
2050			Spl a.a
2055	100	Clst	No Glauc, Nod, else a.a
	Tr	Ls	Wh-v lt gry, sbblky-blky, frm, slily arg I.P, microxln
			- **Cuttings from Brygge core** -
2058	80	Clst	Lt olv gry – grnsh gry, sbblky, frm, non Calc, r slty tr Glauc Nod
	20	Sltst	Brn gry – ovl gry, sft – frm, pred sft, lse Qtz in brn Mtrx, Calc cmt i.p.
2060	90	Clst	a.a., r Pyr, r Mica
	10	Sltst	a.a.
2061,9	90	Clst	a.a.
	10	Sltst	a.a.
2065	70	Clst	a.a.
	30	Sltst	a.a.
	Tr	Ls	Wh – v lt gry, sbblky, sft, frm i.p., slily Arg i.p., Microxln i.p.
2068	70	Clst	a.a.
	30	Sltst	a.a.
	R	Ls	a.a.
2070	70	Clst	a.a, pred grnsh gry – dk grnsh gry i.p., Qtz i.p., frm i.p., sft
	30	Sltst	a.a.
	R	Ls	a.a.
			Core chip evaluation
T2 2057,8	100	Clst	Grnsh blk- dk grnsh gry, sft, soluble, crmbly, sbplty – fis, wxy - soapy
T3 (2067)	100	Clst	Dk grnsh gry, grnsh blk i.p., mod hd, non-soluble, dns, fis, ea, slty, non Calc, tr Glauc Nod, r Mica
B3 (2077)	100	Clst	Med blsh gry - grnsh gry, sft – frm, soluble, crmlby, fis, ea, slty, Calc Nod i.p., tr Glauc, tr Mica, r Pyr, r Glauc Nod
			- **Cuttings from drilling to coring point in Tang Fm.** -
2080		Clst	Lt olv gry – grnsh gry, sbblky, frm, non Calc, r slty tr Glauc Nod
		Sltst	Brn gry – ovl gry, sft – frm, pred sft, lse Qtz in brn Mtrx, Calc cmt i.p.
2085	80	Clst	a.a
	20	Sltst	a.a
	Tr	Ls	a.a
2090	90	Clst	Lt olv gry-gn gry, sbblky-blky, sft-frm, non calc-calc, slily slty I.P, Tr glauc, r micropyr
	10	Ls	Wh-v lt gry, sbblky-blky, arg bnd I.P., microxln
2095	40	Clst	Lt olv gry-gn gry, sbblky-blky, sft-frm, non calc-calc, slily slty I.P, Tr glauc, r micropyr

	60	Sltst	Lt brn gry-brn gry, sbblky-blky, frm, slily calc-calc I.P., occ v arg
	Tr	Ls	Wh-v lt gry, sbblky-blky, arg bnd I.P., microxln
2100	50	Clst	a.a
	40	Sltst	Tr brn blk (org?), else a.a
	10	Ls	a.a
2105	40	Clst	a.a
	30	Sltst	a.a
	30	Ls	a.a
2110			Spl a.a
2115			Spl a.a
2120	40	Clst	a.a
	40	Sltst	Incr dk brn-brn blk, else a.a
	20	Ls	a.a
2125	50	Clst	Occ v calc, else a.a
	30	Sltst	a.a
	20	Ls	a.a
2130	70	Clst	Pred frm, occ mod hd, else a.a
	10	Sltst	a.a
	20	Ls	a.a
2135	20	Clst	a.a
	60	Tf	Gn gry-dk gn gry, occ blk spec, sbblky, pred sft-frm, tr pyr, occ slty
	20	Ls	a.a
2140	20	Clst	Non calc-occ slily calc, else a.a
	70	Tf	a.a
	10	Ls	Occ yel gry, else a.a
2145			Spl a.a
2150			Spl a.a
2155			Spl a.a
2160	20	Clst	Gn gry-lt olv gry, sbblky, sft-frm, non-slily calc, Tr micropyr, r glauc
	30	Tf	Gn gry-dk gn gry, occ blk spec, amor-sbblky, pred sft, occ frm, slily slty
	20	Ls	Wh-v lt gry-yrl gry, sbblky-blky, occ slily arg, r pyr, microxln
	30	Sltst	Brn gry-olv gry, amor-sbblky, occ slily stky, occ v arg, slily calc, r micropyr

Appendix D

Mineralogical analysis tables:

- Well A
- Well B
- Well D
- Well I
- Well H

Heidrun Field: Well A

Whole rock fraction

Formation	Depth mTVD MSL	Qtz	K-fsp	Plag	Chl	Kaol	Mi/Ill	ML	Smec	Calc	Sid	Dol	Pyr	Gyp
Kai (cut)	1751	48,8	2	4,9	3,1	9	15	2,8	4,6	4,1	0,7	0	4,3	0
Kai (cut)	1758	47,5	1,82	1,8	2,5	14,3	13,8	2,6	2	7,3	1,6	0	4,9	0
Brygge (co)	1827	31	2,1	1,5	7,2	6,3	23,1	9,8	2,5	0	5	0,4	9,9	1,1
Brygge (co)	1834	6,6	0,5	2,3	1,3	4,3	17,8	6,9	0,4	51,5	4,4	1,9	1,9	0
Brygge (cut)	1839	16,9	1,7	5,1	10,3	0	9,6	3,7	40,6	2,5	1,7	0	7,6	0
Brygge (co)	1846	6	1	1,2	3,8	9	53,2	19,6	0	0	3,1	0	3,2	0
Brygge (cut)	1846	11	1,7	4,2	8,4	0	11,6	3,5	50,3	0,5	3,4	0	4,2	0
Brygge (cut)	1928	6,6	1,8	3,8	1,4	1,6	1,9	1,5	53,8	8,8	1,2	0,9	8,5	0
Brygge (cut)	1936	15	2,7	3,8	4,6	0,1	5,5	3,5	43,1	4,5	2,5	1,7	10,7	0

Fine fraction

Formation	Depth mTVD MSL	Qtz	K-fsp	Plag	Chl	Kaol	Ill	ML	Smec	Calc	Sid	Dol	Pyr
Brygge (co)	1827	15,7	1	1,3	8,5	11,2	10,5	38,9	0	0	0	0	12,9
Brygge (co)	1834	3	0,5	0,7	4,2	7,1	13,6	7	43,4	19,3	0	0	1,1
Brygge (co)	1846	3	0,5	0,7	3,1	16,7	18,7	1,1	54,7	0	0	0	1,5

Heidrun Field: Well B

Whole rock

Formation	Depth mTVD	Depth mMD	Qtz	K-fsp	Plag	Chert	Chl	kaol	Mi/ill	ML	Smec	Calc	dol	pyr	zeolite
Brygge	1860	2059,62	6,7	0	0	0	0	0	23,6	0	61	0	2,3	6,4	0
Brygge	1861	2060,6	0,8	0	0	4,2	0	0	0	0	11,9	81,6	0	1,4	0
Brygge	1866	2065,63	2,4	0	0	62,1	0	0	7,4	0	14,7	0	0	12,6	0,7
Brygge	1873	2072,24	4	0	0	40,4	0	0	13,8	32,8	0	0	0	7,9	1,1
Brygge	1877	2076,48	2,7	0	0	67,4	0	0	7,9	13,1	0	0	0	7,3	1,7
Brygge	1878	2076,9	0,8	0	0	0	0	0	0	9,5	0	87,6	0	2,1	0

Fine fraction

Formation	Depth mTVD	Depth mMD	Qtz	Plag	Chert	Chl	Kaol	Ill	ML	Smec	Calc
Brygge	1860	2059,62	0	0	0	0	0	0	0	100	0
Brygge	1861	2060,6	0	0	0	0	0	0	0	84,9	15,1
Brygge	1866	2065,63	1,2	0	29,4	0	0	32,5	0	36,9	0
Brygge	1873	2072,24	2	0	9,7	0	0	12,2	76,1	0	0
Brygge	1877	2076,48	0	0	20,6	0	0	0	79,4	0	0
Brygge	1878	2076,9	0	0	0	0	0	0	89,3	0	10,7

Åsgard Field: Well D

Whole rock fraction

Formation	Depth mTVD	Depth mMD	Qtz	Kfsp	plag	Chl	Kaol	Mic/Ill	ML	Smec	Calc	Sid	Dol	Pyr	Gyp	Amp	Opa	Trace
Kai	1496	1540	22,5	10,9	18,7	3,9	9,1	26,8	1,2	0,6	1,7	1,4	0,4	1,2	0	1,4	0	
Kai	1533	1580	24	3,1	18,6	4,1	9,2	31,7	0,6	1,2	3	1,6	0,3	1,2	0	1,5	0	
Kai	1569	1620	22,4	3,2	14,8	5,5	10,3	32,5	2,6	1,9	2,7	2,1	0,5	0,8	0	0,8	0	Clo
Kai	1606	1660	23,2	6,3	17,7	5,9	6,9	27,1	1,8	2,1	3,6	1,3	0,9	1,7	0	1,4	0	Clo
Kai	1643	1700	27,7	2,8	17	3,7	9,7	27,9	2,1	1,7	3,1	1,8	0,5	1,1	0	1	0	Clo
Kai	1679	1740	27,3	4,5	17,4	5	8,9	25,5	1,6	2,6	2,7	1,7	0,6	1,3	0	0,9	0	Clo
Kai	1715	1780	22,6	4,5	16,5	4,6	10,2	29,5	0,8	5,2	1,7	1,9	0,4	1,7	0	0,4	0	
Kai	1752	1820	20,3	2,5	15,3	4	13,2	32,1	0,9	6	1,6	1,7	0,3	1,5	0	0,6	0	Clo
Kai	1788	1860	17,5	3,2	16,7	3	8,4	29	1	7,5	8,6	1,3	0,3	2,8	0,2	0,6	0	Clo
Kai	1824	1900	18,9	4,9	17,6	3,1	7,6	26,6	0,9	9,5	5	0,9	0,4	3,8	0,2	0,7	0	Clo
Kai	1861	1940	23,5	3	12	2,4	13,5	25,3	1,5	11,2	2,9	0,8	0,2	3,5	0	0,3	0	Clo
Brygge	1897	1980	20,8	4,1	8,7	4	12,9	26,2	0,7	12	1,4	0,4	0,4	8,6	0	0	0	Clo
Brygge	1934	2020	19,6	2,1	3,1	3,7	12,1	33,4	1,4	14,3	0,2	0,4	0,1	9,5	0	0	0	
Brygge	1970	2060	11,5	1,5	5,1	2,4	11,4	32,9	0,7	29,7	0,3	0	0,1	4,2	0	0,1	0	
Brygge	2006	2100	8,5	0,5	1,9	2,8	7,5	17,2	1	54,9	0	0,5	0	3,7	0	0	1,6	Clo
Brygge	2043	2140	7,5	1	2,1	1,6	7,4	13,1	0	59	0,3	0,5	0	2,8	0	0	4,7	Clo
Brygge	2052	2152	5,2	0,4	1,4	2,3	3,1	8,1	0,5	69	0,8	0,2	0	2,2	0	0	6,8	Clo

Fine fraction

Formation	Depth mTVD	Depth mMD	qtz	Kfsp	plag	Chl	Kaol	Mic/Ill	ML	Smec	Calc	Sid	Dol	Pyr	Amp	Opa
Kai	1496	1540	4,1	0,8	2,1	15	16,1	45,8	0,4	12	1	2,2	0	0,2	0,2	0
Kai	1533	1580	3,9	0,8	2,2	15,7	12,4	50,4	0,2	10,3	1	2,1	0	0,7	0,2	0
Kai	1569	1620	3,2	0,3	1,2	10,2	18,9	52,4	0,4	11,3	0,6	1,2	0	0,2	0,1	0
Kai	1606	1660	3,3	0,7	1,8	12,8	10,6	47,1	1	18,3	1,7	1,7	0	0,8	0,2	0
Kai	1643	1700	3,6	0,4	1,1	10,8	13	45,3	0,6	22,2	0,9	1,6	0	0,3	0,1	0
Kai	1679	1740	2,4	0,2	1,2	8,5	14,2	35,6	0,4	35,3	0,8	0,7	0	0,6	0	0
Kai	1715	1780	2,3	0,3	0,7	9,2	13,1	42,7	0,3	30,3	0,2	0,7	0	0,3	0	0
Kai	1752	1820	2,9	0,4	0,5	7,1	15,4	37,4	0,4	33,9	0,3	0,9	0	0,7	0	0
Kai	1788	1860	2,8	0,4	0,7	5,5	14,7	27,8	1,1	39,2	5,6	0,6	0	1,7	0	0
Kai	1824	1900	3	0,3	0,5	5,7	15,3	27,8	0,6	42,3	3	0,3	0	1,2	0	0
Kai	1861	1940	1,4	0,2	0,5	4,2	23,3	32,4	1,1	33,4	1,7	0,3	0	1,6	0	0
Brygge	1897	1980	2,9	0,4	0,6	4,1	26,4	25,5	1,8	32,8	0	0	0	5,5	0	0
Brygge	1934	2020	3,7	0	0	4,3	25,4	27,9	3,8	31,1	0	0	0	3,8	0	0
Brygge	1970	2060	2,1	0	0	3	14,5	21,5	0,8	56,7	0	0	0	1,4	0	0
Brygge	2006	2100	1,3	0	0	2,4	5,5	11	0,7	78,3	0	0	0	0,5	0	0,4
Brygge	2043	2140	1	0,1	0,2	1,4	5,1	12,3	0,3	76,5	0	0	0	0,6	0	2,4
Brygge	2052	2152	0,6	0,1	0,1	2,1	2,6	9	0,1	83,7	0	0	0	0,2	0	1,4

Aasta Hansteen Field: Well H

Whole rock fraction

Formation	Depth mTVD	Depth mMD	Qtz	Kfsp	Plag	Chl	Kaol	Mi/ill	Ml	Smec	Ver	Cal	dol	pyr	amp	clo	opa	Gyp	hal	syl
Kai	2116	2140	20,8	3,5	11,4	6,1	13,2	23	0	0	16,8	1,3	0,6	2	0,8	0,6	0	0	2,8	0
Brygge	2216***	2240***	7,6	1,4	0,6	2	8,9	10,8	0	0	64,1	0	0	4,4	0	0	0	0	4,2	0
Brygge	2216**	2240**	13,9	2,3	3	2,4	20,6	21,7	0,7	0	28,5	0	0	7	0	0	0	0	2,5	0
Brygge	2365	2388	7,4	1,5	0,7	0,5	2,5	4,5	0	26,6	0	0,8	0	20,1	0	18,7	16,6	0	4,2	0

Fine fraction

Formation	Depth mTVD	Depth mMD	Qtz	Kfsp	Plag	Chl	Kaol	Ill	ML	Smec	Ver	Cal	dol	pyr	Clo	Opa	Gyp
Kai	2116	2140	6	0,9	3,1	9,7	15,8	33,3	0,6	0	29,7	0	0	0,8	0	0	0
Brygge	2216***	2240***	3,6	0,4	0,3	3,2	9,6	7,4	0,5	0	73	0	0	1,8	0	0	0
Brygge	2365	2388	2,2	1,8	0	8	0,4	12,8	0	61,4	0	0	0	8,8	4,8	23,2	0

Aasta Hansteen Field: Well I

Whole rock fraction

Formation	Depth mTVD	Depth mMD	Qtz	Kfsp	Plag	Chl	Kaol	Mi/ill	Ml	Smec	ver	Cal	dol	pyr	amp	clo	opa	Gyp	hal	syl
Kai	2077	2100	25,6	5,1	13,9	6,2	12,6	24,7	0,6	7	0	1,2	0,8	1,5	0,9	0	0	0	0,2	2,5
Brygge	2127	2150	17,8	8,3	15,2	5,8	10,4	27	0,5	12,1	0	0,4	0,3	1,3	0,8	0	0	0	0,1	1,7
Brygge	2157**	2180**	21,9	2,8	14	6,8	12,6	30,2	0,8	7,4	0	0,6	0,5	1,3	0,9	0	0	0	0,1	1,9
Brygge	2157***	2180***	5,4	6,5	2,4	2,9	2,4	4,6	0,5	75,2	0	0	0	0	0	0	0	0	0,8	7,3

Fine fraction

Formation	Depth mTVD	Depth MD	Qtz	Kfsp	Plag	Chl	Kaol	Ill	Ml	Smec	Ver	Cal	dol	pyr	Clo	Opa	Gyp
Kai	2077	2100	6,5	0,6	3,6	9,3	17,8	34,7	0,4	26,4	0	0	0,1	0,5	0	0	0
Brygge	2127	2150	5,6	0,6	3	10,6	14	33,7	0	31,8	0	0	0	0,9	0	0	0
Brygge	2157**	2180**	5,2	0,5	2,3	11,6	14,2	39,1	0,4	26,1	0	0	0,1	0,5	0	0	0